

LA-UR-06-8372  
November 2006  
EP2006-1039

# **Interim Measures Investigation Report for Chromium Contamination in Groundwater**

Prepared by the Environmental Programs Directorate

Los Alamos National Laboratory, operated by Los Alamos National Security, LLC, for the U.S. Department of Energy under Contract No. DE-AC52-06NA25396, has prepared this document pursuant to the Compliance Order on Consent, signed March 1, 2005. The Compliance Order on Consent contains requirements for the investigation and cleanup, including corrective action, of contamination at Los Alamos National Laboratory. The U.S. government has rights to use, reproduce, and distribute this document. The public may copy and use this document without charge, provided that this notice and any statement of authorship are reproduced on all copies.



## EXECUTIVE SUMMARY

This interim measures investigation report describes work performed to address chromium contamination in groundwater beneath Los Alamos National Laboratory (the Laboratory). The investigation was conducted in accordance with requirements in the March 1, 2005, Compliance Order on Consent (the Consent Order) between the U.S. Department of Energy (DOE), the Regents of the University of California, and the New Mexico Environment Department (NMED). This investigation implemented an interim measures work plan that was prepared in response to a requirement in a letter from NMED dated December 29, 2005. The interim measures investigation was implemented to ensure the protection of drinking water while longer-term corrective action remedies are evaluated and implemented.

The investigations were conducted in the late summer and fall of 2006 to characterize the nature and extent of chromium in surface water, alluvial groundwater, and perched-intermediate groundwater in and beneath the Los Alamos, Sandia, and Mortandad Canyons watersheds. Wells extending into the regional aquifer are also considered. These data are used to evaluate spatial and temporal trends in chromium contamination at a multiple-watershed scale, including variations in contaminant concentration at increasing distances from the source areas and as a function of time since chromium releases were halted.

A review of archival records and interviews identify the cooling towers associated with the Technical Area (TA) 03 power plant (TA-03-22) at the head of Sandia Canyon as the main source of chromium contamination at the Laboratory. An estimated 26,000 to 105,000 kg (58,000 to 230,000 lb) of chromium(VI) was released into the south fork of upper Sandia Canyon from these operations circa 1956 to 1972. Other sources of chromium(VI) include the cooling tower at the Omega West Reactor (TA-02) in Los Alamos Canyon and sites at TA-35 and TA-48 in the Mortandad watershed. The total chromium mass released and effluent volumes in Sandia Canyon were more than an order of magnitude greater than those released in Los Alamos and Mortandad Canyons.

Sampling data from regional groundwater monitoring wells and surrounding production wells shows that only R-11 and R-28 contain clear evidence for Laboratory-derived chromium contamination. A few other regional groundwater monitoring wells (e.g., R-15) may contain slightly elevated chromium but additional monitoring data are needed to further assess whether these results indicate contamination. Installation of R-35a and R-35b will provide further information for the assessment of potential impact to water-supply well PM-3.

The results of this interim measures investigation indicate that the predominant zone of infiltration into the suballuvium vadose zone occurs in the middle reaches of Sandia Canyon as suggested in the initial conceptual model. However, preliminary indication from the water-balance investigation is that the zone of infiltration extends farther upcanyon than initially thought.

Data from core obtained during this investigation from within the predominant zone of infiltration show that the chromium has largely been flushed through this zone and that the geochemical conditions beneath the alluvium are not ideal for reducing and immobilizing chromium(VI). Analytical results for alluvium collected in the characterization core holes and previous sediment data collected from young deposits throughout the canyon, especially in the wetland, indicate that a significant portion of the mass of chromium might remain in those media. That portion of the chromium inventory is expected to be predominantly in the relatively stable trivalent phase due to the abundance of organic matter and other adsorbing phases such as iron oxides. But, present-day detections of low concentrations of chromium(VI) in surface water and alluvial groundwater suggest that geochemical conditions are allowing for some transformation to the mobile form.

It is recommended that the interim measure phase of this investigation be concluded with this report and subsequent work be conducted under the Sandia Canyon and Cañada del Buey pursuant to Section IV.B.5.b of the Consent Order. Modifications to the scope of the work plan would be necessary to account for new information and data gaps identified since preparation of the work plan and in the interim measures phase. Data collection under the modified work plan would focus on characterization of the nature and extent of all contaminants (not just limited to chromium and related contaminants) sufficient to support risk assessments and corrective-action remedy selection.

## CONTENTS

<b>1.0</b>	<b>INTRODUCTION .....</b>	<b>1</b>
<b>2.0</b>	<b>BACKGROUND .....</b>	<b>2</b>
<b>3.0</b>	<b>SCOPE OF ACTIVITIES.....</b>	<b>4</b>
3.1	Quarterly Sampling of Surface Water and Groundwater in Sandia and Mortandad Canyons .....	5
3.2	Investigation of Surface Water and Alluvial Groundwater Infiltration.....	6
3.2.1	Water Infiltration in Upper Sandia Canyon.....	6
3.2.2	Alluvial Groundwater Infiltration in Lower Sandia Canyon .....	6
3.3	Installation of Characterization Core Holes in Lower Sandia Canyon .....	7
3.4	Analysis of Archival Core.....	7
3.5	Installation of Alluvial Wells in Lower Sandia Canyon.....	8
3.6	Rehabilitate Well R-12.....	8
3.7	Background Chromium Concentrations in Groundwater.....	9
3.8	Effects of Seasonal Pumping at Production Wells on Water Table.....	9
<b>4.0</b>	<b>REGULATORY CRITERIA .....</b>	<b>9</b>
<b>5.0</b>	<b>INVESTIGATION RESULTS .....</b>	<b>10</b>
5.1	Surface Water Loss in Sandia Canyon .....	11
5.2	Extent of Alluvial Groundwater as Determined from Drilling .....	12
5.3	Results from Nested Piezometers .....	14
5.4	Suballuvial Moisture Occurrences .....	16
5.5	Contaminant Distributions .....	17
5.5.1	Chromium.....	17
5.5.2	Molybdenum.....	25
5.5.3	Phosphate .....	28
5.5.4	Zinc .....	30
5.5.5	Groundwater Geochemistry of Alluvium .....	33
<b>6.0</b>	<b>SUMMARY OF PHYSICAL SYSTEM CONCEPTUAL MODEL .....</b>	<b>33</b>
<b>7.0</b>	<b>CONCLUSIONS AND RECOMMENDATIONS.....</b>	<b>37</b>
<b>8.0</b>	<b>REFERENCES .....</b>	<b>38</b>

### Appendixes

Appendix A	Acronyms
Appendix B	Field Investigation Methods and Results
Appendix C	Analytical Data Tables and Water-Level Data (on DVDs)

### Figures

Figure 2.0-1	Location of Sandia, Los Alamos, and Mortandad canyons showing major chromium release sites, stream-flow gages, surface water sampling stations, and existing and newly installed boreholes and wells .....	41
--------------	--	----

Figure 5.1-1	Photographs of Parshall flume installed near E123 gaging station in upper Sandia Canyon, looking upstream (upper) and downstream (lower).....	43
Figure 5.1-2	Comparison of hydrographs at gaging station E123 and at collocated Parshall flume (D123), October 20 through October 26, 2006 .....	44
Figure 5.1-3	Photograph of E123.5 gaging station in Sandia Canyon, September 2006, looking downstream.....	44
Figure 5.1-4	Rating curve at gaging station E123.5 .....	45
Figure 5.1-5	Comparison of hydrographs at gaging stations E123 and E123.5 from October 17 to October 23, 2006 .....	45
Figure 5.2-1	Map of eastern extent of alluvial saturation in Mortandad and Sandia Canyons .....	46
Figure 5.2-2	Transducer data collected between October 13th and November 7th 2006, at SCA 2. Screen location is shown .....	46
Figure 5.2-3	Transducer data collected between October 12th and November 7th 2006, at SCP-2a,b (top panel), SCA-4 and nearby piezometers SCP-1a,b,c (midpanel), and SCA-5 (bottom panel).. .....	47
Figure 5.3-1	SCP-1a,b,c piezometer nest water levels .....	48
Figure 5.3-2	SCP-2a,b piezometer nest water levels .....	49
Figure 5.3-3	SCP-1a,b,c vertical gradient and computed seepage velocity .....	50
Figure 5.3-4	SCP-2a,b vertical gradient and computed seepage velocity .....	51
Figure 5.4-1	Borehole stratigraphies with core moisture data and presence of saturated horizons superimposed (all elevations and depths are in feet).....	52
Figure 5.4-2	Histograms of averaged moisture content (100 × g water/g solid) collected from core samples of ash flows of the Otowi Member of the Bandelier Tuff beneath lower Sandia Canyon. Error bars are 1 standard deviation. ....	53
Figure 5.5-1	Profiles of acid-soluble chromium and pore-water dissolved chromium concentrations determined from core samples in core holes SCC-1, SCC-2, SCC-3, SCC-4, SCC-5 and SCC-6 .....	54
Figure 5.5-2	Histograms comparing chromium concentrations in weak nitric acid leachate (3050 method) for combined Qbt 1g, Qct, Qbo, and Qbog core samples collected from Los Alamos, Sandia, Mortandad, and Ten Site canyons.....	55
Figure 5.5-3	Profiles of acid-soluble molybdenum and pore-water dissolved molybdenum concentrations determined from core samples in core holes SCC-1, SCC-2, SCC-3, SCC-4, SCC-5 and SCC-6 .....	56
Figure 5.5-4	Profiles of pore-water dissolved phosphate concentrations determined from core samples in core holes SCC-1, SCC-2, SCC-3, SCC-4, SCC-5 and SCC-6.....	57
Figure 5.5-5	Profiles of acid-soluble zinc and pore-water dissolved zinc concentrations determined from core samples in core holes SCC-1, SCC-2, SCC-3, SCC-4, SCC-5 and SCC-6 .....	58
Figure 6.0-1	Conceptual hydrogeologic cross section showing potential chromium transport pathways and dissolved hexavalent chromium values (µg/L) for surface water, monitoring wells, and water supply wells in the vicinity of Sandia Canyon .....	59

**Tables**

Table 2.0-1	Water Treatment Chemicals Used at the Technical Area 3 Power Plant .....	61
Table 2.0-2	Estimates of Chromium(VI) Releases at the TA-03 Power Plant All estimates assume time period of release from June, 1956 to April, 1972 (5814 days) .....	62
Table 2.0-3	Water Discharge Volumes for 2003, 2004, and 2005 for Five Active NPDES Outfalls Discharging to Sandia Canyon.....	62
Table 5.1-1	Outfall Discharge Data from TA-03 into Upper Sandia Canyon for WY06.....	63
Table 5.1-2	Comparison of Surface Flow at E123 with Outfall Discharges during WY06.....	64
Table 5.1-3	Total Estimated Water Loss above E123 during WY06.....	64
Table 5.2-1a	Initial Observations of Water Occurrence in SC Drill Holes.....	65
Table 5.2-1b	Initial Observations of Water Occurrence in SCC Drill Holes .....	65
Table 5.2-1c	Initial Observations of Water Occurrence in SCA Drill Holes .....	65
Table 5.3-1	Sandia Canyon Piezometer Slug Test Results.....	65

**Plates**

Plate 1.	Depth-Concentration Profiles Showing the Distribution of Acid-Soluble Chromium in Cores Collected from Boreholes in Los Alamos, Sandia, Mortandad, and Ten Site Canyons
----------	---



## **1.0 INTRODUCTION**

This interim measures investigation report (investigation report) describes the work done to date to address chromium contamination detected in groundwater beneath Los Alamos National Laboratory (LANL or the Laboratory). The investigation was conducted in accordance with requirements of the March 1, 2005, Compliance Order on Consent (hereafter, Consent Order) between the U.S. Department of Energy (DOE), the Regents of the University of California, and the New Mexico Environment Department (NMED). The work was initiated in response to a letter from NMED dated December 29, 2005 (NMED 2005, 091683), that required the Laboratory to submit an interim measures work plan pursuant to Section VII.B.2 of the Consent Order. The Laboratory submitted the "Interim Measures Work Plan for Chromium Contamination in Groundwater" (LANL 2006, 091987) on March 31, 2006, and NMED approved the work plan with modifications on May 5, 2006 (NMED 2006, 092543). The Laboratory addressed NMED's approval with modifications in a letter dated August 25, 2006 (LANL 2006, 094129). NMED's approval with modifications required the installation of a regional groundwater well (R-35). A work plan for R-35 was submitted to NMED on July 3, 2006 (LANL 2006, 093388), and it was approved by NMED on July 24, 2006 (NMED 2006, 093530).

The specific goals of the investigation are to support any necessary interim measures decision by

- determining the primary source(s) of chromium contamination and the nature of operations associated with releases,
- characterizing the present-day spatial distribution of chromium and related constituents such as phosphate and zinc,
- collecting data to evaluate the geochemical and physical/hydrologic processes that govern chromium transport, and
- collecting and evaluating data to help guide subsequent investigations and remedy selection.

This report presents the results of the interim measures investigation. Information on radioactive materials and radionuclides, including the results of sampling and analysis of radioactive constituents, is voluntarily provided to NMED in accordance with DOE policy.

Section 2.0 of this report presents an updated review of the chromium sources in and adjacent to Sandia Canyon. Section 3.0 describes the scope of activities performed as part of this investigation. Section 4.0 describes the regulatory framework for addressing the chromium contamination. Section 5.0 discusses results of the characterization of the distribution of chromium and related constituents. Section 6.0 presents the physical system conceptual model that addresses sources and processes related to the chromium contamination, present-day distribution, and hydrologic and geochemical processes that are consistent with the observations of chromium contamination. Three appendixes are also included: abbreviations and acronyms (Appendix A), information on field investigations and results (Appendix B), and analytical results (presented on a DVD in Appendix C). Regional well R-35 has not been completed as of the writing of this report, but the well completion information and results will be issued in a subsequent report.

A primary goal of the interim measures investigation was to collect sufficient data to determine if an interim measure is needed to ensure protection of drinking water while corrective measures are evaluated and implemented, as appropriate. This goal is addressed by defining the nature and extent of mobile (i.e., hexavalent) chromium contamination in surface water, the vadose zone, and groundwater. Installation and monitoring of groundwater at R-35a and R-35b will provide an additional important means of ensuring protection of drinking water because the well will be located along the flow path between the

currently known chromium contamination and water-supply well PM-3. If necessary, well-head treatment can be conducted at a water-supply well if it were to become unacceptably impacted by chromium. Groundwater monitoring will continue to be conducted at an appropriate frequency as described in the Laboratory's "Interim Facility Groundwater Monitoring Plan" (IFGMP) (LANL 2006, 094043), and the analytical results will be reported in periodic monitoring reports.

## **2.0 BACKGROUND**

### **Sources of Chromium**

Several types of historic anthropogenic chromium sources are present in the Sandia, Los Alamos, and Mortandad Canyons watersheds. These include facilities for electroplating and photoprocessing and the use of chromate as a corrosion inhibitor in cooling-tower systems. Based on the review of solid waste management units (SWMUs) in these watersheds performed for the "Interim Measures Work Plan for Chromium Contamination in Groundwater" (LANL 2006, 091987, Appendix 1), the highest chromium usage was as a corrosion inhibitor. Documented usage of chromium in cooling-water systems occurred at the Technical Area (TA) 03 power plant and at the TA-02 Omega West Reactor (OWR) (see Figure 2.0-1) (DOE, 1987 052975), as described below. Chromium may have been used in other smaller-scale cooling systems at the Laboratory. However, its use is undocumented and expected to be of lesser extent because its use was reportedly labor intensive and most practical for larger systems (Birdsell 2006, 091685). A 1971 memorandum (Miller 1971, 003853) reports that other Laboratory cooling towers used a combination of biodegradable and nontoxic chemicals for scale and corrosion control, including amino acids, aminocarboxylic acids, polyacrylates, and organic inhibitors.

### **Sandia Canyon Sources**

The cooling towers for the TA-03 power plant at the head of Sandia Canyon (Consolidated Unit 03-012(b)-00, currently National Pollutant Discharge Elimination System [NPDES] outfall 01A-00, Figure 2.0-1) probably used the largest amounts of potassium dichromate at the Laboratory. The power plant has been operated by the Laboratory's utilities subcontractor (e.g., the Zia Company, Johnson Controls Inc., or KSL) since it opened in 1951. Table 2.0-1 summarizes the history of water treatment chemicals used in cooling water at the power plant from 1951 to 2006 based on records obtained from the power plant water chemist (LANL 2006, 094153). This information indicates that chromate was used from June 1956 to April 1972 as part of a zinc dianodic (blended chromate-phosphate-zinc (Zia 1972, 003855) anticorrosion treatment for the cooling-tower system. The process involved adding sulfuric acid to lower the pH of cooling-tower water to prevent precipitation of silica, calcium carbonate, and other solids. A mixture of potassium dichromate, phosphate, and zinc was then added to coat metal components with a corrosion-inhibiting film (Birdsell 2006, 091685). These chemicals were contained in cooling-tower blowdown released as effluent and in drift emitted with water vapor from the towers.

The Comprehensive Environmental Assessment and Response Program (CEARP) report (DOE 1987, 052975, p. TA3-13) summarizes chromium usage at the power plant as averaging 16.3 kg per day (35.9 lb per day) during that period. This was discharged into upper Sandia Canyon with blowdown water volumes ranging from 485 to 1090 m<sup>3</sup>/day (128,000 to 288,000 gal./day). During this period, hexavalent chromium levels of up to 34 ppm (as chromate, CrO<sub>4</sub><sup>-2</sup>) were reported for discharge concentrations (DOE 1987, 052975, p. TA-3-13). Stream concentrations of 2.4 to 7.3 ppm (as chromate) were also reported below the wetlands from 1969 to 1971 (Purtymun 1975, 011787, p. 115). The total mass of chromium used at and released from the TA-03 power plant is not known. However, Table 2.0-2 provides four estimates of the potential chromate mass released. Estimates 1 and 2 use information obtained from CEARP (DOE 1987, 052975) and its reference documents (Zia 1972, 003855; Reinig 1972, 003848).

Estimate 3 is based on information from a vendor (Phoenix Chemicals) proposing a chemical replacement for chromate at the power plant in 1969 (Birdsell 2006, 091685). Estimate 4 is based on surface water discharge concentrations in power plant effluent from 1968 and 1969 (Kennedy 1971, 033896). Based on these estimates, the likely mass of chromium(VI) released into Sandia Canyon ranged from 26,000 to 105,000 kg (58,000 to 230,000 lb) between June 1956 and April 1972.

Releases of water (as effluent) to upper Sandia Canyon have been significant since the early 1950s and continue today. These discharges along with stormwater runoff have supplied a sufficient water volume to facilitate potential chromium transport in the watershed. Cooling water for the power plant has been one water source. Treated sanitary wastewater is another source. The former TA-03 Wastewater Treatment Plant [legacy waste site 03-014(a)-99] operated from 1951 to 1992 (LANL 2006, 094161). From 1951 to 1985, the power plant recycled the wastewater for use as cooling water. The wastewater met approximately 75% of the power plant's cooling water requirement, with fresh water making up the difference (LANL 2006, 094153; Purtymun 1975, 011787). Presumably, effluent discharges were dominated by power plant effluent during that time period, at roughly 500 to 1000 m<sup>3</sup>/day (130,000 to 260,000 gal./day) (see Table 2.0-2,) and discharged to the south fork of upper Sandia Canyon (currently NPDES outfall 01A001). From 1986 to 1992, we presume that reuse of the treatment plant water stopped and discharges likely increased by approximately 75%.

Since 1992, the TA-46 Sanitary Wastewater System (SWW) has treated the Laboratory's sanitary wastewater. Water quality and effluent volumes from this facility are reported for NPDES outfall 13S. However, the sanitary wastewater has been routed to TA-03 since 1992 for potential reuse as cooling water. Despite being routed to TA-03, the effluent has never been used for that purpose, and it is discharged directly into Sandia Canyon through NPDES outfall 01A001 (Figure 2.0-1) along with cooling water from the power plant. Table 2.0-3 provides effluent volumes for the years 2003 through 2005 for the five outfalls that are currently permitted to discharge to Sandia Canyon. The SWS represents the greatest discharge volume ranging from an average of 960 to 1113 m<sup>3</sup>/day (and is currently the dominant water source to Sandia Canyon. Power plant discharges have dropped significantly from an average of 403 m<sup>3</sup>/day (106,000 gal./day) in 2003 to 49.6 and 34.3 m<sup>3</sup>/day (13,000 and 9060 gal./day) in 2004 and 2005, respectively, because much of the Laboratory's power needs are now supplied from the commercial power grid. This information shows that a significant volume of effluent has been available to drive chromium transport in the subsurface. A more complete summary of effluent volumes will be compiled as part of the upcoming Sandia Canyon investigation.

Phosphates were used as cooling water additives at the TA-03 power plant before, during, and after chromate usage, as indicated in Table 2.0-1, likely from 1951 to 2001. Sodium molybdate was used from 1993 to 2001 (Table 2.0-1). These chemicals were likely released at other outfalls in Sandia Canyon as well. For example, Garratt-Callahan Formula 2010 (see Table 2.0-1) is listed as an additive in the 1998 NPDES permit application for the following outfalls that have released to Sandia Canyon: 03A024 and 03A027 at TA-03, outfall 03A113 at TA-53, and outfall 03A181 at TA-55.

### Los Alamos Canyon Sources

The cooling system for the OWR (Figure 2.0-1) at TA-02 was operated by the Laboratory and used potassium dichromate as a corrosion inhibitor from 1957 to 1973. Chromate use was stopped after the replacement of an aluminum heat exchanger with a stainless steel unit. The cooling tower [SWMU 02-005] is believed to be the second largest source of potassium dichromate to the environment at the Laboratory. An estimated 3000 kg (7000 lb) of chromium(VI) may have been released into Los Alamos Canyon as combined drift and cooling-tower blowdown from the TA-02 cooling tower from 1957 to 1973.

This estimate used normal operating conditions over the 16-yr life of the reactor and chromium usage rates from a 1971 study, for which the cooling tower was operated continuously for 117.9 h and used 67.6 lb of potassium dichromate ( $K_2Cr_2O_7$ ) (Warner 1971, 004251). During the study, an average of 0.023 kg/h (0.05 lb/h) of chromium(VI) was lost through entrainment in drift. Presumably, the remaining 0.07 kg/h (0.15 lb/h) chromium(VI) was discharged with blowdown. Under normal operating conditions, the cooling tower is believed to have operated 8 h/day, Monday through Friday, with a blowdown discharge rate of roughly 46 to 57 m<sup>3</sup>/day (12,000 to 15,000 gal./day) (Birdsell 2006, 091685). This chromium mass estimate differs from an earlier estimate of 2300 kg (5000 lb) (LANL 1993, 015314, p. 7.6-1), which used the same 1971 study results but accounted only for drift losses and assumed a 120-h operating week over 17 yr.

### **Mortandad Canyon Sources**

The SWMU summary presented in Appendix 1 of the “Interim Measures Work Plan for Chromium Contamination in Groundwater” (LANL 2006, 091987), indicates several possible Mortandad Canyon sources including cooling-tower systems (e.g., Consolidated Unit 48-007(a)-00) and plating processes (e.g., 03-045(h)-00). The CEARP report (DOE 1987, 052975) also notes that “According to several employees, cooling tower water for the tower serving TA-3-66 had chromium added during the early years of operation. Blowdown was discharged to Mortandad Canyon.” Chromium is released at low concentrations with treated wastewater from the TA-50 Radioactive Liquid Waste Treatment Facility (RLWTF) into Effluent Canyon, a small tributary of Mortandad Canyon. The estimated mass of chromium released from the RLWTF since 1976 is 26 kg (57 lb) (LANL 2006, 094161). A retired Laboratory employee, John Balagna, who had worked at TA-48, noted that the TA-48 cooling tower constructed circa 1958 had a wooden exterior and turned green when the wood was treated. Copper, chromate, and arsenate preservatives were effective for wooden cooling towers in the 1960s (Betz 1962, 094158, p. 307) and may have been used. These combined sources are assumed to be smaller than the power plant in Sandia Canyon, both in terms of discharge volumes and total chromium mass released, because operations were more limited.

Although the sources are not well defined, field investigations show evidence of near-surface chromium contamination in Mortandad Canyon. Results from the sediment investigation in the Mortandad watershed indicate that the highest chromium concentrations are in reach E-1FW at the head of Effluent Canyon (Figure 2.0-1) at maximum concentrations greater than residential soil screening levels, indicating a TA-48 source (LANL 2005, 89308; LANL 2006, 094161). Arsenic and copper are also elevated in this reach, indicating the plausibility of a wood preservative as a potential chromium source. Elevated levels of chromium in nonfiltered surface and alluvial waters also indicate the presence of chromium(III), presumably from historic Laboratory-derived sources of chromium at TA-03, TA-48, and TA-35 (LANL 2006, 094161).

### **3.0 SCOPE OF ACTIVITIES**

The water investigations presented in this report focus on characterizing the nature and extent of chromium in surface water, alluvial groundwater, the vadose zone, and perched-intermediate groundwater in and beneath the Los Alamos, Sandia, and Mortandad Canyons watersheds. Regional groundwater data are also evaluated for these areas. Data from these components of the hydrogeologic system are used to evaluate spatial and temporal trends in chromium contamination at a multiple-watershed scale, including variations in contaminant concentration at increasing distances from the source areas and as a function of time since chromium releases were halted. The scope of the investigation is described in the “Interim Measures Work Plan for Chromium Contamination in Groundwater” (Interim Measures Work Plan) (LANL 2006, 091987). The investigation methods are discussed Appendix B of this report.

This section describes the investigation activities performed to address chromium contamination in groundwater. These activities were designed to accomplish the goals described in Section 1.0 and to address key uncertainties in the conceptual model in support of optimizing subsequent investigation and/or remediation activities. These activities were to

1. perform quarterly sampling of surface water and groundwater in Sandia and Mortandad Canyons,
2. investigate surface water and alluvial groundwater infiltration in Sandia Canyon using gaging station data and by installing two piezometer sets,
3. determine chromium distributions in the upper vadose zone in lower Sandia Canyon by drilling six new core holes,
4. determine chromium distributions in the upper vadose zone from archival cores from Los Alamos, Sandia, Mortandad, and Ten Site Canyons,
5. determine water quality and extent of alluvial saturation in lower Sandia Canyon by installing five alluvial wells,
6. rehabilitate screens in well R-12 in lower Sandia Canyon,
7. refine the understanding of background concentrations and speciation of chromium in groundwater, and
8. evaluate seasonal water-level variations in monitoring wells due to supply well production.

### **3.1 Quarterly Sampling of Surface Water and Groundwater in Sandia and Mortandad Canyons**

In response to a requirement by NMED (NMED 2005, 091683), a group of intermediate and regional groundwater wells (including water-supply wells) surrounding R-28 was sampled in late January–early February 2006 for an analyte suite intended to help characterize the chromium contamination and define potential sources. Results of that initial investigation were incorporated into the design of the Interim Measures Work Plan (LANL 2006, 091987), and the analytical data are presented in Appendix 6 of that work plan.

This investigation included sampling of surface water, alluvial groundwater, perched-intermediate groundwater, and regional groundwater to provide snapshots of water quality throughout the hydrological system. Water-quality data from this sampling provides information about constituents that can be used to fingerprint potential sources and pathways, leading to improved conceptual models of processes controlling chromium mobility and transport and to subsequent remedy selection. Table 3.1-1 lists the sites that were sampled, and Figure 2.0-1 shows the sampling locations. Both filtered and nonfiltered water samples were collected, and the suite of analytes included general inorganic constituents, metals (including total and hexavalent chromium), stable isotopes of hydrogen, nitrogen, and oxygen, perchlorate, volatile organic compounds (VOCs), high explosive (HE) compounds, total organic carbon (TOC), and tritium as described in the Interim Measures Work Plan (LANL 2006, 091987). The field parameters for groundwater samples include temperature, conductivity, pH, alkalinity, dissolved oxygen, and turbidity. Analytical results for the metals and general chemistry are presented on a DVD in Appendix C. The remaining data will be presented in pending periodic monitoring reports and as appropriate in subsequent documents related to the Sandia Canyon investigation.

### 3.2 Investigation of Surface Water and Alluvial Groundwater Infiltration

This investigation contained two activities designed to assess the infiltration of surface water and alluvial groundwater to deeper bedrock units. These activities include investigations of

- surface water infiltration in upper Sandia Canyon, and
- alluvial groundwater infiltration in lower Sandia Canyon.

Areas of surface water and alluvial groundwater loss probably coincide within those parts of the canyon floor that have been local zones of recharge to deeper perched zones and to the regional aquifer during and after the period of chromium release from the TA-03 power plant cooling tower. Results from these water-loss investigations are used in conjunction with results from the core-hole and alluvial well investigations described below to identify potential deep infiltration pathways.

#### 3.2.1 Water Infiltration in Upper Sandia Canyon

This activity examined surface water and alluvial groundwater loss in two reaches of upper Sandia Canyon by evaluating the water balance using outfall and stream gage data. These reaches are the

- canyon floor wetland bracketed by the TA-03 power plant outfall on the west and surface water gaging station E123 on the east, and
- narrow bedrock-dominated portion of Sandia Canyon located between surface water gaging stations E123 and E123.5.

Figure 2.0-1 shows the locations of these outfalls and stream gages.

Discharge records from the TA-03 power plant outfall (presently 01A-001), the SCC outfall (03A-027) were used to constrain the input water volume entering the wetland. Streamflow-gage data from E123 were used to estimate the water volume exiting the wetland. Different periods of record (e.g., summer vs. autumn) were used to estimate evapotranspiration (ET) associated with cattails and other vegetation in the wetland.

Downstream from the wetland, the stream channel runs for a distance of approximately 2200 m (7218 ft) through a steep-walled canyon incised into unit Qbt 2 of the Tshirege Member of the Bandelier Tuff until the canyon widens and surface water infiltrates into the thickening alluvium. A temporary streamflow-monitoring station (gaging station E123.5 in Figure 2.0-1) was installed in the narrow portion of the canyon near the eastern extent of perennial flow to determine if significant streamflow-infiltration losses occur between E123 and E123.5. Streamflow measured at gages E123 and E-123.5 were compared to determine streambed infiltration losses that occur within this reach.

#### 3.2.2 Alluvial Groundwater Infiltration in Lower Sandia Canyon

Two sets of nested piezometers, SCP-1 and SCP-2, were installed to evaluate potential spatial variations in the rate of infiltration of alluvial groundwater in lower Sandia Canyon. Table 3.2-1 provides information about the location, purpose, and depth of the piezometers. Construction diagrams and lithologic logs for the piezometers are provided in Appendix B-1.6.

Piezometer set SCP-1 was installed in a single borehole next to alluvial well SCA-4 (Figure 2.0-1). Three 2.54-cm (1-in.) PVC piezometers were nested in the borehole with prepacked screens located at depths of 11.52 to 11.67 m (37.8 to 38.3 ft), 12.0 to 12.15 m (39.4 to 39.9 ft), and 12.36 to 12.71 m (41.2 to 41.7 ft), respectively. Piezometer set SCP-2 was installed in two separate boreholes next to alluvial well

SCA-3 (Figure 2.0-1). Two 2.54-cm (1-in.) PVC piezometers with prepacked screens were set at depths of 15.09 to 15.26 m (49.5 to 50 ft) and 13.41 to 13.56 m (44 to 45.5 ft), respectively. The screens in both sets of piezometers are 15 cm (6 in.) long. Continuous-record water-level transducers were installed in the piezometers to investigate vertical gradients in the alluvial aquifer. Water-level data are summarized in Appendix C-7.

### **3.3 Installation of Characterization Core Holes in Lower Sandia Canyon**

Six deep characterization core holes, SCC-1 through SCC-6, were drilled in lower Sandia Canyon to determine the nature and extent of chromium contamination in the upper vadose zone, to identify infiltration pathways, and to provide information for eventual estimates of contaminant inventories. Table 3.2-1 provides information about the location, purpose, and depth of the core holes. The locations of the core holes are shown in Figure 2.0-1. Core samples were collected at a nominal sample interval of 6 m (20 ft) for anions, metals, and cations and at an interval of 12 m (40 ft) for tritium. Both leachable pore water and weak nitric-acid leachates were extracted from the core and analyzed to define contaminant distributions in the upper vadose zone and to assess the geochemical processes controlling chromium mobility. Analytical results for core samples are presented in Appendix C-3. Together with the alluvial wells described in the next section, these core holes also help define the extent of saturation in alluvium.

Results from a direct-current (DC) resistivity survey conducted in the central portion of Sandia Canyon in 2005 (see Figure 2.0-1) and the Advanced Hydrotest Facility (AHF) core holes SC1 through SC5 (Kleinfelder 2002, 091687) were used to site the core holes. A discussion comparing the DC resistivity survey data with resistivity and moisture data from the core holes is provided in Appendix B-1.5.

The six core holes were drilled by using dry air-rotary coring methods. Surface casing was installed in the alluvium to prevent alluvial groundwater from entering the deeper parts of the core hole and impacting moisture-sensitive samples collected during coring operations. Five of the core holes were backfilled with bentonite and/or native material and abandoned after collection of core samples was completed. A perched-intermediate well, SCI-1, was installed in the SCC-1 core hole after perched water was found in the Puye Formation. The SCI-1 well was constructed using 9.5-cm (3.75-in.) inside diameter (I.D.)/10.2-cm (4-in.) outside diameter (O.D.) schedule 80 polyvinyl chloride (PVC), and it includes a 6.1-m (20-ft) well screen with 0.05-cm (0.02-in.) slots. The well targets gravels overlying a possible perching horizon of siltstone in the Puye Formation. The well screen extends from 109.3- to 115.4-m (358.5- to 378.5-ft) depth.

When borehole conditions permitted, borehole camera, gamma, and induction logs were run after the core hole reached the total depth to help define geologic contacts and to assess moisture conditions in the core hole. Samples taken tables and lithologic logs prepared from core and cuttings for each borehole are presented in on a CD in Appendix B-1.6. Screening water samples were collected when perched groundwater was encountered, when possible. Screening samples, listed in Appendix B-1.6, were analyzed for anions, metals, and tritium to provide an indication of whether contaminants are present in perched-intermediate groundwater. Screening water data are presented in Appendix C-3 on a DVD.

### **3.4 Analysis of Archival Core**

Selected archival core samples from Los Alamos, Sandia, Mortandad, and Ten Site Canyons were analyzed to determine the nature and extent of chromium contamination in the upper vadose zone, to identify infiltration pathways, and to provide information for eventual estimates of contaminant inventories. Locations of the core holes sampled are shown on the location map on Plate 1. These data supplement new core data described in Section 3.3 of this report and provide information to evaluate chromium

distributions beneath Los Alamos and Mortandad Canyons. Core samples were selected for analysis at nominal 20-ft intervals in each core hole. Results of archival core analyses are presented in Appendix C-4.

### **3.5 Installation of Alluvial Wells in Lower Sandia Canyon**

Five alluvial wells, SCA-1 through SCA-5, were drilled in lower Sandia Canyon to delineate the extent of alluvial saturation, to determine the nature and extent of chromium contamination within alluvial groundwater, and to provide information for eventual estimates of contaminant inventories. Water-quality data from these wells represent the first significant sampling of persistent alluvial groundwater in Sandia Canyon. These data will be used to determine if alluvial groundwater represents a continuing source of chromium to deeper groundwater. Table 3.2-1 provides information about the location, purpose, and depth of the alluvial wells. Table B-1.0-1 (Appendix B) summarizes the depth intervals over which the wells are screened. Lithologic logs prepared from drill cuttings and cores are presented for the alluvial wells in Appendix B-1.6. The locations of the wells are shown in Figure 2.0-1.

After the alluvial wells were completed and developed, a round of groundwater samples was collected and analyzed for metals (including hexavalent chromium, uranium, boron, and molybdenum), anions, stable isotopes of hydrogen, oxygen, and nitrogen, tritium, HE compounds, VOCs, and TOC. Filtered water samples were collected for analyses of metals, anions, and nitrogen isotopes. Nonfiltered water samples were collected for metals, VOCs, HE compounds, stable isotopes of hydrogen and oxygen, and tritium. The field parameters for groundwater samples include temperature, conductivity, pH, alkalinity, dissolved oxygen, and turbidity. Analytical data for the first round of sampling is presented in Appendix C-2. These wells will continue to be sampled under the Laboratory's IFGMP (LANL 2006 094043), and the analytical results will be reported in periodic monitoring reports.

### **3.6 Rehabilitate Well R-12**

Groundwater data from all three screens at R-12 are presently considered nonrepresentative because of geochemical effects caused by the use of organic additives during drilling (LANL 2005, 091121). This well is equipped with a Westbay multilevel sampling system and has two well screens in perched-intermediate groundwater and one screen in the regional aquifer. R-12 is considered an important monitoring site because of its location along the eastern Laboratory boundary, its proximity to supply well PM-1, and its position potentially downgradient of chromium contamination within the regional aquifer (e.g., R-11 and R-28). In the recently published "Well Screen Analysis Report," the well was rated as fair in its ability to produce reliable and representative water-quality samples for the regional aquifer screen, and the well was rated as poor for the upper perched-zone screen (LANL 2005, 091121, Figure 6-2b). The lower perched-zone screen was not evaluated because of a lack of water-quality data.

Well rehabilitation at well R-12 is currently underway in accordance with the requirement in the "Interim Measures Work Plan" (LANL 2006, 091987) and the Laboratory's "Work Plan for R-Well Rehabilitation and Replacement" (LANL 2006, 092535). Rehabilitation activities consisted of removing the Westbay sampling system, video logging the well interior, conducting specific capacity tests on all three screened intervals, monitoring water-quality parameters during the tests, and collecting groundwater samples for geochemical analyses. Water-quality parameters were within acceptable limits after pumping of isolated screens associated with the specific capacity tests, and further development was not considered necessary. Hydrologic and water-quality data for the R-12 rehabilitation will be presented in a separate report "Well Rehabilitation Report for Characterization Well R-12, Los Alamos National Laboratory, Los Alamos, New Mexico Project No. 73885," which is in preparation.

### **3.7 Background Chromium Concentrations in Groundwater**

An investigation of background concentrations for total dissolved chromium and chromium(VI) was proposed in the "Interim Measures Work Plan" (LANL 2006, 091987). However, it was mutually decided by both NMED and the Laboratory that such an investigation was not necessary, based on recent analytical results for total dissolved chromium and chromium(VI) at numerous wells. These results showed that detectable concentrations of total dissolved chromium consisted mostly of chromium(VI) (LANL 2006, 091987). Sampling stations included Laboratory noncontaminated and contaminated monitor wells, supply wells, and regional off-site wells.

### **3.8 Effects of Seasonal Pumping at Production Wells on Water Table**

The regional aquifer beneath Los Alamos National Laboratory is a major source of water supply for Los Alamos County and the Laboratory. The top of the aquifer is predominantly under water-table conditions, but there are zones of local confinement as well. Municipal wells are generally screened across long intervals deep within the regional aquifer which is predominantly under confined conditions. This activity used a statistical and analytical approach to compare water-level data from regional monitoring wells and municipal supply wells with pumping-rate data from the municipal supply wells. The analysis results in an evaluation of the effects of seasonal variability in the pumping at water-supply wells on the directions and magnitudes on the groundwater flow gradients in the shallow portion of the regional aquifer. In particular, this activity examined whether seasonal pumping affects the equipotential contours of regional water-table map. Information about the elevation of the top of the regional water table was compiled using existing data from nonpumping boreholes and some springs. Data representative of flow conditions in 2005–2006 were analyzed to create water-table maps. The results of this activity are discussed in Appendix B-2.0.

## **4.0 REGULATORY CRITERIA**

The interim measures work plan presented in this report was driven by a letter from NMED dated December 29, 2005, that required preparation and implementation of an interim measures work plan (NMED 2005, 091683). This requirement was made pursuant to Section VII.B.2 of the Consent Order in response to the Laboratory's notification on December 23, 2005 (sent by email), of chromium above state and U.S. Environmental Protection Agency (EPA) groundwater standards in regional aquifer well R-28.

Groundwater cleanup levels are specified in Section VIII.A of the Consent Order. In general, the Consent Order requires groundwater cleanup levels to be based on existing standards when they are available and when their use is protective of current and reasonably expected exposures. These standards include the New Mexico Water Quality Control Commission (WQCC) groundwater standards and federal maximum contaminant levels (MCLs) adopted by EPA. If both a WQCC standard and MCL exist for a contaminant, the Consent Order requires the lower of the two to be used as the groundwater cleanup level.

The concentrations of chromium in groundwater that are presented in this report are compared with both the WQCC groundwater standard and the MCL. The WQCC human-health standard for chromium in groundwater is set at 50 µg/L as described in New Mexico Administrative Code 20.6.2.3103, and it is applied to the dissolved portion of the contaminant. In the case of the chromium contamination, the data indicate that the entire measured concentrations are in the dissolved hexavalent phase.

The MCL, which applies to drinking water, is 100 µg/L and is considered protective of potential health effects. According to information on EPA websites, the MCL has also been set at 100 µg/L because EPA believes, given present technology and resources, this is the lowest level to which water systems can reasonably be required to remove this contaminant if it occurs in drinking water.

## **5.0 INVESTIGATION RESULTS**

This section summarizes the results of the interim measures investigation of chromium contamination in groundwater. The discussion focuses on the sources, nature and extent, and fate and transport of chromium contamination in the Sandia, Los Alamos, and Mortandad watersheds. Particular emphasis is placed on chromium distributions and transport in Sandia Canyon because it is identified as the largest source of chromium released by the Laboratory, and it is the likely source of contamination observed in regional groundwater monitoring wells R-11 and R-28. The results presented in this section form the basis of the physical system conceptual model discussed in Section 6.0.

The following discussion is divided into five sections. Section 5.1 presents the results of a water-balance study that evaluated spatial and temporal trends of surface water loss in Sandia Canyon. Section 5.2 describes the extent of alluvial groundwater in Sandia Canyon. Section 5.3 provides preliminary information on gradients and flux rates in the alluvial groundwater system determined from nested piezometers. Section 5.4 describes the distribution of moisture including perched-intermediate groundwater in Sandia Canyon based on new drilling. Section 5.5 discusses the spatial and temporal trends for contaminants in surface and alluvial water in Sandia Canyon; in pore water and solid core samples from Sandia, Los Alamos, Mortandad, and Ten Site Canyons; and in perched-intermediate and regional groundwater beneath Sandia, Los Alamos, and Mortandad Canyons. Together, the data presented in Sections 5.0 are used to identify contaminant sources and to understand contaminant transport away from the source areas.

The discussion in this section is supported by presentation of more detailed information about investigation methods and topical discussions about components of the hydrogeologic and geochemical system in Appendix B. Appendix B-1 describes the results of drilling investigations in Sandia Canyon including installation of alluvial wells and piezometers, collection of contaminant profiles from core holes, and installation of a perched-intermediate well. Appendix B-1 also contains a discussion of the relationship between core moisture and borehole conductivity and surface-based resistivity measurements. Appendix B-2 provides an analysis of regional water-level data and discusses potential impacts of pumping at supply wells on flow and transport.

Data used to support interpretations about trends in hydrologic conditions and contaminant distributions are presented in Appendix C-1 (surface water chemistry data), C-2 (groundwater chemistry data for Sandia Canyon), C-3 (pore water and acid-soluble analyses for new core), C-4 (acid-soluble analyses for archival core), C-5 (perched-intermediate and regional groundwater chemistry data), C-6 (regional aquifer water-level data), C-7 (nested piezometer water-level data), and C-8 (analytical data packages).

In the following discussion, metric units are generally used, followed by English units. However, some data such as transducer data for piezometers and streamflow-gage data were collected and reported in English units (feet and acre-feet, respectively). Because of the voluminous nature of these data, the original units are maintained in some graphs and tables.

## 5.1 Surface Water Loss in Sandia Canyon

This section summarizes results from investigations of potential surface water loss in Sandia Canyon that were conducted as part of implementation of the “Interim Measures Work Plan for Chromium Contamination in Groundwater” (LANL 2006, 091987). Investigations focused on potential water loss in two areas with perennial surface water supplied from effluent discharges: the Sandia wetland (reach S-2 of Katzman 2000, 064349) and an approximately 3.5-km (2.2-mi) section of canyon east of the wetland. The Sandia wetland is in a broad, relatively low gradient area that occurs upcanyon of exposures of resistant unit Qbt-2 of the Bandelier Tuff (Gardner et al. 1999, 063492). Down to the west, splays of the Rendija Canyon fault also cross Sandia Canyon in this area. The downcanyon investigation area is steeper and has a narrower canyon bottom where the stream first incises through unit Qbt-2 and then through the less resistant, underlying units Qbt-1v and Qbt-1g (Gardner et al. 1999, 063492; Lavine et al. 2003, 092527). Drainage areas are 234 acres (0.95 km<sup>2</sup>) and 825 acres (3.34 km<sup>2</sup>) above the lower ends of the two investigation areas.

Potential water loss through the Sandia wetland was evaluated by comparing discharge records from outfalls at TA-03 with flow measured at the E123 surface water gaging station (e.g., Shaull et al. 2006, 093735), located immediately east of the wetland. The locations of outfalls and gages are shown in Figure 2.0-1. This comparison was made for water year 2006 (WY06) October 2005 through September 2006 to allow examination of potential seasonal variations in water loss. Outfall discharge data for each month in WY06, obtained from the Laboratory’s Environmental Stewardship–Resource and Conservation and Recovery Act group, are presented in Table 5.1-1. A continuous record of gage data for E123 was used in the assessment. Outfall and gaging station data were compared during 12 time periods of 5 to 14 days with no significant precipitation during and 2 days before to avoid uncertainties in discharge that might be associated with stormwater runoff. Data for these 12 time periods are shown in Table 5.1-2 and indicate estimated average daily losses of up to 0.45 acre-ft between the outfalls and E123 caused by ET and/or infiltration from alluvium into bedrock. Table 5.1-3 extrapolates the losses from these 12 time periods to the rest of WY06, providing an estimate of approximately 68 acre-ft of annual loss, which is 16% of the total WY06 outfall discharge of 426 acre-ft. This may be an underestimate of combined losses from ET and infiltration into underlying bedrock because some of the discharge measured at E123 may represent slow drainage of stormwater that had previously infiltrated into alluvium in the wetland.

Constraints on potential ET in this area can be made using evaporation pan data from the region and relations between pan data and ET as provided in the literature. For March through November, average pan loss is 62.3 in. over a 21-yr period at a station in Santa Fe at a similar elevation as the Sandia wetland (station 8072; 7205-ft elevation; data from 1951 to 1971, downloaded from [http://weather.nmsu.edu/Pan\\_Evaporation/](http://weather.nmsu.edu/Pan_Evaporation/)), which is equivalent to 28.5 acre-ft over an area of 5.5 acres (22,215 m<sup>2</sup>, the area of reach S-2). The relation of ET to pan evaporation rates varies with vegetation, but ET is generally lower (e.g., Dunne and Leopold 1978, 084459, pp. 128–129), indicating that potential ET should be less than 28.5 acre-ft. Experimental studies using cattails also indicate rates of ET less than pan evaporation (e.g., Kirkpatrick 2005, 094133, p. 41, ET ~75% of pan evaporation). Net ET is further reduced by plant utilization of precipitation. Potential ET is therefore significantly less than the calculated loss between the outfalls and E123, indicating infiltration from the alluvium into bedrock. Assuming total ET of 14-20 acre-ft/yr (50%–70% of pan evaporation rates) for reach S-2, including both cattail and noncattail areas, and assuming 68 acre-ft of total loss, yields an estimated 48–54 acre-ft of water loss into bedrock in WY06, or 11%–13% of the total outfall discharge volume.

The accuracy of the rating curve for the E123 gaging station during periods with no stormwater runoff was confirmed using measurements at a portable 6-in. Parshall flume that was collocated with E123 for a 7-day period in October 2006. Water level (stage) in the Parshall flume was recorded with a Milltronics

ultrasonic level monitor. A photograph of the Parshall flume adjacent to E123 is shown in Figure 5.1-1. The accuracy of Parshall flumes is  $\pm 3\%$  (Dodge 1990, 094146, p. 3), and total flow measured at the flume from October 22 to October 27 (3.42 acre-ft) was within 1% of flow estimated using the E123 rating curve (3.38 acre-ft). Figure 5.1-2 shows a comparison of hydrographs obtained using the Parshall flume and the E123 rating curve.

Potential water loss along the ~3.5 km (2.2 mi) of canyon below the Sandia wetland was evaluated by comparing discharge records from the E123 surface water gaging station with discharge estimated at a temporary gaging station, E123.5, installed as part of this investigation. Station E123.5 is located between two boulders where flow drops into a small pool, in an area with perennial effluent-derived flow upcanyon of where the canyon bottom widens and alluvium thickens. The canyon bottom here is narrow, incised into Bandelier Tuff unit Qbt-1g and bounded by bouldery colluvium, with little opportunity for underflow within the alluvium. A photograph of gaging station E123.5 is shown in Figure 5.1-3. Stage height was measured with a transducer and calibrated between September 27 and October 4, 2006, with a 6-in.-Parshall flume installed immediately above the transducer location. Transducer readings were also calibrated with field measurements of water depth. The resultant rating curve is shown in Figure 5.1-4. A comparison of estimated discharge at E123 and E123.5 for 23 days within the period between October 6 and November 8, 2006, is shown in Table 5.1-4 and indicates a reduction in flow between these stations due to infiltration into the subsurface. A comparison of hydrographs obtained at E123 and E123.5 for the period October 17 to October 23 is shown in Figure 5.1-5. Total flow during the 23-day period is estimated as 23.19 acre-ft at E123 and 14.96 acre-ft at E123.5 for a 35% loss along the intervening portion of Sandia Canyon. An uncertainty of  $\pm 10\%$  is estimated for the discharge at E123.5, which is much less than the calculated water loss and indicates some infiltration into bedrock between E123 and E123.5.

Flow is ephemeral at the next downcanyon gaging station, E124 (Shaull et al. 2006, 093735), located approximately 0.9 km (0.6 mi) downcanyon from E123.5, and indicates complete infiltration of the remaining effluent into alluvium in this reach. Only stormwater, estimated as about 19% of the total flow in WY06 (based on data from E123), extends downcanyon past E124 in some events.

## 5.2 Extent of Alluvial Groundwater as Determined from Drilling

Alluvial saturation, or saturation in shallow bedrock beneath alluvium, was encountered during drilling at several of the AHF holes (SC series) drilled in Sandia Canyon during July–August 2002 (Kleinfelder 2002, 91687) and in several of the SCC-series holes and all of the SCA-series and SCP-series holes drilled for this investigation report. Details of water encountered during drilling of the SCC and SCA holes are provided in Appendix B-1.1; notes on occurrences of water in the SC drill holes, with revised stratigraphy, are provided in Appendix Table B-1.1-1. Tables 5.2-1a–c summarize the depths below ground surface and elevations of first occurrence of water, or absence of shallow groundwater, as observed in the SC, SCC, and SCA drill holes.

It was known at the start of this project that alluvial storage and saturation would be significant along Sandia Canyon where it broadens by lateral incision into the weaker, nonwelded base of the Tshirege Member of the Bandelier Tuff (i.e., to the east of SCA-2). As a result of this project, it is evident that the alluvium in this broader portion of the canyon is typically ~15–21 m (~50–70 ft) thick near the present canyon axis; however, lateral variations in alluvium thickness and transitions in the nature of the underlying bedrock from Tshirege unit Qbt 1g, to the Cerro Toledo Interval, and finally to Otowi ash flows, indicate potentially complex and localized recharge through the alluvium into the deeper vadose zone. A notable result of the drilling investigations conducted for this project is the determination that saturation in the alluvium, under present conditions, extends eastward to a point between SCA-5 and SCC-6 (Figure 5.2-1).

Observations from closely spaced holes indicate that saturation may extend laterally from the alluvium along specific suballuvial stratigraphic boundaries, such as the Qbt 1g/Qct contact (see Appendix B.1-6). Thus, some of the holes listed in Tables 5.2-1a and 5.2-1b indicate encounters with shallow perched water not in the alluvium but in immediately underlying units such as nonwelded vitric Tshirege (Qbt 1g) and the Cerro Toledo Interval (Qct). These very shallow occurrences of saturation in bedrock are considered to be connected with and part of the alluvial groundwater system.

Figure 5.2-1 compares the extent of alluvial saturation as observed in Mortandad Canyon with the extent of alluvial or shallow suballuvial saturation observed in Sandia Canyon. The extent of shallow saturation in Sandia Canyon is based on the data from Tables 5.2-1a–c; the extent of alluvial saturation in Mortandad Canyon is as described in the “Mortandad Canyon Investigation Report” (LANL 2006, 094161). As in Mortandad Canyon, the canyon bottom widens, and alluvial volume and depth increase where canyon incision passes through the vitric, nonwelded lower section of the Tshirege Member; in Sandia Canyon this widening and deepening occur east of SCA-2. The measured extent of alluvial saturation in Sandia Canyon extends ~1 km (0.6 mi) farther east than the alluvial saturation in Mortandad Canyon. Alluvial saturation in Sandia Canyon is shown as narrowing beyond SCA-4 to honor the lack of evidence for shallow saturation at SC-4, SCC-5, R-11, and SC-5; alternatively, shallow saturation may be wider but discontinuous in this region.

Observations of water during drilling of alluvial boreholes were used to determine screen depths in alluvial well design and to design the piezometer sets located near SCA-3 (piezometers SCP-2a and SCP-2b) and SCA-4 (nested piezometers SCP-1a, b, c). Details of relative screen depths and of well and piezometer design are shown in Appendix B-1.6. Full stratigraphic summaries for all of the SCA, SCP, and SCC holes with drilling information are in Appendix B-1.6 (on CD).

Transducers have been used to monitor water levels in all of the alluvial wells and piezometers. Initial transducer data were collected hourly, with some interruptions, over a period of 25 days from mid-October to mid-November 2006. Manual measurements of depth to water were collected to verify transducer function. Further data will be obtained to monitor flow events and seasonal variability; the October–November 2006 data collected before the preparation of this report are in Appendix C-7 (on DVD). Preliminary temporal trends discussed briefly here. The following section (Section 5.3) provides a more detailed analysis of head values, vertical gradients, and seepage velocities derived from the transducer data in the SCP holes (piezometers).

Transducer data for SCA-1 are not yet analyzed, pending acquisition of data from a vented system. Transducer data at SCA-2 are plotted in Figure 5.2-2. The alluvial well at SCA-2 was designed with a screen across the top of saturation (2053.3-m [6736.7-ft] elevation) observed when the drill hole was hand augered. Cycles of water level at SCA-2 fluctuate with streamflow events along the adjacent stretch of Sandia Canyon; the approximately diurnal cycle seen at SCA-2 reflects daily (generally weekday) discharges into upper Sandia Canyon from facility operations (see Section 5.1).

Figure 5.2-3 summarizes transducer data collected from the alluvial wells and piezometers farther downcanyon in reaches beyond gaging station E-124, where the canyon widens and alluvial accumulation is thicker. No data are shown for alluvial well SCA-3 because water levels fell significantly below the 2039.8-m (~6692.4-ft) elevation observed during drilling to an elevation of ~2038.8 m (~6689 ft) (base of the screen at SCA-3 is at 2039.3-m [6690.7-ft] elevation; see Appendix B-1.6). However, piezometers SCP-2a and SCP-2b just east of SCA-3 provided continuous transducer data for the October–November 2006 period considered here. Water levels peaked between October 20th and 21st but declined steadily thereafter. The transducer curves for these piezometers and for all of the alluvial wells and piezometers farther east differ significantly from those in the narrower canyon to the west in that

no diurnal cycle is observed. Apparently, the increased storage volume of alluvium in the wider canyon damps out these fluctuations. Also notable in the comparison of SCP-2a and SCP-2b is the 0.7-m (~2.3-ft) head difference between the higher piezometer (red curve) and the lower piezometer (blue curve), suggesting significant downward flow into suballuvial horizons (see Section 5.3).

The middle panel of Figure 5.2-3 summarizes the October–November 2006 transducer data for SCA-4 and the three nearby nested piezometers, SCP-1a, b, and c. An early peak water level followed by continuous decline is also observed at this site. The peak water-level measurement before decline is observed in the SCA-4 data on about October 15th, 5 days before the decline began at SCP-2a, b. A similar trend is observed in the alluvial well farthest east, SCA-5, although here the transducer record appears to have begun after peak water level was reached, and peak saturation predates October 12th. When considered together, the three localities summarized in Figure 5.2-3 suggest an alluvial system where recent recharge by late summer rainstorms has increased the late-October saturated thickness at SCP-2a, b, whereas the damping effect of alluvial dispersion pushes the decline from summer peak saturation to earlier dates in the eastern part of the system.

### **5.3 Results from Nested Piezometers**

Nested piezometers were installed at two locations for the purpose of investigating vertical gradients and seepage velocities in the alluvium. Piezometer nest SCP-1 consists of three piezometers installed in a single borehole with bentonite seals placed between their screens to isolate them hydraulically from each other. Piezometer nest SCP-2 consists of two piezometers installed in separate boreholes located 1.7 m (5.5 ft) apart (see Appendix B-1.6). Each piezometer consists of a 1-in. (2.5-cm) I.D. PVC tube with a prepacked 15.2-cm (0.5-ft) long 0.25-mm (0.01-in.) slotted screen. Within each nest, each piezometer's screen was set at a specific depth within the saturated alluvium. At SCP-1, the screen-bottom depths were 11.7 m (38.3 ft), 12.2 m (39.9 ft), and 12.7 m (41.7 ft) for the SCP-1a, SCP-1b, and SCP-1c piezometers, respectively. At SCP-2, the screen-bottom depths were 13.7 m (45.0 ft) and 15.2 m (50.0 ft) for the SCP-2a and SCP-2b piezometers, respectively.

Pressure transducers were installed in each piezometer to record water levels in the alluvial aquifer. Water-level readings were recorded at hourly intervals. Hydrographs showing preliminary water-level data collected during October–November 2006 along with screen-bottom elevations are provided in Figures 5.3-1 and 5.3-2. At SCP-1, water levels declined by approximately 36.6 cm (1.2 ft) during the initial observation period, which occurred during a generally dry period following a wet summer rainy season. Relative pressure-head relationships between each piezometer at SCP-1 were consistent during this time, aside from the fact that the alluvial saturation level dropped below the screen at SCP-1a on October 21. The highest water levels were recorded in SCP-1c, the deepest piezometer, indicating a consistent upward gradient at this location. However, the water levels in SCP-1a were higher than those recorded in SCP-1b, indicating a downward gradient within the SCP-1a to SCP-1b interval. A consistent pressure head differential of about 76.2 cm (2.5 ft) between the SCP-2a and SCP-2b piezometers shows a strong downward gradient at this location.

Vertical seepage velocities were computed from the piezometer data using the following equation applying Darcy's law:

$$v_z = \frac{K}{n_e} \frac{dh}{dz}$$

Where

$v_z$  is the vertical seepage velocity,

$K$  is the saturated hydraulic conductivity,

$n_e$  is the effective porosity, and

$dh/dz$  is the vertical gradient.

Hydraulic conductivity values were determined from slug tests performed in each piezometer. The results of the slug test analyses are shown in Table 5.3-1. Detailed descriptions of the slug tests are provided in Appendix B-1.6.

The aquifer material in SCP-1 was described as well-sorted coarse sand with 95% to 100% sand and 0% to 5% silt. The same lithology was described for all three screened intervals in this piezometer nest. The reported hydraulic conductivity values are generally similar and consistent with literature reported values for coarse sand. The aquifer material in SCP-2 was described as silty, clayey sand with 70% fine to coarse sand and 30% silt/clay. The same lithology was described for both screened intervals in this piezometer nest, even though reported hydraulic conductivity values vary by 2 orders of magnitude. Representative literature reported values for silty sand range from  $10^{-3}$  to  $10^{-5}$  cm/s (Fetter 1994, 070942). Hydraulic conductivity values applied in the seepage velocity computations for SCP-1 were the averages of the bounding screens for each interval. The hydraulic conductivity value applied for the SCP-2 computations was the lower value, determined from SCP-2b, since this value falls within the reported range of literature values, and attempting to use the average of the reported slug test results from SCP-2a resulted in unreasonably high computed seepage velocities. A representative porosity value of 0.41 for coarse sand alluvium was assumed for the SCP-1 computations, while a representative porosity of 0.34 for clayey silt was assumed for SCP-2 (Spitz and Moreno 1996, 085503, p. 343).

Time-varying vertical gradients and computed seepage velocities are shown in Figures 5.3-3 and 5.3-4 for piezometer sets SCP-1 and SCP-2, respectively. In these graphs, a positive gradient and seepage velocity represents a downward component of groundwater flow while a negative value represents an upward component of flow. At SCP-1, the SCP-1a to SCP-1b interval exhibited downward vertical gradients ranging from about 0.02 to 0.09 with associated vertical seepage velocities ranging from about 12 to 61 cm/day (0.4 to 2 ft/day). However, the SCP-1b to SCP-1c interval exhibited upward vertical gradients ranging from about 0.13 to 0.18 with associated upward seepage velocities ranging from about 116 to 155 cm/day (3.8 to 5.1 ft/day). At SCP-2, the SCP-2a to SCP-2b interval exhibited consistently strong downward vertical gradients ranging from about 0.51 to 0.53 with associated vertical seepage velocities ranging from about 46 to 49 cm/day (1.5 to 1.6 ft/day). This represents an annual average rate of infiltration loss from the base of the alluvium of about 172.5 m/yr (566 vertical ft/yr) at this location.

These results reflect a preliminary analysis of a relatively short period (less than 4 weeks) of data collection following a wet rainy season. Thus, the observed conditions may not be representative of longer-term trends. The piezometer nests will continue to be monitored, and future reporting will provide assessments of the longer period of record.

## 5.4 Suballuvial Moisture Occurrences

The only perched-intermediate groundwater observed as part of this investigation occurs as water stored in Puye sedimentary deposits above relatively impermeable weathering and soil zones at the top of the Cerros del Rio lavas. The saturated zones in the SCC-series holes are summarized in Figure 5.4-1, which places these holes in west-to-east relation by relative elevation. Similar to the alluvial system, water storage above the Puye/Cerros del Rio contact extends only as far downcanyon as the vicinity of SCC-4. The perched-intermediate groundwater is generally thicker between holes SCC-4 and SCC-1. The gradient within the perched system includes a westward component that parallels the contact between the Puye Formation and the Cerros del Rio lavas.

Figure 5.4-1 also shows core-derived moisture contents plotted against stratigraphy for all of the SCC-series holes. Included with the six SCC-series holes in Figure 5.4-1 is the moisture profile obtained from comparable core samples taken at the R-11 phase 1 core hole, superimposed on the combined magnetic resonance (CMR)-calculated saturation obtained at the adjacent phase 2 drill hole by Schlumberger (Kleinfelder 2005, 094154). Figure 5.4-1 illustrates relatively consistent increased moisture content near the Qbt 1g/Qct contact in all three SCC-series holes where this contact was present (SCC-2, SCC-3, and SCC-4). This rise in moisture at the Qbt 1g/Qct contact is not necessarily associated with actual saturation, but it may indicate that this horizon is susceptible to vadose-zone water movement in periodic wetting cycles. A second, deeper horizon of high core moisture content is observed in the Guaje Pumice Bed (Qbog) in SCC-1 through SCC-5, but comparable Guaje saturation is not present at R-11 and is only poorly developed at SCC-6. This observation is in accord with the occurrence of sub-Guaje perched water in the western set of SCC holes.

The data from R-11 (Figure 5.4-1) are informative because they provide a core-derived moisture profile that can be compared with the CMR-calculated saturation profile in an adjacent hole. The CMR-calculated saturation in the colluvial section (Qc) is higher than in the underlying Otowi ash flows, yet the core moisture in the middle of the colluvium is low. This discrepancy is likely the result of intact core obtained from a block of tuff within the colluvium rather than from the matrix seen by the CMR tool. Note that the core sample from the top of the colluvium does have a high moisture content (unfortunately, this horizon was behind casing when the CMR tool was run, so comparable CMR saturation could not be calculated). A more direct comparison can be made at the bottom of the R-11 moisture profile in the Guaje Pumice Bed (Qbog). Even though the moisture content here does not rise as sharply as in the Guaje Pumice Bed at holes SCC-2 to SCC-5, the calculated saturation in the pumice bed is significantly higher than in the overlying Otowi ash flows. Although there are inherent uncertainties in the calculation of saturation from CMR logs (e.g., porosity allocation to magnetic resonance properties in particular units), the R-11 data illustrate the large saturation effects that even small amounts of moisture increase can have. Such a situation may be poised at a moisture content where even small water influxes could lead to transient saturation and enhanced vadose-zone flow.

Moisture profiles through the Otowi ash flows in the section of Sandia Canyon from SCC-1 to SCC-6 are not always smooth. Recently obtained moisture profiles from Mortandad Canyon also indicate that moisture distribution in the Otowi can be highly variable, and it is likely affected by small variations in the ash-flow matrix properties of this otherwise massive and homogeneous, poorly fractured unit (LANL 2006, 094161). On average, however, the moisture contents in the Otowi ash flows beneath Sandia Canyon are highest (>20%) in the canyon section from SCC-2 to SCC-4 and lower (<20%) to the west (SCC-1) and east (SCC-5 to SCC-6). These relationships are summarized in Figure 5.4-2. Given the observation from R-11 cited above that small amounts of moisture increase may lead to greatly increased saturation, this distribution of moisture in the Otowi may indicate that the likeliest pathways from the alluvial system through the Otowi are centered in the stretch of canyon from SCC-2 to SCC-4.

As discussed in Section 5.3, the piezometer set at SCP-2a, b, with strong evidence of downward flow, is adjacent to deeper borehole SCC-2, which is the SCC borehole with the highest moisture content in the

underlying Otowi ash flows (Figure 5.4-2). Although the variability of moisture measurements in the Otowi ash flows can be large in specific drill holes, moisture data from all SCC holes and from R-11 supports the hypothesis that infiltration from alluvium into underlying bedrock units may be concentrated in the portion of Sandia Canyon between SCC-2 and SCC-4. Future data from the piezometers sets at SCP-2a, b, and SCP-1a–c will provide some of the data needed to test this hypothesis.

## 5.5 Contaminant Distributions

This section describes analytical results for the primary chemicals present in the TA-03 power plant cooling tower discharges including chromium, molybdenum, phosphate ( $\text{PO}_4^{3-}$ ), and zinc. Sections of this report that follow describe the nature and extent of these chemicals in water and core. For each chemical, its current distribution is described, and time histories are presented to illustrate the evolution of the chemical in the environment.

The following format is used to describe chemical distributions in hydrogeologic media (core samples), surface water, unsaturated zone pore water, and groundwater.

Contaminant depth profiles of chromium, molybdenum, phosphate, and zinc show concentrations as a function of core-hole depth for pore water, obtained by deionized water leachate, and for metals-trace elements associated with solid phases, determined from EPA 3050 digestion (acid leach), in core.

- Time series concentrations for chromium are presented for some perched-intermediate zones, and contaminant trends for these groundwaters are discussed.
- Time series plots of total dissolved chromium concentration trends are shown for the regional aquifer, and contaminant trends for these groundwaters are discussed.

The following discussion and supporting plots presented in this section provide information about the spatial and temporal distributions of chromium in key areas of the Sandia, Los Alamos, and Mortandad watersheds. Additional plots in Appendix C provide an overview of the spatial trends of acid soluble and pore-water concentrations of dissolved chromium in the unsaturated zone beneath Sandia Canyon. Distributions of acid-soluble chromium in core holes (termed “archival core”) previously drilled in the Los Alamos, Mortandad, and Sandia watersheds are presented in Plate 1.

### 5.5.1 Chromium

Concentrations of total dissolved chromium in groundwater are compared with background ranges (LANL 2005, 090580) to evaluate the origin of this trace metal within alluvial and perched groundwater and the regional aquifer. Chromium is stable in the +III and +VI oxidation states in aqueous solution, in which chromium(VI) is the soluble form of this metal (Rai and Zachara 1986, 091684). Chromium(III) is associated with minerals and volcanic glass comprising aquifer material and suspended particles in surface water and groundwater samples, whereas dissolved chromium is largely chromium(VI) (LANL 2006, 091987). Anthropogenic chromium is detected in surface water, alluvial and perched-intermediate groundwater, and/or the regional aquifer beneath Mortandad and Sandia Canyons. This section describes the distributions of total chromium in core samples, surface water, alluvial and perched-intermediate groundwater, and the regional aquifer.

#### 5.5.1.1 Chromium in Surface Water and Alluvial Groundwater Chemistry

Figure 2.0-1 shows the locations of surface water gaging stations, core holes, and wells discussed in this section. Appendix C-1 provides analytical results for surface water samples collected within the Sandia

watershed. Present-day effluent from the TA-03 cooling towers does not contain chromium(VI) (see Section 2, Table 2-0.1). At the head of Sandia Canyon west of the wetland near gaging station E122 (Figure 2.0-1, Appendix C-1), concentrations of total dissolved chromium in surface water (8.2 and 9.2 µg/L) are higher than those at gaging station E123 east of the wetland (2.5 to 5.3 µg/L). Concentrations of chromium(VI) were 9.2 µg/L in two surface water samples (one filtered and one nonfiltered) collected at gaging station E122 (Appendix C-1). This indicates that surface water mobilizes chromium(VI) from a residual chromium source in sediments west of the wetland and that much of this dissolved chromium is removed from the surface water as it passes through the wetland. At gaging station E123, concentrations of total chromium (10 to 261 µg/L) in nonfiltered samples are elevated relative to the filtered samples (Appendix C-1). This observation suggests that the nonfiltered samples contain chromium(III) adsorbed onto suspended material. The suspended material may largely consist of solid organic matter transported from the wetland and coatings of ferric (oxy)hydroxide and/or clay minerals based on measured concentrations of iron and aluminum in nonfiltered, surface water samples.

At the terminus of persistent surface water base flow in Sandia Canyon below gaging station E123.5, concentrations of total chromium are similar in both filtered (9.7 µg/L) and nonfiltered (11.7 µg/L) samples (Appendix C-1), suggesting that chromium(VI) dominates at this location. The increase of chromium(VI) in surface water between gaging station E123 and the terminus of surface flow suggests that surface water mobilizes chromium(VI) from contaminated sediments downcanyon of the wetland.

Maximum, mean, and median groundwater background concentrations of dissolved chromium are 5, 1.3, and 1 µg/L, respectively, within alluvial groundwater (LANL 2005, 090580). Alluvial wells SCA-1 and SCA-5 were sampled on October 16 and 11, 2006, respectively, and analytical results for these two wells are presented in Appendix C-2. The results from the three other wells (SCA-2, SCA-3, and SCA-4) will be delivered to NMED when they become available. Wells SCO-1 and SCO-2 previously drilled in Sandia Canyon were dry during the times of sampling. At SCA-1, chromium concentrations in filtered and nonfiltered samples were 2.8 and 10.7 µg/L (Appendix C-2), respectively, suggesting that chromium(III) is associated with suspended particles within the wetland. At SCA-5, average concentrations of total chromium in two filtered and two nonfiltered samples were 9.7 and 13.5 µg/L (Appendix C-2), respectively, suggesting that chromium(VI) dominates.

### 5.5.1.2 Chromium in Vadose Zone

Six core holes were drilled in Sandia Canyon for the current study and designated as SCC-1 through SCC-6 (Figure 2-0.1). Core samples were analyzed for chromium and other constituents using both deionized water leaching and the EPA 3050 digestion method, which is referred to as the acid-soluble (digested) fraction. Analytical results for core samples digested by the EPA 3050 method are reported in units of milligrams per kilograms and are provided in Appendix C-3. Pore-water concentrations of analytes are reported in units of milligrams per liters, which is considered to be equivalent to parts per million for solutions having a TDS content less than 1000 and a solution density of 1 g/mL or 1 g/cm<sup>3</sup>. Collocated core samples leached with deionized water provide pore-water concentrations of soluble or dissolved chromium and other solutes. Analytical results for pore-water solutes are provided in Appendix C-3. Figure 5.5-1 shows acid-soluble chromium and pore-water chromium as a function of depth and stratigraphy. The pore-water concentrations of dissolved chromium are much lower than solid-bound chromium at the six boreholes (note the different concentration scales). Appendix Figures B-1.7-1 through B-1.7-6 show distributions of both fractions of chromium at each core hole using a logarithmic concentration scale to emphasize details in the variation of pore-water concentrations of chromium.

Maximum concentrations of dissolved chromium in pore water increase with depth from SCC-1 to SCC-5, possibly showing the distribution of residual chromium left by recharge through the subsurface beneath

Sandia Canyon. A single background upper tolerance limit (UTL) was established for acid-soluble chromium in Tshirege Member unit Qbt 1g, Cerro Toledo deposits, and the Otowi Member because of the geochemical similarity of these units (Ryti et al. 1998, 059730). These combined units have a mean background concentration of 0.9 mg/kg, a median of 0.81 mg/kg, and a UTL of 2.6 mg/kg. Potential anthropogenic chromium was identified in the SCC samples at concentrations slightly exceeding the background UTL for the Bandelier Tuff-Cerro Toledo interval (Ryti et al. 1998, 059730) at SCC-1 through SCC-6. Core samples from the alluvium at SCC-1 through SCC-6 contained chromium concentrations slightly greater than the background UTL for this unit. The background UTL for chromium is 10.5 mg/kg in sediments, including the alluvium in Sandia Canyon which largely consists of weathered Bandelier Tuff (Ryti et al. 1998, 059730). Core samples from the Guaje Pumice Bed at SCC-2, SCC-3, and SCC-6 contained acid-soluble chromium concentrations significantly greater than the background UTL for the Bandelier Tuff and Cerro Toledo interval.

Chromium(III) dominates in the core samples based on higher concentrations of acid-soluble chromium in comparison to pore-water chromium. Sporadic concentrations of elevated chromium occur within the alluvium, Tshirege Member unit Qbt 1g, Cerro Toledo interval, Otowi Member, and/or Guaje Pumice Bed. The highest concentration of acid-soluble chromium (38.3 mg/kg) was detected in core collected at SCC-3 within the depth interval from 101 to 103 m (332 to 339 ft) within the Cerros del Rio basalt (Figures 5-5.1 and C-3.3). This could result from natural chromium concentrated within iron and magnesium-rich minerals comprising the basalt. Iron and magnesium were also concentrated in the partly digested sample at 2.54 and 4.37 weight percent (wt %), respectively (Appendix C-3). Appendix Figures B.1-7-7 through B.1-7-12 show acid-soluble concentrations of iron and chromium within the different hydrostratigraphic units including the alluvium, Bandelier Tuff, Cerro Toledo interval, Puye Formation, and Cerros del Rio basalt. The Cerros del Rio basalt contains the highest concentrations of chromium, likely associated with iron-rich volcanic glass, oxides, and silicate minerals.

Concentrations of TOC coating the core samples ranged from 0.00365 wt % (36.5 mg/kg) at SCC-1 to 0.223 wt % (2230 mg/kg) at SCC-5 (Appendix C-3). Based on the small concentrations of solid-bound TOC, it is unlikely that any appreciable amounts of chromium(VI) were reduced to chromium(III) within the unsaturated zone beneath Sandia Canyon at the SCC core holes. The reduction of chromium(VI) (as  $\text{CrO}_4^{2-}$ ) to  $\text{Cr}(\text{OH})_3$  by solid organic matter, consisting of humic substances containing hydroquinone ( $\text{C}_6\text{H}_6\text{O}_2$ ), a redox-active functional group (McBride 1994, 058947), requires that there are 3 moles of hydroquinone to every 2 moles of chromate. A discussion on the reductive capacity of solid organic matter is provided in Section 5.5.1.5, Chromium Geochemistry.

It is most likely that a large but unknown quantity of chromium(VI) previously migrated through the upper 122 m (400 ft) of the vadose zone in Sandia Canyon because elevated concentrations of other mobile chemicals such as molybdenum used more recently than chromium at the cooling towers at the TA-03 power plant (Table 2-1) are present in the subsurface. Detectable pore-water concentrations of dissolved chromium extracted from the SCC core holes by deionized water leaching ranged from 0.003 to 1.329 mg/L, with the highest value observed in SCC-2 alluvium (Appendix C-3). Chromium concentrations less than analytical detection in pore water occurred in 50% of the samples, with instrument detection limits (IDLs) ranging from 0.003 to 0.024 mg/L using inductively coupled plasma-mass spectrometry (ICP-MS) at the Hydrology, Geochemistry, and Geology (EES-6) analytical laboratory (Appendix C-3). In all but one sample (collected from 6- to 7-m [20- to 24-ft] depth at SCC-2), dissolved concentrations of chromium in pore water were up to 3 orders of magnitude less than acid-soluble chromium (Figures 5-5.1 and Appendix Figures B-1.7-1 through B-1.7.6). Usually, both fractions correlate with each other in the samples, suggesting that equilibrium occurs between dissolved chromium and the solid phase(s) either through adsorption or precipitation. Under acidic pH conditions,  $\text{CrO}_4^{2-}$  and  $\text{HCrO}_4^-$  adsorb onto ferric (oxy)hydroxide to a greater extent than under alkaline pH conditions (Rai et al. 1987,

091686; Rai and Zachara 1986, 091684) that are characteristic of the unsaturated pore water beneath Sandia Canyon. Pore-water pH values ranged from 7.13 at SCC-1 to 8.98 at SCC-6 (Appendix C-3), supporting the hypothesis that most of the chromium(VI) migrating through the upper vadose zone beneath Sandia Canyon remained mobile.

Distinguishing anthropogenic from natural chromium is not entirely conclusive with the available chemical data obtained from the core holes. Guidelines are presented to help differentiate between sources of chromium in the unsaturated zone based on concentration data and on the similar distributions of chromium(III), associated with solids and dissolved chromium, and chromium(VI), in pore water. If acid-soluble chromium, dominantly occurring as chromium(III), is within background concentrations and both fractions correlate with each other, then pore-water chromium most likely represents natural chromium(VI) in equilibrium with the solid. If concentrations of acid-soluble chromium exceed background for a particular host rock or soil, then it is reasonable to assume that pore-water chromium(VI) contains an unknown amount of anthropogenic chromium. This is the case for the dissolved chromium in pore water collected from SCC-1 at a depth of 12.2 to 12.7 m (40 to 41.5 ft) (Appendix Figure B-1.7-1) that contained 11.4 mg/kg acid-soluble chromium. Another example of the occurrence of anthropogenic chromium is where relatively high concentrations of pore-water chromium correlate with relatively low amounts of acid-soluble chromium. This is the case for a sample collected from SCC-5 at a depth interval of 49 to 50 m (160 to 163 ft) (Appendix Figure B-1.7-5). Using one or more of these criteria, residual anthropogenic chromium sporadically occurs within the alluvium at SCC-1 and possibly within the Cerro Toledo interval at SCC-4. Some anthropogenic chromium occurs within the Cerro Toledo interval at SCC-2, -3, -4, and -6, and also within the Otowi Member at SCC-1, -2, -3, -4, -5, and -6 (Figures 5-5.1 and Appendix Figures Bb-1.7-1 through B-1.7-6).

Archival core samples were analyzed for chromium and other constituents as part of this investigation to provide supplemental information about chromium distributions in Sandia Canyon and to evaluate the extent of chromium contamination in the upper vadose zone beneath Los Alamos, Mortandad, and Ten Site Canyons. The archival core samples were analyzed using the EPA 3050 digestion method to determine the fraction of acid-soluble chromium. Analytical results for chromium and other constituents measured on the archival core samples are presented in Appendix C-4.

As discussed above, most of the chromium determined by the EPA 3050 digestion method is probably in the form of relatively immobile chromium(III). Part of the acid-soluble chromium is leached from naturally occurring minerals such as trace iron oxides and pyroxenes in the rhyolitic Bandelier Tuff and Cerro Toledo interval; pyroxenes, amphiboles, and iron oxides in the dacitic sedimentary deposits of the Puye Formation; and olivine, pyroxene, and iron oxides of the Cerros del Rio basalt. Chromium-bearing minerals are more abundant in dacitic and basaltic rocks, and natural chromium background should be greater in these rocks compared with rhyolites. The archival core may also contain anthropogenic chromium that originated as chromium(VI) in pore water that was reduced to chromium(III) and precipitated from solution or was adsorbed onto ferric (oxy)hydroxide and clay minerals. The anthropogenic contribution to the EPA 3050 analytical results is identified by concentrations that exceed the background UTL for chromium within the Bandelier Tuff and Cerro Toledo interval.

A histogram showing the distribution of acid-soluble chromium background concentrations for samples used to establish the background UTL for the combined units Tshirege Member unit Qbt 1g, Cerro Toledo deposits, and the Otowi Member is presented in Figure 5-5.2. For comparison, Figure 5-5.2 also contains histograms showing acid-soluble chromium concentrations for core samples representing these same units in Los Alamos, Sandia, Mortandad, and Ten Site Canyons. Many of the core samples from Los Alamos, Sandia, and Mortandad Canyons contain acid-soluble chromium concentrations above the background UTL, indicating that anthropogenic chromium is present in the vadose zone in these three

canyons. Ten Site Canyon has few acid-soluble chromium concentrations above the background UTL, and in general it seems to contain relatively little chromium contamination.

Depth-concentration profiles for acid-soluble chromium were prepared for selected core holes in Los Alamos, Sandia, Mortandad, and Ten Site Canyons to determine the spatial distribution of chromium as a function of depth and position within the watersheds (Plate 1). In Los Alamos Canyon, the depth-concentration profiles show that exceedances of the background UTL for the Bandelier Tuff units are more frequent with increasing distance downcanyon of the chromium source at the former OWR site at TA-02 (see Section 2.0). The highest concentrations of acid-soluble chromium in the Bandelier Tuff units occur within the central part of the Otowi Member at core holes LAOI-3.2/3.2a (Plate 1). Elevated concentrations of acid-soluble chromium in the Bandelier Tuff continue downcanyon as far as R-8, but concentrations decline east of LAOI-3.2/3.2a. Where penetrated, the Puye Formation and Cerros del Rio basalt contain relatively greater concentrations of acid-soluble chromium compared with the overlying Bandelier Tuff units (Plate 1). Although higher concentrations of naturally occurring acid-soluble chromium are expected in these dacitic and basaltic rocks, identification of natural versus anthropogenic chromium cannot be determined because background values for deeper rock units have not been established.

Acid-soluble chromium concentration data for the new SCC core holes in Sandia Canyon are described in the section above. Additional archival samples from Sandia Canyon were analyzed for boreholes SC-2 through SC-5 and boreholes R-11 and R-12. The SCC and archival core data are shown together in Plate 1 so that all available data for each watershed can be compared in a spatial context. The distribution of acid-soluble chromium in Sandia Canyon shows few clear spatial patterns. There is a tendency for acid-soluble chromium concentrations to be greatest in the alluvium, but except for a few scattered exceedances of the alluvium UTL, this represents higher background in alluvium relative to the underlying bedrock tuffs. Cerro Toledo interval deposits, and to a lesser extent, the upper part of the Otowi Member, exceed the background UTL in the part of the canyon bracketed by core hole SC-3 (Plate 1). For most core holes, concentrations of acid-soluble chromium are generally below the background UTL in the lower Otowi Member. However, samples from the Guaje Pumice Bed at R-11 (and in SCC-2, SCC-3, and SCC-6 as noted above) contain acid-soluble chromium concentrations significantly greater than the background UTL, suggesting that preferential pathways or some retention of chromium may occur in this unit (Plate 1). The Puye Formation and Cerros del Rio basalt contain relatively greater concentrations of acid-soluble chromium compared with the overlying Bandelier Tuff units, but the presence or absence of anthropogenic chromium cannot be determined without comparison to background values.

Mortandad Canyon core data are characterized by generally sporadic occurrences of acid-soluble chromium concentrations above the background UTL for most boreholes. Like Sandia Canyon, there is a tendency for acid-soluble chromium concentrations to be elevated in alluvium relative to deeper bedrock units, reflecting higher background chromium in the alluvium (Plate 1). Alluvium in core holes MCB-14, MCOI-6, and MC-2AHF contains a few samples that exceed the background UTL. Many bedrock units contain a few isolated elevated chromium values, but there are few spatial trends. One notable exception is MCB-14 where cores collected between depths of 55 and 70 m (180 and 230 ft) contain acid-soluble chromium concentrations significantly greater than the background UTL (Plate 1). MCB-14 core also contains elevated concentrations of pore-water nitrate and perchlorate (see "Mortandad Canyon Investigation Report," LANL 2006, 094161, Appendix Figure D-2.3-11, p. D-204), indicating indicating the borehole is located where contaminants migrate with preferential percolation of moisture through the vadose zone.

Ten Site Canyon boreholes contain few acid-soluble chromium concentrations greater than the background UTL, suggesting that this canyon was a relatively minor source of chromium compared with

Los Alamos, Sandia, and Mortandad Canyons. Alluvium was sampled only in MCB-15, and the chromium values were within background values (Plate 1). MCB-15 contains elevated acid-soluble chromium concentrations in the Cerro Toledo interval and at the top of the Otowi Member. R-14 contains a single isolated acid-soluble chromium concentration of 1020 mg/kg at a depth of 79.8 m (262 ft) in the Otowi Member (Plate 1). This is the single highest chromium value found in the archival cores analyzed for this investigation; however, the very low chromium concentrations found in samples above and below this sample suggest that the result is spurious.

### **5.5.1.3 Temporal Trends of Chromium in Perched Intermediate Groundwater**

Screening groundwater samples were collected during drilling of the SCC core holes and analytical results are provided in Appendix C-3. Because chromium was the primary analyte of importance during drilling, analyses of a broad suite of analytes was not specified for screening groundwater samples collected at the SCC core holes. Screening results for the core-hole water samples suggest that low concentrations of residual chromium are present in perched-intermediate groundwater beneath Sandia Canyon. A core-hole screening water sample collected during drilling at SCC-1, at a depth of 116 m (382 ft) bgs within the Puye Formation, contained 0.005 ppm (5 ppb) of total dissolved chromium (Appendix C-3). This core hole was completed as an intermediate well designated SCI-1. Core-hole screening water samples collected during drilling at SCC-2 contained concentrations of total dissolved chromium of 0.013 ppm (13 ppb) within unit Qbt 1g of the Tshirege Member at a depth of 17 m (55 ft) bgs and 0.007 ppm (7 ppb) within the Puye Formation at a depth of 109 m (357 ft) bgs (Appendix C-3). A third core-hole water screening sample collected at SCC-2, at a depth of 113 m (370 ft) bgs, contained 0.006 ppm (6 ppb) of total dissolved chromium. Another screening groundwater sample collected at SCC-2 contained 0.009 ppm (9 ppb) of total dissolved chromium within the Puye Formation, when the core hole was deepened to 101 m (332 ft) bgs and penetrated the top of the Cerros del Rio basalt. A core-hole screening water sample collected during drilling at SCC-3, at a depth of 97 m (319 ft) bgs within the Puye Formation, contained 0.008 ppm (8 ppb) of total dissolved chromium (Appendix C-3). The total depth of the core hole was 98 m (323 ft) bgs when this sample was collected. At SCC-4, a core-hole screening water sample collected at a depth of 34 m (111 ft) bgs within the Otowi Member, possibly representing a thin saturated zone or leaching of vadose-zone material with water used during drilling, contained 0.007 ppm (7 ppb) of total dissolved chromium (Appendix C-3). No samples were collected at SCC-4 when a thin saturated zone was encountered at 98 m (322 ft) bgs because of an insufficient volume of water available for chromium analysis, and no perched groundwater was present at either SCC-5 or SCC-6.

Monitoring wells completed in the regional aquifer consist of both single- and multiscreen construction. Groundwater chemistry data from the single-screen completions are representative of predrilling conditions. However, one multiscreen well in Sandia Canyon does not provide fully representative data for the groundwater, especially for certain constituents subject to chemical reduction, precipitation, dissolution and desorption resulting from the effects of reducing conditions (for example, chromium, iron, manganese, perchlorate, and nitrate). The affected well/screens are R-12, screens 1, 2, and 3. This well has undergone rehabilitation consisting of temporarily removing Westbay components and pumping the three screens. Analytical results for groundwater samples collected during well rehabilitation at R-12 will be provided in a separate report.

Maximum, mean, and median groundwater background concentrations of dissolved chromium are 2, 0.73, and 0.99 µg/L, respectively, within perched groundwater in volcanic rocks (Bandelier Tuff and Tschicoma Formation, and phreato-magmatic desposits of the Cerros del Rio lavas) (LANL 2005, 090580). Elevated chromium(VI) concentrations are observed in perched-intermediate zones located beneath Mortandad Canyon. The presence of deep contamination indicates that there are some

pathways through the vadose zone that have transported unknown masses of chromium to depths below the Otowi Member (LANL 2006, 094161). The perched-intermediate wells sampled during 2002, 2003, 2005, and 2006 include MCOI-4, -5, -6, and -8, and MCOBT-4.4 (Figure 2.0-1). Appendix Figure B-1.7-13 shows concentrations of total dissolved chromium in perched-intermediate and regional aquifer wells in Mortandad Canyon. Additional analytical data presented in LANL (2006,094161) show spatially variable results with chromium(VI), represented by similar concentrations of total chromium in filtered and nonfiltered pairs, dominating in some of the perched zones and chromium(III) at others. Chromium(III) is associated with suspended particles in groundwater samples. Concentrations of total chromium in filtered samples decreased from 53.3 to 37.4 µg/L at MCOBT-4.4 during this period (Appendix Figure B-1.7-13). Concentrations of total chromium in filtered and nonfiltered samples were similar, indicating that chromium(VI) dominates over chromium(III) at MCOBT-4.4 (LANL 2006, 094161).

Concentrations of total chromium in filtered samples collected at MCOI-4 have generally decreased from 29.4 to 16.7 µg/L during the sampling period (Appendix Figure C-3.13). A sample collected on June 28, 2006, at MCOI-4 confirmed the presence of chromium(VI) at 17.7 µg/L (Appendix C-5 through speciation analysis using ion chromatography and/or mass spectrometry). Concentrations of total chromium in filtered samples collected at MCOI-5 decreased from 3.5 to 2.9 µg/L (Appendix Figure B-1.7.13). At MCOI-6, concentrations of total chromium in filtered samples varied from 43.9 to 58.2 µg/L, and concentrations of chromium(VI) ranged from 41.4 to 53.2 µg/L, as determined by speciation analyses (Appendix C-5). At MCOI-8, the concentration of total dissolved chromium was less than analytical detection (1 µg/L). This sample was collected on January 30, 2006. A more recent sample collected from the well on June 30, 2006, detected total dissolved chromium at 1.7 µg/L.

In Los Alamos Canyon, concentrations of total chromium in filtered samples collected at LAOI-3.2a, LAOI-7, R-6i, and R-9i varied from 0.25 to 3.6 µg/L (Figure C-3.14, Appendix C-5). A groundwater sample collected on March 1, 2006, at R-6i confirmed the presence of chromium(VI) at 1.7 µg/L through speciation analysis using ion chromatography. These results suggest the perched-intermediate zones at these wells presently do not contain anthropogenic chromium.

#### 5.5.1.4 Temporal Trends of Chromium in the Regional Aquifer

Maximum, mean, and median groundwater background concentrations of total dissolved chromium are 7, 4.1, and 3 µg/L, respectively, within the regional aquifer (LANL 2005, 090580). A contract analytical laboratory, however, reported an anomalous dissolved chromium concentration of 44.1 µg/L in a filtered sample collected from Otowi(O)-4 on September 28, 1998, as part of the LANL groundwater background investigation (LANL 2005, 090580). A split sample collected from the well on the same date and analyzed by EES-6 contained 6 µg/L of dissolved chromium. Other dissolved chromium concentrations ranged between 2 and 7 µg/L at O-4 (LANL 2005, 090580). Regional aquifer wells recently sampled include R-1, R-6, R-9, R-10a, R-11, R-13, R-14, R-15, R-28, R-33, R-34, and TW-8 (Appendix C-2 and C-5). Appendix Figures B-1.7.13, B-1.7.14, and B-1.7.15 show concentrations of total dissolved chromium in samples collected from perched-intermediate and/or regional aquifer wells within the Mortandad, Los Alamos, and Sandia watersheds, respectively. Concentrations of total dissolved chromium within the regional aquifer in the Puye Formation and underlying pumiceous sediments are highest beneath Mortandad Canyon east of the sediment traps (at R-28) and decrease to the east and southwest (at R-13 and R-15) (LANL 2006, 094161). Water-supply wells O-4, PM-1, and PM-3 were also sampled during 2005 and 2006 and concentrations of dissolved chromium ranged from 3.4 to 4.2 µg/L (Appendix C-5, Appendix Figures B-1.7-14 and B-1.7.15).

Concentrations of total chromium at R-28 generally increased from 375 to 428 µg/L in filtered samples collected during 2005 and 2006 (Appendix Figure B-1.7-13, Appendix C-5). Concentrations of chromium(VI), determined from speciation analyses, ranged from 376 to 423 µg/L in both filtered and nonfiltered samples collected at the well (Appendix C-5). These are the highest concentrations of total chromium(III, VI) and chromium(VI) measured in the regional aquifer beneath the Laboratory. The increasing trend in chromium concentrations at R-28 suggests that the well is located within the leading edge of a chromium plume. Presence of nitrate, perchlorate, and tritium in addition to chromium(VI) at R-28 suggest that several sources of contaminants are likely (Appendix C-5).

Concentrations of total chromium at R-11 generally increased from 18.4 to 29.4 µg/L in filtered samples collected during 2005 and 2006 (Appendix Figure B-1.7-15, Appendix C-2). Concentrations of chromium(VI) were 26.0 and 26.4 µg/L in filtered and nonfiltered samples, respectively, collected on February 3, 2006. The increasing trend in chromium concentrations at R-11 suggests that the well is also located within the leading edge of a chromium plume.

Concentrations of total chromium varied from 2.6 to 7.9 µg/L in filtered samples collected at R-15 (Appendix Figure C-3-13). Concentrations of chromium(VI) were 7 and 7.1 µg/L in filtered and nonfiltered samples, respectively, collected on January 30, 2006. These total dissolved chromium and chromium(VI) concentrations are slightly elevated compared with background chromium concentrations for the regional aquifer.

Detectable concentrations of total chromium in nonfiltered and filtered samples ranged from 2.73 to 12.3 µg/L and from 0.93 to 8.2 µg/L, respectively, at R-1, R-6, R-9, R-10a, R-13, R-14, R-33, R-34, and TW-8 (Appendix C-5). Well R-33 (screen 1) contained a concentration of dissolved chromium of 8.2 µg/L in a sample collected on September 14, 2005. Duplicate samples collected on February 14, 2006, for R-33 (screen-1) showed total dissolved chromium concentrations of 4.3 and 4.9 µg/L (Appendix C-5). Concentrations of total chromium varied from 3.36 to 7.92 µg/L in nonfiltered samples collected at TW-8 from 2001 to 2006 (LANL 2006, 094161). Concentrations of total chromium in three filtered samples were less than analytical detection (<1 µg/L) at R-14 in 2004 and 2005 (LANL 2006, 094161). The majority of water samples from R-14 contained detectable total chromium. Nondetection of total chromium is most likely caused by the presence of residual drilling fluid at R-14, screen 2.

#### 5.5.1.5 Chromium Geochemistry

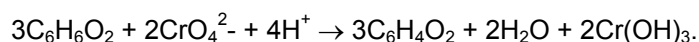
This section summarizes a conceptual model for chromium geochemistry focusing on speciation, adsorption, and precipitation, which influence migration of this metal in surface water and groundwater environments. Chromate ( $\text{CrO}_4^{2-}$ ) and bichromate ( $\text{HCrO}_4^-$ ) from dissociated potassium dichromate ( $\text{K}_2\text{Cr}_2\text{O}_7$ ) were released into Sandia Canyon from 1956 to 1972 (Section 2.0). Bichromate and chromate are hypothesized to be the dominant mobile species in surface water and groundwater depending on pH. Bichromate dominates below pH 6.5 in aqueous solution. Analytical results show that chromium(VI) is the dominant species when concentrations of chromium in filtered and nonfiltered sample pairs are similar. Chromium(VI) adsorbs onto ferric (oxy)hydroxide, which is characterized by a net-negative surface charge under acidic pH conditions (Rai et al. 1987, 091686; Rai and Zachara 1986, 091684). Ferric (oxy)hydroxide and iron oxide are stable under oxidizing conditions and are commonly found in most hydrogeologic settings (Langmuir 1997, 056037; Lindsay 1979, 071512). Adsorption of chromium(VI) onto iron-rich phases may account for the presence of residual chromium within the vadose zone beneath Sandia and Mortandad watersheds. Chromium(VI) reduces to chromium(III) in the presence of chemical reductants including ferrous iron, dissolved sulfide, and solid organic matter. Once reduced, chromium(III) is insoluble and precipitates from solution initially as amorphous  $\text{Cr}(\text{OH})_3$ , which converts to crystalline

$\text{Cr}(\text{OH})_3$ . Chromium(III) also co-precipitates with ferric iron as  $(\text{Fe}_x\text{Cr}_{1-x})(\text{OH})_3$  (Rai et al. 1987, 091686; Rai and Zachara 1986, 091684) and precipitates are subsequently much less mobile in groundwater.

Adsorbing chromium(III) binds to sediment to become part of the sediment load, as described in Section 5.5.1.1 and either stays relatively close to the release location or is transported downcanyon with surface flow events. Nonadsorbing chromium(VI) in the forms of bichromate and chromate travel with groundwater and follow the same flow paths that water takes under alkaline pH conditions. Strongly adsorbing chromium(III) may adsorb onto immobile rock surfaces. Therefore, chromium(III) tends to exhibit retarded migration in the environment, and nonadsorbing chromium(VI) migrates in surface water, vadose-zone pore water, and groundwater.

Reoxidation of chromium(III) to chromium(VI), however, has been shown experimentally to occur in the presence of manganese(IV) solids (Rai et al. 1987, 091686; Rai and Zachara 1986, 091684). This depends on the abundance, reactivity, and availability of the oxidant, and concentrations of acid-soluble manganese are typically in the low mg/kg range in soils at the Laboratory (Ryti et al. 1998, 059730). In the presence of sufficient concentrations of solid organic matter and ferrous iron in anaerobic environments, it is likely that chromium(III) will not readily reoxidize to chromium(VI). East of the wetland, however, reoxidation of chromium(III) to chromium(VI) occurs with concentrations of dissolved chromium increasing in surface water. This reoxidation could result from dissolved oxygen and/or manganese(IV) solids reacting with chromium(III) as stream sediments interact with aerated surface waters flowing downcanyon.

Chromium(VI) in alluvial groundwater infiltrates the vadose zone and travels as the mobile solutes  $\text{CrO}_4^{2-}$  and  $\text{HCrO}_4^-$ , depending on pH. A fraction of chromium(VI) potentially is reduced to chromium(III) along vadose-zone flow paths provided that there are sufficient amounts of dissolved ferrous iron and naturally occurring iron(II)-rich minerals and volcanic glass that act as reducing agents. Here is one reaction describing the reduction of chromium(VI) to chromium(III) in the presence of solid organic matter consisting of humic substances containing hydroquinone ( $\text{C}_6\text{H}_6\text{O}_2$ ) that provide the reduction capacity (McBride 1994,058947):



According to this reaction, 1.5 moles of hydroquinone are required to reduce 1.0 mole of chromate. This is easily accomplished with excess solid organic matter present within the Sandia Canyon wetland. In the above reaction, hydroquinone oxidizes to quinone ( $\text{C}_6\text{H}_4\text{O}_2$ ), releasing two electrons for each mole of quinone produced. Concentrations of TOC coating the core sediments ranged from 0.00365 wt % (36.5 mg/kg) at SCC-1 to 0.223 wt % (2230 mg/kg) at SCC-5 (Appendix C-3). An unknown amount of hydroquinone occurs in the sediment TOC that is capable of initiating chromium(VI) reduction. Dissolved concentrations of chromium in pore water ranging from 3 to 1329 ppb or  $\mu\text{g}/\text{L}$  suggest that residual chromium(VI) is present and that it has not completely reduced to chromium(III) in the upper 122 m (400 ft) of the upper vadose zone within Sandia Canyon. It is also possible that short groundwater residence times occurring within the unsaturated zone do not allow for sufficient reaction times for reduction of chromium(VI) by solid organic matter (humic substances).

## 5.5.2 Molybdenum

Molybdenum is detected in surface water and alluvial and perched-intermediate groundwater beneath Sandia Canyon. There are both natural and anthropogenic sources of molybdenum within the watershed, with Laboratory-derived molybdenum produced from the dissociation of sodium molybdate ( $\text{Na}_2\text{MoO}_4$ ) used as a corrosion inhibitor in the cooling towers at the TA-03 power plant and in several other cooling

towers that discharged to Sandia Canyon (Section 2.0). In the discussion that follows, molybdenum concentrations within unsaturated-pore water and saturated zones are summarized.

### 5.5.2.1 Molybdenum in Surface Water and Alluvial Groundwater

Dissolved molybdenum concentrations of 2.8, 3.2, and 3.3 µg/L were measured in surface water samples collected at the head of Sandia Canyon west of the wetland at gaging station E122 (Appendix C-1). Surface water samples (nonfiltered) collected at this location contained 3, 3.7, and 3.8 µg/L of molybdenum. At gaging station E123 located east of the wetland, concentrations of molybdenum were 9 and 9.5 µg/L and 8.5 and 9 µg/L in filtered and nonfiltered surface water samples, respectively (Appendix C-1). This indicates that a residual molybdenum source is present within the wetland. At this location, molybdenum is probably stable in the +VI oxidation state, occurring as  $\text{MoO}_4^{2-}$ , based on similar concentrations of this trace element in both filtered and nonfiltered samples. At the terminus of persistent base flow below gaging station E123.5, concentrations of molybdenum (13.7 and 17.2 µg/L) in nonfiltered samples slightly exceed concentrations (13.3 and 16.7 µg/L) in filtered samples, suggesting that molybdenum(VI) dominates at this site (Appendix C-1).

Maximum, mean, and median groundwater background concentrations of dissolved molybdenum are 5, 1.5, and 1 µg/L, respectively, within alluvial groundwater (LANL 2005, 090580). The dissolved concentration of molybdenum was 52.7 µg/L (Appendix C-2) at SCA-1, indicating that anthropogenic molybdate dominates within the Sandia Canyon wetland. At SCA-5, average concentrations of molybdenum in two filtered and two nonfiltered samples were 3.1 and 2.3 µg/L, respectively (Appendix C-2). Molybdenum concentrations in filtered and nonfiltered samples of alluvial groundwater do not exceed 1 mg/L (1000 µg/L), the New Mexico WQCC groundwater standard.

### 5.5.2.2 Molybdenum in Vadose Zone

Molybdenum has migrated from the surface water and alluvial groundwater into the deeper vadose zone, probably since cooling tower releases containing molybdenum began in the Sandia watershed. At the TA-03 power plant, this occurred from 1993 to 2001 (Table 2-1). Sodium molybdate was used at other cooling towers during approximately the same time period. Analytical results for acid-soluble molybdenum and pore-water dissolved molybdenum are provided in Appendix C-3. Depth profiles of acid-soluble molybdenum and pore-water concentrations of dissolved molybdenum at SCC-1 through SCC-6 are provided in Figure 5-5.3. Pore-water concentrations of dissolved molybdenum reflect releases to the Sandia watershed (Figure 5-5.3). Background concentrations of molybdenum in soils, sediments, and volcanic rocks have not been established at the Laboratory.

Detectable pore-water concentrations of dissolved molybdenum ranged from 0.008 to 1.06 mg/L, with the highest value observed in the Otowi Member at SCC-2 (Appendix C-3). Molybdenum concentrations less than analytical detection in pore water occurred in 8% of the samples, with the instrument detection limit ranging from 0.007 to 0.013 mg/L using ICP-MS (Appendix C-3). Concentrations of molybdenum in pore water were within 1 order of magnitude of acid-soluble molybdenum (Figure 5.5-3). Usually, both fractions strongly correlate with each other in the samples, suggesting that most of the molybdenum is weakly adsorbed onto vadose-zone material. Because sodium molybdate was used 20 yr or more after potassium dichromate at the TA-03 power plant, molybdenum trails chromium migration through the vadose zone beneath Sandia Canyon.

### 5.5.2.3 Temporal Trends of Molybdenum in Perched-Intermediate Groundwater

Screening results for core-hole water analyses suggest that concentrations of residual anthropogenic molybdenum are present in the upper portion of the vadose zone beneath Sandia Canyon. A core-hole screening water sample collected during drilling at SCC-1, at a depth of 116 m (382 ft) bgs within the Puye Formation, contained 0.062 ppm (62 ppb) of dissolved molybdenum (Appendix C-3). Core-hole screening water samples collected during drilling at SCC-2 contained 0.040 ppm (40 ppb) of dissolved molybdenum within Qbt 1g of the Tshirege Member at a depth of 17 m (55 ft) bgs and 0.028 ppm (28 ppb) within the Puye Formation at a depth of 109 m (357 ft) bgs (Appendix C-3). A third core-hole water screening sample collected at SCC-2, at a depth of 113 m (370 ft) bgs, was not analyzed for molybdenum because a sample collected at 109 m (357 ft) bgs was analyzed for this trace metal. At SCC-4, a core-hole screening water sample collected at a depth of 34 m (111 ft) bgs that possibly represents a thin saturated zone or leaching of vadose-zone material with water used during drilling contained 0.333 ppm (333 ppb) of dissolved molybdenum. This screening sample was collected within the Otowi Member (Appendix C-3). No samples were collected at SCC-4 when a thin saturated zone was encountered at 98 m (322 ft) bgs because of an insufficient volume of water being available for molybdenum analysis.

In Mortandad Canyon, migration of molybdenum to perched-intermediate groundwater is not as extensive as chromium migration, based on analytical results. Maximum, mean, and median groundwater background concentrations of dissolved molybdenum are 4, 1.4, and 1 µg/L, respectively, within perched groundwater in volcanic rocks (LANL 2005, 090580). Natural and/or anthropogenic molybdenum is observed in perched-intermediate groundwater at MCOBT-4.4, MCOI-4, MCOI-5, and MCOI-6 (Appendix C-5). Concentrations of molybdenum in filtered samples ranged from 0.74 to 2.5 µg/L at MCOBT-4.4 and MCOI-4, which are within background ranges (LANL 2005, 090580). Dissolved concentrations of molybdenum that are mostly anthropogenic in origin decreased from 56.1 to 32.2 µg/L at MCOI-6 and from 8.1 to 2.6 µg/L at MCOI-5 (Appendix C-5) during 2005 and 2006.

In Los Alamos Canyon, concentrations of dissolved molybdenum within perched-intermediate groundwater at R-6i slightly increased from 1.3 to 2.3 µg/L during 2005 and 2006 (Appendix C-5). Dissolved concentrations of this trace element decreased from 21 to 9.5 µg/L during 2001 and 2002 at R-9i (Appendix C-5). Dissolved concentrations of molybdenum were less than analytical detection (2 µg/L) at LAOI-3.2a and LAOI-7 during 2006 (Appendix C-5). Dissolved concentrations of molybdenum were 2.9 and 3.3 µg/L at LAOI-3.2 (Appendix C-5).

### 5.5.2.4 Temporal Trends of Molybdenum in the Regional Aquifer

Anthropogenic molybdenum is not detected within the regional aquifer based on dissolved concentrations that are typically less than 3 µg/L, the upper limit of background concentration. Maximum, mean, and median groundwater background concentrations of dissolved molybdenum are 3, 1.3, and 1 µg/L, respectively, within the regional aquifer (LANL 2005, 090580). Several supply wells including O-4, PM-1 and PM-3 were also sampled during 2005 and 2006, and the concentration of dissolved molybdenum was 2.4 µg/L at PM-1 (Appendix C-5). Nonfiltered water samples were collected at O-4 and PM-3 and analytical results for molybdenum are provided in Appendix C-5. Dissolved concentrations of molybdenum generally increased from 0.78 to 2.2 µg/L in samples collected from R-28 during 2005 and 2006 (Appendix C-5). At R-11, dissolved concentrations of molybdenum generally increased from 2 to 3.2 µg/L during 2005 and 2006. Concentrations of detectable molybdenum stayed at 0.95 to 1 µg/L in filtered samples collected from R-15 in 2005 (Appendix C-5). Detectable concentrations of molybdenum in filtered samples ranged from 0.5 to 3 µg/L at R-1, R-6, R-9, R-10a, R-13, R-14, R-33, R-34, and TW-8.

Although the highest concentration of molybdenum was in a groundwater sample at R-33 (screen 1); most concentrations of dissolved molybdenum were less than 2 µg/L at this well.

### 5.5.2.5 Molybdenum Geochemistry

Molybdenum is stable in the +II, +III, +IV, +V, and +VI oxidation states in aqueous solution. Molybdenum(VI) is the most common oxidation state in oxidizing groundwater and undergoes hydrolysis reactions forming metal-oxyanions (Lindsay 1979, 071512). Because of the multiple redox range across which molybdenum species vary, the environmental chemistry of this trace metal is complex. Molybdate ( $\text{MoO}_4^{2-}$ ) is the dominant aqueous species above pH 4.3 under oxidizing conditions. Molybdate complexes influence the solubility of molybdenum(VI) solids. Below pH values of 6, molybdenum(VI) species, primarily  $\text{HMoO}_4^-$  and  $\text{MoO}_4^{2-}$ , weakly adsorb onto ferric( oxy)hydroxide under acidic conditions in the presence of other more strongly adsorbing species including phosphate (Rai et al. 1987, 091686). Molybdate is not expected to adsorb onto solid organic matter, which is characterized by a net-negative surface charge, nor is it expected to form complexes with dissolved organic carbon stable.

In the presence of sulfate-reducing bacteria, dissolved molybdate becomes reduced to molybdenum sulfide (molybdenite) and dissolved molybdenum sulfide complexes. Such conditions may occur in organic-rich groundwater environments isolated from the atmosphere. Groundwater beneath the wetland, however, contains sulfate (well SCA-1) (Appendix C-2), which limits the precipitation of molybdenite.

Under oxidizing and circumneutral pH conditions, molybdenum may precipitate from solution as calcium molybdate (Lindsay 1979, 071512). Calcium molybdate is thermodynamically stable under alkaline pH conditions and has been observed in soils at power plant facilities across the United States (Rai et al. 1987, 091686). Using thermodynamic data presented in Lindsay (1979, 071512), precipitation of calcium molybdate at the Sandia Canyon wetland requires 1.77 mg/L of dissolved molybdenum in the presence of 25 mg/L of dissolved calcium as measured at SCA-1. Dissolved concentrations of molybdenum are much less in Sandia Canyon, and precipitation of calcium molybdate is not feasible under existing conditions. Dilution and adsorption may decrease the concentration of molybdenum in the subsurface beneath Sandia and Los Alamos Canyons.

### 5.5.3 Phosphate

Phosphate is an anthropogenic chemical present in Laboratory outfall discharges. In cooling tower blowdown, it was used as zinc phosphate and polyphosphate compounds. Phosphate is also present in treated sewage effluent as a constituent in detergents. In the discussion that follows, phosphate concentrations within unsaturated-zone pore water and saturated zones are summarized.

#### 5.5.3.1 Phosphate in Surface Water and Alluvial Groundwater

A dissolved phosphate(P) concentration of 2.9 mg/L was measured in a surface water sample collected on October 17, 2006, at gaging station E122 (Appendix C-1). The concentration of phosphate(P) was 3.58 mg/L in a nonfiltered surface water sample collected at this location on the same date (Appendix C-1). Concentrations of phosphate(P) were 2.18 and 2.21 mg/L in filtered and nonfiltered surface water samples, respectively, at the eastern end of the wetland at gaging station E123 (Appendix C-1). At the terminus of persistent base flow, the concentration of phosphate(P) (2.52 mg/L) in a nonfiltered sample was similar in analytical error to that for the filtered sample (2.61 mg/L).

Maximum, mean, and median groundwater background concentrations of total dissolved phosphate(P) are 0.08, 0.02, and 0.02 mg/L, respectively, within alluvial groundwater (LANL 2005, 090580).

Concentrations of total phosphate(P) were 2.31 and 4.38 mg/L, respectively, in filtered and nonfiltered samples at SCA-1 (Appendix C-2). A fraction of total phosphate(P) is associated with suspended material in groundwater beneath the wetland. At SCA-5, average concentrations of phosphate in filtered and nonfiltered samples were 0.37 and 0.42 mg/L, respectively (Appendix C-2).

### 5.5.3.2 Phosphate in Vadose Zone

Phosphate has migrated from the surface water and alluvial groundwater into the deeper vadose zone, probably since cooling tower releases began in the Sandia watershed at TA-03 in 1951 until 2001 (Table 2-1). Other cooling towers releasing to the Sandia Canyon watershed may have also released phosphate (Section 2.0). Analytical results for pore-water concentrations of phosphate extracted from the SCC samples are provided in Appendix C-2, and depth versus concentration profiles for pore-water phosphate are shown in Figure 5-5.4. Phosphate was commonly detected in most SCC cores analyzed in the Sandia watershed, and vadose-zone pore-water concentrations frequently exceed 2 mg/L.

Detectable pore-water concentrations of total dissolved phosphate (as  $PO_4$ ) extracted from the SCC holes ranged from 0.11 to 34.7 mg/L (equivalent to total dissolved phosphate[P] of 0.04 to 11.3 mg/L), with the maximum concentration measured in the alluvium at SCC-1 (Appendix C-3), although cores from alluvial perched zones at SCC-2 to SCC-4 had similar concentrations. Total dissolved phosphate concentrations in pore water less than analytical detection occurred in 18% of the samples, with IDLs ranging from 0.03 to 0.12 mg/L (total phosphate[P] ranging from 0.01 to 0.04 mg/L) using ion chromatography (Appendix C-3). The highest concentrations of total dissolved phosphate in pore water typically occurred within the alluvium at the SCC holes (Figure 5-5.5). Total dissolved phosphate is also elevated within some samples from the Cerro Toledo interval, Puye Formation, and Cerros del Rio basalt (Figure 5-5.5). The lowest concentrations of total dissolved phosphate were measured in the Otowi Member of the Bandelier Tuff.

### 5.5.3.3 Temporal Trends of Phosphate in Perched-Intermediate Groundwater

Migration of phosphate to perched-intermediate zones encountered during drilling of the SCC core holes generally was not extensive. Maximum, mean, and median groundwater background concentrations of total dissolved phosphate(P) are 0.05, 0.01, and 0.008 mg/L, respectively, within perched groundwater in volcanic rocks (LANL 2005, 090580). A core-hole screening water sample collected during drilling at SCC-1, at a depth of 116 m (382 ft) bgs within the Puye Formation, contained 0.04 ppm (40 ppb) of dissolved phosphate (phosphate[P] 0.01 ppm) (Appendix C-3). Core-hole screening water samples collected during drilling at SCC-2 contained 7.98 ppm (7980 ppb) concentrations of dissolved phosphate (phosphate[P] 2.61 ppm) within Qbt 1g of the Tshirege Member at a depth of 17 m (55 ft) bgs. This anion was not detected (less than 0.01 ppm) in perched water within the Puye Formation at depths of 109 and 113 m (357 and 370 ft) bgs at SCC-2. Phosphate was not analyzed in the two core-hole screening water samples collected during drilling at SCC-3 collected at a depth of 97 m (319 ft) bgs. At SCC-4, a core-hole screening water sample at a depth of 34 m (111 ft) bgs within the Otowi Member, possibly representing a thin saturated zone or leaching of vadose-zone material with water used during drilling, contained 0.06 ppm (60 ppb) of dissolved phosphate (phosphate[P] 0.02 ppm) (Appendix C-3). No samples were collected at SCC-4 when a thin saturated zone was encountered at 98 m (322 ft) bgs because of an insufficient volume of water available for phosphate analysis.

Total phosphate(P) concentrations within perched-intermediate zones beneath Mortandad Canyon are less than 0.5 mg/L, suggesting that the introduced mass of this adsorbing anion has not migrated to deeper saturated zones. Detectable concentrations of total dissolved phosphate(P) ranged from 0.059 to 0.182 mg/L at MCOBT-4.4, MCOI-4, MCOI-5, MCOI-6, and MCOI-8 (Appendix C-5).

#### 5.5.3.4 Temporal Trends of Phosphate in the Regional Aquifer

Anthropogenic phosphate(P) is only detected at low concentrations within the regional aquifer where dissolved concentrations are typically less than 0.05 mg/L. Maximum, mean, and median groundwater background concentrations of total dissolved phosphate(P) are 0.03, 0.01, and 0.003 mg/L, respectively, within the regional aquifer (LANL 2005, 090580). Concentrations of total phosphate(P) at R-28 ranged from 0.01 to 0.11 mg/L and from 0.02 to 0.095 mg/L, respectively, in filtered and nonfiltered samples collected during 2005 and 2006 (Appendix C-5). Concentrations of total phosphate(P) at R-11 ranged from 0.04 to 0.11 mg/L and from 0.01 to 0.05 mg/L, respectively, in filtered and nonfiltered samples collected during 2005 and 2006 (Appendix C-2-5).

#### 5.5.3.5 Phosphate Geochemistry

Orthophosphate is the stable form of phosphorus in soils, surface water, and groundwater occurring as  $\text{H}_3\text{PO}_4^0$ ,  $\text{H}_2\text{PO}_4^-$ ,  $\text{HPO}_4^{2-}$ , and  $\text{PO}_4^{3-}$  (Lindsay 1979, 071512). Phosphoric acid is stable under acidic conditions and phosphate dominates under alkaline conditions. Between pH values of 6 and 9, orthophosphate is stable dominantly as  $\text{H}_2\text{PO}_4^-$  and  $\text{HPO}_4^{2-}$  (Lindsay 1979, 071512). Phosphate also forms complexes with many metals including aluminum, calcium, iron, magnesium, strontium, uranium, and zinc (Lindsay 1979, 071512). Phosphate adsorbs onto ferric (oxy)hydroxide and competes with chromate, bichromate, and molybdate for adsorption sites under acidic pH conditions (Langmuir 1997, 056037). It is possible that metal-phosphate complexes enhance the mobility of this chemical in groundwater beneath the Laboratory.

#### 5.5.4 Zinc

Zinc is detected in surface water and alluvial and perched-intermediate groundwater beneath Sandia Canyon. Zinc is also detected within perched-intermediate zones beneath Mortandad Canyon. There are both natural and anthropogenic sources of zinc within both watersheds. Laboratory-derived zinc was associated with zinc phosphate ( $\text{Zn}_3(\text{PO}_4)_2$ ) and zinc dichloride ( $\text{ZnCl}_2$ ), which were used as corrosion inhibitors in the cooling towers at the TA-03 power plant. In the discussion that follows, zinc concentrations within unsaturated-pore water and saturated zones are summarized.

##### 5.5.4.1 Zinc in Surface Water and Alluvial Groundwater

A detectable concentration of dissolved zinc of 9.7  $\mu\text{g/L}$  was measured in a surface water sample collected at the head of Sandia Canyon west of the wetland at gaging station E122 (Appendix C-1). Nonfiltered surface water samples collected at this location contained 14.5 and 14.4  $\mu\text{g/L}$  of zinc. At gaging station E123 located east of the wetland, average concentrations of detectable zinc were 30.8  $\mu\text{g/L}$  and 313  $\mu\text{g/L}$  in five filtered and six nonfiltered surface water samples, respectively (Appendix C-1). This indicates that a residual zinc source occurs within the wetland. At the terminus of persistent base flow, concentrations of zinc (17.6 and 25.8  $\mu\text{g/L}$ ) in two nonfiltered samples slightly exceed concentrations (15.8 and 20.3  $\mu\text{g/L}$ ) in two filtered samples, suggesting that a fraction of zinc is adsorbed onto suspended particles (Appendix C-1).

Maximum, mean, and median groundwater background concentrations of dissolved zinc are 21, 4.6, and 2.5  $\mu\text{g/L}$ , respectively, within alluvial groundwater (LANL 2005, 090580). Dissolved and total concentrations of zinc were 16 and 29.2  $\mu\text{g/L}$ , respectively, in groundwater (Appendix C-2) at SCA-1. At SCA 5, average concentrations of zinc in filtered and nonfiltered samples were 7.7 and 29.6  $\mu\text{g/L}$ , respectively (Appendix C-2). Zinc concentrations in filtered and nonfiltered groundwater samples do not exceed 10 mg/L (10,000  $\mu\text{g/L}$ ), the New Mexico WQCC domestic water supply standard.

#### 5.5.4.2 Zinc in Vadose Zone

Zinc has migrated from the surface water and alluvial groundwater into the deeper vadose zone, probably since cooling tower releases containing zinc occurred in the Sandia watershed at TA-03 from 1956 to 1972 and from 2001 to 2006. The background UTL for zinc is 40 mg/kg within the Cerro Toledo interval, unit 1g of the Tsirege Member, and Otowi Member (Ryti et al. 1998, 059730). The background UTL for zinc is 60.2 mg/kg in sediments, including the alluvium within Sandia Canyon (Ryti et al. 1998, 059730). Analytical results for acid-soluble zinc and pore-water dissolved zinc are provided in Appendix C-3. Depth profiles of acid-soluble zinc and pore-water concentrations of dissolved zinc at SCC-1 through SCC-6 are provided in Figure 5-5.5. Pore-water concentrations of dissolved zinc reflect releases to the Sandia watershed (Figure 5-5.5).

Detectable pore-water concentrations of dissolved zinc ranged from 0.001 mg/L at SCC-1 to 0.472 mg/L at SCC-2 (Appendix C-3), with the highest concentration occurring in the Cerros del Rio basalt. Zinc was detected in all core samples leached with deionized water using ICP-MS and inductively coupled plasma optical emission spectroscopy (Appendix C-3). Dissolved concentrations of zinc in pore water were within a factor of 2 of the acid-soluble zinc associated with solids (Figure 5.5-5). Usually, both fractions strongly correlate with each other in the samples, suggesting that most of the zinc is weakly adsorbed onto vadose-zone material. Because zinc dichloride was used after zinc phosphate at the TA-03 steam plant, zinc continues to migrate through upper portions of the vadose zone beneath Sandia Canyon.

#### 5.5.4.3 Temporal Trends of Zinc in Perched-Intermediate Groundwater

Zinc was not analyzed in a core-hole screening water sample collected during drilling at SCC-1. Core-hole screening water samples collected during drilling at SCC-2 contained 0.004 ppm (4 ppb) concentrations of dissolved zinc within Qbt 1g of the Tshirege Member at a depth of 17 m (55 ft) bgs. The concentration of dissolved zinc was 0.002 ppm (2 ppb) in two screening water samples collected within the Puye Formation at depths of 109 and 113 m (357 and 370 ft) bgs at SCC-2. Zinc was not analyzed in the two core-hole screening water samples collected during drilling at SCC-3. At SCC-4, a core-hole screening water sample collected at a depth of 34 m (111 ft) bgs within the Otowi Member, possibly representing a thin saturated zone or leaching of vadose-zone material with water used during drilling, contained 0.002 ppm (2 ppb) of dissolved zinc (Appendix C-3). No samples were collected at SCC-4 when a thin saturated zone was encountered at 98 m (322 ft) bgs because of an insufficient volume of water available for zinc analysis.

Maximum, mean, and median groundwater background concentrations of dissolved zinc are 33, 5.3, and 5 µg/L, respectively, within perched groundwater in volcanic rocks (LANL 2005, 090580). In Mortandad Canyon, natural and anthropogenic zinc are observed in perched-intermediate groundwater at MCOBT-4.4, MCOI-4, MCOI-5, MCOI-6, and MCOI-8 (Appendix C-5). Concentrations of zinc in filtered samples ranged from 1.06 to 3.18 µg/L at MCOBT-4.4, within background ranges for perched-intermediate groundwater (LANL 2005, 090580). Dissolved concentrations of zinc ranged from 24.7 to 294 µg/L at MCOI-4, suggesting an anthropogenic origin for zinc at this well. From 2005 to 2006, concentrations of zinc in filtered samples decreased from 145 to 123 µg/L at MCOI-5. Dissolved concentrations of zinc varied from 51.5 to 151 µg/L at MCOI-6 and increased from 19.3 to 46.1 µg/L at MCOI-8 (Appendix C-5) during 2005 and 2006. Concentrations of dissolved zinc at MCOI-6 and -8 are mostly anthropogenic in origin.

In Los Alamos Canyon, concentrations of dissolved zinc varied from 12.9 to 45.7 µg/L within perched-intermediate groundwater at R-6i during 2005 and 2006 (Appendix C-5). During 2001, one groundwater sample contained a detectable concentration of dissolved zinc at 4 µg/L at R-9i (Appendix C-5).

Concentrations of dissolved zinc are within background ranges (LANL 2005, 090580) at LAOI-7, LAOI-3.2, and LAOI-3.2a. Dissolved concentrations of this trace element varied from 8.3 to 16 µg/L during 2006 at LAOI-7 (Appendix C-5). Dissolved concentrations of zinc decreased from 12.2 to 4.5 µg/L at LAOI-3.2 (Appendix C-5). The dissolved concentration of zinc was 2.7 µg/L at LAOI-3.2a during 2006 (Appendix C-5).

#### 5.5.4.4 Temporal Trends of Zinc in the Regional Aquifer

Maximum, mean, and median groundwater background concentrations of dissolved zinc are 80, 13.3, and 5 µg/L, respectively, within the regional aquifer (LANL 2005, 090580). Anthropogenic zinc was detected at some of the regional aquifer wells. Otowi-4 contained 80 µg/L of dissolved zinc in a sample collected on May 29, 1997, and several other samples from this supply well had similar concentrations of zinc. The source(s) of zinc at O-4 are not known but may include corrosion of well material and/or Laboratory-derived zinc present in discharges to Los Alamos Canyon. Since 2002, concentrations of zinc generally have been less than 15 µg/L in nonfiltered samples (Appendix C-5). Several supply wells including O-4, PM-1, and PM-3 were also sampled during 2006. Dissolved concentrations of zinc were 2.9 and 6 µg/L at PM-1 and PM-3, respectively (Appendix C-5). Nonfiltered water samples were collected at O-4 and analytical results for zinc are provided in (Appendix C-5). Dissolved concentrations of zinc generally varied from 3.1 to 13.6 µg/L in samples collected at R-28 during 2005 and 2006 (Appendix C-5). At R-11, dissolved concentrations of zinc generally increased from 8.9 to 37 µg/L during 2005 and 2006. Concentrations of detectable zinc varied from 3.2 to 9.1 µg/L in filtered samples collected from R-15 during 2005 and 2006 (Appendix C-5). Concentrations of zinc in filtered samples ranged from 1 to 392 µg/L at R-1, R-6, R-9, R-10a, R-13, R-14, R-33, R-34, and TW-8. The highest concentration of dissolved zinc was in a groundwater sample from TW-8, suggesting that corrosion of carbon steel is occurring at this well. The highest concentrations of dissolved zinc were 111 and 38.6 µg/L at R-10a and R-33, respectively (Appendix C-5). Concentrations of dissolved zinc were less than 20 µg/L at the other R-wells.

#### 5.5.4.5 Zinc Geochemistry

Zinc is stable in the +II oxidation state in aqueous solution (Lindsay 1979, 071512). In typical surface water environments,  $Zn^{2+}$  dominates below pH 8.4 when the activity of sulfate is 10-3.0 (96 mg/L) and the partial pressure of carbon dioxide gas is 10-3.5 atmospheres (Rai et al. 1987, 091686). The complex  $ZnSO_4^0$  can be present in appreciable amounts at higher concentrations of sulfate, which is relevant to the unsaturated zone at the SCC core holes containing sulfate concentrations exceeding 96 mg/L. Between pH values of 8.4 and 11.9, the dissolved complex  $ZnCO_3^0$  dominates based on thermochemical calculations performed by Rai et al. (1987, 091686). The solubility of zinc in soil environments is considered to be controlled by  $Zn_5(OH)_6(CO_3)_2$  under oxidizing, alkaline conditions (Rai et al. 1987, 091686). Adsorption of zinc onto ferric (oxy)hydroxide and clay minerals controls the transport of this metal in groundwater in the absence of solubility-controlling solids. Zinc adsorption increases with increasing pH, and zinc has been shown experimentally to adsorb onto ferric (oxy)hydroxide stronger than nickel, cobalt, and cadmium (Rai et al. 1987, 091686). Zinc, in the form of  $Zn^{2+}$ , is expected to adsorb onto solid organic matter, which is characterized by a net-negative surface charge. The association of zinc with suspended material downcanyon from the Sandia Canyon wetland at gaging station E123 can be explained by adsorption of zinc onto solid organic matter. Zinc(II) is also expected to form complexes with dissociated organic acids present in dissolved organic carbon (McBride 1994, 058947). These zinc-organic complexes can be mobile in groundwater especially if they occur as neutral or negatively charged solutes. Analytical results for zinc in nonfiltered samples at SCA-1 and SCA-5 suggest that this trace metal is associated with suspended material, possibly consisting of ferric (oxy)hydroxide and/or clay minerals, through adsorption processes. Adsorption of zinc, however, does not

entirely apply to the perched-intermediate zones beneath Mortandad Canyon based on elevated concentrations of dissolved zinc at several of the wells. The apparent mobility of zinc in the vadose zone beneath Mortandad Canyon is controlled by the metal's speciation in which zinc could be stable as  $ZnCO_3^0$  and/or  $ZnSO_4^0$  complexes that do not completely adsorb onto ferric (oxy)hydroxide because of their neutral charge.

### 5.5.5 Groundwater Geochemistry of Alluvium

Alluvial well SCA-1 is completed within the Sandia Canyon wetland (Figure 2.0-1). Groundwater beneath the wetland is chemically unique from other shallow alluvial groundwater within the Sandia watershed based on available data from SCA-5. Groundwater beneath the wetland is reducing in comparison to alluvial groundwater farther east within the watershed (Appendix C-2). Because the wetland contains abundant solid organic matter, the concentration of TOC is high (5.11 mg/L) (Appendix C-2). It is likely that the wetland is an effective scavenger for chromium. This metal is hypothesized to become reduced by dissolved and suspended organic matter followed by adsorption of chromium(III) onto solid organic matter and initial precipitation of amorphous  $Cr(OH)_3$ . Anions including molybdate, sulfate, chromate, and bichromate, however, are not expected to adsorb onto solid organic matter, which is characterized by a net-negative surface charge. These oxyanions also are not expected to form complexes with dissolved organic carbon stable. The elevated concentration of molybdenum (52.7  $\mu\text{g/L}$ ) supports the hypothesis that this trace element does not adsorb onto solid organic matter.

Groundwater at SCA-1 had a TDS of 455 mg/L, consisting mainly of dissolved sodium (99.1 mg/L) and of bicarbonate (161 mg/L) calculated from total carbonate alkalinity. Concentrations of ammonia(N) were 0.06 and 0.152 mg/L in filtered and nonfiltered samples, respectively, at SCA-1. The concentration of dissolved nitrate(N) was 5.94 mg/L (Appendix C-2). Reducing conditions occurring within the wetland are also characterized by dissolved concentrations of iron and manganese of 512 and 514  $\mu\text{g/L}$ , respectively, at SCA-1. Particulate iron and manganese are also present in the wetland as indicated by iron and manganese concentrations of 3010 and 1400  $\mu\text{g/L}$ , respectively, in the nonfiltered sample (Appendix C-2). Concentrations of total iron suggest that ferric (oxy)hydroxide and/or clay minerals were present as suspended material.

At SCA-5, the average TDS was 222 mg/L with sodium and bicarbonate being the dominant solutes. Average dissolved concentrations of sodium and bicarbonate, calculated from total carbonate alkalinity, were 35.5 and 105 mg/L, respectively (Appendix C-2). Groundwater from SCA-5 contained an average concentration of TOC of 1.55 mg/L (Appendix C-2). Average concentrations of iron and manganese in two filtered and two nonfiltered samples collected from SCA-5 were 200 and 5135  $\mu\text{g/L}$  and 37.8 and 119.5  $\mu\text{g/L}$ , respectively. Concentrations of iron in the nonfiltered samples suggest that ferric (oxy)hydroxide and/or clay minerals were present as suspended material. The average concentration of aluminum, which is an essential component of clay minerals, was 1.25 wt % in the two nonfiltered samples. This suggests that clay minerals and/or other aluminosilicates were present in the nonfiltered samples

## 6.0 SUMMARY OF PHYSICAL SYSTEM CONCEPTUAL MODEL

This section summarizes the main elements of the physical system conceptual model based on data presented in Section 5.0 and in the Appendixes. The primary focus of this section is to summarize the sources(s) of chromium found in the regional groundwater at R-11 and R-28 and to discuss the physical, chemical, and hydrologic processes that govern the fate and transport of chromium and associated contaminants, including molybdenum, sulfate, and zinc. Figure 6.0-1 illustrates key aspects of the physical system conceptual model.

A review of archival records and interviews identify the cooling towers associated with the TA-03 power plant (TA-03-22) at the head of Sandia Canyon as the main source of chromium contamination at the Laboratory (Figures 2.0-1 and 6.0-1). Chromium usage for power plant cooling appears to have averaged 16.3 kg (35.9 lb) per day from circa 1956 to 1972. This resulted in an estimated total release of approximately 26,000 to 105,000 kg (58,000 to 230,000 lb) of chromium(VI) into the south fork of upper Sandia Canyon. Effluent containing up to 40 ppm of chromate ( $\text{CrO}_4$ ) was discharged to Sandia Canyon at rates between 485 to 1090  $\text{m}^3$  (128,000 to 288,000 gal.) per day. Effluent discharges to the head of Sandia Canyon have continued at average rates probably exceeding 1000  $\text{m}^3$  (288,000 gal) per day since chromium releases were discontinued. These exert a hydrologic driving force that facilitates transport of chromium.

Other sources of chromium(VI) include the cooling tower at the OWR (TA-02) in Los Alamos Canyon and possible release sites at TA-35 and TA-48 in the Mortandad watershed (Figure 2.0-1). In Los Alamos Canyon, the cooling tower at the OWR released an estimated 3000 kg (7000 lb) of chromium(VI) between 1957 and 1973, including stack emissions and blowdown. Effluent discharges from the reactor cooling tower were approximately 12,000 to 57,000 L (3100 to 15,000 gal.) per day, 5 days a week. TA-35 and TA-48 sites in the Mortandad watershed included small cooling towers and electroplating facilities. These sites are believed to be relatively small sources of chromium releases compared with Sandia and Los Alamos Canyons, both in terms of total chromium mass released and associated discharge volumes that might have served as a hydrologic driver. Sediment investigations indicate that TA-48 at the head of the Effluent Canyon tributary was the primary source of chromium contamination in the Mortandad watershed, and the downcanyon extent of residual chromium contamination in sediment is limited spatially (LANL 2006, 091461)

The total chromium mass released and effluent discharge volumes in Sandia Canyon were more than an order of magnitude greater than those released in Los Alamos and Mortandad Canyons. Nonetheless, data from archival core show that chromium(III) occurs above background concentrations in the upper vadose zone, indicating vertical migration of chromium in all three canyons. Elevated chromium(VI) in perched-intermediate groundwater beneath Mortandad Canyon provides additional evidence that chromium(VI) is being transported within the vadose zone there. Thus, while Sandia Canyon likely is the main source of chromium observed in R-11 and R-28, relatively small contributions of chromium from Los Alamos and Mortandad Canyons sources cannot be ruled out for these or other wells (e.g., R-15).

The remaining discussion in this section focuses on the fate and transport of contaminants released from the power plant at the head of Sandia Canyon. Many elements of the conceptual model discussed below also apply to the fate and transport of chromium in Los Alamos and Mortandad Canyons.

Initially, dissolved chromium(VI) was released from the TA-03 power plant. Some chromium(VI) was adsorbed onto soils and sediments near the outfall, but most was transported by surface flow down the south fork drainage at the head of Sandia Canyon to the wetland located just below the confluence of the south and north forks (Figure 2.0-1). The wetland did not exist at the current size at the time of the initial releases but is known to have been substantial in size (LANL 1999, 064617). At all stages of its evolution, the wetland contained abundant solid organic matter that served as both a chemical reductant and adsorbent, and the chromium(VI) was reduced to its trivalent state. The reduced chromium precipitated or was adsorbed onto organic matter or oxide, hydroxide, and clay minerals as chromium(III). Evidence for this process is based on elevated concentrations of trivalent chromium in sediments found within the wetland and low concentrations of dissolved chromium(VI) in present-day alluvial groundwater within the wetland. Additionally, present-day surface water (filtered samples) entering the wetland contains higher concentrations of chromium(VI) than does surface water exiting the wetland (Figure 6.0-1). Thus, the wetland is an effective a geochemical sink that inhibits the migration of chromium, and a significant portion of the chromium released to the canyon likely remains within the sediments there. However, it is

apparent that not all chromium(VI) released from the power plant was immobilized within the wetland. Stream concentrations of 2.4 to 7.3 mg/L (as chromate) were reported below the wetland from 1969 to 1971 (Purtymun 1975, 011787), indicating that significant amounts of chromium were transported down canyon by surface flow, probably both as a dissolved phase and as suspended material. Sediment samples collected downstream from the wetland also contain chromium above the sediment background value, further indicating transport of some chromium past the wetland.

Redistribution of chromium by surface water, sediment transport, and groundwater is an ongoing process within the Sandia watershed. Once adsorbed onto organic material and sediment particles in the wetland, chromium-bearing sediments are transported downcanyon by floods that scour the streambed and mobilize the bed sediment. Data collected in the Sandia Canyon after the Cerro Grande fire indicate elevated chromium contamination as far east as reach S-5 west (LANL 2006, 091987). Reoxidation of chromium(III) to chromium (VI) within suspended material and stream sediments could be significant in the absence of chemical reductants as surface water moves from the organic-rich environment of the wetland to less reducing conditions in downcanyon reaches. This may account for the observed increase of dissolved chromium concentrations in surface water at the eastern terminus of surface water flow relative to surface water exiting the wetland near gaging station E123 (Figure 6.0-1).

The transport of contaminants by surface water is facilitated where thin alluvium overlies relatively impermeable bedrock in the stream channel; this limits the amount of infiltration along the stream channel and results in greater movement of surface water downcanyon. The downcanyon extent of surface water flow varies with discharge from the TA-03 power plant, treated sewage effluent discharge rates, runoff from storm events and snowmelt, and prior moisture conditions along the channel. Under baseflow conditions with minimal stormwater contribution, an estimated 11% to 13% of effluent flow infiltrates bedrock units across the wetland (Figure 6.0-1). The wetland is underlain by relatively impermeable Bandelier Tuff, unit Qbt 2 and part of the water loss might be caused by infiltration along fractures associated with splays of the Rendija Canyon fault zone that cross the lower wetland area. Approximately 35% of the effluent flow infiltrates bedrock units between gaging stations E123 and E123.5. This part of the canyon is steep and has a narrow canyon bottom where the stream first incises through unit Qbt 2 and then through the less resistant units Qbt 1v and Qbt 1g. Much of the infiltration may occur in the eastern third of this canyon segment where Qbt 1v and Qbt 1g underlie the stream channel (Figure 6.0-1). The remaining effluent (approximately 50% of the effluent released) is lost over a short canyon segment (300 to 700 m [900 to 2300 ft]) below gaging station E123.5 (Figure 2.0-1). This portion of the canyon is characterized by rapidly thickening alluvium as the canyon floor widens eastward, resulting in greater alluvial groundwater storage (Figure 6.0-1). Runoff from storm events and snowmelt sometimes causes ephemeral flow and episodic infiltration to occur through the remaining portion of Sandia Canyon on Laboratory property, and possibly as far east as the Rio Grande, but these events are infrequent.

The infiltration of water near the eastern limit of surface flow recharges alluvial groundwater that generally accumulates in the lower part of the alluvial deposits, most often perching on or within shallow bedrock units. This alluvial groundwater is a major pathway for additional downcanyon transport of soluble chromium and mobile constituents. In Sandia Canyon, the thickest and most persistent perched alluvial groundwater occurs between alluvial wells SCA-2 and SCA-5 (Figure 6.0-1). The region between these two alluvial wells is identified by water-level measurements as contributing to alluvial groundwater loss to bedrock units beneath the canyon floor. This interpretation is supported by downward pressure gradients and high seepage velocities measured at the newly installed nested piezometers. These data should be viewed as preliminary because of the short period of record and the high heads imposed on the alluvial groundwater system after large floods in August 2006. High rates of infiltration in this area are also supported by core measurements at SCC-2 through SCC-4 that show the Otowi Member is characterized by relatively high moisture contents and that moisture contents are relatively higher in the westernmost

coreholes. The western boundary of the main zone of bedrock infiltration is uncertain, but it possibly extends up to 1000 m (3280 ft) west of gaging station E123.5 (Figure 6.0-1) in an area where the steep, narrow nature of the canyon prevents access by drill rigs.

Infiltration of alluvial groundwater to bedrock units results in the vertical transport of mobile contaminants into suballuvium bedrock units. Movement of moisture and contaminants probably occurs as gravity-driven porous flow. Transport of contaminants to these deeper zones is generally limited to soluble constituents such as chromium(VI), molybdenum(VI), nitrate, and sulfate. Results of this investigation suggest that dissolved chromium beneath the middle reaches of the canyon has been flushed out of the upper 122 m (400 ft) of the vadose zone by chromium-free water following cessation of the releases. Residual concentrations of chromium are observed in pore water and adsorbed onto rock matrices within the unsaturated zone, but the concentrations are generally low and the occurrence of elevated concentrations is sporadic.

A thin zone of perched-intermediate groundwater occurs within the Puye Formation atop the Cerros del Rio basalt between SCC-1 and SCC-4. This perched system appears to thicken westward, and it probably is recharged by percolation of moisture from the overlying rocks. Contaminant concentrations in screening samples for this perched zone are slightly elevated with respect to background. These data combined with the generally low concentrations of contaminants in the overlying pore waters suggest that years of recharge and high hydraulic fluxes have flushed the soluble contaminants out of the upper vadose zone and into deeper sections of the vadose zone. Most likely, moisture carrying these dissolved contaminants percolated into the lower vadose zone, with some portion entering the regional groundwater system, which lies approximately 253 m (830 ft) below the canyon floor at R-11 (Figure 6.0-1).

Dissolved-phase contaminants, including chromium(VI), nitrate, perchlorate, and tritium, are observed only in the shallow zone of the regional aquifer. Some wells, such as R-11, R-15, and R-28, show indications of increasing concentrations of some of these contaminants over time. Differences in nitrogen isotopic ratios for some wells (e.g., R-28 vs. R-11) indicate that contamination in regional groundwater beneath Sandia Canyon includes contributions from mixed source areas including Mortandad Canyon.

The regional aquifer is a complex, heterogeneous system that includes confined and unconfined zones. The degree of hydraulic communication between these zones is believed to be spatially variable. The shallow portion of the regional aquifer (along the water table) is predominantly under phreatic (unconfined) conditions and has limited thickness (approximately 30–50 m [98–164 ft]). Groundwater flow and contaminant transport directions in this zone generally follow the gradient of the regional water table; the flow is generally east/southeastward. The direction and gradient of flow at the regional water table is predominantly controlled by areas of recharge (e.g., the Sierra de los Valles and variably within some Pajarito Plateau canyons) and discharge (White Rock Canyon springs and the Rio Grande).

The deep portion of the regional aquifer is predominantly under confined conditions, and it is stressed by Pajarito Plateau water-supply pumping. The pumping likely has a small impact on the flow directions in the phreatic zone because of poor hydraulic communication (cf. Appendix B-2). Capture of contaminants by supply well PM-3, which is screened approximately 56 to 536 m (183 to 1759 ft) below the regional water table, seems unlikely because of this poor vertical hydraulic communication. However, the poor hydraulic communication does not preclude the possibility that some contaminant migration may occur between the shallow and deep zones. Between the two zones, the hydraulic gradient has a downward vertical component due to water-supply pumping, creating the possibility that downward contaminant flow may occur along “hydraulic windows.” However, upward vertical gradients near PM-3 might provide natural protection against entry of contaminants from the phreatic zone into the well screen.

As presented in the “Interim Measures Work Plan for Chromium Contamination in Groundwater” (LANL 2006, 091987), transport of the chromium contamination observed at R-28 is expected to travel in

the general direction of water-supply well PM-3. To date, chromium concentrations in the water-supply wells, including PM-3, are within background levels. Installation of the monitoring wells R-35a and R-35b will test components of the conceptual model with respect to the fate and transport of chromium migration within the regional aquifer.

## **7.0 CONCLUSIONS AND RECOMMENDATIONS**

Sampling data from regional groundwater monitoring wells and surrounding production wells shows that only R-11 and R-28 contain clear evidence for Laboratory-derived chromium contamination. A few other regional groundwater monitoring wells (e.g., R-15) may contain slightly elevated chromium but additional monitoring data are needed to further assess whether these results indicate contamination. Installation of R-35a and R-35b will provide further information for the assessment of potential impact to water-supply well PM-3.

The results of this interim measures investigation indicate that the predominant zone of infiltration into the suballuvium vadose zone occurs in the middle reaches of Sandia Canyon as suggested in the initial conceptual model. However, preliminary indication from the water-balance investigation is that the zone of infiltration extends farther up canyon than initially thought.

Data from core obtained during this investigation from within the predominant zone of infiltration show that the chromium has largely been flushed through this zone and that the geochemical conditions beneath the alluvium are not ideal for reducing and immobilizing chromium(VI). The presence in the vadose zone of the less-mobile constituents of the initial corrosion-inhibiting compound used from circa 1956 to 1972 provides a record that the infiltration pathway was, at least in part, in the area of investigation. The presence of highly mobile molybdenum, which was used many years after the chromium, also supports this conclusion. Analytical results for alluvium collected in the characterization coreholes and previous sediment data collected from young deposits throughout the canyon, especially in the wetland, indicate that a significant portion of the mass of chromium might remain in those media. That portion of the chromium inventory is expected to be predominantly in the relatively stable trivalent phase due to the abundance of organic matter and other adsorbing phases such as iron oxides. But, present-day detections of low concentrations of chromium(VI) in surface water and alluvial groundwater suggest that geochemical conditions are allowing for some transformation to the mobile form.

It is recommended that the interim measure phase of this investigation be concluded with this report and subsequent work be conducted in the context of the work plan for Sandia Canyon and Cañada del Buey (LANL 1999, 064617) pursuant to Section IV.B.5.b of the Consent Order. Modifications to that work plan would be necessary to account for new information and data gaps identified since preparation of the work plan and in the interim measures phase. Examples of potentially important data gaps are the need to characterize the spatial distribution and mass of chromium and related contaminants in the near surface sediment and alluvium (including the wetland area in upper Sandia Canyon), and to further constrain potential infiltration pathways using additional temporary stream gages. The need for deep drilling, in addition to planned R-35a and R-35b, will be assessed as part of the next-phase work plan in the context of project goals agreed to between the Laboratory and NMED.

Data collection under the modified work plan would focus on characterization of the nature and extent of all contaminants (not just limited to chromium and related contaminants) sufficient to support risk assessments and corrective-action remedy selection. Presently, the schedule set forth by NMED for the chromium investigation requires a "Phase 2 Interim Measures Work Plan" due 30 days following receipt of NMED comments on this report. The Laboratory's recommendation would substitute submittal of a phase 2 work plan with modifications to the existing approved work plan for Sandia Canyon and Cañada del Buey.

## 8.0 REFERENCES

*The following list includes all documents cited in this report. Parenthetical information following each reference provides the author(s), publication date, and ER ID number. This information is also included in text citations. ER ID numbers are assigned by the Environmental Programs Directorate's Records Processing Facility (RPF) and are used to locate the document at the RPF and, where applicable, in the master reference set.*

*Copies of the master reference set are maintained at the NMED Hazardous Waste Bureau; the U.S. Department of Energy–Los Alamos Site Office; the U.S. Environmental Protection Agency, Region 6; and the Directorate. The set was developed to ensure that the administrative authority has all material needed to review this document, and it is updated with every document submitted to the administrative authority. Documents previously submitted to the administrative authority are not included.*

Betz 1962. "Betz Handbook of Industrial Water Conditioning," Betz Laboratories Inc., Trevose, Pennsylvania. (Betz 1962, 094158)

Birdsell, K., March 2006. "Documentation of Discussions with Various People Concerning LANL and Zia Operations Specific to Cooling Towers and the Use of Chromium," memorandum to Los Alamos National Laboratory Environmental Restoration Records Processing Facility file from K. Birdsell, Los Alamos, New Mexico. (Birdsell 2006, 091685)

Dodge, R. A., February 1990. "Effects of Mountain Stream Topography on the Accuracy of Small Parshall Flumes," U.S. Department of Interior Bureau of Reclamation Report R-90-03, Denver, Colorado. (Dodge 1990, 094146)

DOE (U.S. Department of Energy), October 1987. "Phase 1: Installation Assessment, Los Alamos National Laboratory, Volumes 1 and 2, Comprehensive Environmental Assessment and Response Program," Albuquerque Operations Office, Albuquerque, New Mexico. (DOE 1987, 052975)

Dunne, T., and L.B. Leopold, 1978. "Water in Environmental Planning," W.H. Freeman and Company, San Francisco, California, pp. 128–129. (Dunne and Leopold 1978, 084459)

Fetter, C.W., 1994. Applied Hydrogeology, 3rd Ed., Macmillan College Publishing Company, New York, New York. (Fetter 1994, 070942)

Gardner, J.N., A. Lavine, G.WoldeGabriel, D. Krier, D. Vaniman, F. Caporuscio, C. Lewis, P. Reneau, E. Kluk, and M.J. Snow, March 1999. "Structural Geology of the Northwestern Portion of Los Alamos National Laboratory, Rio Grande Rift, New Mexico: Implications for Seismic Surface Rupture Potential from TA-3 to TA-55," Los Alamos National Laboratory report LA-13589-MS, Los Alamos, New Mexico. (Gardner et al. 1999, 063492)

Katzman, D., February 2000. "Summary Status of Environmental Restoration Project Investigations in Upper Sandia Canyon," Los Alamos National Laboratory document LA-UR-00-777, Los Alamos, New Mexico. (Katzman 2000, 064349)

Kennedy, W.R., May 11, 1971, "Radiochemical and Chemical Analyses of Water," letter to W.E. Hale, (U.S. Geological Survey, Albuquerque, New Mexico) from W.R. Kennedy (Associate Group Leader, H 8-468, Los Alamos Scientific Laboratory), Los Alamos, New Mexico. (Kennedy 1971, 033896)

Kirkpatrick, A.D., January 2005. "Assessing Constructed Wetlands for Beneficial Use of Saline-Sodic Water," M.S. Thesis, Montana State University, Bozeman, Montana. (Kirkpatrick 2005, 094133)

Kleinfelder, September 2002. "Report of Pre-Conceptual Geotechnical Investigations, Advanced Hydrotest Facility Project, TA-53, Los Alamos National Laboratory, Los Alamos, New Mexico," Project No. C59010120, Albuquerque, New Mexico. (Kleinfelder 2002, 091687)

Kleinfelder, February 2005. "Final Completion Report, Characterization Well R-11, Los Alamos National Laboratory, Los Alamos, New Mexico," Project No. 37151, Albuquerque, New Mexico. (Kleinfelder 2005, 094154)

Kleinfelder, 2006. "Well Rehabilitation Report for Characterization Well R-12, Los Alamos National Laboratory, Los Alamos, New Mexico," Project No. 73885, Albuquerque, New Mexico. (Kleinfelder 2006, in preparation)

Langmuir, D. 1997, *Aqueous Environmental Geochemistry*, Prentice-Hall, Inc., Upper Saddle River, New Jersey. (Langmuir 1997, 056037)

LANL (Los Alamos National Laboratory), September 1999, "Work Plan for Sandia Canyon and Canada Del Buey," Los Alamos National Laboratory document LA-UR-99-3610, Los Alamos, New Mexico. (LANL 1999, 064617)

LANL (Los Alamos National Laboratory), June 2005. "Groundwater Background Investigation Report," Los Alamos National Laboratory document LA-UR-05-2295, Los Alamos, New Mexico. (LANL 2005, 090580)

LANL (Los Alamos National Laboratory), November 2005. "Well Screen Analysis Report," Los Alamos National Laboratory document LA-UR-05-8615, Los Alamos, New Mexico. (LANL 2005, 091121)

LANL (Los Alamos National Laboratory), March 2006. "Interim Measures Work Plan for Chromium Contamination in Groundwater," Los Alamos National Laboratory document LA-UR-06-1961, Los Alamos, New Mexico. (LANL 2006, 091987)

LANL (Los Alamos National Laboratory), June 2006. "Interim Facility-Wide Groundwater Monitoring Plan, Revision 1.1.2," Los Alamos National Laboratory document LA-UR-06-4975, Los Alamos, New Mexico. (LANL 2006, 094043)

LANL (Los Alamos National Laboratory), June 2006. "Work Plan for R-Well Rehabilitation and Replacement," Los Alamos National Laboratory document LA-UR-06-3687, Los Alamos, New Mexico. (LANL 2006, 092535)

LANL (Los Alamos National Laboratory), July 2006. "Drilling Work Plan for Regional Monitoring Well R-35," Los Alamos National Laboratory document LA-UR-06-3964, Los Alamos, New Mexico. (LANL 2006, 093388)

LANL (Los Alamos National Laboratory), August 25, 2006. "Response to the Approval with Modification Letter Issued by NNMED on May 8, 2006, to the Interim Measures Work Plan for Chromium Contamination in Groundwater," Los Alamos National Laboratory letter to J. Bearzi (NMED HWB) from A. Phelps (Associate Director, Environmental Programs, LANL) and D. McInroy (Deputy Program Director, Corrective Actions), Los Alamos, New Mexico. (LANL 2006, 094129)

LANL (Los Alamos National Laboratory), October 2006. "Mortandad Canyon Investigation Report," Los Alamos National Laboratory document LA-UR-06-6752, Los Alamos, New Mexico. (LANL 2006, 094161)

LANL (Los Alamos National Laboratory), November 2006. "History of Water Treatment Chemicals Used at TA-03 Power Plan from 1951 through November 2006," prepared by J.V. Ortiz for Los Alamos National Laboratory Site Support Services, Los Alamos, New Mexico. (LANL 2006, 094153)

Lavine, A., C. Lewis, D. Katcher, J. Gardner, and J. Wilson, June 2003. "Geology of the North-Central to Northeastern Portion of Los Alamos National Laboratory New Mexico," Los Alamos National Laboratory report LA-14043-MS, Los Alamos, New Mexico. (Lavine et al. 2003, 092527)

- Lindsay, W.L. 1979, *Chemical Equilibria in Soils*, John Wiley & Sons, New York, New York. (Lindsay 1979, 071512)
- McBride, M. B. 1994, *Environmental Chemistry of Soils*, Oxford Press, New York, New York. (McBride 1994, 058947)
- Miller, E.L., July 30, 1971. "Effluent from Plant Cooling Towers," Los Alamos Scientific Laboratory memorandum to C. Christenson, Los Alamos Scientific Laboratory, Los Alamos, New Mexico. (Miller 1971, 03853)
- NMED (New Mexico Environment Department), December 29, 2005. "Interim Measures Work Plan Requirement, Groundwater Contaminants Detected in the Regional Aquifer at R-28," Los Alamos National Laboratory (LANL), EPA ID# NM0890010515, HWB-LANL-GW-MISC," New Mexico Environment Department letter to M. Johansen (DOE-LASO) and D. McInroy (EP-CA) from J. Bearzi (NMED-HWB), Santa Fe, New Mexico. (NMED 2005, 091683)
- NMED (New Mexico Environment Department), May 5, 2006. "Approval with Modifications for the Interim Measures Work Plan for Chromium in Groundwater," New Mexico Environment letter to M. Johansen (DOE-LAAO) from J. Bearzi (NMED), Santa Fe, New Mexico. (NMED 2006, 092543)
- NMED (New Mexico Environment Department), July 24, 2006. "Approval for the Drilling Work Plan for Regional Aquifer Wells R-35a and R-35b," New Mexico Environment letter to M. Johansen (NNSA), and D. McInroy (EP-CA), from J. Young (HWB-NMED), Santa Fe, New Mexico. (NMED 2006, 093530)
- Purtymun, W.D., December 1975. "Geohydrology of the Pajarito Plateau with Reference to Quality of Water, 1949–1972," Los-Alamos Scientific Laboratory document LA-UR-02-4726, Los Alamos, New Mexico. (Purtymun 1975, 011787)
- Rai, D., C.C. Ainsworth, L.E. Eary, S.V. Mattigod, and D.R. Jackson, August 1987. "Inorganic and Organic Constituents in Fossil Fuel Combustion Residues, Volume 1: A Critical Review, " (Electric Power Research Institute. (Rai et al 1987, 091686)
- Rai, D., and J.M. Zachara, May 1986."Geochemical Behavior of Chromium Species," Electric Power Research Institute. (Rai and Zachara 1986, 091684)
- Reinig, L.P., March 7, 1972. "Preliminary Report – Chromate Problem," memorandum to distribution, Los Alamos Scientific Laboratory from L.F. Reinig, Los Alamos, New Mexico. (Reinig 1972, 003848)
- Ryti, R., P.A. Longmire, D.E. Broxton, S.L. Reneau, and E.V. McDonald, May 1998. "Inorganic and Radionuclide Background Data for Soils, Canyon Sediments, and Bandelier Tuff at Los Alamos National Laboratory," Los Alamos National Laboratory document LA-UR-98-4847, Los Alamos, New Mexico. (Ryti et al. 1998, 059730)
- Shaul, D.A., D. Ortiz, M.R. Alexander, and R.P. Romero, May 2006. "Surface Water Data at Los Alamos National Laboratory 2005 Water Year," Los Alamos National Laboratory report LA-14239-PR, Los Alamos, New Mexico. (Shaul et al. 2006, 093735)
- Spitz, K., and J. Moreno, 1996. *A Practical Guide to Groundwater and Solute Transport Modeling*. John Wiley & Sons, Inc., New York, New York. (Spitz and Moreno, 1996, 085503)
- Warner, C.L., December 10, 1971. "Potassium Dichromate Entrainment in OWR Cooling Tower Drift," memo to OWR Committee, Los Alamos Scientific Laboratory, Los Alamos, New Mexico. (Warner 1971, 04251)
- Zia Company, February 1, 1972. "Conceptual Design Report for Chemical Reduction System, TA-3 Power Plant, Los Alamos, New Mexico." (Zia 1972, 003855)

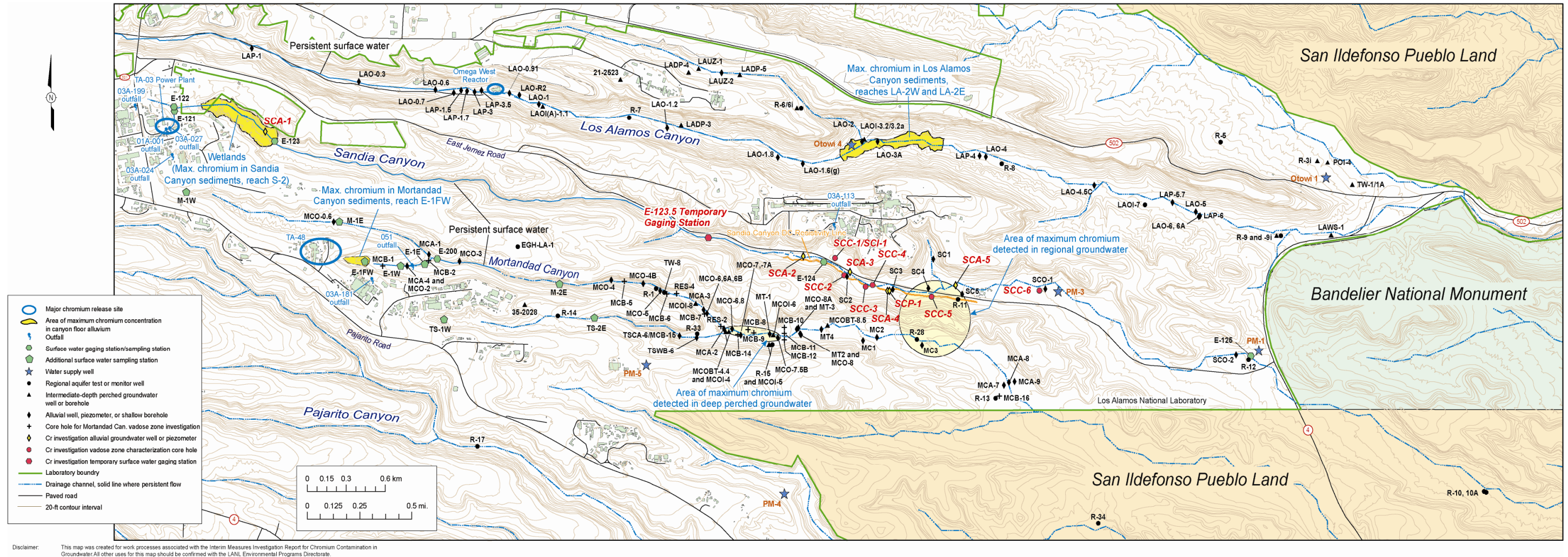


Figure 2.0-1. Location of Sandia, Los Alamos, and Mortandad canyons showing major chromium release sites, stream-flow gages, surface water sampling stations, and existing and newly installed boreholes and wells.

This page intentionally left blank.



**Figure 5.1-1.** Photographs of Parshall flume installed near E123 gaging station in upper Sandia Canyon, looking upstream (upper) and downstream (lower).

Los Alamos National Laboratory

HYPLOT V129 Output 11/13/2006

Period 8 Day PlotStart 00:00\_10/20/2006

2006

Interval 20 Minute PlotEnd 00:00\_10/28/2006

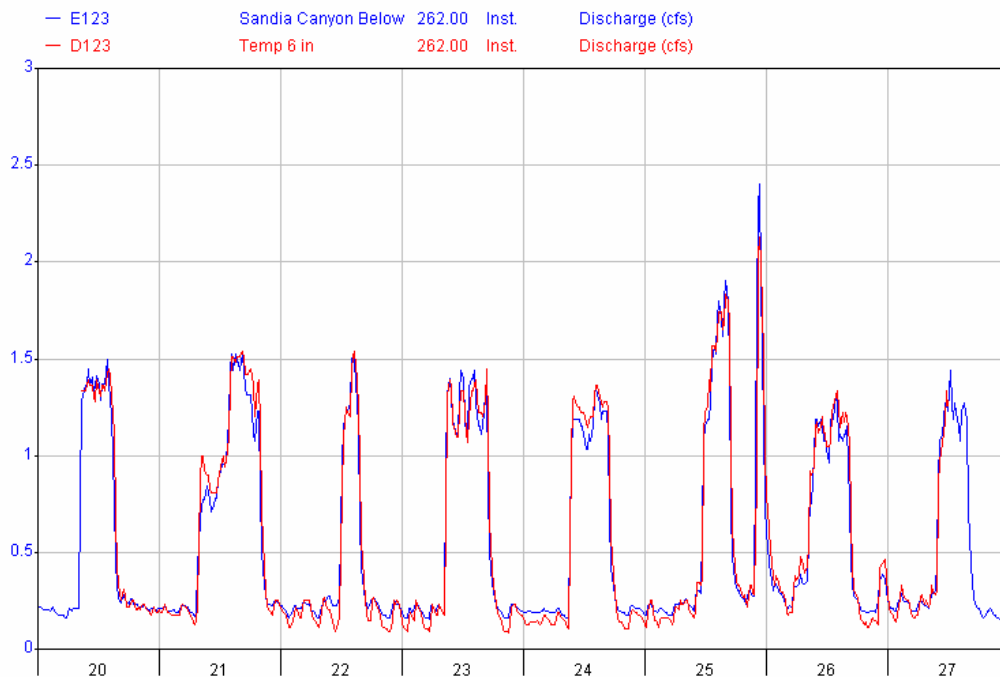


Figure 5.1-2. Comparison of hydrographs at gaging station E123 and at collocated Parshall flume (D123), October 20 through October 26, 2006.



Figure 5.1-3. Photograph of E123.5 gaging station in Sandia Canyon, September 2006, looking downstream.

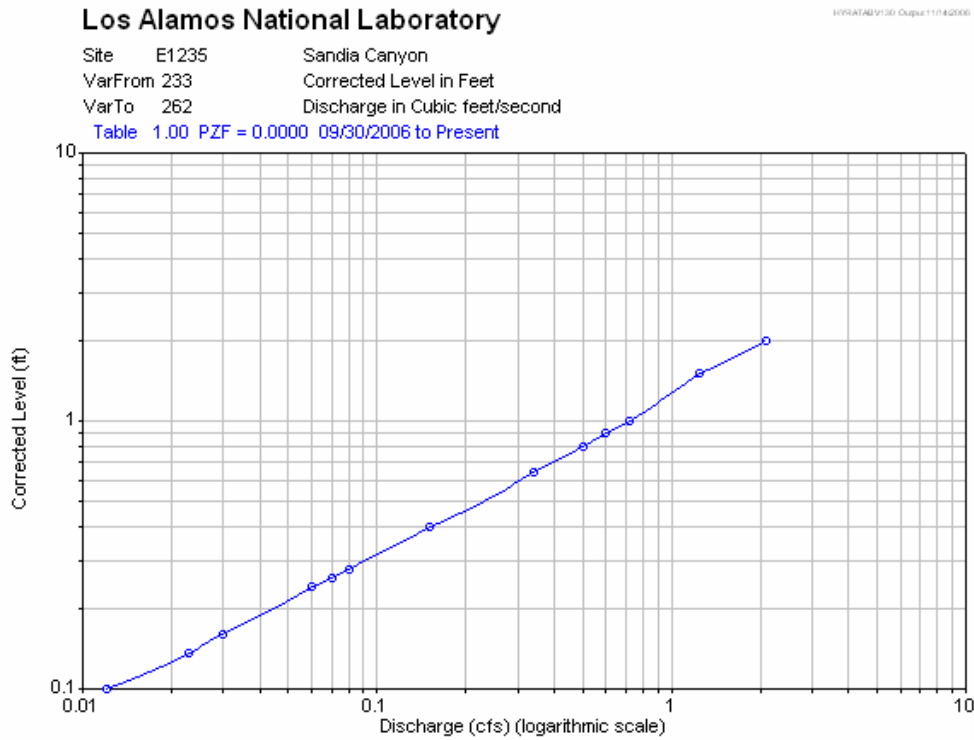


Figure 5.1-4. Rating curve at gaging station E123.5

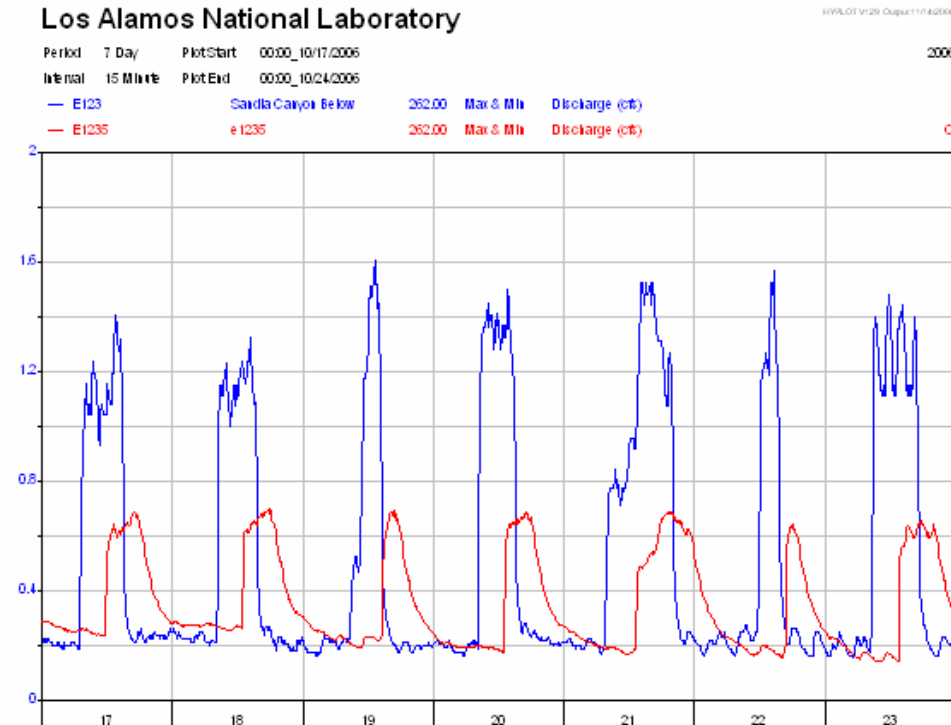


Figure 5.1-5. Comparison of hydrographs at gaging stations E123 and E123.5 from October 17 to October 23, 2006.

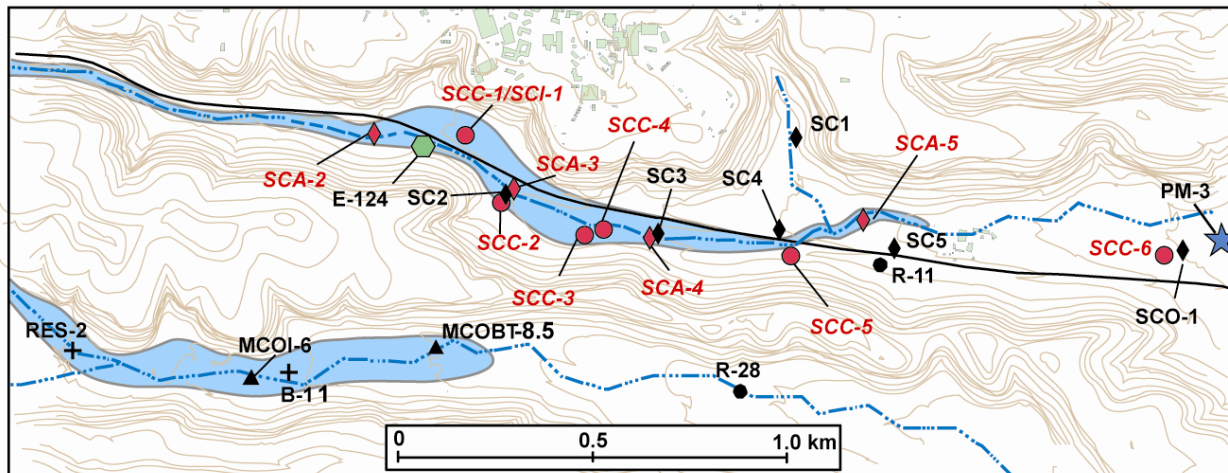


Figure 5.2-1. Map of eastern extent of alluvial saturation in Mortandad and Sandia Canyons

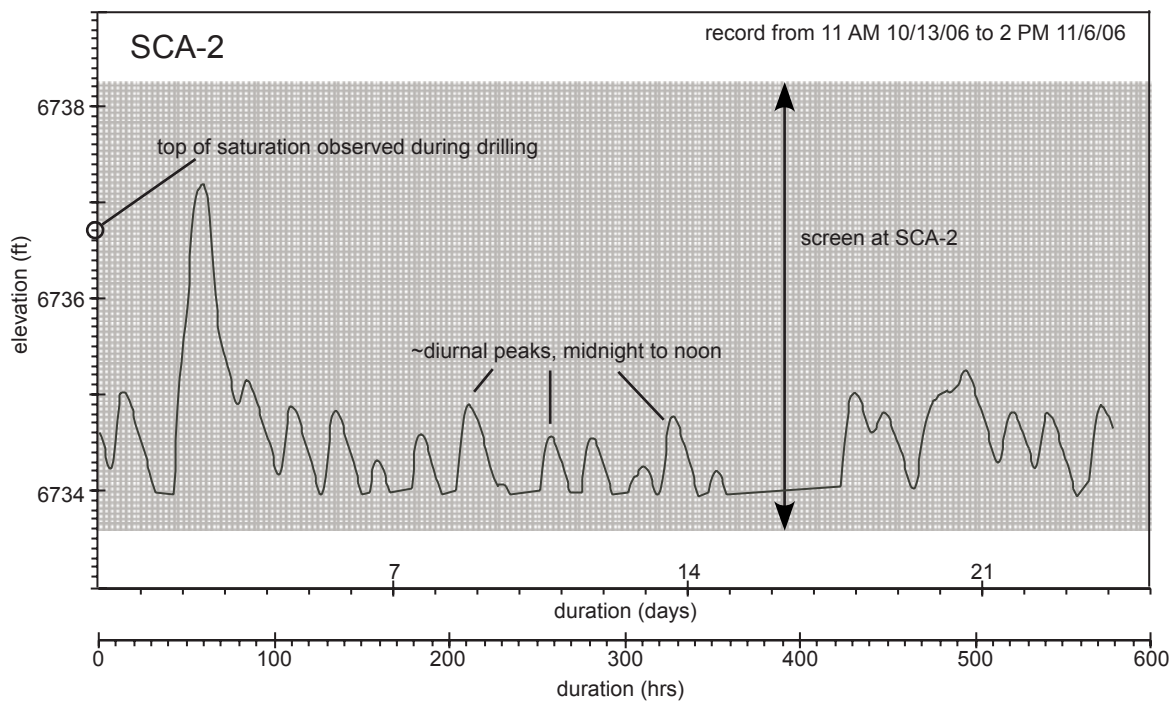
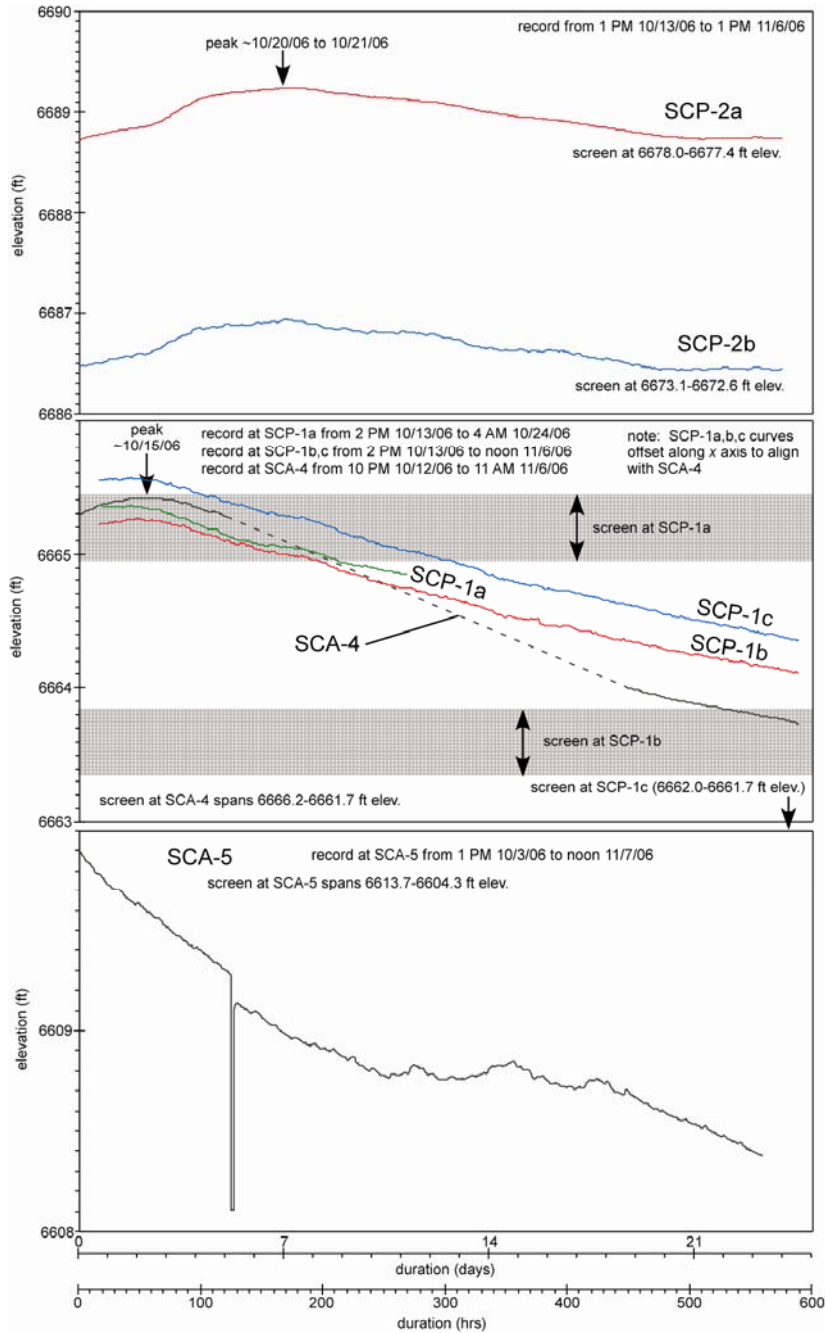


Figure 5.2-2. Transducer data collected between October 13th and November 7th 2006, at SCA 2. Screen location is shown.



**Figure 5.2-3.** Transducer data collected between October 12th and November 7th 2006, at SCP-2a,b (top panel), SCA-4 and nearby piezometers SCP-1a,b,c (midpanel), and SCA-5 (bottom panel). The record at SCP-1a ends where the top of saturation dropped below the screen in that piezometer. The record at SCA-4 includes a data gap (dashed line). The record at SCA-5 shows a sharp water-level decline during the 5th day of data collection as a result of sampling.

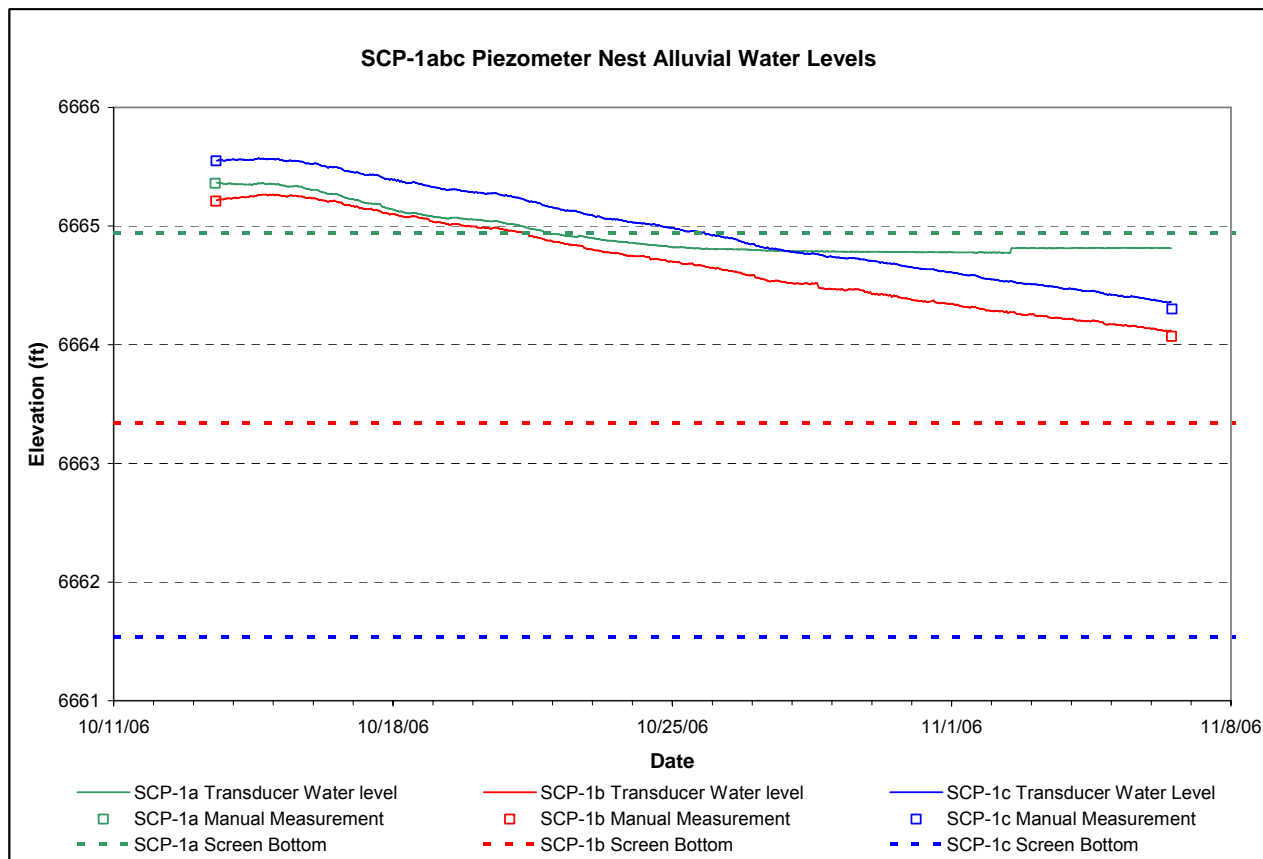


Figure 5.3-1. SCP-1a,b,c piezometer nest water levels

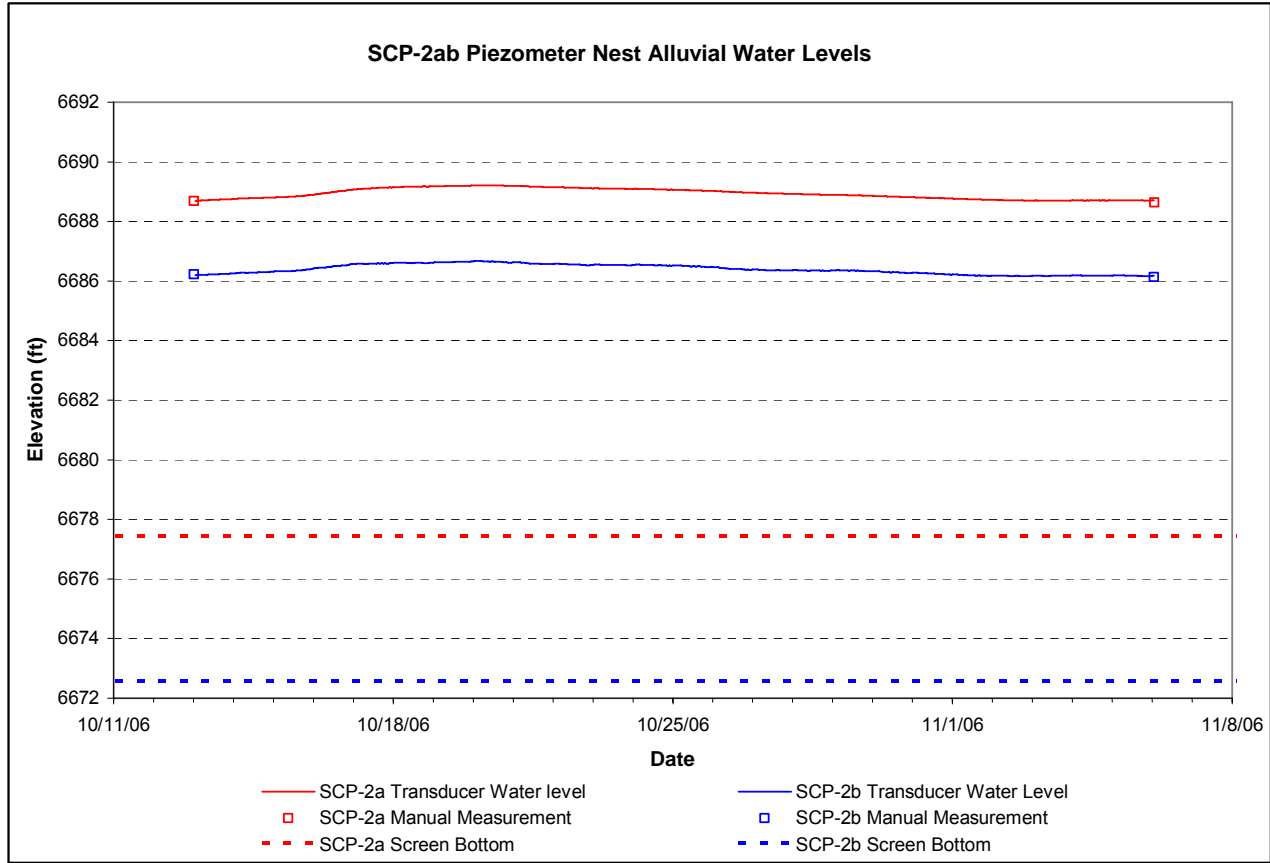


Figure 5.3-2. SCP-2a,b piezometer nest water levels

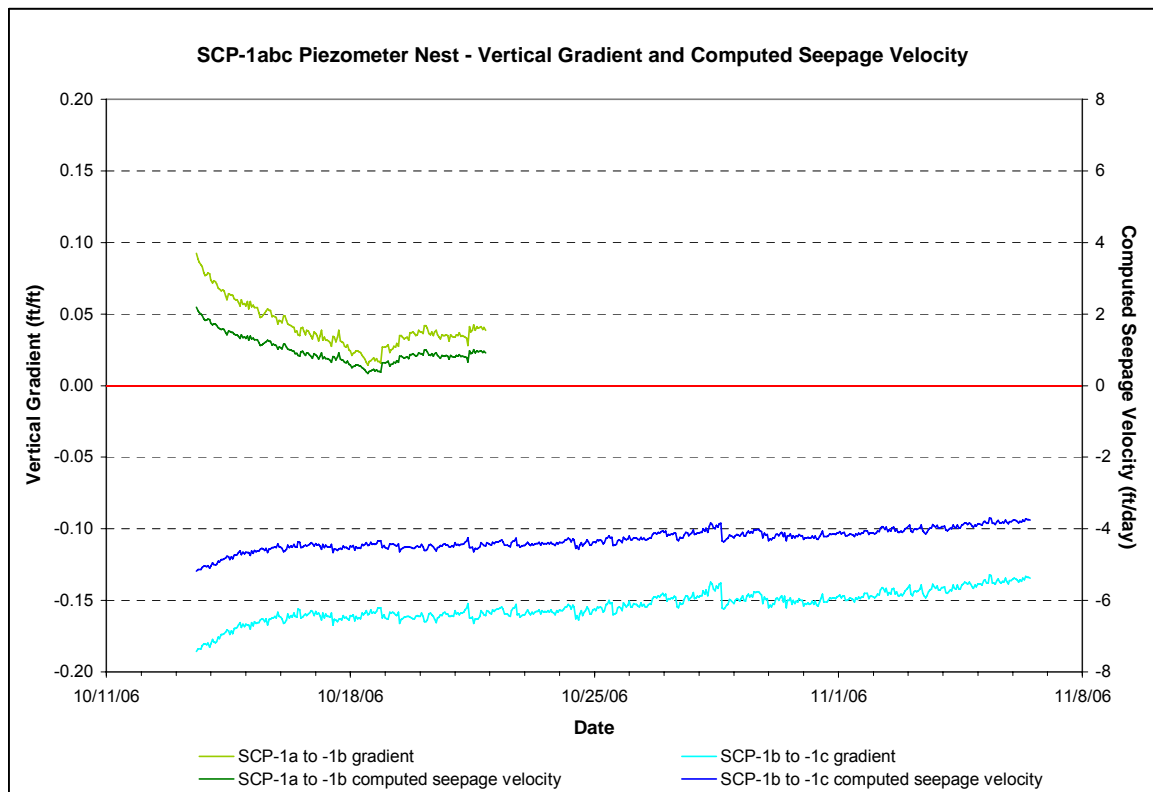


Figure 5.3-3. SCP-1a,b,c vertical gradient and computed seepage velocity

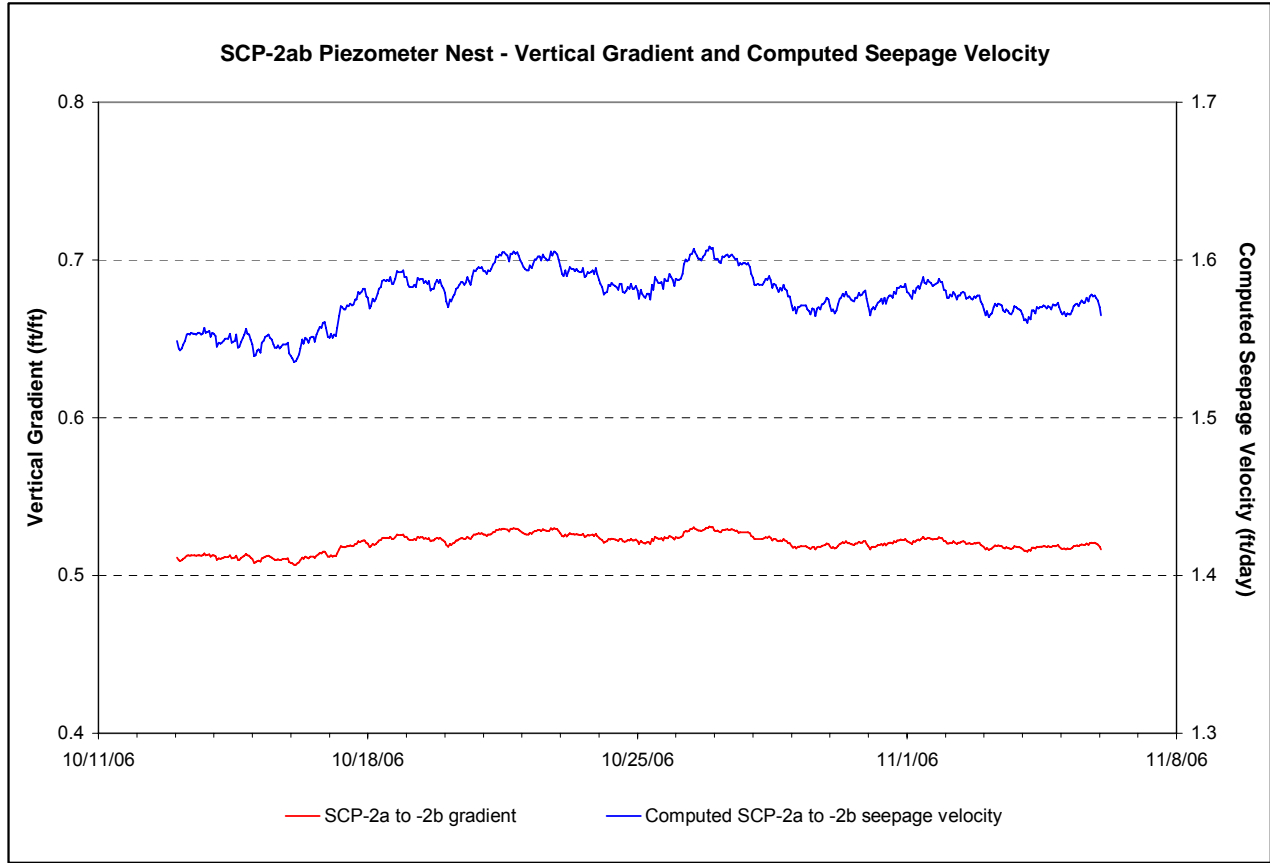
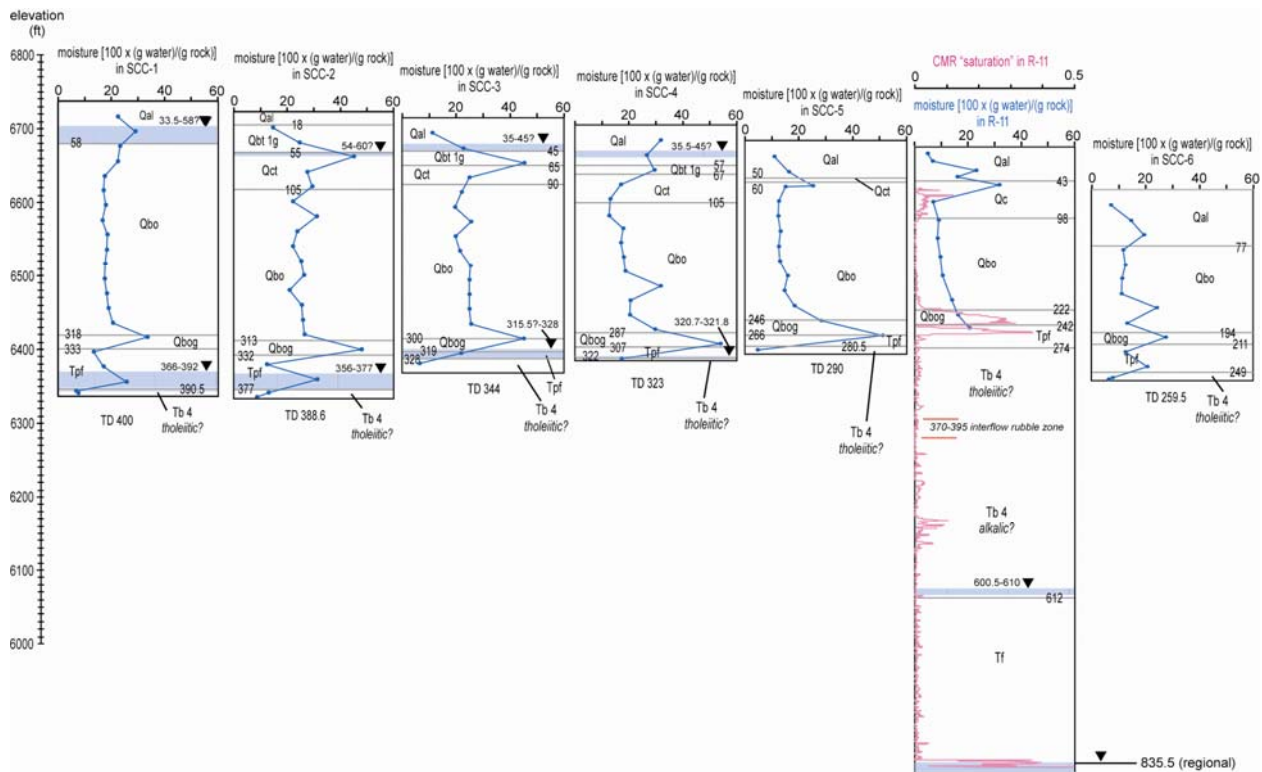
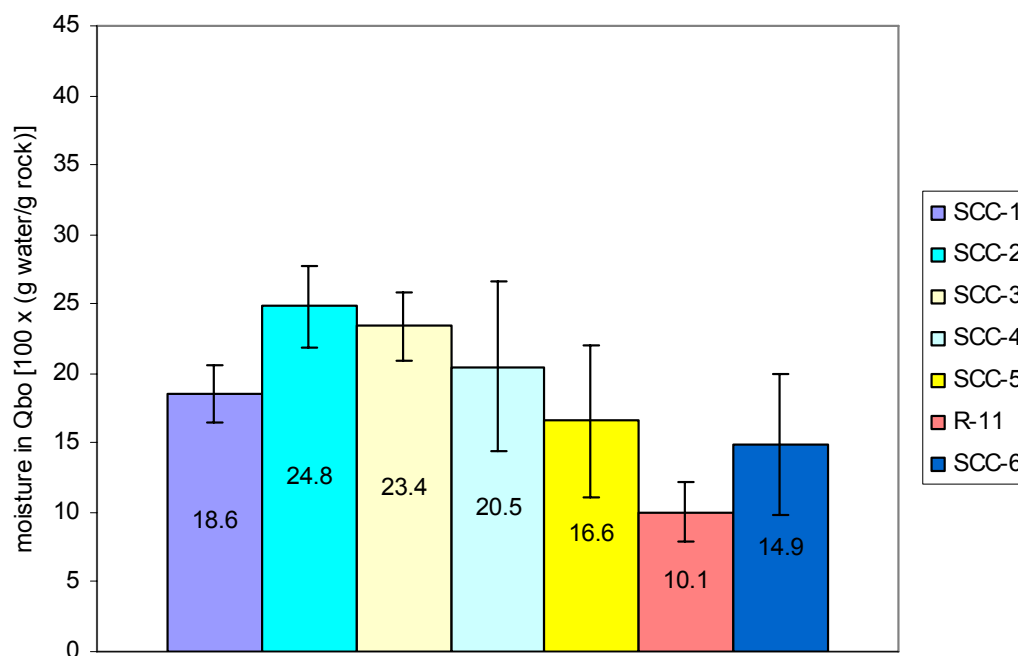


Figure 5.3-4. SCP-2a,b vertical gradient and computed seepage velocity



**Figure 5.4-1. Borehole stratigraphies with core moisture data and presence of saturated horizons superimposed (all elevations and depths are in feet). For regional drill hole R-11, the calculated volume fraction of pore space “saturated” is shown as estimated from the Schlumberger combined magnetic resonance (CMR) log.**



**Figure 5.4-2. Histograms of averaged moisture content (100 x g water/g solid) collected from core samples of ash flows of the Otowi Member of the Bandelier Tuff beneath lower Sandia Canyon. Error bars are 1 standard deviation.**

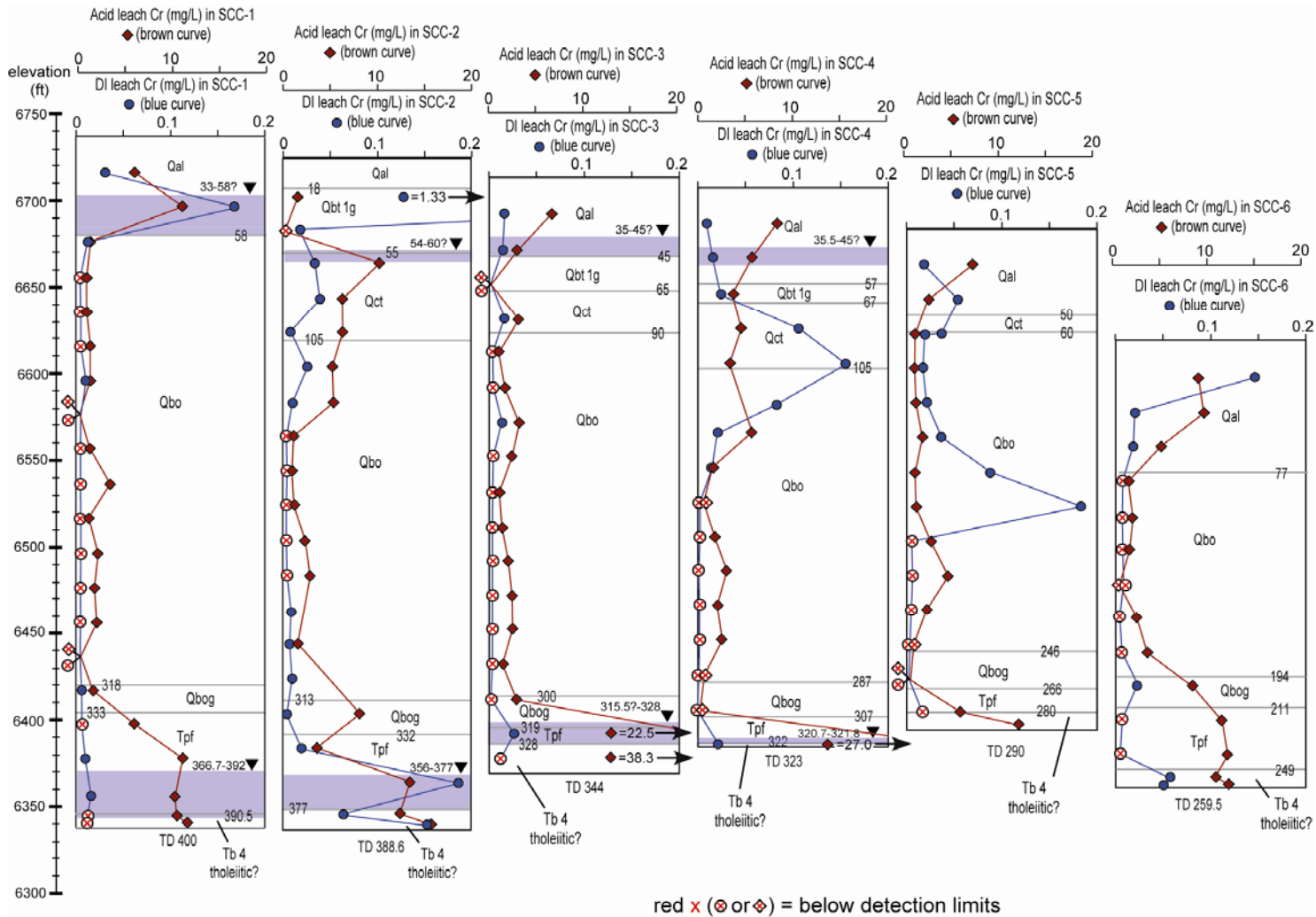
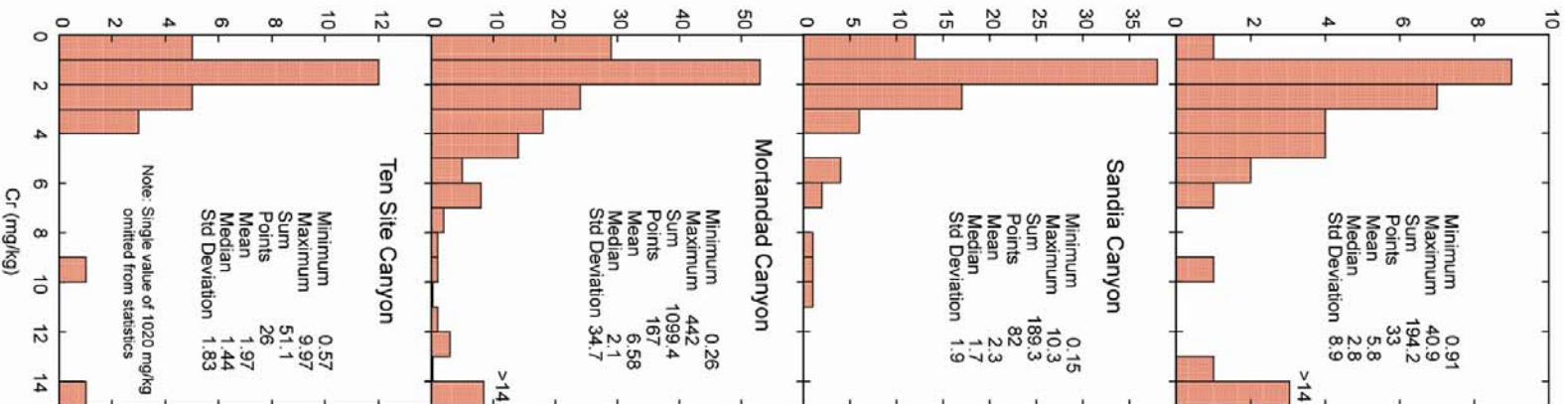
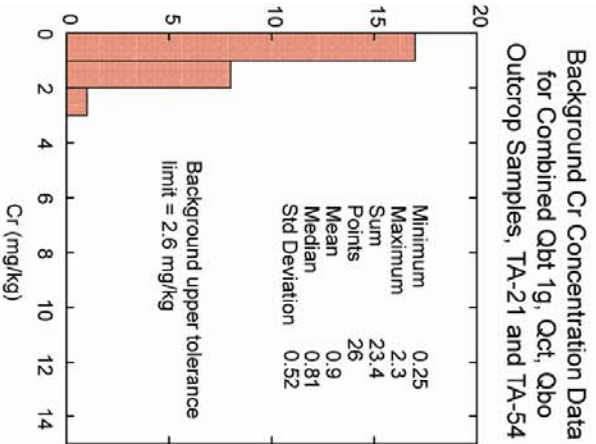


Figure 5.5-1. Profiles of acid-soluble chromium and pore-water dissolved chromium concentrations determined from core samples in core holes SCC-1, SCC-2, SCC-3, SCC-4, SCC-5 and SCC-6.



**Figure 5.5-2.** Histograms comparing chromium concentrations in weak nitric acid leachate (3050 method) for combined Qbt 1g, Qct, Qbo, and Qbog core samples collected from Los Alamos, Sandia, Mortandad, and Ten Site canyons. Chromium data used to compute the LANL background value for the combined Qbt 1g, Qct, Qbo, and Qbog back ground unit (Ryti et al. 1998, 59730) is shown on the left for comparison.

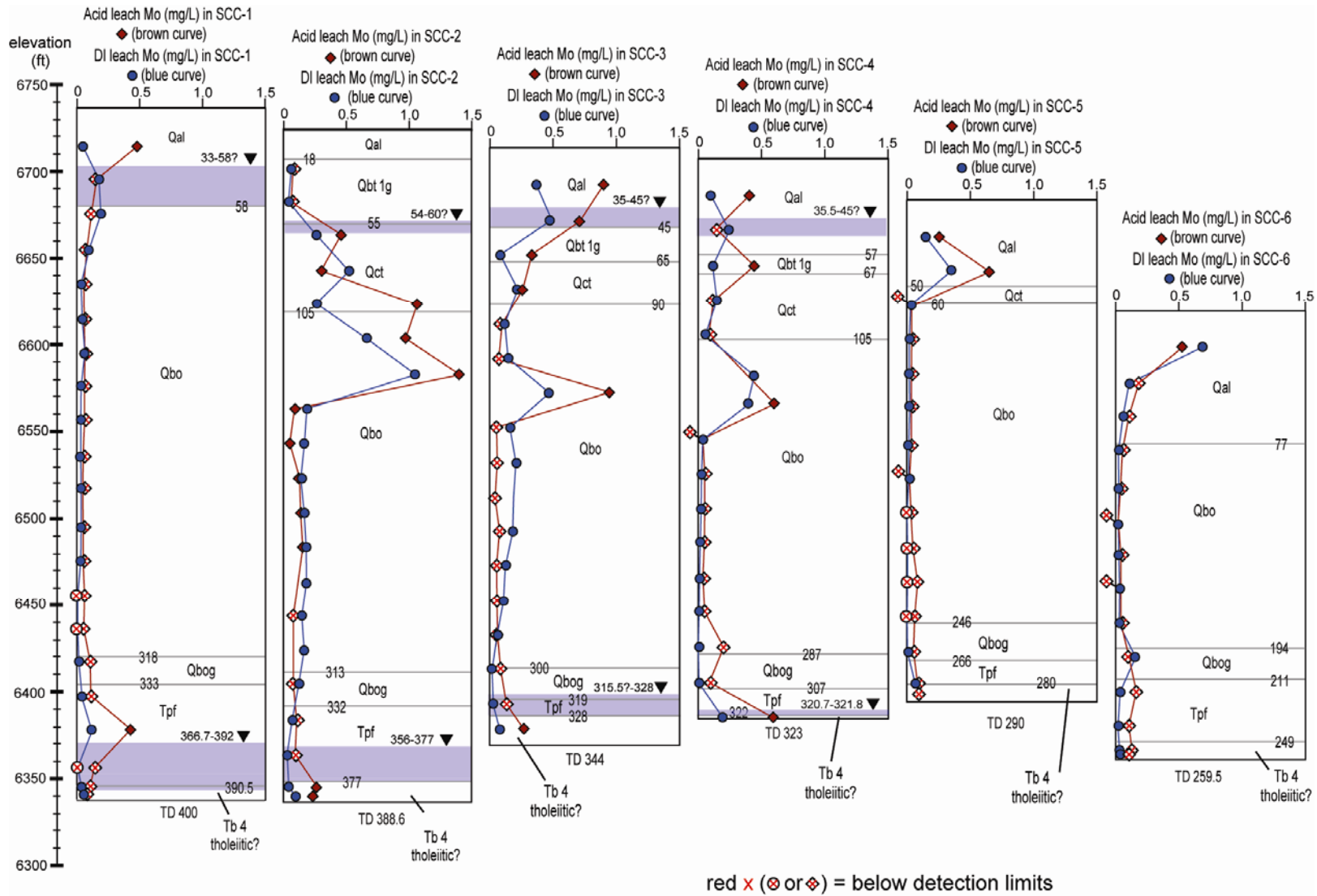


Figure 5.5-3. Profiles of acid-soluble molybdenum and pore-water dissolved molybdenum concentrations determined from core samples in core holes SCC-1, SCC-2, SCC-3, SCC-4, SCC-5 and SCC-6.

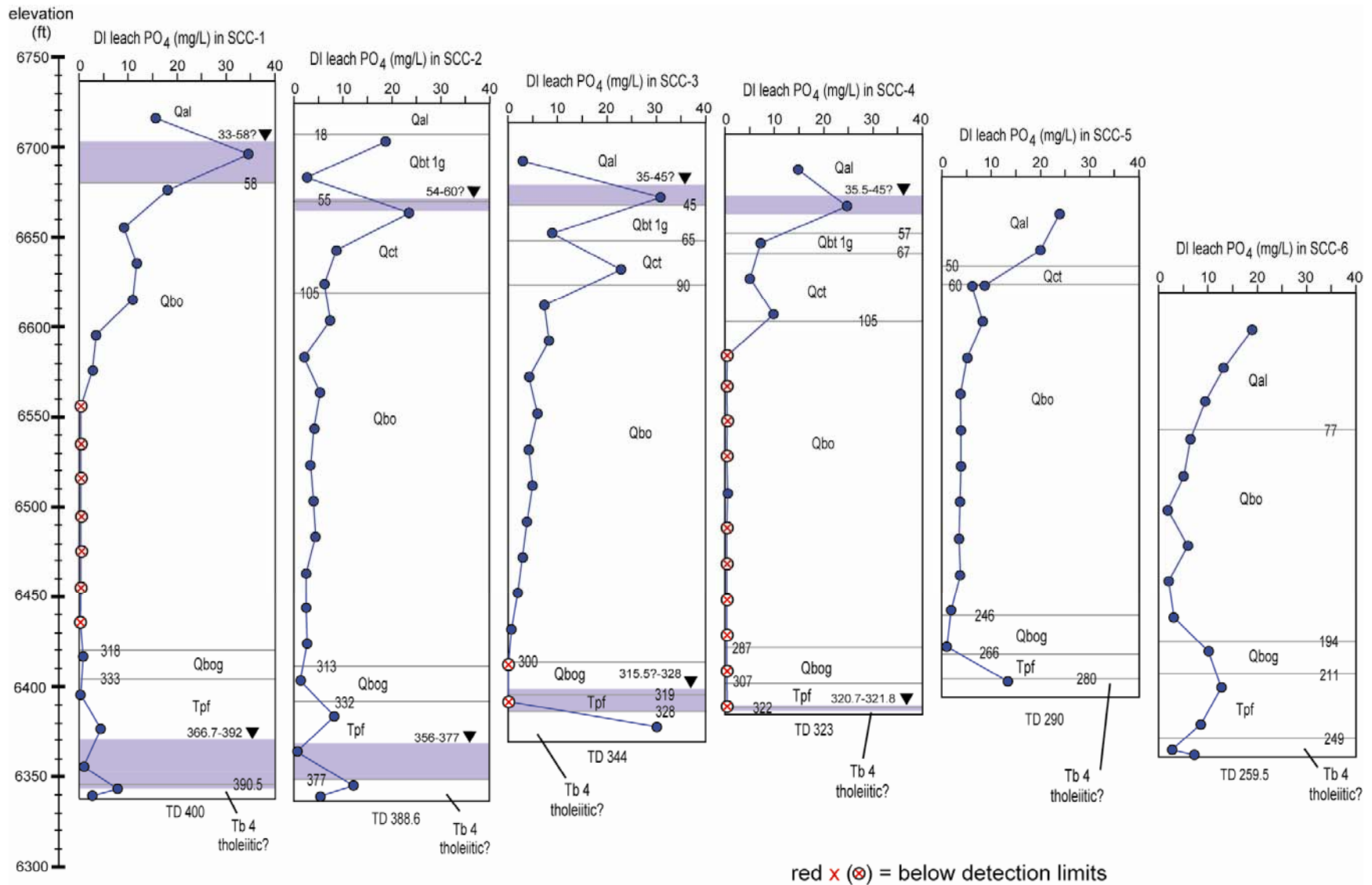


Figure 5.5-4. Profiles of pore-water dissolved phosphate concentrations determined from core samples in core holes SCC-1, SCC-2, SCC-3, SCC-4, SCC-5 and SCC-6.

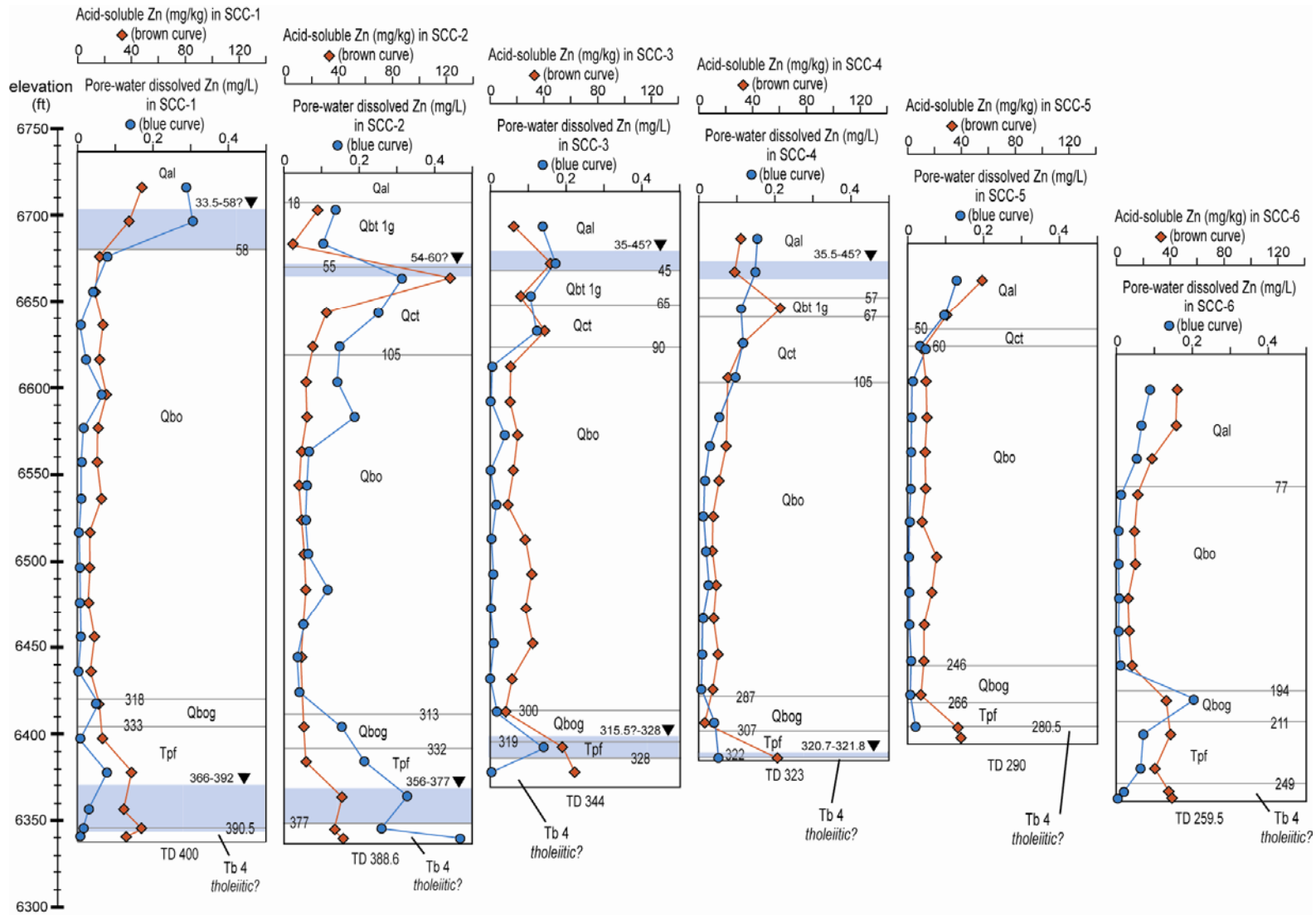


Figure 5.5-5. Profiles of acid-soluble zinc and pore-water dissolved zinc concentrations determined from core samples in core holes SCC-1, SCC-2, SCC-3, SCC-4, SCC-5 and SCC-6.

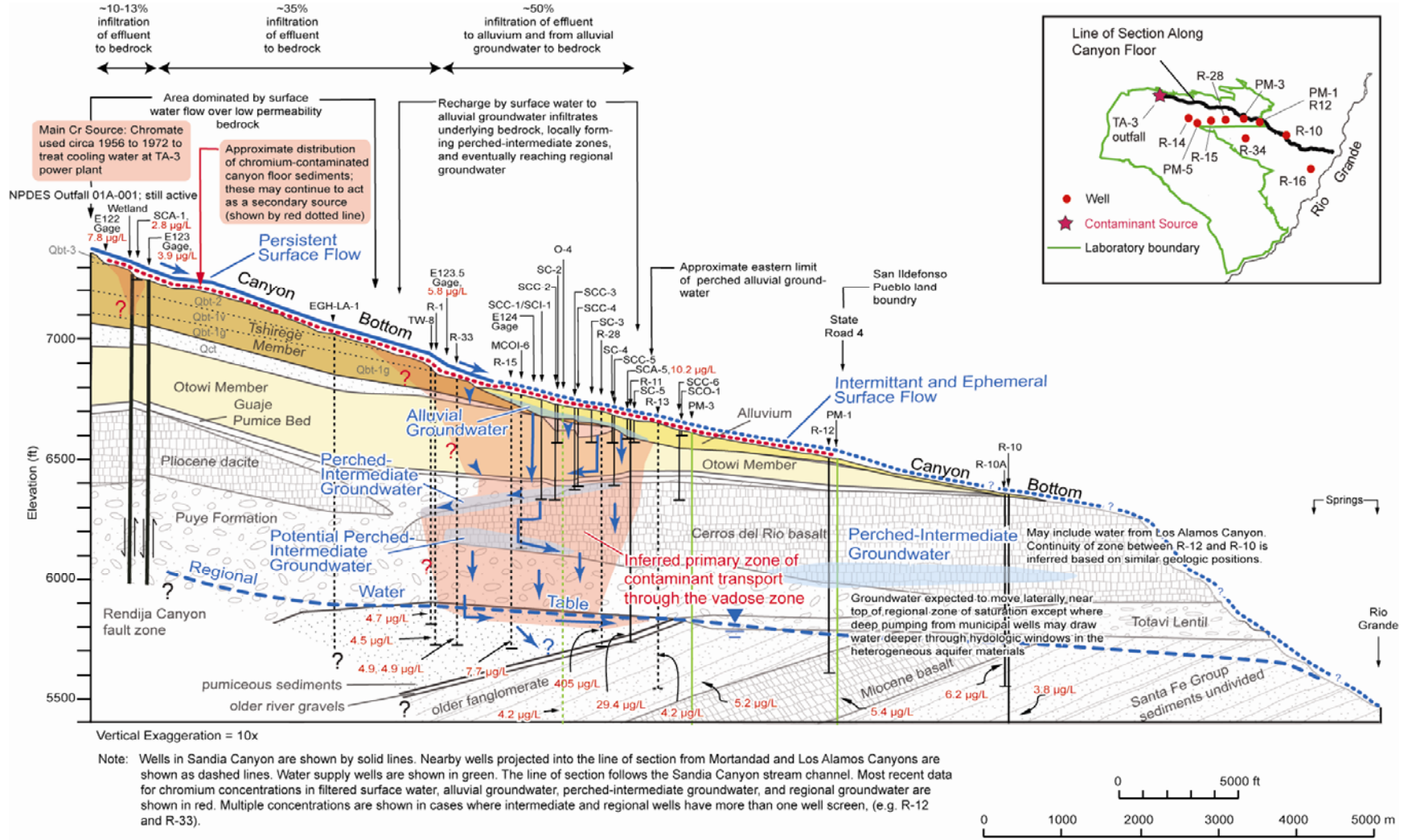


Figure 6.0-1. Conceptual hydrogeologic cross section showing potential chromium transport pathways and dissolved hexavalent chromium values (µg/L) for surface water, monitoring wells, and water supply wells in the vicinity of Sandia Canyon.

This page intentionally left blank.

**Table 2.0-1  
Water Treatment Chemicals Used at the Technical Area 3 Power Plant**

Date	Product	Use	Chemicals	Notes
1951 to June 1956	Unknown	Corrosion/deposition control	Polyphosphate/Sulfuric acid	
June 1956 to April 1972	Betz (formula not known)	Corrosion/deposition control	Phosphate/chromate/zinc	Zinc dianodic treatment. (Phosphate may have been as hexametaphosphate); various Betz fungicides, biocides and dispersants added at various times
April 1972 to November 1975	Betz 602 & 419	Corrosion and scale control; dispersant		Chromate use stopped April 1972 replaced with polynodic phosphonate
November 1975 to December 1980	Betz 602 & 431	Corrosion and scale control; dispersant	Polynodic phosphonate	Changed from Betz 419 dispersant to Betz 431 dispersant
December 1980 to 1993	Betz 2020	Scale inhibitor	Calcium phosphate	Part of Dianodic II program (non-chromate based)
	Betz 562C	Corrosion inhibitor	NaOH and 1-H-benzotriazole, methyl	Part of Dianodic II program (non-chromate based)
1993 to 2001	Garratt-Callahan Formula 314-T	Biocide (organic halogen donor)	Chlorine and Bromine	None
	Garratt-Callahan Formula 2010	Cooling water corrosion and scale control	2-phosphono-1,2,4-butane-carboxylic acid, sodium molybdate, benzotriazole	None
	Garratt-Callahan Formula 159	Boiler feedwater oxygen scavenger	Sodium bisulfite	None
2001 to 2006 (present)	Nalco Stabrex ST20	Microorganism control	Alkaline liquid bromine, sodium hydroxide (1-5%)	None
	Nalco 7408	Chlorine scavenger	Sodium bisulfite (30-60%)	None
	Nalco 7384	Corrosion inhibitor	Inorganic salts, zinc chloride (60-100%)	None
	Nalco Trasar 23268	Cooling water treatment	Acrylate polymers, organic compound, listed hazard: sodium tolyltriazole (1-5%)	None

**Table 2.0-2**  
**Estimates of Chromium(VI) Releases at the TA-03 Power Plant**  
**All estimates assume time period of release from June, 1956 to April, 1972 (5814 days)**

Estimates	Information used	Total release of chromium(VI), kg (lb)	Reference
Estimate 1	16.3 kg/day (35.9 lb/day as CrO <sub>4</sub> )	43,000 kg (94,000 lb)	(DOE 1987, page TA3-13, 52975);(Reinig 1972, 3848)
Estimate 2	30 to 35 ppm (as CrO <sub>4</sub> ); 485 to 1091 m <sup>3</sup> /day (128,000 to 288,000 gal/day) as blowdown	38,000 to 100,000 kg (83,000 to 220,000 lb)	(DOE 1987, page TA3-13, 52975); (Reinig 1972, 3848); (Zia 1972, 3855)
Estimate 3	30 to 40 ppm (as CrO <sub>4</sub> ); 947 m <sup>3</sup> /day (250,000 gal/day) as blowdown	74,000 to 99,000 kg (163,000 to 220,000 lb)	Estimate from Phoenix Industrial and Nuclear Products Company, Inc. (Birdsell 2006, 091685)
Estimate 4	9.6 (+0.3) to 16.3 (+0.3) (Cr <sup>+6</sup> , mg/L); 485 to 1091 m <sup>3</sup> /day (128,000 to 288,000 gal/day) as blowdown	26,000 to 105,000 kg (58,000 to 230,000 lb)	(Kennedy 1971, Table IV, 33896), (DOE 1987, page TA3-13, 52975); (Reinig 1972, 3848); (Zia 1972, 3855)

**Table 2.0-3**  
**Water Discharge Volumes for 2003, 2004, and 2005 for Five Active NPDES Outfalls Discharging to Sandia Canyon**

Name	Outfall	2003		2004		2005	
		MG/Y	(m <sup>3</sup> /day)	MG/Y	(m <sup>3</sup> /day)	MG/Y	(m <sup>3</sup> /day)
SWWS	13S	92.527	959.56	104.07	1079.23	107.30	1112.73
POWER PLANT	001	38.9	403.42	4.78	49.61	3.31	34.33
<b>Total Power Plant plus SWWS</b>	<b>001</b>	<b>131.427</b>	<b>1362.98</b>	<b>108.85</b>	<b>1128.84</b>	<b>110.61</b>	<b>1147.06</b>
Sigma Complex	03A024	0	0.00	0.00	0.00	0.00	0.00
SCC	03A027	8.02	83.17	6.93	71.86	9.58	99.33
LANSCE	03A113	0.9673	10.03	0.65	6.75	0.39	4.07
<b>Total flow to Watershed</b>		<b>140.41</b>	<b>1456.19</b>	<b>116.43</b>	<b>1207.45</b>	<b>120.58</b>	<b>1250.45</b>

**Table 5.1-1**  
**Outfall Discharge Data from TA-03 into Upper Sandia Canyon for WY06**

Month	Average Daily Discharge <sup>a</sup> , Outfall 001 (MG) <sup>b</sup>	Average Daily Discharge, Outfall 03A027 (MG)	Average Daily Discharge, Outfall 03A199 (MG)	Estimated Total Average Daily Discharge (MG)	Estimated Total Average Daily Discharge (acre-ft)	Estimated Monthly Discharge (acre-ft)
October 2005	0.315	0.0264	0.0432	0.3846	1.180	36.6
November 2005	0.2798			0.3494	1.072	32.2
December 2005	0.3013			0.3709	1.138	35.3
January 2006	0.3274	0.02823	0.0576	0.4132	1.268	39.3
February 2006	0.2844			0.3702	1.136	31.8
March 2006	0.31814			0.4040	1.240	38.4
April 2006	0.2879	0.03616	0.0360	0.3601	1.105	33.1
May 2006	0.2892			0.3614	1.109	34.4
June 2006	0.29290			0.3651	1.120	33.6
July 2006	0.30900	0.03161	0.0432	0.3838	1.178	36.5
August 2006	0.35026			0.4251	1.304	40.4
September 2006	0.29888			0.3737	1.147	34.4
Total						426

<sup>a</sup> Outfall data obtained from Environmental Stewardship–Resource Conservation and Recovery Act.

<sup>b</sup> MG = millions of gallons.

**Table 5.1-2  
Comparison of Surface Flow at E123 with Outfall Discharges during WY06**

Period	Length of Period (days)	Total Discharge at E123 (acre-ft) <sup>a</sup>	Estimated Discharge from TA-03 Outfalls (acre-ft) <sup>b</sup>	Estimated Loss Between Outfalls and E123 (acre-ft)	Estimated Average Daily Loss (acre-ft)	Average Temperature (degrees C) <sup>c</sup>	Precipitation in Previous 7 Days (in.) <sup>c</sup>
10/21/05-10/29/05	9	9.70	10.62	0.92	0.102	8.5	0.54
11/01/05-11/10/05	10	9.21	10.72	1.51	0.151	9.6	0.01
11/21/05-11/30/05	10	10.50	10.72	0.22	0.022	1.7	0.00
12/20/05-12/29/05	10	9.40	11.38	1.98	0.198	4.0	0.01
1/12/06-1/22/06	11	12.62	13.95	1.33	0.121	-0.8	0.00
3/14/06-3/18/06	5	5.16	6.20	1.04	0.208	5.5	0.13
4/13/06-4/26/06	14	11.37	15.47	4.10	0.293	12.2	0.01
5/24/06-5/31/06	8	6.25	8.87	2.62	0.328	18.4	0.06
6/12/06-6/21/06	10	6.66	11.20	4.54	0.454	22.7	0.22
7/11/06-7/17/06	7	8.57	8.25	-0.33	-0.047	22.6	1.07
8/27/06-08/31/06	5	5.50	6.52	1.02	0.204	18.8	2.55
9/24/06-9/30/06	7	7.52	8.03	0.51	0.073	13.2	0.19

<sup>a</sup> Discharge data obtained from Hydstra database.

<sup>b</sup> Based on average daily discharge data from Table B-x-1.

<sup>c</sup> Values from TA-06 meteorological station; data downloaded from <http://weather.lanl.gov/>.

**Table 5.1-3  
Total Estimated Water Loss above E123 during WY06**

Month	Days in Month	Calculated Average Daily Loss (acre-ft) <sup>*</sup>	Calculated Monthly Loss (acre-ft)
October 2005	31	0.102	3.2
November 2005	30	0.087	2.6
December 2005	31	0.198	6.1
January 2006	31	0.121	3.7
February 2006	28	0.164	4.6
March 2006	31	0.208	6.4
April 2006	30	0.293	8.8
May 2006	31	0.328	10.2
June 2006	30	0.454	13.6
July 2006	31	0.000	0.0
August 2006	31	0.204	6.3
September 2006	30	0.073	2.2
<b>Total</b>			<b>68</b>

<sup>\*</sup> Values based on data in Table B-x-2; no reliable data available for February and value for this month assumed to be average of adjacent months; value for July (a negative number) replaced by zero.

**Table 5.2-1a**  
**Initial Observations of Water Occurrence in SC Drill Holes**

Drill Hole	Depth to Water Encounter	Elevation of Water Encounter
SC-1	no alluvial or shallow suballuvial perched water noted	
SC-2	18.1 m (59.3 ft, in Qct)	2031.1 m (6663.7 ft)
SC-3	10.7 m (35 ft, in Qct)	2032 m (6668 ft)
SC-4	no alluvial or shallow suballuvial perched water noted	
SC-5	no alluvial or shallow suballuvial perched water noted	

**Table 5.2-1b**  
**Initial Observations of Water Occurrence in SCC Drill Holes**

Drill Hole	Depth to Water Encounter	Elevation of Water Encounter
SCC-1	10.1 m (33 ft, in Qal)	2043.6 m (6704.8 ft)
SCC-2	16.5 m (54 ft, in basal Qbt 1g)	2032.8 m (6669.3 ft)
SCC-3	10.7 m (35 ft, in Qal)	2035.3 m (6677.6 ft)
SCC-4	10.8 m (35.5 ft, in Qal)	2034.1 m (6673.5 ft)
SCC-5	no alluvial or shallow suballuvial perched water noted	
SCC-6	no alluvial or shallow suballuvial perched water noted	

**Table 5.2-1c**  
**Initial Observations of Water Occurrence in SCA Drill Holes**

Drill Hole	Depth to Water Encounter	Elevation of Water Encounter
SCA-1	Qal fully saturated to surface	2197.9 m (7211.2 ft)
SCA-2	3.63 m (11.9 ft, in Qal)	2053.3 m (6736.7 ft)
SCA-3	~9.2 m (~30.3 ft, in Qal)	~2039.8 m (~6692.4 ft)
SCA-4	~11 m (~36 ft, in Qal)	~2032.2 m (~6667.2 ft)
SCA-5	17.25 m (56.6 ft, in Qal)	2015.4 m (6612.1 ft)

**Table 5.3-1**  
**Sandia Canyon Piezometer Slug Test Results**

Piezometer	K (ft/day)*	K (cm/sec)
SCP-1a	8.53	3.01E-03
SCP-1b	10.87	3.83E-03
SCP-1c	12.03	4.24E-03
SCP-2a	90.00	3.18E-02
SCP-2b	1.03	3.63E-04

\* Summary of data from Table 3 in Appendix B-1.6.

This page intentionally left blank.

# **Appendix A**

---

## *Acronyms*



AHF Advanced Hydrotest Facility  
bgs below ground surface  
CEARP Comprehensive Environmental Assessment Response Program  
CMR combined magnetic resonance  
DC direct current  
DOE Department of Energy (U.S.)  
EES-6 Hydrology, Geochemistry, and Geology  
EPA Environmental Protection Agency (U.S.)  
ET evapotranspiration  
HE high explosive(s)  
HAS hollow-stem auger  
ICP inductively coupled plasma  
I.D. inside diameter  
IFGMP Interim Facility Groundwater Monitoring Plan  
LC liquid chromatography  
MCL maximum contaminant level  
MS mass spectrometry  
NMED New Mexico Environment Department  
NPDES National Pollutant Discharge Elimination System  
O.D. outside diameter  
PVC polyvinyl chloride  
SWC Sanitary Wastewater System  
SWMU solid waste management unit  
TA technical area  
TAL target analyte list  
TOC total organic carbon  
VOC volatile organic compound  
WQCC Water Quality Control Commission  
wt % weight percent  
WY water year



# **Appendix B**

---

*Field Investigation Methods and Results*



Field investigations for the “Interim Measures Work Plan for Chromium Contamination in Groundwater” (LANL 2006, 091987) included drilling investigations of alluvial and intermediate depth (Section B-1); collection, synthesis, and analysis of regional water-level data (Section B-2); and analysis of existing and new gage data for estimation of water balance and infiltration in Sandia Canyon (Section 5.1).

### **B-1.0 Drilling Investigations in Sandia Canyon for the Chromium Interim Measures Work Plan**

Drilling investigations in Sandia Canyon for the “Interim Measures Work Plan for Chromium Contamination in Groundwater” were conducted using three different methods. Using hand-auger methods, two alluvial wells were emplaced, one in the wetlands of upper Sandia Canyon (SCA-1) and one in a narrow reach downcanyon (SCA-2; location map, Figure 2.0-1). A CME 55 hollow-stem auger (HSA) track-mounted rig was used to install three other alluvial wells and two associated piezometer sets farther downcanyon (SCA-3 with associated piezometers SCP-2a,b; SCA-4 with associated piezometer nest SCP-1a,b,c; and SCA-5 without associated piezometers). Finally, a Speedstar 50K truck-mounted rig was used to collect both cuttings and core at six deeper holes (SCC-1 through SCC-6) that penetrated down to the top of the Cerros del Rio lavas. Several of the SCC-series holes were drilled at locations selected to investigate conductive (SCC-1, SCC-2, SCC-4, SCC-5) or resistive (SCC-3) zones as indicated from surface geophysics; all of the SCC-series holes investigated water and contaminant distributions through the vadose zone down to the Cerros del Rio lavas. Table B-1.0-1 summarizes some basic comparative information for all of the alluvial and intermediate holes. Table B-1.0-2 summarizes information for the two piezometers localities.

Core and borehole water samples were collected for analysis only from the SCC-series holes. Initial water sampling at some of the alluvial wells has taken place; data from these samples are in Appendix C-2 (on DVD). Piezometers will be used only for monitoring water levels and head data; no sampling of core, cuttings, or water was scheduled for the piezometers holes. Observations of drilling conditions and water occurrences are discussed below in Section B-1.1, along with a stratigraphic summary of the new geological data obtained through this drilling program. A summary of coring methods and core samples taken is provided in Section B-1.2; a comparable summary of water-sample collection during drilling is provided in Section B-1.3.

Borehole geophysics data (natural gamma and induction) were collected only for the SCC-series holes. The natural gamma data provide significant input to determining stratigraphic contacts, particularly for Tshirege unit Qbt 1g, the Cerro Toledo interval, and the Guaje Pumice Bed (Qbog). The natural gamma data also provide a means of mapping internal stratigraphy of the Otowi ash flows (Qbo). These data are described in Section B-1.4. Since the placement of core holes SCC-1 through SCC-5 was based in part on surface DC resistivity data for Sandia Canyon, a brief comparison of down-hole moisture and conductivity data from these holes with surface-based electrical data is provided in Section B-1.5.

Throughout the discussion in this appendix, reference can be made to Section B-1.6 for details of drilling history; core and water samples taken; logs collected; and features of hole completion as either well, piezometer, or abandonment. Section B-1.6 (on CD) provides the full text of the drill hole summaries prepared by Kleinfelder Inc. Included in these summaries, on a hole-by-hole basis, are tables listing core and water samples taken for analysis. Analysis results for these samples are tabulated in Appendix C (on DVD).

## B-1.1 Drilling Observations and Stratigraphic Summary

### Alluvial Wells

Alluvial well SCA-1 was hand augered to 0.67 m (2.2 ft) in fully saturated soil and organic matter at the eastern end of the wetlands at the Sandia Canyon headwaters (location map, Figure 2.0-1). Wooden planking provided access across saturated, spongy wetlands to the auger site. The upper 0.61 m (2.0 ft) of section is composed largely of silt with organic mat and phreatophyte root-zone growth. Below 0.61 m (2.0 ft) there is a transition to sandy silt composed largely of detritus from the devitrified Tshirege Member of the Bandelier Tuff. The prepack screen at SCA-1 (0.40-0.58-m [1.3-1.9-ft] depth) is above the stratigraphic transition at 0.61 m (2.0 ft), but the filter pack of 10/20 sand extends from 0.24 m (0.8 ft) slightly beyond this contact to 0.64-m (2.1-ft) depth.

Alluvial well SCA-2 was hand augered to 5.79 m (19.0 ft) in a narrow stretch of Sandia Canyon 349.3 m (1146) ft west-northwest of alluvial well SCA-3 (location map, Figure 2.0-1). SCA-2 is located on the stream bank adjacent to and ~2.3 m (~7.5 ft) above the active channel. During drilling, water was encountered at 3.63-m- (11.9-ft-) depth. The augered section consisted of silt to gravel detritus derived from both devitrified and vitric portions of the Tshirege Member of the Bandelier Tuff, with some gravels of intermediate-composition lavas likely derived from the population of lithic clasts within the tuff. The deposits encountered were silty to sandy, except for a coarser gravel zone extending from 1.52- to 3.41-m (5.0- to 11.2-ft) depth. The prepack screen at SCA-2 (3.08–4.51-m [10.1–14.8-ft] depth) includes the lower part of this coarser interval.

Alluvial well SCA-3 was drilled with the CME-55 HSA rig. SCA-3 is located on the stream bank north of and ~0.8 m (~2.5 ft) above the active stream channel (location map, Figure 2.0-1). Considerable difficulty was encountered beginning at ~9.1-m (~30-ft) depth, where flowing silts and sands began to rise into the hollow auger. Depth-to-water tags during drilling were consistently at ~9.2-m (~30.3-ft) depth. At depths greater than ~12.2 m (~40 ft), reliable tags to depth of water were not possible because of wet slurry coating the interior of the auger flights; beginning at 13.3 m (43.5 ft), coring was difficult because flowing sand locked the core barrel. The auger rig could not advance beyond 16.3 m (53.5 ft) because of the problem with flowing silts and sands; depth to bedrock beneath the alluvium could not be reached. Throughout the drilled depth, sand and silt predominated, with few gravels present and those encountered well rounded and typically <1 cm. To install a well at this site, the rig was moved 4.5 m (14.7 ft) to the east, and a second hole was drilled to 17.8-m (58.5-ft) depth by inserting a wooden plug into the mouth of the HSA to prevent inflow of liquefied alluvium; the well was then constructed inside the HSA using 5.8 cm (2.3 in.) outside diameter (O.D.) polyvinyl chloride (PVC) with a prepack screen at 8.41-9.75-m (27.6–32.0-ft) depth. Liquefied alluvium rose to 9.60 m (31.5 ft) during well construction; above this depth the prepack screen is behind 10/20 sand that rises to 7.32 m (24 ft) below ground surface (bgs).

Adjacent to SCA-3 and to the east, two separate holes were drilled, using the HSA and the same wooden plug method to install piezometers SCP-2a and SCP-2b. A nested installation was not attempted because of the problems with flowing sand. The deeper piezometer, SCP-2b (total depth (TD) of 15.7 m (51.5 ft) with a prepack screen at 15.09–15.24 m (49.5–50.0 ft). SCP-2b is 1.62 m (5.3 ft) east-southeast of SCA-3. The shallower piezometer, SCP-2a has a TD of 13.9 m (45.6 ft) with a prepack screen at 13.56-13.72-m (44.5–45.0-ft) depth and is 1.68 m (5.5 ft) east-southeast of SCP-2b. Figure B-1.1-1 illustrates the configuration of SCA-3 and the adjacent piezometers.

Alluvial well SCA-4 was also drilled with the CME-55 (HSA rig; this hole is 340 m (1117 ft) east-southeast of SCA-3 (location map, Figure 2.0-1). At SCA-4 severe problems with flowing sands as at SCA-3 were not encountered. Sands and clasts of devitrified portions of the Tshirege Member to ~5 cm (2 in.)

predominated throughout the drilled interval to a depth of 12.7 m (41.8 ft), where unit Qbt 1g of the Tshirege Member was encountered. TD was at 13.4 m (43.8 ft) in Qbt 1g. First tags of depth to water began at ~11-m (~36ft) depth; examination of core saturation during drilling suggested that saturation decreased significantly below the contact with Qbt 1g at 12.74 -m (41.8-ft) depth. Alluvial well SCA-4 was constructed inside the HSA using 5.8 cm (2.3 in.) O.D. PVC with a prepacked screen interval at 11.28-12.65 m (37.0–41.5 ft).

Adjacent to SCA-4 and 1.8 m (5.9 ft) to the west, three 3.3 cm (1.3 in.) O.D. piezometers were nested through the HSA in a single borehole drilled to 13.4-m (43.8-ft) depth. Screens on each piezometer are 15.2 cm (6 in.) in length and represent depth intervals of 11.52-11.67 m (37.8–38.3 ft) at SCP-1a; 12.01-12.16 m (39.4-39.9 ft) at SCP-1b; and 12.56–12.71 m (41.2–41.7 ft) at SCP-1c. Thin bentonite seals were placed between the piezometers as the auger flights were retracted, 21 cm (0.7 ft) of bentonite between piezometers b and c and 9 cm (0.3 ft) between a and b. Figure B-1.1-1 shows the configuration of SCA-4 and the associated nest of three piezometers.

Alluvial well SCA-5 was drilled with the CME-55 HSA rig, 495.4 m (1625 ft) northeast of SCA-4 (location map, Figure 2.0-1). At SCA-5, sands and clasts of devitrified portions of the Tshirege Member to several centimeters predominate, although some vitric pumice from the lower Tshirege or upper Otowi Member is present, and a small colluvial block of devitrified upper Tshirege occurs at 18.3–18.6-m (60–61-ft) depth. The contact with vitric nonwelded tuff of the Otowi Member was encountered at 22.1-m (72.5-ft) depth; the contact observed in the core was at angled at ~40° from horizontal, and a 0.3 m (1 ft) colluvial block of devitrified Tshirege was observed right above the contact. TD was at 23.9 m (78.5 ft) in the Otowi Member. The first water tag during drilling was at 17.25 m (56.6 ft) when the auger was at 17.83-m-(58.5-ft) depth; tagged water levels fell as coring advanced, with water tagged at 19.8 m (65 ft) when the auger was at 20.9-m (68.5-ft) depth; drying out of the core suggested that a productive zone in the alluvium may have been sealed off below ~19.4 m (~63.5 ft). A prepack screen was installed at 16.76-19.63-m (55.0–64.4-ft) depth; depth to water 9 days after well construction was 17.6 m (57.8 ft).

### **Characterization Drill Holes**

All of the deep characterization holes, SCC-1 through SCC-6, were drilled with the Speedstar 50K drill rig. All of these holes attained their goal of using air-rotary methods to collect 0.46–0.91-m (1.5–3-ft) lengths of core at 6.1-m (20-ft) intervals down into the top of the Cerros del Rio lavas. Dry drilling methods were used to the extent possible. In practice, all of these holes required addition of small amounts of water once the Otowi Member was encountered, to prevent the drill bit from caking up with the moist, readily powdered vitric tuff. As planned, only one of the characterization holes was completed as a well (SCC-1 was selected; the intermediate well designation is SCI-1); all of the others were plugged and abandoned. Stratigraphy for all of the SCC-series holes is summarized in Figure B-1.1-2, along with the upper portion of the stratigraphy of the only regional borehole in this stretch of the canyon, R-11 (Kleinfelder 2005, 094154). This figure can be referred to for cross-hole comparisons along with the following discussion of drilling observations from each hole.

Hole SCC-1 was drilled north of East Jemez Road in Sandia Canyon, opposite gaging station E-124 (location map, Figure 2.0-1). At 17.7-m (58-ft) depth the stratigraphy encountered in SCC-1 passed from alluvium with sand and gravel dominated by clasts of devitrified Tshirege Member tuff into nonwelded vitric ash flows of the Otowi Member. Alluvial saturation was present with a fairly constant level of 10 m (33 ft) bgs; declining moisture in cuttings suggested a base of alluvial saturation at ~16.2-17.7 m (53-58 ft). The Guaje Pumice Bed was encountered from 96.9 to 101.5-m (318 to 333-ft) depth. Beneath the Guaje Pumice Bed are gravels and sands of the Puye Formation, extending to the top of the Cerros del Rio lavas at 119.0-m (390.5-ft) depth. The upper part of the Puye, to 115.8-m (380-ft) depth, is

dominated by gravel-rich sands with rounded clasts of intermediate-composition lavas up to 25 cm (10 in.) in diameter (upper size limit based on borehole video). From 115.8 m- (380 ft-) to 119.0-m (390.5 ft) depth, the Puye Formation is finer grained, composed of sandy silt. With the drill casing at 118.1 m (387.5 ft), water level in the hole remained steady or declined slowly. When the drill casing was retracted from 118.1 m (387.5 ft) to 109.0 m (357.5 ft), water in the hole rose from 120.6 m (395.6 ft) to 119.9 m (393.3 ft). With casing further retracted to 102.9 m (337.5 ft), water levels rose to 115.60 m (379.25 ft) within 3 h. A borehole video was then collected with drill casing at 102.7 m (337 ft); the video showed water seeping into the upper Puye Formation at 102.7-m (337-ft) depth, with stronger flow appearing at 111.6–111.9 m (366–367 ft) and a depth to standing water at 115.1 m (377.5 ft). Based on these observations and a conductivity log (see Section B-1.4), a well design with 10.2 cm (4 in.), O.D. PVC casing was prepared with a screen at 109.7–115.8-m (360–380-ft) depth. Because of slough in the borehole, the final screen interval was slightly higher, at 109.2–115.2-m (358.4–377.9-ft) depth. A few days after well construction, filter-pack sand was noticed rising into the screen, indicating that the end cap had been ruptured. To remedy this fault, a plug was inserted and set on November 3, 2006.

The “Interim Measures Work Plan for Chromium Contamination in Groundwater” (LANL 2006, 091987) specified completion of only one of the SCC-series holes as a well. Well SCC-1 was drilled next to last in sequence (only SCC-6 followed); SCC-1 was selected for emplacement of an intermediate well (designated SCI-1) based on experience with limited deep perched zones at the other holes. Only SCC-2 had a comparable extent of saturation at depth. Well construction is described in Section B-1.6 (on CD).

Drill hole SCC-2 was drilled south of East Jemez Road and southeast of SCC-1 (location map, Figure 2.0-1). At this site, close to outcrops of Tshirege Member Qbt 1g in the south wall of the canyon, only a thin, unsaturated interval of alluvium was encountered, to 5.5-m (18-ft) depth. Beneath the alluvium, unit Qbt 1g extended to 16.8-m (55-ft) depth, with Cerro Toledo sediments beneath Qbt 1g to 32.0-m (105-ft) depth. Saturation was encountered not in the alluvium but at 15.3-m (50.2-ft) depth in Qbt 1g. The base of this upper saturation is poorly constrained but believed to be within the Cerro Toledo sediments at ~18.3-m (~60-ft) depth. Nonwelded vitric ash flows of the Otowi Member extended beneath the Cerro Toledo from 32.0- to 95.4-m (105- to 313-ft) depth, with the Guaje Pumice Bed at 95.4–101.2-m (313-332-ft) depth. Beneath the Guaje Pumice Bed are deposits of the Puye Formation analogous to those at SCC-1, with gravel-bearing deposits above ~106.7-m (~350-ft) depth and sandy silt beneath these gravels to the top of the Cerros del Rio lavas at 114.9-m (377-ft) depth. With drill casing at 108.9-m (357.3-ft) depth and hole depth of 109.7 m (360 ft), water levels rose very slowly (over 1.5 h) from 108.84 to 108.72 m (357.1 to 356.7 ft) bgs. With drill casing advanced to 115.0 m (377.3 ft) and hole at TD of 118.4 m (388.6 ft) in Cerros del Rio basalt, water rose very slowly into the hole (from 113.72 m [373.1 ft] to 113.52 m [372.45 ft] in 1.5 h). Poor rates of flow and indications of saturation entirely within the silty and relatively tight portion of the Puye contraindicated emplacement of a well in this hole.

Drill hole SCC-3 was also drilled south of East Jemez Road and southeast of SCC-2 (location map, Figure 2.0-1). At this site, as at SCC-2, alluvium lies on top of Tshirege unit Qbt 1g. Saturation was observed in the alluvium beginning at 10.7-m (35-ft) depth; the base of saturation is poorly constrained but is believed to be close to the contact with Qbt 1g at 13.7-m (45-ft) depth. At 19.8 m (65 ft) Qbt 1g overlies the Cerro Toledo Interval, which extends to 27.4-m (90-ft) depth. The lower portion of the Cerro Toledo contains well-rounded cobbles of intermediate-composition volcanic lavas. Beneath the Cerro Toledo, nonwelded vitric ash flows of the Otowi Member of the Bandelier Tuff extend to 91.4-m (300-ft) depth, with the Guaje Pumice Bed at 91.4–97.2 m (300-319 ft). The Puye Formation is both higher in elevation (Figure B-1.1-2) and much thinner than at SCC-3 than at SCC-1 and SCC-2 (2.7 m [9 ft] vs. 17.5 to 13.7 m [57.5 to 45 ft]). In addition, the sequence of gravels over silts observed in the Puye at SCC-1 and SCC-2 does not occur at SCC-3; instead, thicker silts (97.2–99.1-m [319-325-ft] depth) overlie a thin gravel horizon (99.1–100.0-m [325–328-ft] depth) with dacite cobbles up to ~6 cm

(2.4 in.). The Cerros del Rio lavas beneath 100.0 m (328 ft) are vesicular to about 100.6 m (330 ft), where vesicles diminish; TD is at 104.9 m (344 ft) in competent but still vesicular basalt. With drill casing at 99.7-m (327-ft) depth and the hole at TD, the water level fell from 99.50 to 99.83 m (326.45 to 327.55 ft) in a few minutes. When the casing was pulled up to 78.3 m (257 ft), the water level rose from a depth in the Puye gravel bed at 99.64 m (326.9 ft) into the Guaje Pumice Bed at 96.16 m (315.5 ft) in about 6 h. The limited thickness of the saturated zone and the apparent lack of productive gravels argued against placement of a well in this hole.

Drill hole SCC-4 was drilled close to SCC-3, just 54 m (176 ft) to the northeast (location map, Figure 2.0-1). This close location was based on a surface DC resistivity profile, indicating that the upper ~76.2 m (250 ft) of the vadose zone at SCC-4 was much more conductive than the equivalent section at SCC-3 (see discussion of surface DC resistivity profile in Section B-1.5, below). The locations of these two holes were chosen to test whether any gross differences in saturation accounted for the variability seen in the resistivity profile. The stratigraphic sequence at SCC-4 is similar to that at SCC-3. At SCC-4, 17.4 m (57 ft) of alluvium overlies a thin horizon of Qbt 1g (17.4–20.4 m [57–67 ft]). Saturation in the alluvium was encountered at 10.8 m (35.5 ft), but alluvial saturation appeared to end at ~13.7 m (~45 ft), at a depth internal to the alluvial sequence. The Cerro Toledo Interval at SCC-4 is slightly thicker (11.6 m [38 ft]; 20.4–32.0-m [67–105 ft] depth) than at SCC-3 (7.6 m [25 ft]). Nonwelded vitric ash flows of the Otowi extend from 32.0- to 87.5-m (105- to 287-ft) depth, with the Guaje Pumice Bed at 87.5–93.6 m (287–307 ft). As at SCC-3, the Puye Formation at SCC-4 consists of fine sediments (silty sand to 96.9 m [318 ft]) overlying a thinner gravel horizon (dacite gravels to 98.1 m [322 ft], the contact with Cerros del Rio lavas). The top of the Cerros del Rio basalt contains both clay and pedogenic carbonate with fossil root casts. With the hole at TD (98.5 m [323 ft]), water was tagged at 98.27 m (322.4 ft) depth; maximum rise was to only 97.75 m (320.7 ft), far too thin a zone of saturation to consider emplacement of a well. Results from the paired holes SCC-3 and SCC-4 suggest that the differences seen in the DC resistivity profile are not related to major variability in vadose-zone saturation (see Section B-1.5 for more detailed discussion).

Drill hole SCC-5 was drilled 438 m (1437 ft) east of SCC-4 and very close to the southern wall of the canyon (location map, Figure 2.0-1). Here the alluvium is 15.2 m (50 ft) thick and overlies a thin horizon (15.2–18.3-m [50–60-ft] depth) of the Cerro Toledo Interval; the Tshirege Qbt 1g interval that persists beneath the southern part of the canyon from SCC-2 to SCC-4 is no longer present. No saturation was observed in the alluvium. Beneath the Cerro Toledo, Otowi ash flows extend from 18.3- to 75.0-m (60- to 246-ft) depth, and the Guaje Pumice Bed from 75.0- to 81.1-m- (246- to 266-ft-) depth. The Puye Formation here is deposited on a high stand of the Cerros del Rio basalt and thus is relatively thin, with an upper sequence of gravels and sands from 81.1 to 83.8 m (266 to 275 ft) and silt from 83.8 m (275 ft) to the top of the Cerros del Rio at 85.5 m (280 ft). The hole TD in the Cerros del Rio basalt was 88.4 m (290 ft). Throughout the Puye section, samples were damp, but no standing water was observed.

Drill hole SCC-6 was drilled much farther downcanyon, 895 m (2936 ft) east-northeast of SCC-5 (location map, Figure 2.0-1). Here the alluvium is thicker (23.5 m [77 ft]) and directly overlies vitric nonwelded ash flows of the Otowi Member. As at SCC-5, no saturation was found in the alluvium. The Otowi ash flows extend from 23.5- to 59.1-m (77- to 194-ft) depth, overlying the Guaje Pumice Bed (59.1–64.3 m [194–211 ft]). Puye Formation sediments were thicker and more complex than in the other core holes, including an upper silt zone (64.3–67.1 m [211–220 ft]), a horizon with abundant vitric plagioclase-porphyrific dacite pumice (67.1–68.6 m [220–225 ft]), another silt horizon (68.6–70.1 m [225–230 ft]), dacitic gravels (70.1–71.6 m [230–235 ft]), another silt zone (71.6–73.2 m [235–240 ft]), and a basal gravel sequence (73.2–75.9 m [240–249 ft]). Final depth was at 79.1 m (259.5 ft) in Cerros del Rio basalt (upper contact at 75.0 m [249 ft]) with some pedogenic carbonate coating basalt rubble).

## **Comparisons between Closely Spaced Drill Holes**

There are now locations in Sandia Canyon where drilling conducted for the "Interim Measures Work Plan for Chromium Contamination in Groundwater" (LANL 2006, 091987) has placed SCC or SCA holes in proximity or where drill holes for this project and other projects are close together. Although most of the holes that are close together are shallow, close spacing allows an investigation of local variability in the transition from alluvium to bedrock. Figure B-1.1-3 illustrates three situations in Sandia Canyon where holes are within 61.0 m (200 ft) of each other: (1) SCC-2, SC-2, and SCA-3; (2) SCC-5 and SC-4; and (3) regional well R-11 and SC-5. In each of the three comparisons, the drill holes are shown arranged from south to north (left to right in Figure B-1.1-3). The SC core holes were installed in 2002 to evaluate rock properties of the Otowi Member for a potential underground laboratory as part of a proposed Advanced Hydrotect Facility. The cores from the SC holes were reexamined as part of this investigation, and the geologic contacts listed in the project report (Kleinfelder 2002, 091687) were modified in some cases. Table B-1.1-1 summarizes these modifications to the SC-hole stratigraphies; the original descriptions of these boreholes are attached to this report as Appendix B-1.6 on CD).

In the associated set of holes from SCC-2 to SCA-3, the alluvium is saturated only in the northernmost hole, SCA-3, near the active stream channel. To the south, likely associated saturation was found only near the contact between Tshirege unit Qbt 1g and the underlying Cerro Toledo Interval (it is likely that the Cerro Toledo Interval underlies alluvium at SCA-3, but problems with flowing sand during drilling prevented the auger rig from going deep enough to reach the contact). From SC-2 to SCC-2, the depth of erosion into Otowi ash flows beneath the Cerro Toledo channel increases to the south.

In closely spaced holes SCC-5 and SC-4, alluvial saturation was found in the northern hole but not the southern one (although this may merely reflect ephemeral variation in saturation related to the time of drilling). Here the Cerro Toledo deposits have thinned considerably; they are absent in SC-4 and only 10 ft thick at SCC-5. Nevertheless, the Cerro Toledo channel cut into the Otowi is deeper to the south, just as seen in the comparison between SCC-2 and SC-2.

Deeper incision into the Otowi along the southern wall of the canyon is even more pronounced in the comparison between R-11 and SC-5. Accumulation of colluvial blocks of devitrified upper Tshirege units occurs at R-11 where erosion into the Otowi ash flows is 11.3 m (37 ft) lower in elevation than to the north at SC-5. No alluvial saturation was noted in either hole, but the Schlumberger combined magnetic resonance (CMR) results at R-11 show that calculated saturation in the colluvium is distinctly higher than in the underlying Otowi ash flows.

In summary, the comparison between closely located holes shows that (1) alluvial saturation can vary markedly, in some cases over distances of <12.2 m (<40 ft), and (2) incision into the Otowi along the stretch of canyon from SCC-2 to R-11 tends to increase away from the current active channel and to the south, possibly indicating a more southerly channel or channels during the period of Cerro Toledo deposition at ~1.6-1.2 million years ago.

### **B-1.2 Coring Methods and Core Samples**

#### **Alluvial Wells**

Core was collected from alluvial boreholes SCA-3, SCA-4, and SCA-5. The core samples were collected only for the purpose of defining stratigraphy and examining samples for saturation; the core was not collected for developing contaminant profiles within alluvium. A continuous sampler was used at SCA-3 from 4.1 m (13.5 ft) to 13.3 m (43.5 ft), where problems with flowing sand precluded use of this system; with addition of water a final sample was collected from 16.3 m (53.5 ft) to TD at 17.8 m (58.5 ft), but this

deeper sample may be compromised by disturbance during drilling. At SCA-4, core was collected with the continuous sampler from 7.3 m (23.8 ft) to TD at 13.4 m (43.8 ft), allowing precise definition of the contact between alluvium and Tshirege unit Qbt 1g at 12.74 m (41.8 ft). Similarly, at SCA-5, the continuous sampler was used to collect core from 11.7 m (38.3 ft) to TD at 23.9 m (78.5 ft) with identification of the contact between alluvium and Otowi ash flows at 22.1-m (72.5-ft) depth.

### **Characterization Drill Holes**

Core collection in the deep characterization holes SCC-1 through SCC-6 was accomplished using three different methods. At shallower depths within the alluvium, core was collected with the continuous sampler. At greater depths, the drill rods were retracted and the hole was reentered with a Shelby Tube to collect core. In the Cerros del Rio lavas, shallow penetration was possible with the Shelby Tube, but greater lengths of core required a core barrel. Coring plans developed in the "Interim Measures Work Plan for Chromium Contamination in Groundwater" (LANL 2006, 091987) specified core collection in the SCC holes at 6.1-m (20-ft) intervals from the surface to total depth. This schedule of core collections was maintained with few deviations. A total of 104 core samples were collected, 13 with the continuous sampler, 82 with the Shelby Tube, and 9 with the core barrel. Those cores collected with the continuous sampler were collected without addition of water, but small amounts of water had to be added while drilling through most intervals between core runs within and below the Otowi ash flows in order to maintain hole advancement.

Core samples were sealed in the field in plastic bags for metals, tritium, and nitrogen isotope analyses; splits were sealed in preweighed glass jars for moisture, anions, and total organic carbon analyses. In addition to the core samples taken at 6.1 m (20 ft) intervals, additional samples were collected at every other core run to provide bag-sealed samples for radiological screening and tritium analyses at 12.2-m (40-ft) intervals. Details of the core samples taken are provided in tabular form for each of the SCC holes on a hole-by-hole basis in Section B-1.6 (on CD). An annotated summary of the core sample distribution and collection methods is given in Table B-1.2-1.

#### **B-1.3 Water Collection Methods and Water Samples**

No water samples were collected during the drilling of alluvial wells or piezometers; water was sampled from the alluvial wells after well completion and development when sufficient water was present. Analytical results for alluvial water from SCA-1 and SCA-5 are presented in Appendix C-2 (on DVD).

Water samples were collected during drilling of four characterization holes (SCC-1 through SCC-4; Table B-1.0-1). Water samples were collected by plastic bailer. At SCC-1 a bailer was lost down-hole when the hole was at TD; after unsuccessful fishing, Kleinfelder reentered the hole with the coring bit and retrieved the lost bailer. All water samples were collected in 2.0-L quantities (500 mL nonfiltered and nonpreserved, 500 mL filtered and preserved with nitric acid, and 1 L additional for tritium analysis). Details of the groundwater samples taken are provided in tabular form for each of the SCC holes in Section B-1.6 (on CD). An annotated summary of the groundwater sample distribution by borehole and host stratigraphic unit is given in Table B-1.3-1.

#### **B-1.4 Borehole Geophysics**

Geophysical logging was conducted in all of the SCC series boreholes. Logging used the Laboratory-owned Mount Sopris natural gamma and induction tools operated following standard operating procedure (SOP) 05.07. In addition to collection of natural gamma and induction logs, borehole videos were obtained following the same SOP. Table B-1.4-1 summarizes the geophysical logs and borehole videos obtained from each of the SCC holes.

The natural gamma profiles are superimposed on stratigraphy in Figure B-1.1-2. The natural gamma tool is particularly useful in refining stratigraphic contacts for Qbt 1g (which has considerably higher natural gamma activity than the adjacent alluvium or Cerro Toledo Interval), the Cerro Toledo contact with the Otowi ash flows (the natural gamma signal generally rises from Cerro Toledo to Otowi), the contacts of the Guaje Pumice Bed (which has higher natural gamma than the Otowi ash flows or the Puye Formation), and the top of the Cerros del Rio basalts (which have very low natural gamma). Also indicated on Figure B-1.1-2 by red dashed lines between holes are characteristic, laterally mappable inflections in the natural gamma profile within the Otowi ash flows. These same inflections are seen at other localities, and in Mortandad Canyon they have been found to correspond with variations in moisture and contaminant distributions in some boreholes (LANL 2006,094161). An integrated, multihole comparative analysis of stratigraphy, moisture, and contaminants within the Otowi ash flows is beyond the scope of this report, but the features observed in Sandia and Mortandad Canyons indicate that both contaminant and moisture inventories are affected by stratigraphic variability within the Otowi.

The induction data collected from the SCC-series boreholes are summarized in Figure B-1.4-1. Also shown is the CMR-calculated saturation profile from R-11. To provide sufficient stratigraphic detail in this figure, particularly in the Puye Formation (Tpf), only the portion of each hole below 1981-m (6500-ft) elevation is shown. Because drill casing had to be carried to depth in order to seal off alluvial water and provide borehole stability, the induction tool could be run only in the lower 12.2 to 24.4 m (40 to 80 ft) of open borehole in each SCC hole. However, these short intervals span the critical lower saturation zones, helping to assess the potential for well construction in each hole and to guide the design of well SCI-1 in borehole SCC-1. Increased conductivity in the lower Puye Formation at SCC-1 and SCC-2 corresponds with the perched saturation above Cerros del Rio lavas. A somewhat similar but less explicit correlation is seen in the thin saturation interval at SCC-3, where water rose into the Guaje Pumice Bed in an interval where conductivity is low and the estimation of top of saturation is questionable. Farther east, conductivity profiles in the lower Puye are similar and have no correlation with perched-water bodies, indicating that the conductivity data require supporting and more direct observations of perched water to infer the distribution of such saturation. It is of interest to note the generally low conductivity within the Guaje Pumice Bed where core data indicate high moisture content (see Figure 5.4-1); apparently the porous pumice in the Guaje can accumulate significant amounts of water without an increase in conductivity. This conclusion is supported by the calculated CMR saturation in the Guaje at R-11, which is high despite only moderate water content (see discussion in text Section 5.4).

The conductivity data from the SCC holes could only be obtained beneath an elevation of 1969 m (6460 ft) because of the presence of casing at higher elevations in the drill holes. This severely limits direct comparison with the DC resistivity profile that was obtained in this stretch of Sandia Canyon, which only extends down to elevations of 1981–1958 m (6500–6425 ft). The core moisture data, however, do provide a means of comparison with the surface DC resistivity data because the moisture data extend to the surface. These comparisons are considered in the following section.

### **B-1.5 Relation of Core Moisture and Borehole Conductivity to Surface Geophysics**

Several boreholes and monitoring wells in Sandia Canyon provide important information on vadose-zone water. However, even closely spaced boreholes are limited in regard to lateral variation in perched groundwater, infiltration pathways, and contaminant inventories in the subsurface. As part of a Laboratory-wide effort to provide a more synoptic understanding of subsurface hydrogeologic conditions while minimizing the need for further, expensive drilling, a series direct current- (DC-) (or, “electrical-”) resistivity surveys were conducted in selected canyons, including Sandia Canyon, on and near Los Alamos National Laboratory during 2002–2005.

Use of DC-resistivity surveys in hydrogeologic investigations assumes that an important or dominant control on subsurface electrical resistivity (reciprocal of conductivity) is the presence and composition of groundwater, but other important factors include the lithologic properties of subsurface rock units and the presence of clay. A previous study on the Pajarito Plateau (Baldrige et al. 2006, 094048) established that with the exception of specific clay-rich units, groundwater is the chief control on electrical resistivity. In the present work, this relationship is investigated further for Sandia Canyon.

A 5215-ft long DC resistivity survey was acquired in Sandia Canyon in November 2005. The present report summarizes the results of the survey, integrates the results with borehole and other data, and presents interpretations of these data.

## **Methodology**

The DC-resistivity method measures the resistivity of the earth by introducing a near-DC signal into the ground and measuring the resulting voltages created in the earth. From these data, the electrical properties of the earth can be derived, and thereby, the geologic and hydrologic properties can be inferred. The depth of investigation is a function of the length of the survey line, and the resolution is a function of the electrode spacing. The greater the spacing between the outer (current) electrodes, the deeper the electrical currents will flow in the earth, hence the greater the depth of exploration. The depth of investigation is generally 20% to 40% of the outer electrode spacing, depending on the earth resistivity structure.

The resistivity data are used to create a hypothetical model of the resistivity structure of the earth (geoelectric sections). Resistivity models are generally not unique; i.e., a large number of earth models can produce the same observed data. In general, resistivity methods determine the "conductance" of a given stratigraphic layer or unit. The conductance is the product of the resistivity and the thickness of a unit. Hence, that layer could be thinner and more conductive or thicker and less conductive and could produce essentially the same results. Therefore, constraints on the model, such as borehole data or assumed unit resistivities, can greatly enhance the interpretation.

The end product of a DC resistivity survey is generally a "geoelectric" cross section (model) showing thicknesses and values of resistivity of all the geoelectric units or layers. If borehole data or a conceptual geologic model is available, then a geologic identity can be assigned to the geoelectric units.

Electrical resistivity is a fundamental property of rocks and soil that is controlled by rock type, clay content, porosity, and the quantity and quality of the water contained in the rock or soil. Within a given rock or soil type, the resistivity of the rock is primarily dependent on the quality and quantity of water and the amount of clay. Generally, higher clay content and/or poorer quality (higher total dissolved solids [TDS] and/or chlorides) groundwater lowers the resistivity. The electrical resistivity survey, conducted by Geophex, Ltd, comprised a dipole-dipole array with an electrode spacing of 6.0 m (19.6 ft). Each spread consisted of 56 electrodes (including 2 current electrodes), comprising a length of about 318 m (1043 ft). Five spreads were aligned end-to-end so as to obtain a total line length of about 1590 m (5215 ft). The effective depth of sounding was about 76 m (250 ft). (Geophex 2005, 094157; Geophex 2006, 094047).

All boreholes (Figures B-1.2-1 and B-1.1-3) in lower Sandia Canyon were drilled after the electrical resistivity survey was conducted. A variety of geophysical logs and downhole hydrogeologic data was collected, depending on the purposes of each borehole. Induction logs were acquired in several boreholes, but because the shallow parts of the boreholes were cased, they are too deep to overlap with the DC-resistivity survey. Specifically, borehole SCC-3 was drilled into a region that appears relatively resistive (~500-800  $\Omega$ -m) in the lower part (18–79 m [60–260 ft] of the section (Figure B-1.5-1). In contrast, boreholes SCC-4 and -5 were drilled into regions that appear relatively more conductive (~100 to >118  $\Omega$ -m). The resistivity of these boreholes is discussed further below.

In boreholes SCC-1 through SCC-6, core samples were collected for analysis of water content. Samples were sealed in preweighed containers at the drill site to prevent moisture loss. Gravimetric water analyses were performed at Los Alamos National Laboratory using techniques described in Vaniman et al. (2005, 094046). Gravimetric water contents obtained from perched zones are estimates only.

## Results

### Geoelectric Sections

Electrical resistivity in the shallow subsurface (uppermost 69 m [225 ft]) of lower Sandia Canyon ranges significantly from  $<18 \Omega\text{-m}$  to  $\sim 1900 \Omega\text{-m}$  (Figure B-1.5-1). Yet overall, this reach of Sandia Canyon is less resistive than the lower part of Mortandad Canyon just to the south (LANL 2006, 094161). Generally, the upper part of the section, from the surface to a depth of 15–23 m (50–75 ft), is characterized by low resistivity ( $\leq 100 \Omega\text{-m}$ ). Locally, regions of higher resistivity ( $\sim 350\text{--}700 \Omega\text{-m}$ ) are present at or near the surface (upper 9 m [30 ft]) along portions of the survey line (mainly at ranges of 1200–1600 ft and 1850–3650 ft, Figure B-1.5-1).

Below a depth of 15–23 m (50–75 ft), the geoelectric section is characterized by narrow, vertical-oriented regions (“streaks”) of alternately high and low resistivity. Because all boreholes in this part of Sandia Canyon were drilled after the DC-resistivity survey was completed, these low-resistivity streaks cannot be related to the effect of the boreholes.

### Correlation with Perched-Groundwater Zones

Because the boreholes were located very close to the survey line, perched-groundwater zones can be related fairly accurately to the geoelectric section. Overall, the depths and thicknesses of perched-groundwater zones encountered in the boreholes correspond reasonably well with regions of low ( $<120 \Omega\text{-m}$ ) electrical resistivity (Figure B-1.5-1). This correlation is prominent, for example, in boreholes SSC-2 and SC4. In SCC-4, a saturated zone correlates with a region of slightly higher resistivity (300–650  $\Omega\text{-m}$ ), but it is located adjacent to regions of lower resistivity. Altogether, values of 120  $\Omega\text{-m}$  or less are compatible with the resistivity of surface and groundwater of 7–130  $\Omega\text{-m}$  (Baldrige et al., 2006, 094048). Obviously, not all regions of low resistivity ( $\leq 120 \Omega\text{-m}$ ) are apparently associated with the presence of free water (i.e., saturated zones). Thus, the correlation of low resistivity with the free water is not simple. No induction logs were acquired in the upper parts of the boreholes corresponding with the depth region sampled by the DC-resistivity survey because of the presence of casing.

### Interpretations and Conclusions

The dominant control on low DC-resistivity (high electrical conductivity) is the presence of water. Low electrical resistivity ( $\leq 120 \Omega\text{-m}$ ) indicates high moisture, but we cannot confidently assign specific values of resistivity to full saturation. Uncertainties regarding precise correlation of resistivity to the presence of saturated zones also results from the fact that thicknesses of some perched zones are significantly thinner than the electrode spacing (6 m [19.6 ft]; cf. Figure B-1.1-3) of the Sandia Canyon survey. Because resolution decreases downward, deeper aquifers are more poorly resolved.

Clay, especially in the presence of water, can also result in low electrical resistivity, but we have no specific information about amounts or compositions of clay in this reach of Sandia Canyon.

We interpret the overall low-resistivity signature of the upper 15–23 m (50–75 ft) (with the exception of some alluvium in the upper  $\sim 9$  m [30 ft] near the middle of the section) to be caused by the presence of moisture. The low-resistivity zone generally correlates with the alluvium, the Tshirege Member of the Bandelier Tuff (where present), and the Cerro Toledo interval. In this part of Sandia Canyon, the Tshirege

Member wedges out eastward, bringing alluvium into direct contact with the Cerro Toledo interval (Figure B-1.5-1). The interpretation that low electrical resistivity indicates relatively high moisture is consistent with the presence of saturated zones in the alluvium and at the interface between the Tshirege Member of the Bandelier Tuff and the Cerro Toledo interval (Figure B-1.5-1).

At depths >15–23 m (50–75 ft) the resistivity structure of Sandia Canyon is characterized by laterally alternating, dominantly vertically oriented regions of high and low electrical resistivity. At least two mutually exclusive interpretations (conceptual models) may apply to this region. First, regions of low resistivity may indicate fault zones or regions of closely spaced fractures intersecting the geoelectric section at a perpendicular or oblique angle to the axis of the canyon and which together control movement of water in the vadose zone. Regions of high resistivity presumably contain fewer fractures or faults and are relatively dry. If this explanation is correct, then these fault/fracture zones provide potential transport pathways oblique to the orientation of Sandia Canyon. Because many of the vertical zones extend downward at least as deep as the maximum depth imaged by the resistivity survey, they may conduct water to even deeper levels of the vadose zone. If correct, this conceptual model could imply that water, and potentially contaminants, are carried perpendicularly away from Sandia Canyon in the vadose zone. However, this interpretation is not supported by the borehole gravimetric water data. For example, boreholes SCC-3 and SCC-4 were drilled respectively in high (306–1021  $\Omega$ -m)- and low ( $\leq 103$   $\Omega$ -m) resistivity fingers. Yet gravimetric moisture is similar in both holes and, in fact, is slightly higher in SCC-3. A second hypothesis is that water in the subsurface occurs as pods, “ribbons,” and channels of wetter or possibly saturated sediments and/or rock, which are interconnected laterally and vertically to form a three-dimensional network. The electrical-resistivity line thus alternately crossed regions of high and low resistivity. In addition, conductive regions lying close to but not beneath the line may “short circuit” electrical currents, the effect of which is to artificially “map” these low-conductivity regions into the plane of the section. That is, conductive volumes are mapped from the 3rd dimension into the geoelectric section. Thus, the streaks may be real, but they are not necessarily correctly positioned with respect to the section.

Because of the possible complex 3-D geology of Sandia Canyon (and other canyons on the Pajarito Plateau), 2-D electrical profiles should be used with caution for siting wells.

Section B-1.6 is attached as a CD with this report. The CD includes drilling summaries, lithologic logs, and (as applicable) well construction details for the alluvial wells (SCA series), piezometers (SCP series) and coreholes (SCC series) that were drilled for the “Interim Measures Work Plan for Chromium Contamination in Groundwater” (LANL: 2006, 091987). Included as appended material on the CD are listings of the core and groundwater samples collected from SCC holes, results of slug tests in the piezometers (SCP series), geodetic survey data for all of the boreholes and wells, a table describing deviations from as-planned work, and a summary of waste characterization sampling.

#### **B-1.6 Well, Piezometer, and Core Hole Summaries, with Samples Taken Tables**

Section B-1.6 is attached as a CD with this report. The CD includes drilling summaries, lithologic logs, and (as applicable) well construction details for the alluvial wells (SCA series), piezometers (SCP series) and coreholes (SCC series) that were drilled for the “Interim Measures Work Plan for Chromium Contamination in Groundwater” (LANL: 2006, 091987). Included as appended material on the CD are listings of the core and groundwater samples collected from SCC holes, results of slug tests in the piezometers (SCP series), geodetic survey data for all of the boreholes and wells, a table describing deviations from as-planned work, and a summary of waste characterization sampling.

#### **B-1.7 Supplemental Plots of Geochemical Data for Core Samples**

Appendix Figures B-1.1 through B-1.15 are supplemental plots of geochemical data for cores collected from SCC-1 through SCC-6.

## **B-2.0 Analysis of Seasonal Variability in the Water-Table Elevation of the Regional Aquifer**

The regional aquifer beneath the Los Alamos National Laboratory is a complex hydrogeological setting. The shallow portion of the regional aquifer (along the water-table) is predominantly under phreatic (unconfined) conditions and has limited thickness. The deep portion of the regional aquifer is predominantly under confined conditions and is heavily stressed by the Pajarito Plateau water-supply pumping. The gradients and flow directions in the phreatic zone are predominantly controlled by the areas of regional recharge (flanks of Sierra de los Valles and along segments of some of the canyons on the plateau) and discharge to the east (the Rio Grande and the White Rock Canyon Springs). The gradients and flow directions in the deep confined zone are predominantly controlled by the water-supply pumping. Here we analyze the existing data to estimate what is the impact of the deep water-supply pumping on the gradients and flow directions in the phreatic zone.

Information about elevation of the regional water table is provided by existing data from nonpumping monitoring wells and some of the springs (discharge elevation) (Figure B-2.0-1). From all the springs existing at the Laboratory site and its vicinity, a subset is discharging the regional aquifer (predominantly, the springs located close to the Rio Grande); only those are considered in our analysis.

Los Alamos County operates 12 water-supply wells: 5 in the Guaje well field, 2 in the Otowi well field, and 5 in the Pajarito Mesa well field (Figure B-2.0-1). The wells screens are located in deep confined portions of the regional aquifer. Pressures at the supply wells are highly transient and typically are not representative of the water-table elevations and therefore are not considered in the water-table analysis.

### **Water-Supply Production**

Figure B-2.0-2a shows the monthly production for 2005 and 2006 from each well field and the total monthly production from Los Alamos County water-supply wells. Figure B-2.0-2b also shows production variability of individual wells. Production in 2005 ranged from 76.5 million gallons in January and February to nearly 210 million gallons in July. Production in 2006 ranged from about 75 million gallons in February to 155 million gallons in July. Because of rains in August and September 2006, seasonal production requirements in 2006 were less than during 2005. Production from the Otowi well field is almost entirely from well O-4 because well O-1 has not been used on a regular basis for the past several years. Well O-4 produces about as much as the entire five-well Guaje field. Typically, the majority of water production (53% to 66% from January to August 2006) is from the Pajarito well field.

In addition, there is a substantial variability of the water-supply pumping rates on a daily scale. Most of the Los Alamos County water-supply wells are electric, except PM-4, which operates on natural gas. To avoid peak electrical rate periods, the electric wells are operated at night and on weekends. Thus, static groundwater level conditions are rarely if ever attained in these water-supply wells when they are in normal use. In addition, the frequent swapping between pumping and nonpumping periods for all the wells except PM-4 allows for partial recovery of the aquifer pressures near the wells.

Groundwater levels, specific yields, and drawdown characteristics of the water-supply wells were summarized by Koch and Rogers (2003, 088425). Recent aquifer tests were performed at PM-2 in January 2003 (McLin 2005, 090073) and at well PM-4 in February 2005 (McLin 2006, 092218). A summary of all the aquifer tests conducted at the water-supply wells is provided in (McLin 2006a, 093670).

## Groundwater Level Summary

Figure B-2.0-3 shows the mean monthly water levels in selected monitoring wells for 2005 and 2006. The mean monthly data remove or dampen most atmospheric pressure fluctuations and spurious water level fluctuations that may result from abnormal pumping stress, etc.; the mean monthly time series data reveal seasonal transient water level responses to supply well pumping. Although monthly data are shown for 2005 and 2006, this analysis of seasonal transient responses was performed for 2006 because data were available for more wells through the 2006 stress period than in 2005.

Figure B-2.0-4 shows the time series of mean daily groundwater levels for 2005 and 2006 for selected monitoring wells. The groundwater levels are potentially representative of the elevation of the regional water table. Groundwater levels at most of the wells show seasonal variations in response to supply well pumping. Figure B-2.0-4 indicates that in 2005, the maximum transient responses were in August or September, which reflects the pumping stresses associated with the summer drought in 2005. The 2006 water-level data indicate that the highest water levels are generally observed in March, and the lowest water levels occur in most wells in June 2006. This variation corresponds with the maximum and minimum in the pumping stresses (Figure B-2.0-2).

Table B-2.0-1 summarizes the March and June 2006 average monthly water levels at the top of the regional aquifer; the table also lists the number of measurements considered in our statistical analysis, the mean and the standard deviation of the monthly water level for each well.

The water levels of single completion wells shown in Table B-2.0-1 are corrected to compensate for atmospheric pressure differences (see Appendix C-6). Monitoring wells that do not show a significant transient response to seasonal pumping at the top of the regional aquifer (less than 0.25 ft decline in 2006) include R-5, R-7, R-9, R-12, R-22, R-23, R-32, and R-34. Some of these monitoring wells show a decline from March to June 2006, but the time series of the water level does not indicate the decline is related to the seasonal transient pumping, e.g., R-5 and R-7. Monitoring wells that show significant transient seasonal response to pumping in 2006 (greater than 0.25 ft) at the top of the regional aquifer include R-1, R-4, R-6, R-8, R-11, R-13, R-14, R-15, R-20, R-24, and R-28.

The largest seasonal transient responses in 2006 were observed at monitoring wells R-15 (-1.42 ft) and R-8 (-2.03 ft).

R-15 appears to respond primarily to pumping supply well PM-4 (McLin 2006, 092218) and to a lesser extent, supply well PM-5 (Figure B-2.0-5). R-15 has an approximately 60-ft long well screen (Table B-2.0-2) that intersects laterally extensive Miocene pumicious sedimentary deposits that are highly permeable (Puye formation). These deposits are overlaying the even more permeable riverbed deposits (Totavi Lentil). R-15 was initially drilled to a depth exceeding the location of the installed screens which revealed Totavi Lentil below Puye, but Totavi Lentil is not tapped by the existing well screens. All these factors might be causing the observed magnitude of pumping drawdowns at R-15.

The two screens at R-8 respond primarily to pumping of supply well PM-3 (Figure B-2.0-6). The top screen which is supposed to represent the water-table elevation is approximately 50ft in length (Table B-2.0-2). In addition, there is a slough below the top screen that potentially causes the observed water-levels to be representative of aquifer sections deeper than the bottom of the screen. Taking into account that there is a slough below the top screen, we can conclude that (1) the effective section is tapped by the top screen to about 100 ft, and (2) the top and bottom screens are tapping aquifer intervals that are separated by only about 14 ft of clay. The large effective length of the top screen and the small separation distance between the two regional screens at R-8 most probably explains the observed magnitude of pumping drawdowns at the top screen.

In summary, the water levels at the top screens of R-15 and R-8 might not be representative of the water-table elevation nearby the wells.

R-20 responds to pumping of nearby supply well PM-2 (McLin 2005, 090073), and it has a seasonal water-level change at the top of the regional aquifer in 2006 of  $-0.83$  ft. Water-level data for monitoring well R-20 end on June 1, 2006, because the transducers were removed for the well rehabilitation; thus, the total amount of seasonal transient response may not have been observed at this monitoring well. Still, the top screen of R-20 might not be representative of the water-table conditions of the regional aquifer (Table B-2.0-2).

During June, standard deviations greater than about 0.2 ft (Table B-2.0-1) indicate a monitoring well that is responding to supply well pumping; these wells include: R-15, R-24, R-4, and R-8. Monitoring wells R-4 and R-24 appear to respond to pumping of the Guaje well field.

The top of the regional aquifer is predominantly under phreatic, unconfined conditions. However, there appear to be areas of local confinement that are caused by the strong heterogeneity of the flow medium and complexity of groundwater flow structure. Such areas of local confinement near the water-table have been observed during drilling. However, for some of the monitoring wells, the water-table screen may be tapping a confining zone that might be a more dominant, nonlocal confinement feature. In these cases, the regional phreatic water-table zone might have limited thickness, which was too thin for a placement of a well screen, or the phreatic zone may not exist at all at some locations. A good example for such a case is R-24. The screen is representing a zone confined by thick Miocene basalts that are laterally extensive. In this case, clearly the pressures measured at the screen are not representative of the water-table elevation and cannot be used in the generation of phreatic water-table maps. A similar confined zone within the Puye formation might be also observed at R-4.

Other monitoring wells that exhibited confined conditions when drilled include TW-3 in Los Alamos Canyon (installed in 1950) and TW-8 in Mortandad Canyon (installed in 1960). Confined conditions were not reported when monitoring well R-1 was drilled near TW-8 in 2003 or when monitoring well R-15 was drilled in 1999; however, the use of drilling fluids during drilling may have obscured detection of confined conditions.

Table B-2.0-2 summarizes information for monitoring well screen locations at the top of the regional aquifer. Several monitoring wells have screens that are located significantly below the top of the regional water table. Of 40 screens that monitor at or near the top of the regional aquifer, 11 screens (28%) appear to straddle the phreatic water table and provide appropriate water-level data for the water table; 10 screens (25%) are located from 8 to 30 ft below the water table and potentially provide appropriate water-level data for the phreatic water table; and 15 screens (37%) are located greater than 30 ft below the water table, which may not provide appropriate data for the phreatic water table. Water-pressure data from multiple completion wells R-8 and R-33 indicate that screens located 100 ft below the water table have significantly lower head values ( $>20$  ft lower) than the water table screens. Thus, contouring the water table using data from screens in Laboratory monitoring wells should account for the difference in depth of the well screens.

Screens in R-9 and R-12 that supposedly represent the top of the regional aquifer are located in Miocene basalt that has significantly lower head values than surrounding monitoring wells. These head values are not considered to be representative of the phreatic portion of the regional aquifer. The head values observed in these screens do not respond to pumping of nearby supply wells (PM-1, PM-3, O-1) and appear to represent an isolated region of head within the local Miocene basalt.

The complexity of the regional water table is even more pronounced close to the regions of mountain-block recharge. The strong heterogeneity of the flow medium and complexity of groundwater flow structure can cause the flow to form multiple zones of vertical fingering flow through high permeable zones sandwiched between zones of low permeability. The low permeability zones might not be fully saturated or may be incorrectly identified as unsaturated zones due to their properties. The high permeability zones might appear to be separate water-table (or perched) zones. However, most probably these zones merge into a single saturated zone downgradient of the area of recharge and vertical fingering. A very good example for such a case is R-25 where both screens 4 and 5 seem to be under water-table (phreatic) conditions. Still, screen 4, or some average pressure of screens 4 and 5, might be considered to be representative of the regional water-table elevation at this location.

Figure B-2.0-7 shows a section of the water table contour map near the chromium contamination in the regional aquifer using the average March 2006 water-level data for the top of the regional aquifer (green contours). Also shown on this figure are the June 2006 contours of the water table (red contours). In addition on the figure, the water-table elevations are posted at each well for March 2006 (green value) and June 2006 (red value). All data from screens located at the top of the regional aquifer were used to create these water-table contours with no smoothing of the contours. As discussed above, all data may not appropriately represent the phreatic water table. Note the primary differences in the map contours near R-15 where the 5850- and 5860-ft contours are displaced to the west during the higher pumping stress of the aquifer. Water-level contours around R-8 also show a slight transient lowering of the water table by about 2 ft. The June 2006 water-table contours do not indicate a significant change in flow directions at the top of the water table toward supply wells when compared with the March 2006 contours.

The water-table map shows a steeply dipping water table from the western part of the Pajarito Plateau to the central part of the plateau. A break in slope is approximately demarked by a line from about R-7 to R-14 to R-19. East of this line, in the central part of the plateau, the water table flattens and dips to the east-northeast. East of a line from wells R-24 to R-13 to R-32, the water table appears to dip more steeply to the east and southeast, but as mentioned above, the water levels observed at R-9 and R-12 are probably not associated with the phreatic water table observed in the central part of the plateau. The relatively flat section of the water table in the central portion of the Plateau (between PM-5 and R-28) is probably defined by the spatial extent of the highly permeable Miocene sediments (part of the Miocene trough) in the shallow zones of the regional aquifer (LANL 2006, 093196, Plate 6-1).

A water-table mound about 18 ft high is indicated by monitoring well R-8 in Los Alamos Canyon. Most probably, the mound is caused by local canyon-bottom recharge.

Monitoring wells R-11 in Sandia Canyon and R-28 in Mortandad Canyon appear to respond to pumping of each of the supply wells PM-2, PM-4, and PM-5 (Figures B-2.0-8 and B-2.0-9) and have seasonal transient decline of about 0.3 to 0.4 ft. Monitoring well R-1 in Mortandad Canyon responds primarily to pumping of supply well PM-5 with little or no response to pumping PM-4 (Figure B-2.0-10).

Monitoring wells R-4 and R-24 in Pueblo Canyon and Bayo Canyon, respectively, respond primarily to pumping of the Guaje well field. Thus, it appears that the transient response to pumping in the Pajarito Mesa well field does not extent north of approximately Los Alamos Canyon or to the southeast as far as R-22. A small seasonal transient response is noted in monitoring wells DT-5A, DT-9, and DT-10 (Allen and Koch 2005, 093652). Figure B-2.0-8 shows the approximate extent of the transient response observed on monitoring wells. Additional analyses of water-level data from monitoring wells are needed to ascertain more accurately the extent of responses to pumping of supply wells.

In conclusion, the deep portion of the regional aquifer is predominantly under confined conditions, and it is stressed by Pajarito Plateau water-supply pumping. The analyzed water-table data suggest that the

pumping likely has a small impact on the flow directions in the shallow phreatic zone of the regional aquifer. Capture of contaminants by supply wells might be unlikely because of this poor vertical hydraulic communication. However, the poor hydraulic communication does not preclude the possibility that some contaminant migration may occur between the shallow and deep zones. In general, the hydraulic gradient between the two zones has a substantial downward vertical component due to water-supply pumping, creating the possibility that downward contaminant flow may occur along hydraulic windows. As a result, the contaminant flow in the regional aquifer should be predominantly to the east (following the water-table gradients) without substantial temporal changes due to pumping effects.

## **Introduction**

The regional aquifer beneath Los Alamos National Laboratory is a complex hydrogeological setting. The shallow portion of the regional aquifer (along the water-table) is predominantly under phreatic (unconfined) conditions and has limited thickness. The deep portion of the regional aquifer is predominantly under confined conditions and is heavily stressed by the Pajarito Plateau water-supply pumping. The gradients and flow directions in the phreatic zone are predominantly controlled by the areas of regional recharge (flanks of Sierra de los Valles and along segments of some of the canyons on the plateau) and discharge to the east (the Rio Grande and the White Rock Canyon Springs). The gradients and flow directions in the deep confined zone are predominantly controlled by the water-supply pumping. Here we analyze the existing data to estimate what is the impact of the deep water-supply pumping on gradients and flow directions in the phreatic zone.

Information about elevation of the regional water table is provided by existing data from nonpumping monitoring wells and from some of the springs (discharge elevation) (Figure B-2.0-1). From all the springs at the Laboratory site and its vicinity, a subset is discharging the regional aquifer (predominantly, the springs located close to the Rio Grande); only those are considered in our analysis.

Los Alamos County operates 12 water-supply wells: 5 in the Guaje wellfield, 2 in the Otowi well field, and 5 in the Pajarito Mesa well field (Figure B-2.0-1). The well screens are located in deep confined portions of the regional aquifer. Pressures at the supply wells are highly transient and typically are not representative of the water-table elevations; therefore, they are not considered in the water-table analysis.

## **Water-Supply Production**

Figure B-2.0-2a shows the monthly production for 2005 and 2006 from each well field and the total monthly production from Los Alamos County water-supply wells. Figure B-2.0-2b also shows production variability of individual wells. Production in 2005 ranged from 76.5 million gallons in January and February to nearly 210 million gallons in July. Production in 2006 ranged from about 75 million gallons in February to 155 million gallons in July. Because of rains in August and September 2006, seasonal production requirements in 2006 were less than during 2005. Production from the Otowi well field is almost entirely from well O-4 because well O-1 has not been used regularly for the past several years. Well O-4 produces about as much as the entire five-well Guaje field. Typically, the majority of water production (53% to 66% from January to August 2006) is from the Pajarito well field.

In addition, there is a substantial variability of the water-supply pumping rates on a daily scale. Most of the Los Alamos County water-supply wells are electric, except PM-4, which operates on natural gas. To avoid peak electrical rate periods, the electric wells are operated at night and on weekends. Thus, static groundwater level conditions are rarely if ever attained in these water-supply wells when they are in normal use. In addition, the frequent swapping between pumping and nonpumping periods, for all the wells except PM-4 allows for partial recovery of aquifer pressures near the wells.

Groundwater levels, specific yields, and drawdown characteristics of the water-supply wells were summarized by Koch and Rogers (2003, 088425). Recent aquifer tests were performed at PM-2 in January 2003 (McLin 2005, 090073) and at well PM-4 in February 2005 (McLin 2006, 092218). A summary of all the aquifer tests conducted at the water-supply wells is provided in (McLin 2006 093670).

### **Groundwater Level Summary**

Figure B-2.0-3 shows the mean monthly water levels in selected monitoring wells for 2005 and 2006. The mean monthly data remove or dampen most atmospheric pressure fluctuations and spurious water level fluctuations that may result from abnormal pumping stress, etc.; the mean monthly time series data reveal seasonal transient water level responses to supply well pumping. Although monthly data are shown for 2005 and 2006, this analysis of seasonal transient responses was performed only for 2006 because data were available for more wells through the 2006 stress period than in 2005.

Figure B-2.0-4 shows the time series of mean daily groundwater levels for 2005 and 2006 for selected monitoring wells. The groundwater levels are potentially representative of the elevation of the regional water table. Groundwater levels at most of the wells show seasonal variations in response to supply well pumping. Figure B-2.0-4 indicates that in 2005, the maximum transient responses were in August or September, which reflects the pumping stresses associated with the summer drought in 2005. The 2006 water-level data indicate that the highest water levels are generally observed in March, and the lowest water levels occur in most wells in June 2006. This variation corresponds with the maximum and minimum in pumping stresses (Figure B-2.0-2).

Table B-2.0-1 summarizes the March and June 2006 average monthly water levels at the top of the regional aquifer; the table also lists the number of measurements considered in our statistical analysis, the mean and the standard deviation of the monthly water level for each well.

The water levels of single completion wells shown in Table B-2.0-1 are corrected to compensate for atmospheric pressure differences (see Appendix C-6). Monitoring wells that do not show a significant transient response to seasonal pumping at the top of the regional aquifer (less than 0.25-ft decline in 2006) include R-5, R-7, R-9, R-12, R-22, R-23, R-32, and R-34. Some of these monitoring wells show a decline from March to June 2006, but the time series of the water level does not indicate the decline is related to the seasonal transient pumping, e.g., R-5 and R-7. Monitoring wells that show significant transient seasonal response to pumping in 2006 (greater than 0.25 ft) at the top of the regional aquifer include R-1, R-4, R-6, R-8, R-11, R-13, R-14, R-15, R-20, R-24, and R-28.

The largest seasonal transient responses in 2006 were observed at monitoring wells R-15 (-1.42 ft) and R-8 (-2.03 ft).

R-15 appears to respond primarily to pumping supply well PM-4 (McLin 2006 092218) and to a lesser extent, supply well PM-5 (Figure B-2.0-5). R-15 has an approximately 60-ft long well screen (Table B-2.0-2) that intersects laterally extensive Miocene (pre-Puye) pumiceous sedimentary deposits that are highly permeable (Puye formation). These deposits are overlaying the even more permeable riverbed deposits (Totavi Lentil). R-15 was initially drilled to a depth exceeding the location of the installed screens which revealed Totavi Lentil below Puye, but the Totavi Lentil is not tapped by the existing well screens at R-15. All these factors might be causing the observed magnitude of pumping drawdowns at R-15.

The two screens at R-8 respond primarily to pumping of supply well PM-3 (Figure B-2.0-6). The top screen which is supposed to represent the water-table elevation is approximately 50 ft in length (Table B-2.0-2). In addition, there is a slough below the top screen that potentially causes the observed

water levels to be representative of aquifer sections deeper than the bottom of the screen. If we can consider the slough below the top screen, the effective section tapped by the top screen to about 100 ft and the top and the bottom screen tapping aquifer intervals are separated by only about 14 ft of clay. The large effective length of the top screen and the small separation distance between the two regional screens at R-8 most probably explain the observed magnitude of pumping drawdowns at the top screen.

In summary, the water levels at the top screens of R-15 and R-8 might not be representative of the water-table elevation nearby the wells.

R-20 responds to pumping of nearby supply well PM-2 (McLin 2005 090073), and it has a seasonal water-level change at the top of the regional aquifer in 2006 of  $-0.83$  ft. Water-level data for monitoring well R-20 end on June 1, 2006, because the transducers were removed for the well rehabilitation; thus, the total amount of seasonal transient response may not have been observed at this monitoring well. Still, the top screen of R-20 might not be representative of the water-table conditions of the regional aquifer (Table B-2.0-2).

During June, standard deviations greater than about 0.2 ft (Table B-2.0-1) indicate a monitoring well that is responding to supply well pumping; these wells include: R-15, R-24, R-4, and R-8. Monitoring wells R-4 and R-24 appear to respond to pumping of the Guaje well field.

The top of the regional aquifer is predominantly under phreatic, unconfined conditions. However, there appear to be areas of local confinement that are caused by the strong heterogeneity of the flow medium and complexity of groundwater flow structure. Such areas of local confinement near the water table have been observed during drilling. However, for some of the monitoring wells, the water-table screen may be tapping a confining zone that might be a more dominant, nonlocal confinement feature. In these cases, the regional phreatic water-table zone might have limited thickness, which was too thin for a placement of a well screen, or the phreatic zone may not exist at all at some locations. A good example for such a case is R-24. The screen is in a zone confined by thick Miocene basalts that are laterally extensive. In this case, clearly the pressures measured at the screen are not representative of the water-table elevation and cannot be used in the generation of phreatic water-table maps. A similar confined zone within the Puye formation may be also occur at R-4.

Other monitoring wells that exhibited confined conditions when drilled include TW-3 in Los Alamos Canyon (installed in 1950) and TW-8 in Mortandad Canyon (installed in 1960). Confined conditions were not reported when monitoring well R-1 was drilled near TW-8 in 2003 or when monitoring well R-15 was drilled in 1999; however, the use of drilling fluids during drilling may have obscured detection of confined conditions.

Table B-2.0-2 summarizes information for monitoring well screen locations at the top of the regional aquifer. Several monitoring wells have screens that are located significantly below the top of the regional water table. Of 40 screens that monitor at or near the top of the regional aquifer, 11 screens (28%) appear to straddle the phreatic water table and provide appropriate water-level data for the water table; 10 screens (25%) are located from 8 to 30 ft below the water table and potentially provide appropriate water-level data for the phreatic water table; 15 screens (37%) are located greater than 30 ft below the water table, which may not provide appropriate data for the phreatic water table. Water-pressure data from multiple completion wells R-8 and R-33 indicate that screens located 100 ft below the water table have significantly lower head values ( $>20$  ft lower) than the water-table screens. Thus, contouring the water table using data from screens in Laboratory monitoring wells should account for the difference in depth of the well screens.

Screens in R-9 and R-12 that supposedly represent the top of the regional aquifer are located in Miocene basalt that has significantly lower head values than surrounding monitoring wells. These head values are not considered to be representative of the phreatic portion of the regional aquifer. The head values observed in these screens do not respond to pumping of nearby supply wells (PM-1, PM-3, O-1) and appear to represent an isolated region of head within the local Miocene basalt.

The complexity of the regional water table is even more pronounced close to the regions of mountain-block recharge. The strong heterogeneity of the flow medium and complexity of groundwater flow structure can cause the flow to form multiple zones of vertical fingering flow through high permeable zones sandwiched between zones of low permeability. The low permeability zones might not be fully saturated or may be incorrectly identified as unsaturated zones due to their properties. The high permeability zones might appear to be separate water-table (or perched) zones. However, most probably these zones merge into a single saturated zone downgradient of the area of recharge and vertical fingering. A very good example for such a case is R-25 where both screens 4 and 5 seem to be under water-table (phreatic) conditions. Still, screen 4, or some average pressure of screens 4 and 5, might be considered to be representative of the regional water-table elevation at this location.

Figure B-2.0-7 shows a section of the water-table contour map near the chromium contamination in the regional aquifer using the average March 2006 water-level data for the top of the regional aquifer (green contours). Also shown on this figure are the June 2006 contours of the water table (red contours). In addition on the figure, the water-table elevations are posted at each well for March 2006 (green value) and June 2006 (red value). All data from screens located at the top of the regional aquifer were used to create these water-table contours with no smoothing of the contours. As discussed above, all data may not appropriately represent the phreatic water table. Note the primary differences in the map contours near R-15 where the 5850- and 5860-ft contours are displaced to the west during the higher pumping stress of the aquifer. Water-level contours around R-8 also show a slight transient lowering of the water table by about 2 ft. The June 2006 water-table contours do not indicate a significant change in flow directions at the top of the water table toward supply wells when compared with the March 2006 contours.

The water-table map shows a steeply dipping water table from the western part of the Pajarito Plateau to the central part of the plateau. A break in slope is approximately demarked by a line from about R-7 to R-14 to R-19. East of this line, in the central part of the plateau, the water table flattens and dips to the east-northeast. East of a line from wells R-24 to R-13 to R-32, the water table appears to dip more steeply to the east and southeast, but as mentioned above, the water levels observed at R-9 and R-12 are probably not associated with the phreatic water table observed in the central part of the plateau. The relatively flat section of the water table in the central portion of the Plateau (between PM-5 and R-28) is probably defined by the spatial extent of the highly permeable Miocene sediments (part of the Miocene trough) in the shallow zones of the regional aquifer (LANL 2006, 093196, Plate 6-1).

A water-table mound about 18 ft high is indicated by monitoring well R-8 in Los Alamos Canyon. Most probably, the mound is caused by local canyon-bottom recharge.

Monitoring wells R-11 in Sandia Canyon and R-28 in Mortandad Canyon appear to respond to pumping of each of the supply wells PM-2, PM-4, and PM-5 (Figures B-2.0-8 and B-2.0-9) and have seasonal transient decline of about 0.3 to 0.4 ft. Monitoring well R-1 in Mortandad Canyon responds primarily to pumping of supply well PM-5 with little or no response to pumping PM-4 (Figure B-2.0-10).

Monitoring wells R-4 and R-24 in Pueblo Canyon and Bayo Canyon, respectively, respond primarily to pumping of the Guaje well field. Thus, it appears that the transient response to pumping in the Pajarito Mesa well field does not extent north of approximately Los Alamos Canyon or to the southeast as far as R-22. A small seasonal transient response is noted in monitoring wells DT-5A, DT-9, and DT-10 (Allen

and Koch 2005, 093652). Figure B-2.0-8 shows the approximate extent of the transient response observed on monitoring wells. Additional analyses of water-level data from monitoring wells are needed to ascertain more accurately the extent of responses to pumping of supply wells.

In conclusion, the deep portion of the regional aquifer is predominantly under confined conditions, and it is stressed by Pajarito Plateau water-supply pumping. The analyzed water-table data suggest that the pumping likely has a small impact on the flow directions in the shallow phreatic zone of the regional aquifer. Capture of contaminants by supply wells might be unlikely because of this poor vertical hydraulic communication. However, the poor hydraulic communication does not preclude the possibility that some contaminant migration may occur between the shallow and deep zones. In general, the hydraulic gradient between the two zones has a substantial downward vertical component due to water-supply pumping, creating the possibility that downward contaminant flow may occur along hydraulic windows. As a result, the contaminant flow in the regional aquifer should be predominantly to the east (following the water-table gradients) without substantial temporal changes due to pumping effects.

## **REFERENCES**

*The following list includes all documents cited in this appendix. Parenthetical information following each reference provides the author(s), publication date, and ER ID number. This information is also included in text citations. ER ID numbers are assigned by the Environmental Programs Directorate's Records Processing Facility (RPF) and are used to locate the document at the RPF and, where applicable, in the master reference set.*

*Copies of the master reference set are maintained at the NMED Hazardous Waste Bureau; the U.S. Department of Energy—Los Alamos Site Office; the U.S. Environmental Protection Agency, Region 6; and the Directorate. The set was developed to ensure that the administrative authority has all material needed to review this document, and it is updated with every document submitted to the administrative authority. Documents previously submitted to the administrative authority are not included.*

Allen, S.P., and Koch, R.J., 2006, "Groundwater Level Status Report for 2005, Los Alamos National Laboratory," Los Alamos National Laboratory report LA-14292-PR, Los Alamos, New Mexico. (Allen and Koch 2006, 093652)

Baldrige, S.W., G.L. Cole, B.A. Robinson, and G.R. Jiracek, June 2006. "Application of Time-Domain Airborne Electromagnetic Induction to Hydrogeologic Investigations: The Pajarito Plateau, Los Alamos, New Mexico," *Geophysics* (in press). (Baldrige et al. 2006, 094048)

Geophex, October 2005. "Geophysical Survey Plan for Surface DC Resistivity Data Collection in Pajarito, Sandia, DP, Los Alamos, and Pueblo Canyons, Los Alamos National Laboratory, Los Alamos County, New Mexico." (Geophex 2005, 094157)

Geophex, January 2006. "DC Resistivity profiling in DP, Los Alamos, Pajarito, Pueblo and Sandia Canyons, Los Alamos National Laboratory, Los Alamos, NM," Unpublished report. (Geophex 2006, 094047)

Kennedy, W.R., May 11, 1971. "Radiochemical and Chemical Analyses of Water," letter to W.E. Hale, Los Alamos Scientific Laboratory from W.R. Kennedy (Group Leader, H-8-468) Los Alamos, New Mexico. (Kennedy 1971, 33896)

Kleinfelder, September 2002. "Report of Pre-Conceptual Geotechnical Investigations, Advanced Hydrotest Facility Project, TA-53 Los Alamos National Laboratory Los Alamos, New Mexico," Project No. C59010120, Albuquerque, New Mexico. (Kleinfelder 2002, 091687)

Kleinfelder, February 2005. "Final Completion Report Characterization Well R-11 Completion Report Los Alamos National Laboratory, Los Alamos, New Mexico," Albuquerque, New Mexico. (Kleinfelder 2005, 094154)

Kleinfelder, January 2006. "DC Resistivity Profiling in DP, Los Alamos, Pajarito, Pueblo, and Sandia Canyons, Los Alamos National Laboratory, Los Alamos, New Mexico," Geophex Job # 1333, Albuquerque, New Mexico. (Kleinfelder 2006, 094047)

Koch, R.J., and Rogers, D.B., March 2003, "Water Supply at Los Alamos, 1998–2001," Los Alamos National Laboratory report LA-13985-PR, Los Alamos, New Mexico. (Koch and Rogers 2003, 088425)

LANL (Los Alamos National Laboratory), June 1993. "RFI Work Plan for Operable Unit 1098," Los Alamos National Laboratory document LA-UR-92-3825, Los Alamos, New Mexico. (LANL 1993, 015314)

LANL (Los Alamos National Laboratory), June 2005. "Groundwater Background Investigation Report," Los Alamos National Laboratory document LA-UR-05-2295, Los Alamos, New Mexico. (LANL 2005, 090580)

LANL (Los Alamos National Laboratory), March 2006, "Interim Measures Work Plan for Chromium Contamination in Groundwater," Los Alamos National Laboratory document LA-UR-06-1961, Los Alamos, New Mexico. (LANL 2006, 091987)

LANL (Los Alamos National Laboratory), June 2006, "2006 Hydrogeologic Site Atlas," Los Alamos National Laboratory document LA-UR-06-0358, Los Alamos, New Mexico. (LANL 2006, 093196)

LANL (Los Alamos National Laboratory), July 2006. "Summary of Watersheds Potentially Impacted by the Los Alamos National Laboratory," Los Alamos National Laboratory document LA-UR-06-5387, Los Alamos, New Mexico. (LANL 2006, 094004)

LANL (Los Alamos National Laboratory), October 2006. "Mortandad Canyon Investigation Report," Los Alamos National Laboratory document LA-UR-6752, Los Alamos, New Mexico.

LANL (Los Alamos National Laboratory), November 2006. "History of Water Treatment Chemicals Used at TA-03 Power Plant from 1951 through November 2006," prepared by J.V. Ortiz for the LANL Site Support Services, Los Alamos, New Mexico. (LANL 2006, 094153)

McLin, S.G., 2005, "Analyses of the PM-2 Aquifer Test Using Multiple Observation Wells," Los Alamos National Laboratory report LA-14225-MS, Los Alamos, New Mexico. (McLin 2005, 090073)

McLin, S.G., 2006, "Analyses of the PM-4 Aquifer Test Using Multiple Observation Wells," Los Alamos National Laboratory report LA-14252-MS, Los Alamos, New Mexico. (McLin 2006, 092218)

McLin, S.G., 2006a, "A Catalogue of Historical Aquifer Tests on Pajarito Plateau," Los Alamos National Laboratory document LA-UR-06-3789, Los Alamos, New Mexico. (McLin 2006a, 093670)

Vaniman, D., Broxton, D., and Chipera, S., 2005, "Vadose Zone Clays and Water Content beneath Wet and Dry Canyons of the Pajarito Plateau, New Mexico," *Vadose Zone Journal*, Vol. 4, pp. 453–465. (Vaniman et al. 2005, 094046)

This page intentionally left blank.

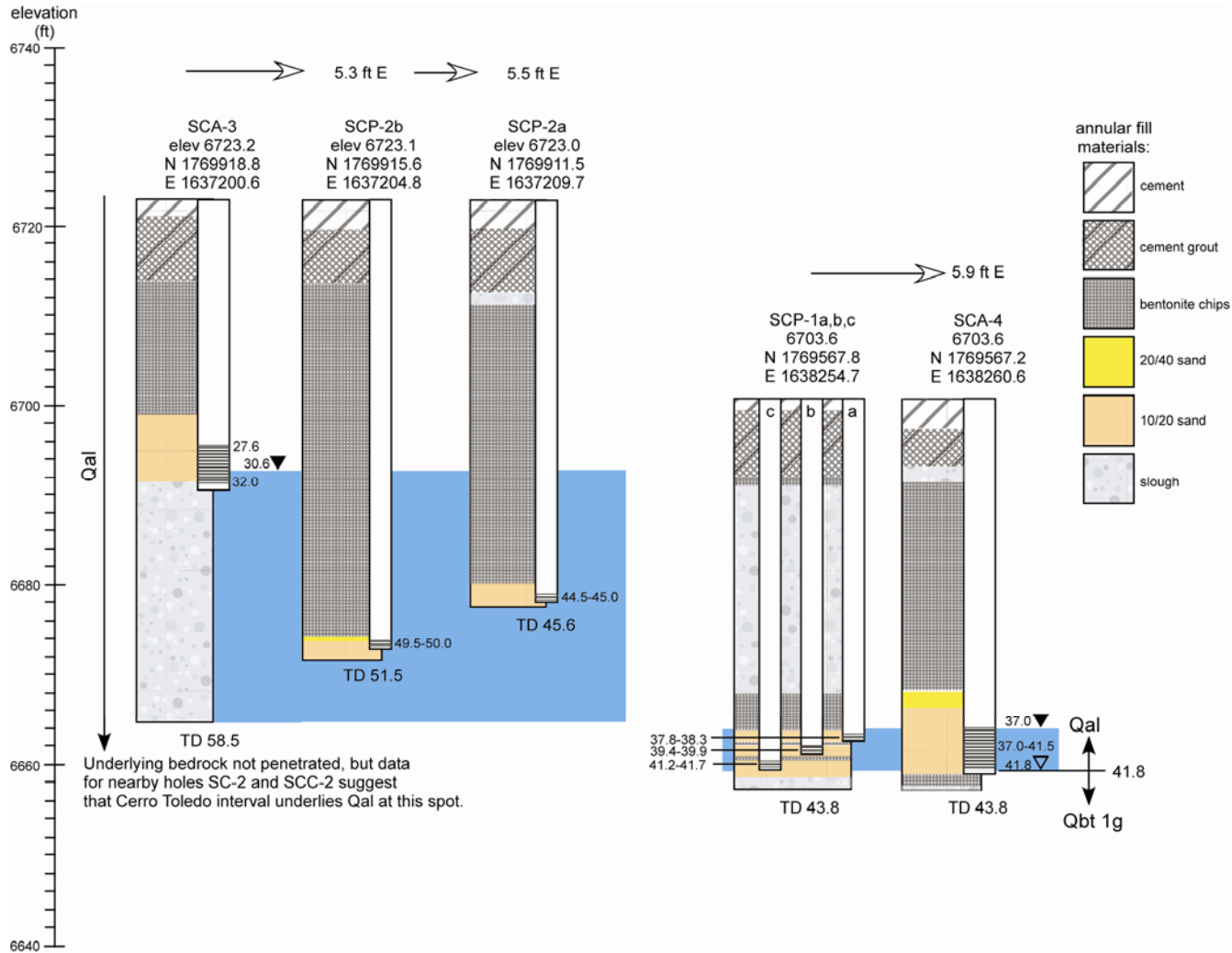


**Figure B-1.1-1. Summary construction and saturation data for SCA alluvial wells that have adjacent sets of SCP piezometers (all elevations and depths are in feet). Depth to saturation is variable over time; saturation shown here represents conditions immediately following construction of the alluvial wells. Detailed descriptions of all alluvial wells and piezometers are provided in Section B-1.6.**

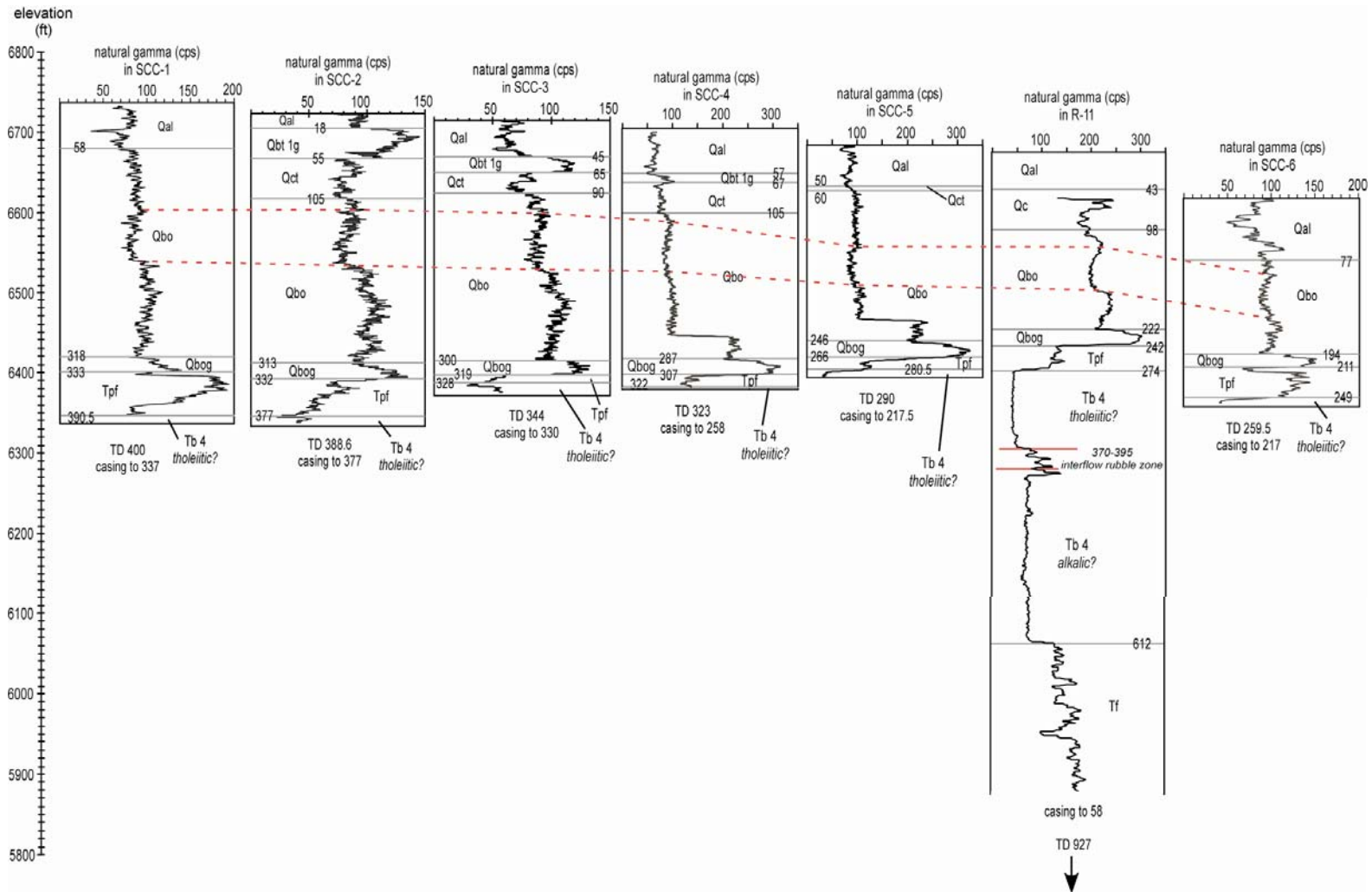


**Figure B-1.1-2. Stratigraphic summary for all SCC-series holes in Sandia Canyon, with comparable stratigraphy for the vadose zone in regional drill hole R-11 (all elevations and depths are in feet). Each stratigraphic column shows the natural gamma log used to help refine stratigraphic contacts, with depth of casing at the time the natural gamma log was collected. Red dashed lines connect stratigraphically significant inflections within gamma profiles of the Otowi ash flows (discussion in Section B-1.4).**

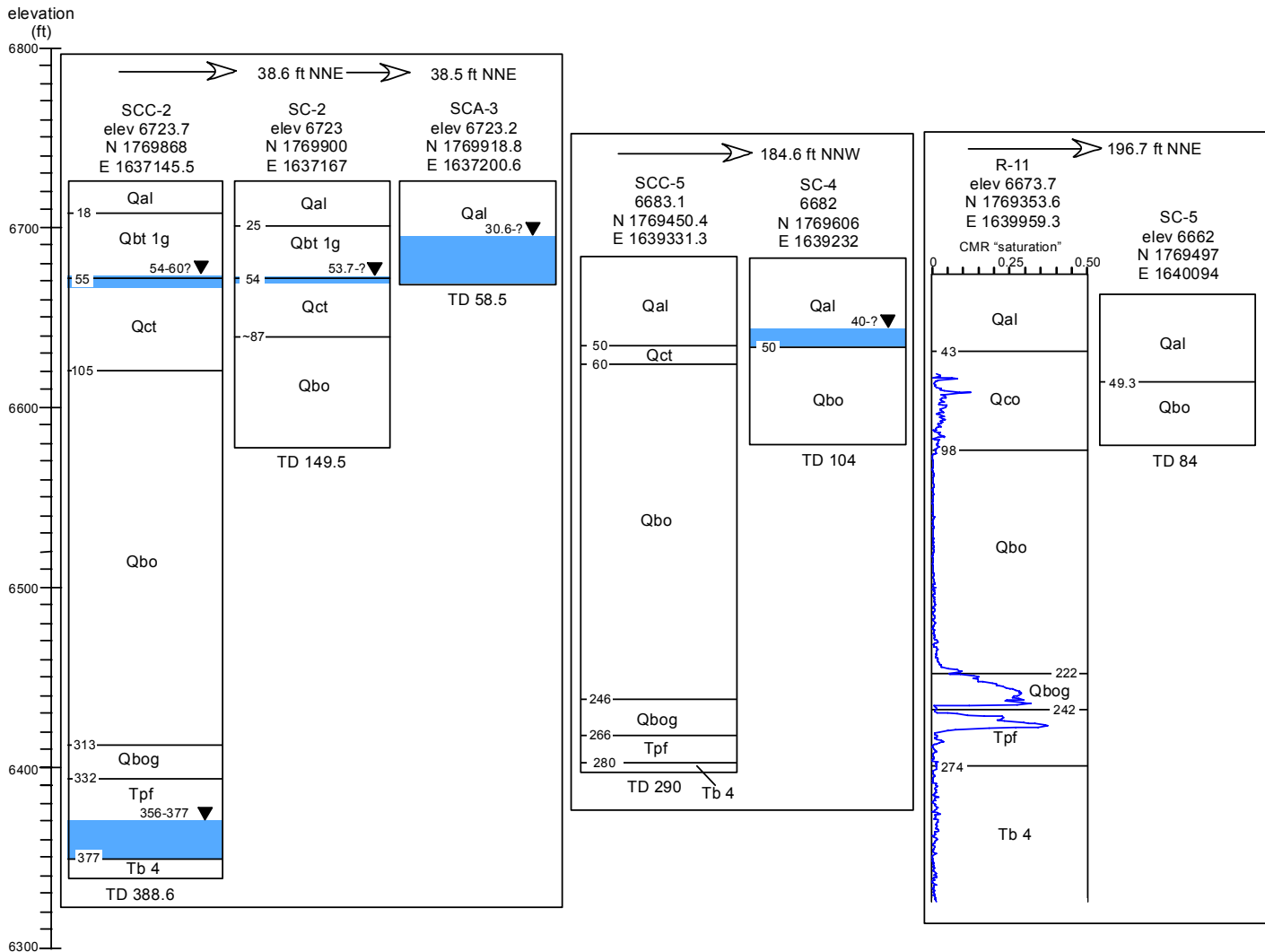


**Figure B-1.1-3. Small-scale (<61-m [ $<200$ -ft] lateral range) in variability of depth of alluvium, stratigraphy beneath alluvium, and occurrence of saturation in three closely spaced sets of drill holes (discussion in Section B-1.1, Comparisons between Closely Spaced Drill Holes). All elevations and depths are in feet.**

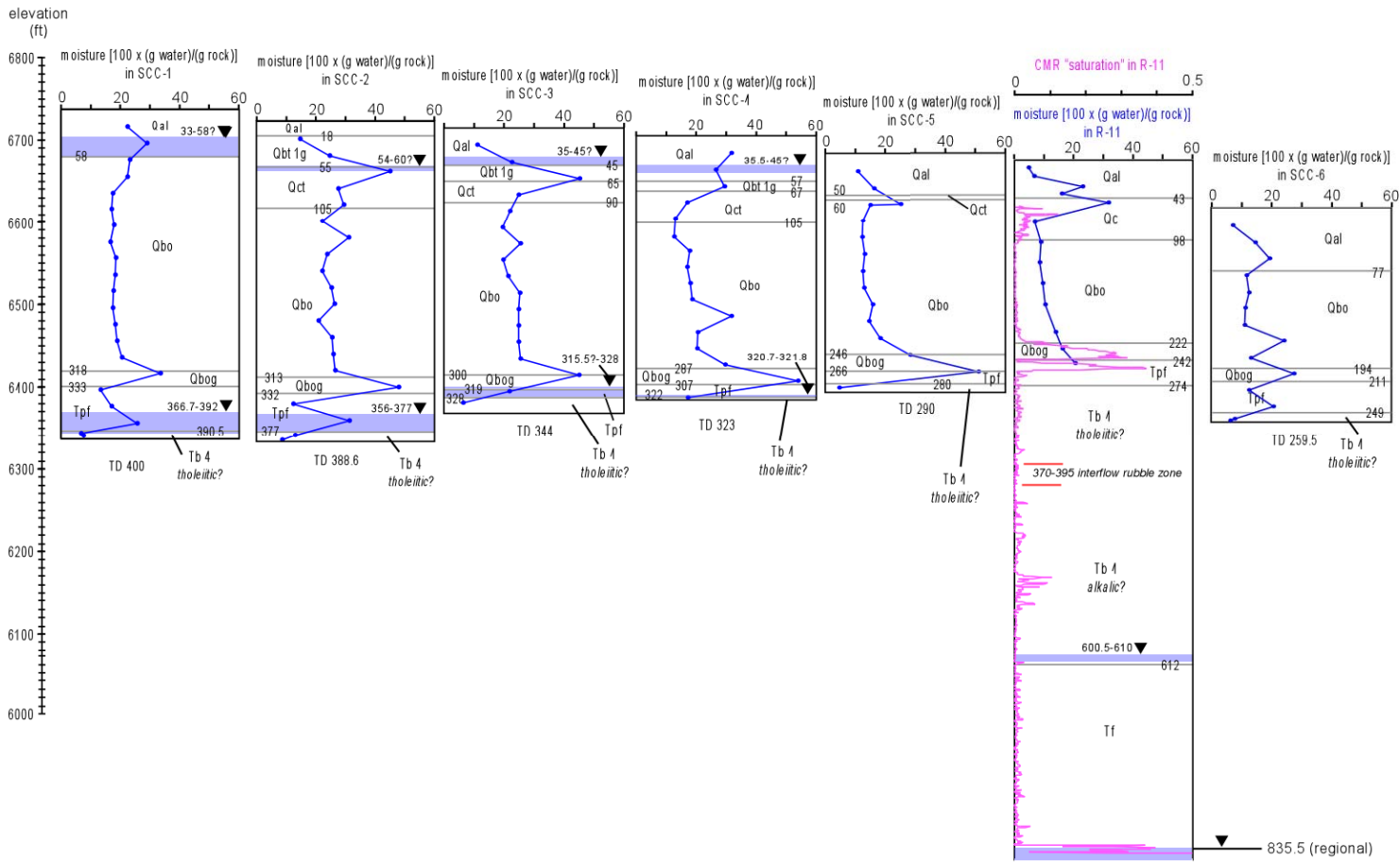
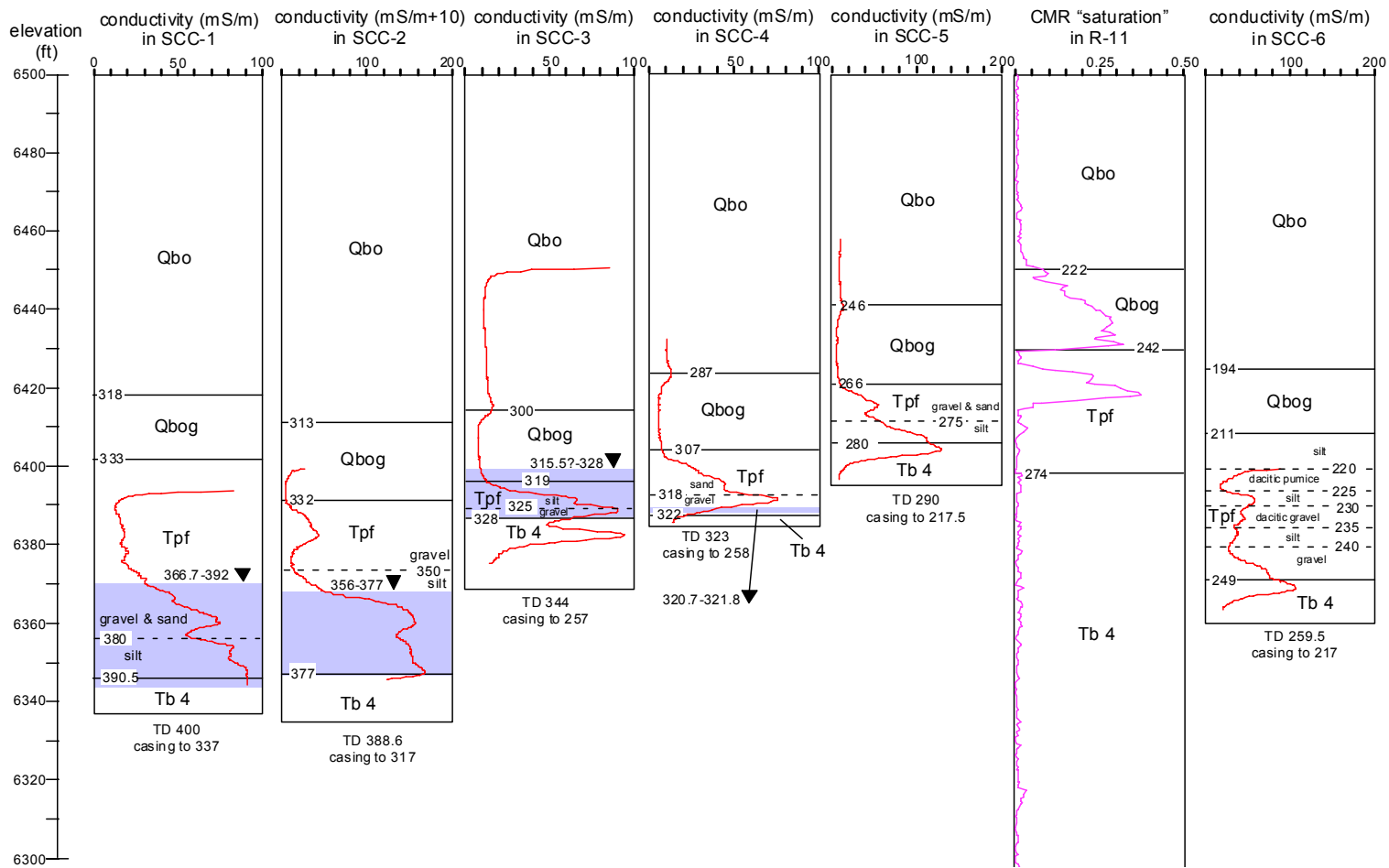
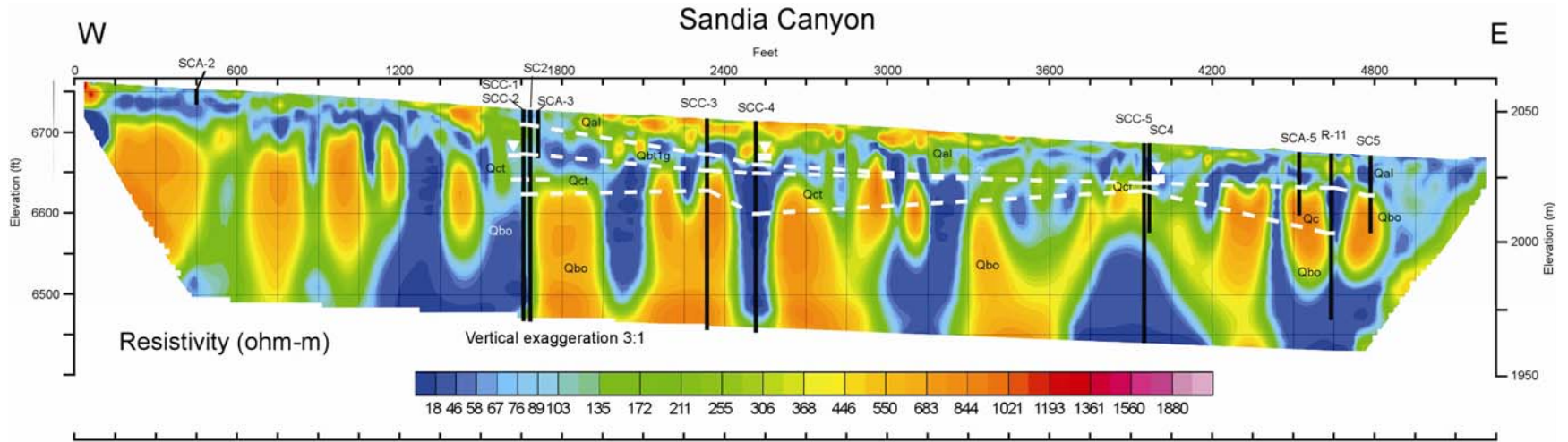


Figure B-1.2-1. Borehole stratigraphies of Figure B-1.1.2 with core moisture data and presence of saturated horizons superimposed (all elevations and depths are in feet). For regional drill hole R-11, the calculated volume fraction of pore space “saturated” is shown as estimated from the Schlumberger combined magnetic resonance (CMR) log. See section B-1.2, *Discussion of Core Moisture Stratigraphy*.



**Figure B-1.4-1. Induction tool conductivity profiles (red curves) in the lower portions (uncased) of the SCC-series drill holes (note that a sharp rise in conductivity at the top of a conductivity curve indicates proximity to steel casing). All elevations and depths are in feet. To provide an expanded and relevant depth scale, only to portion of each drill hole below 1981 m (6500 ft) elevation is shown. The calculated saturation for R-11 is derived from the Schlumberger combined magnetic resonance (CMR) tool.**



**Figure B-1.5-1. DC-resistivity profile of lower Sandia Canyon. Major lithologic units are shown as white dashed lines, queried where significantly uncertain. Lithologic control at wells is indicated by short horizontal white lines. Inverted triangles with horizontal bars indicate perched-groundwater zones. No control on lithologic boundaries or zones of perched water exists between wells. Data on lithologic contacts and perched zones are summarized in Figures B-1.2-1 and B-1.1-3 and in Appendix B-1.6 (on CD) Well, Piezometer, and Core Hole Summaries, with Samples Taken Tables.**

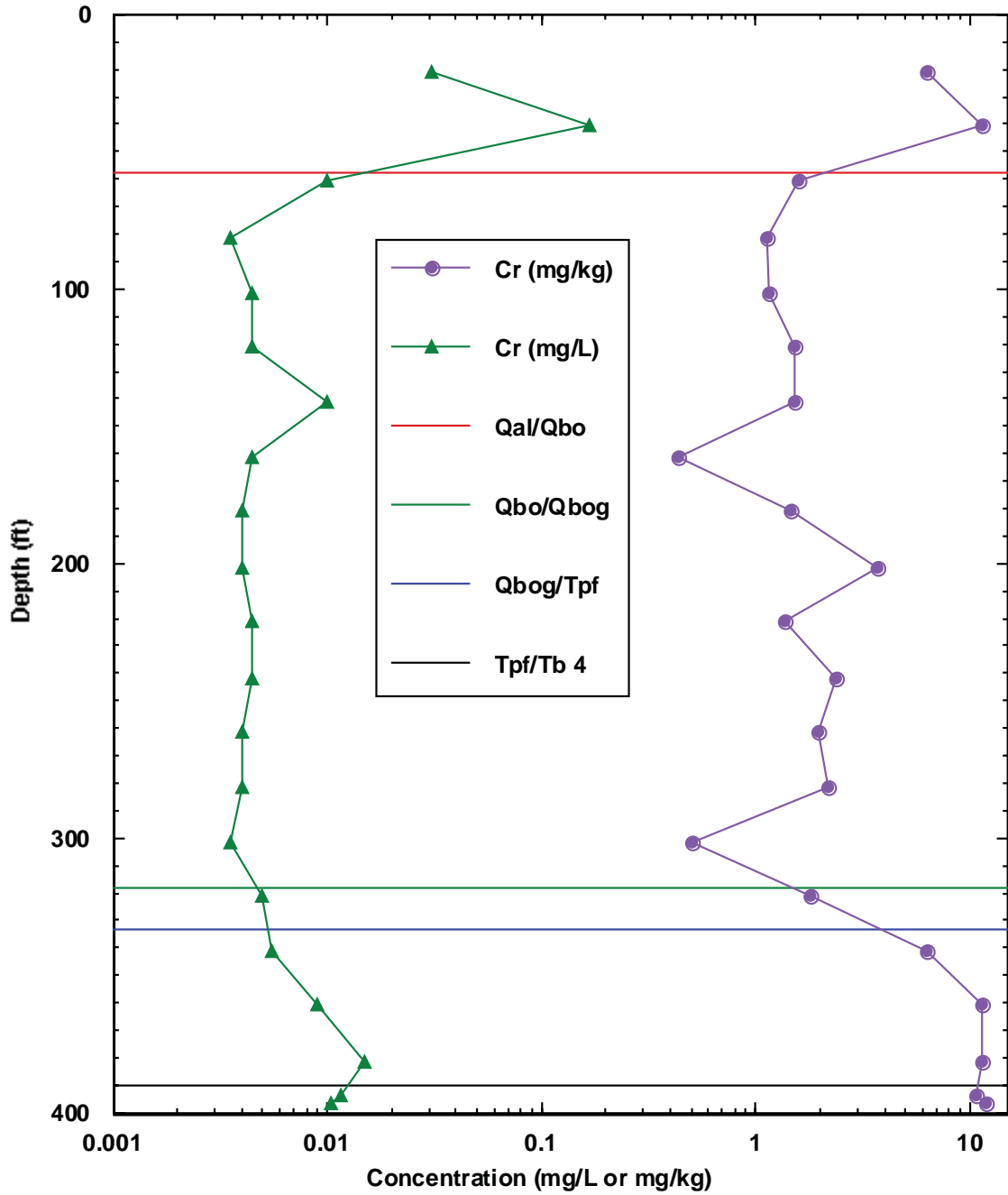


Figure B-1.7-1. Distributions of acid-soluble chromium (mg/kg) and dissolved chromium in pore water (mg/L) at core hole SCC-1, Sandia Canyon, New Mexico.

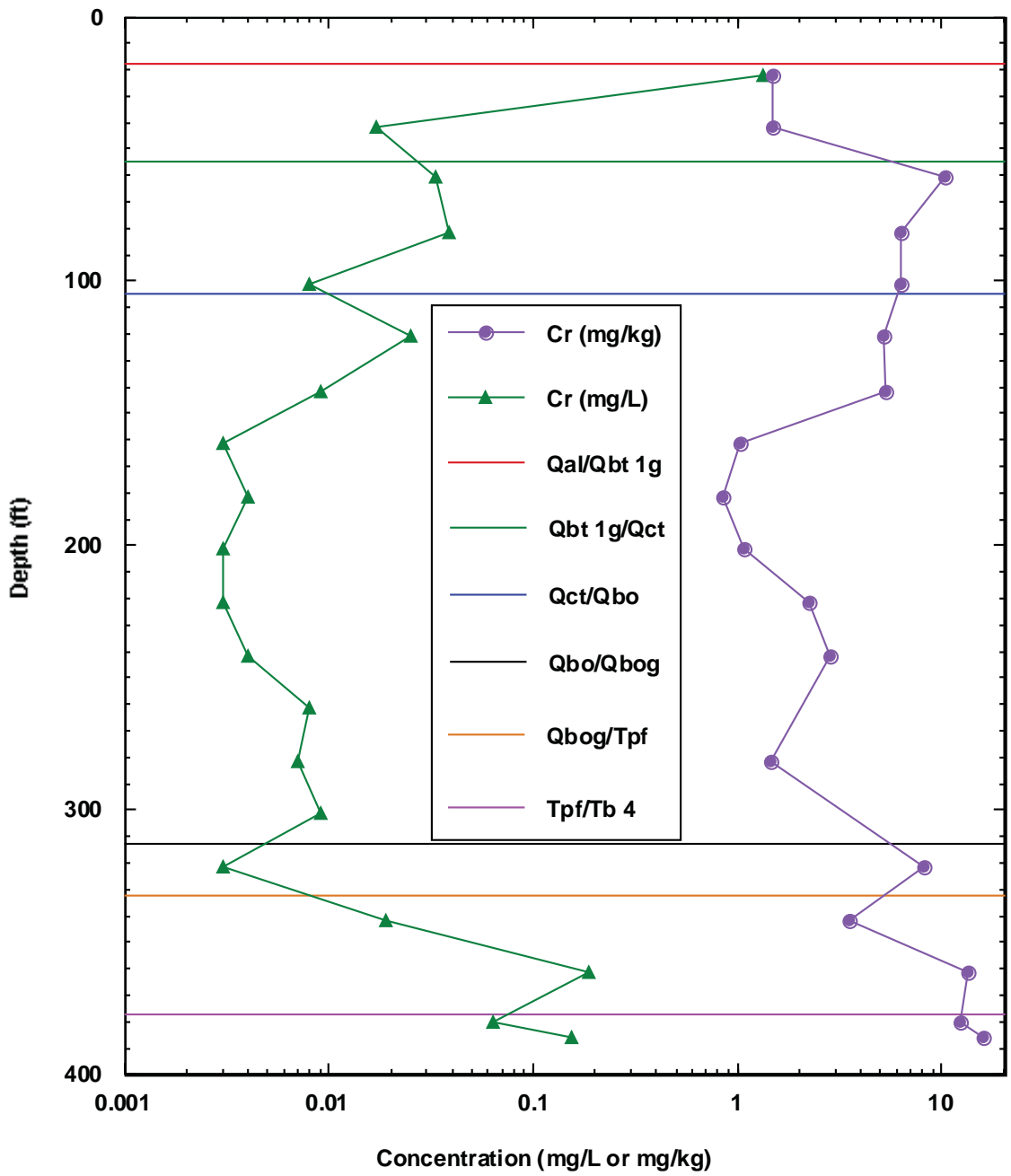


Figure B-1.7-2. Distributions of acid-soluble chromium (mg/kg) and dissolved chromium in pore water (mg/L) at core hole SCC-2, Sandia Canyon, New Mexico.

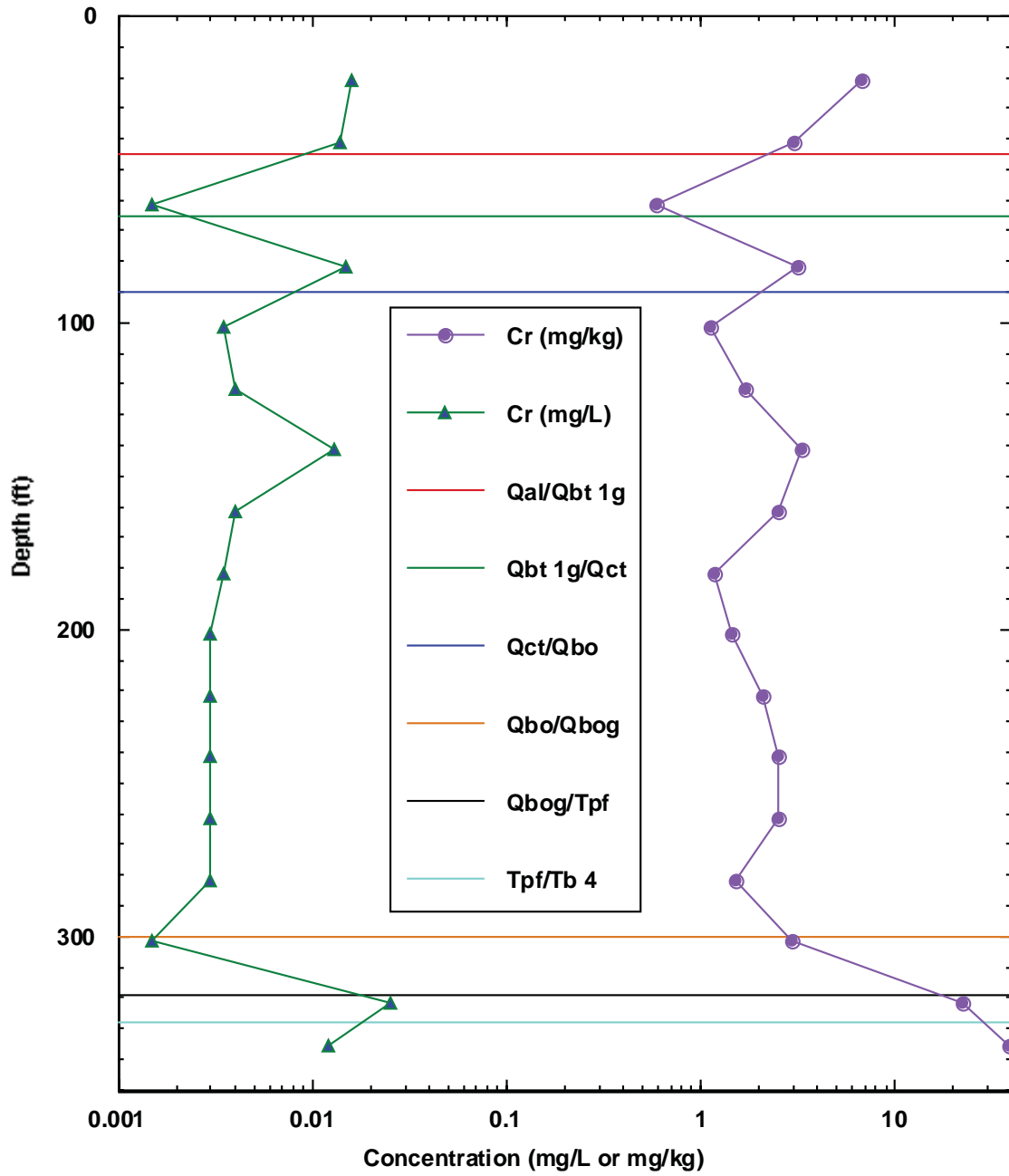


Figure B-1.7-3. Distributions of acid-soluble chromium (mg/kg) and dissolved chromium in pore water (mg/L) at core hole SCC-3, Sandia Canyon, New Mexico.

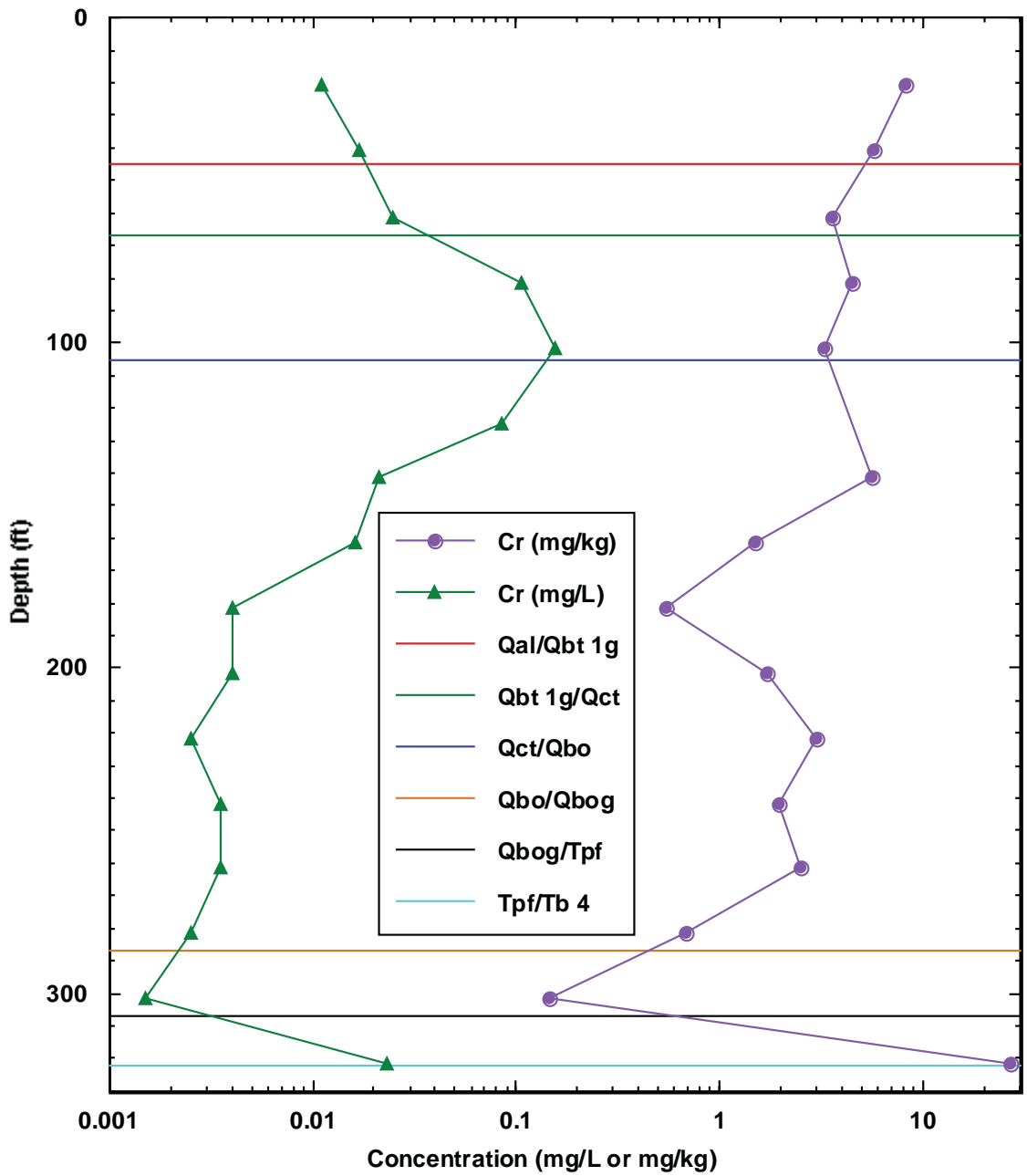


Figure B-1.7-4. Distributions of acid-soluble chromium (mg/kg) and dissolved chromium in pore water (mg/L) at core hole SCC-4, Sandia Canyon, New Mexico.

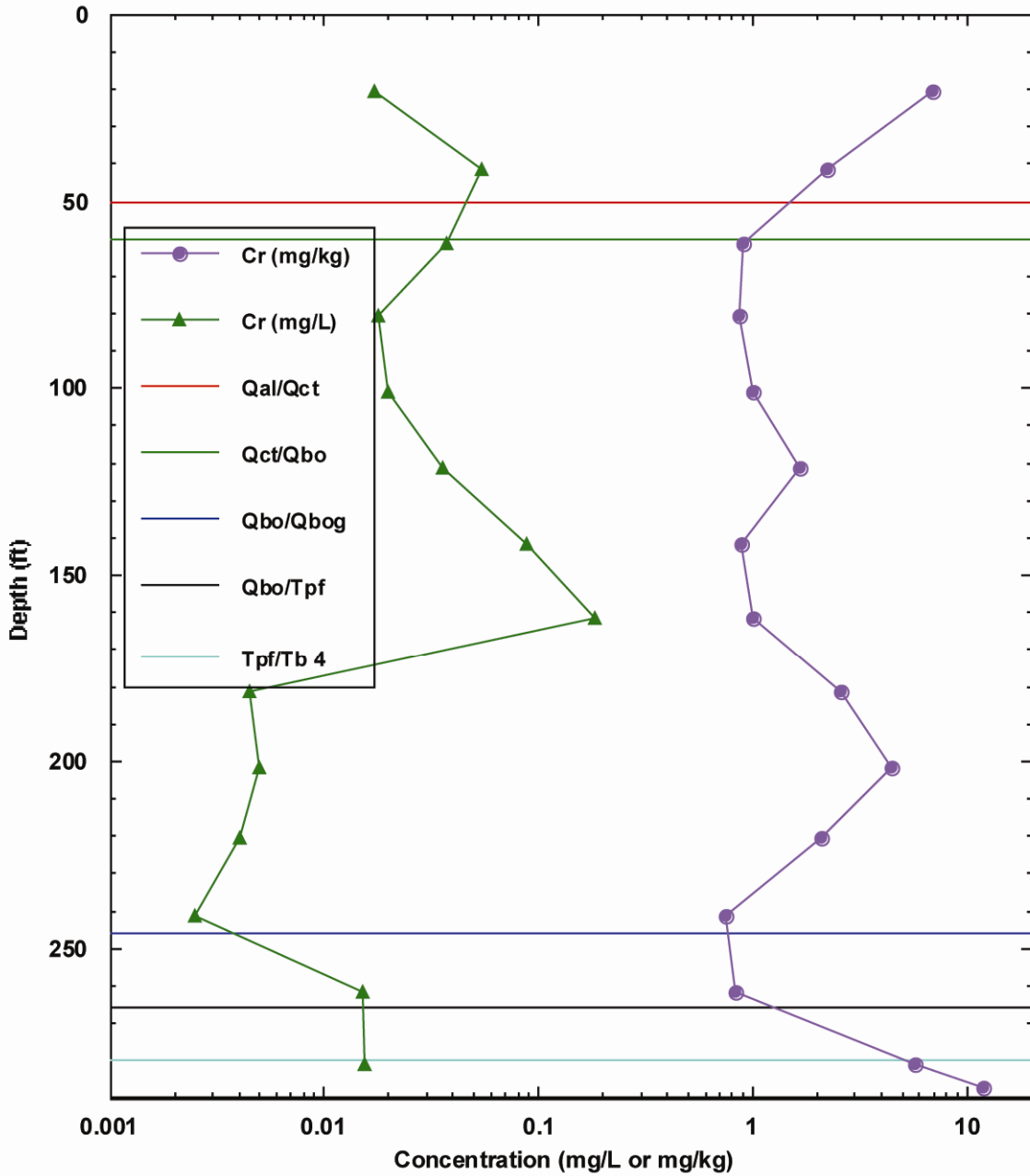


Figure B-1.7-5. Distributions of acid-soluble chromium (mg/kg) and dissolved chromium in pore water (mg/L) at core hole SCC-5, Sandia Canyon, New Mexico.

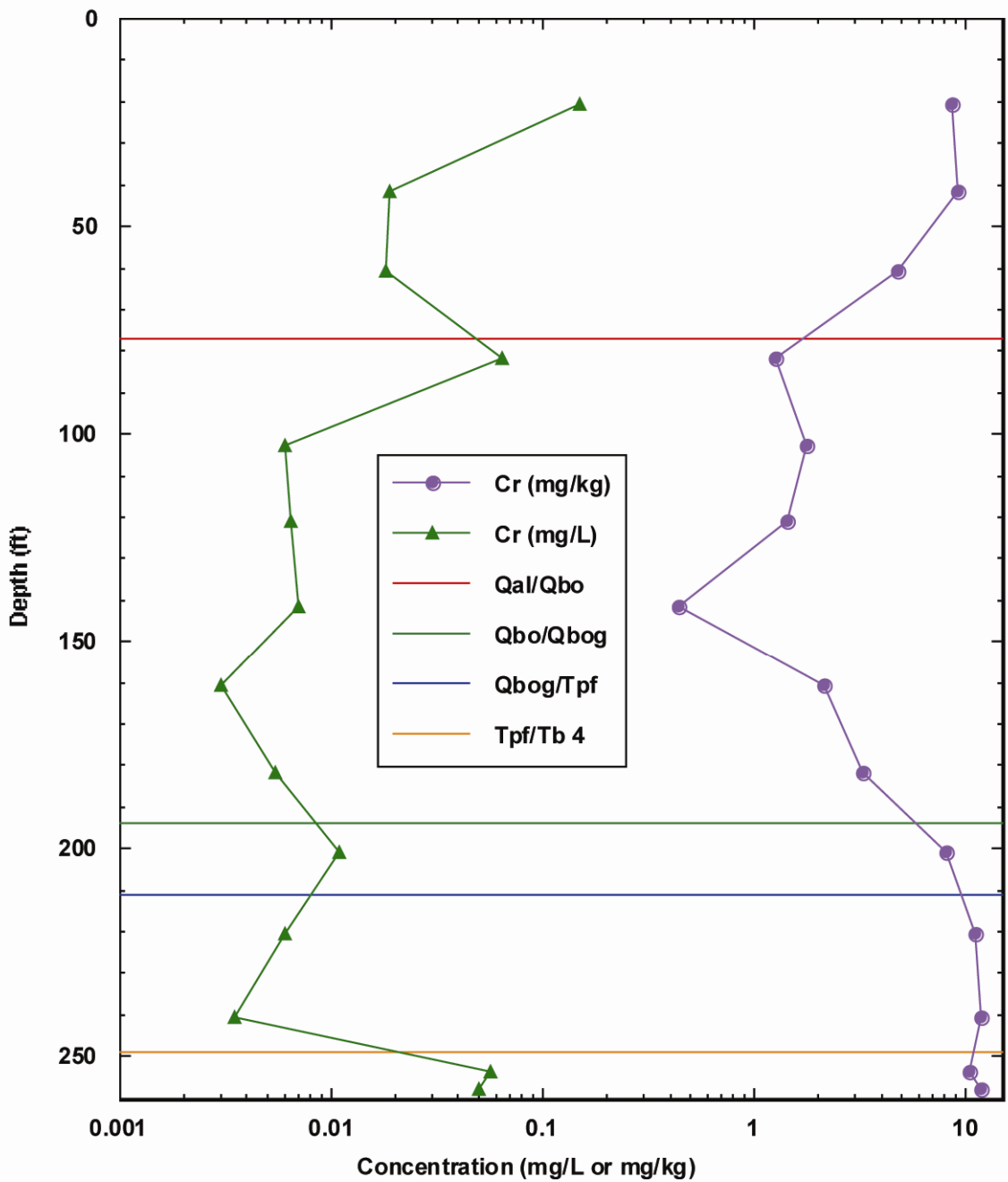


Figure B-1.7-6. Distributions of acid-soluble chromium (mg/kg) and dissolved chromium in pore water (mg/L) at core hole SCC-6, Sandia Canyon, New Mexico.

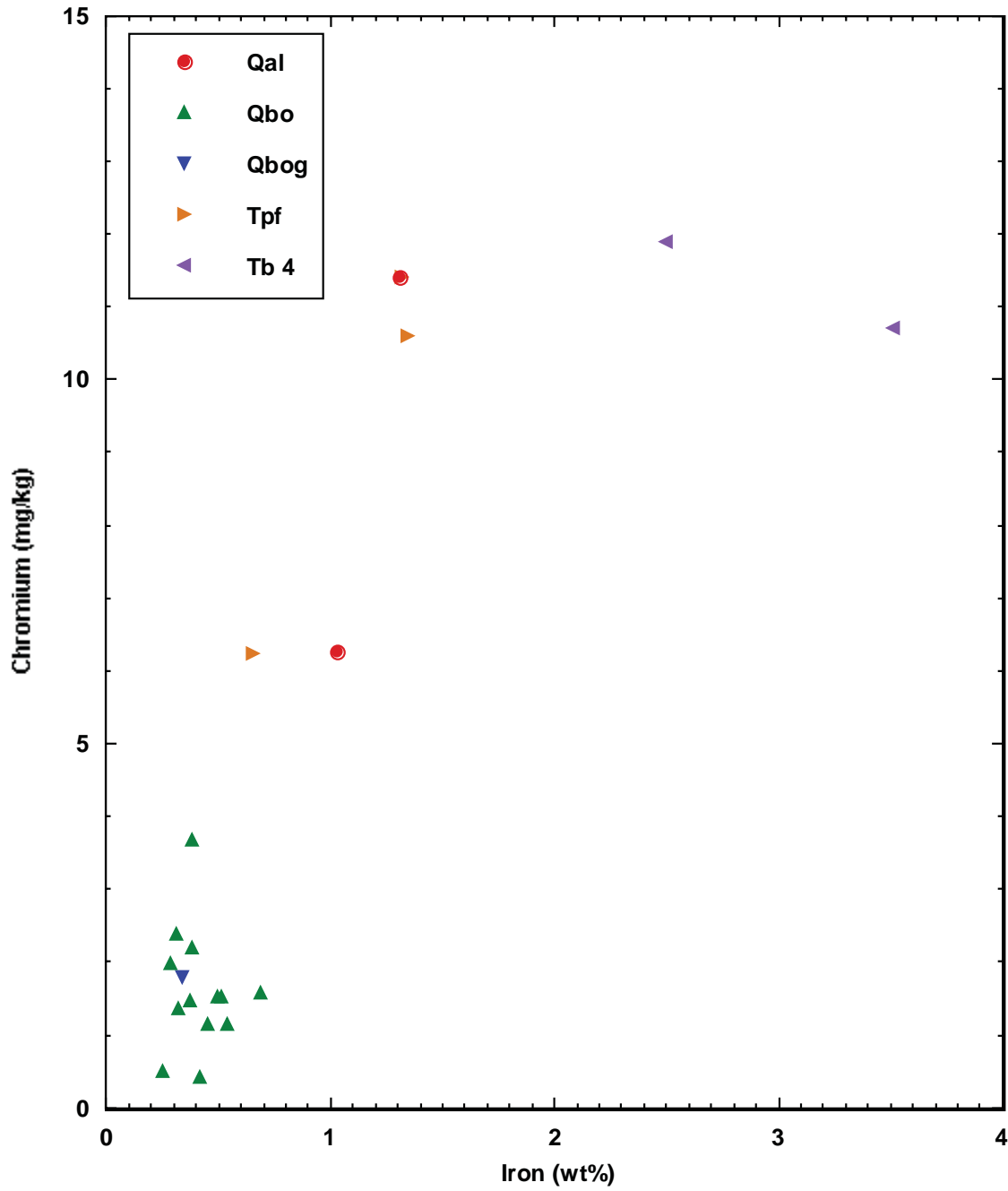


Figure B-1.7-7. Acid-soluble iron (wt%) versus acid-soluble chromium (mg/kg) at core hole SCC-1, Sandia Canyon, New Mexico.

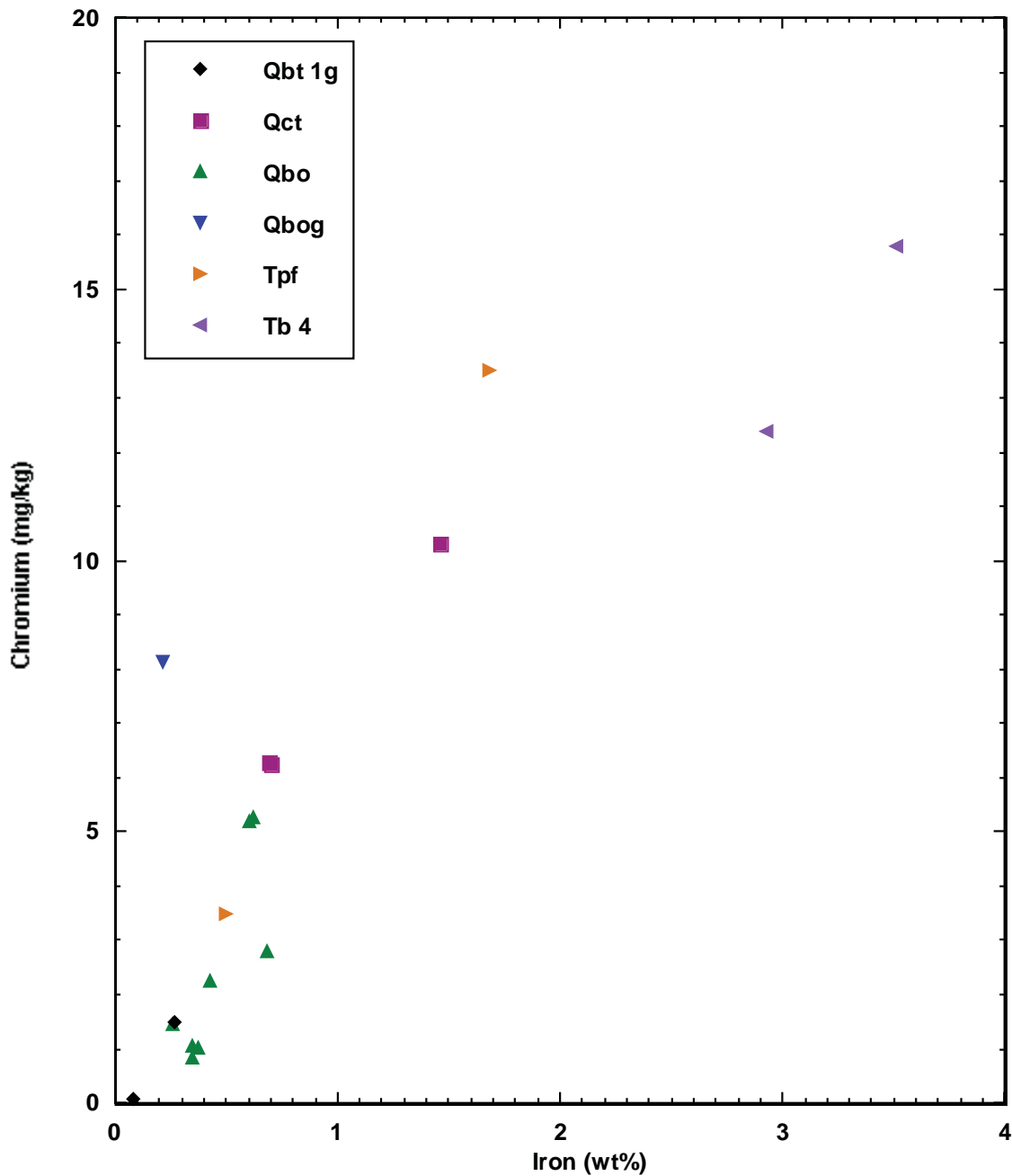


Figure B-1.7-8. Acid-soluble iron (wt%) versus acid-soluble chromium (mg/kg) at core hole SCC-2, Sandia Canyon, New Mexico.

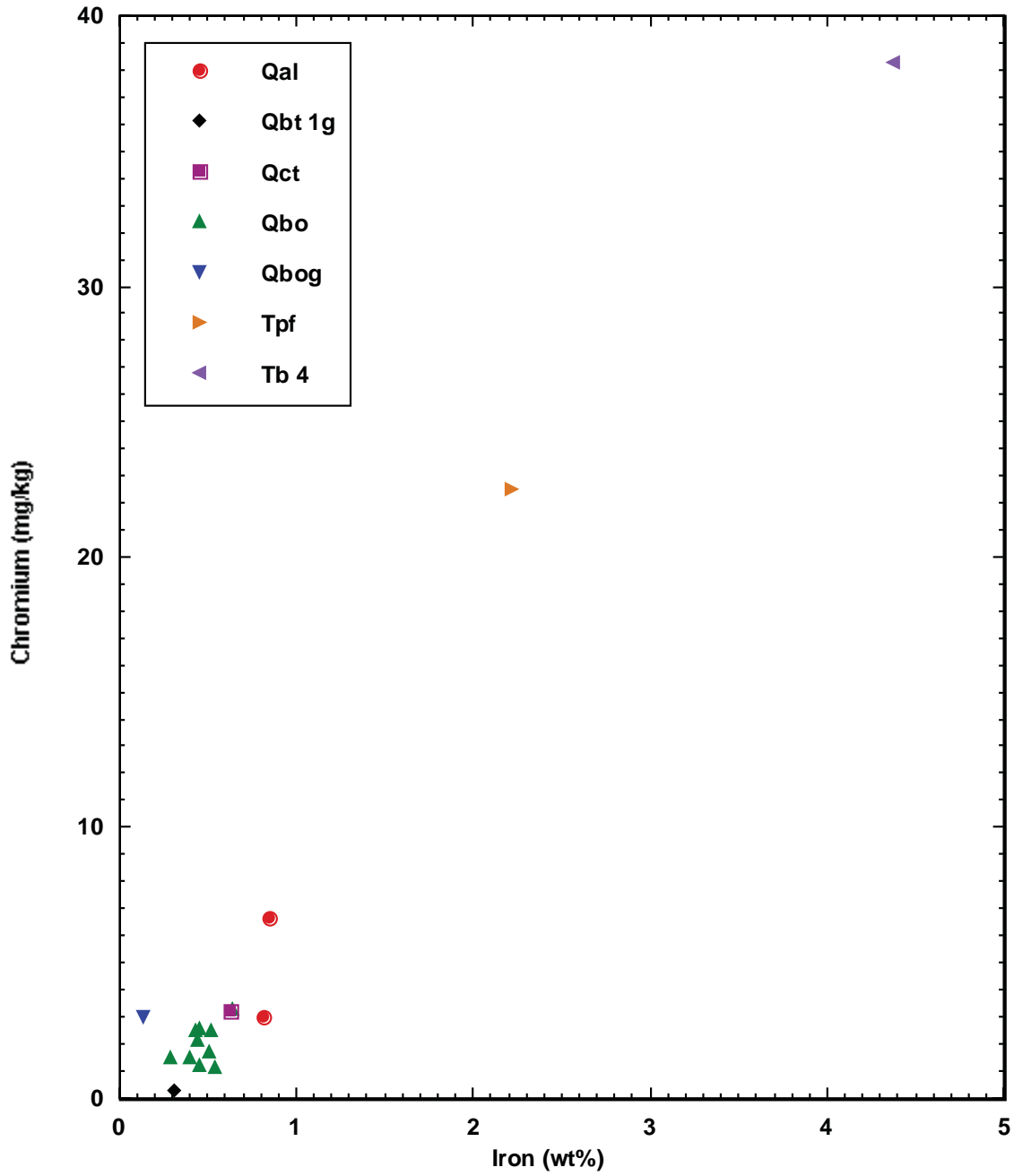


Figure B-1.7-9. Acid-soluble iron (wt%) versus acid-soluble chromium (mg/kg) at core hole SCC-3, Sandia Canyon, New Mexico.

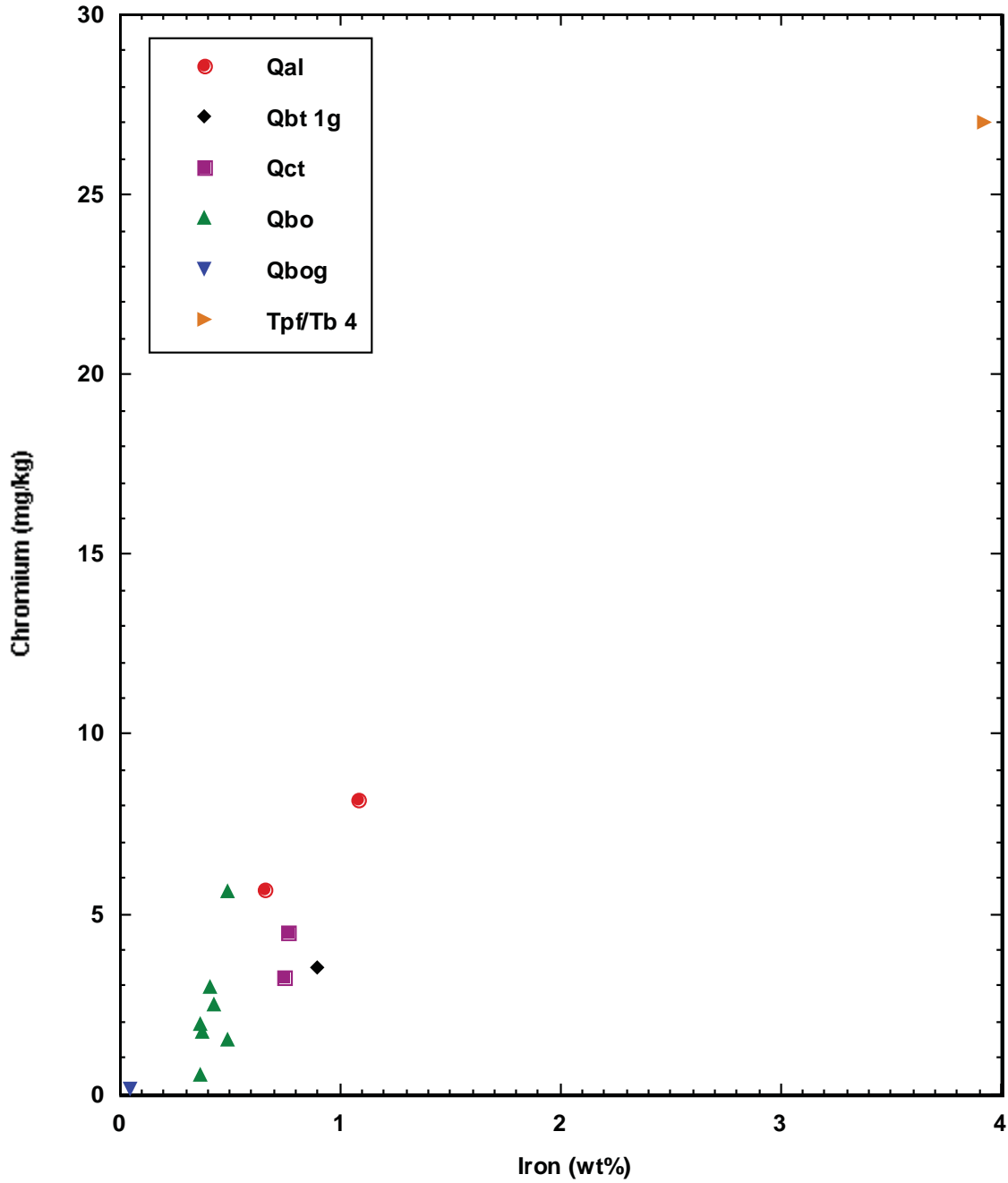


Figure B-1.7-10. Acid-soluble iron (wt%) versus acid-soluble chromium (mg/kg) at core hole SCC-4, Sandia Canyon, New Mexico.

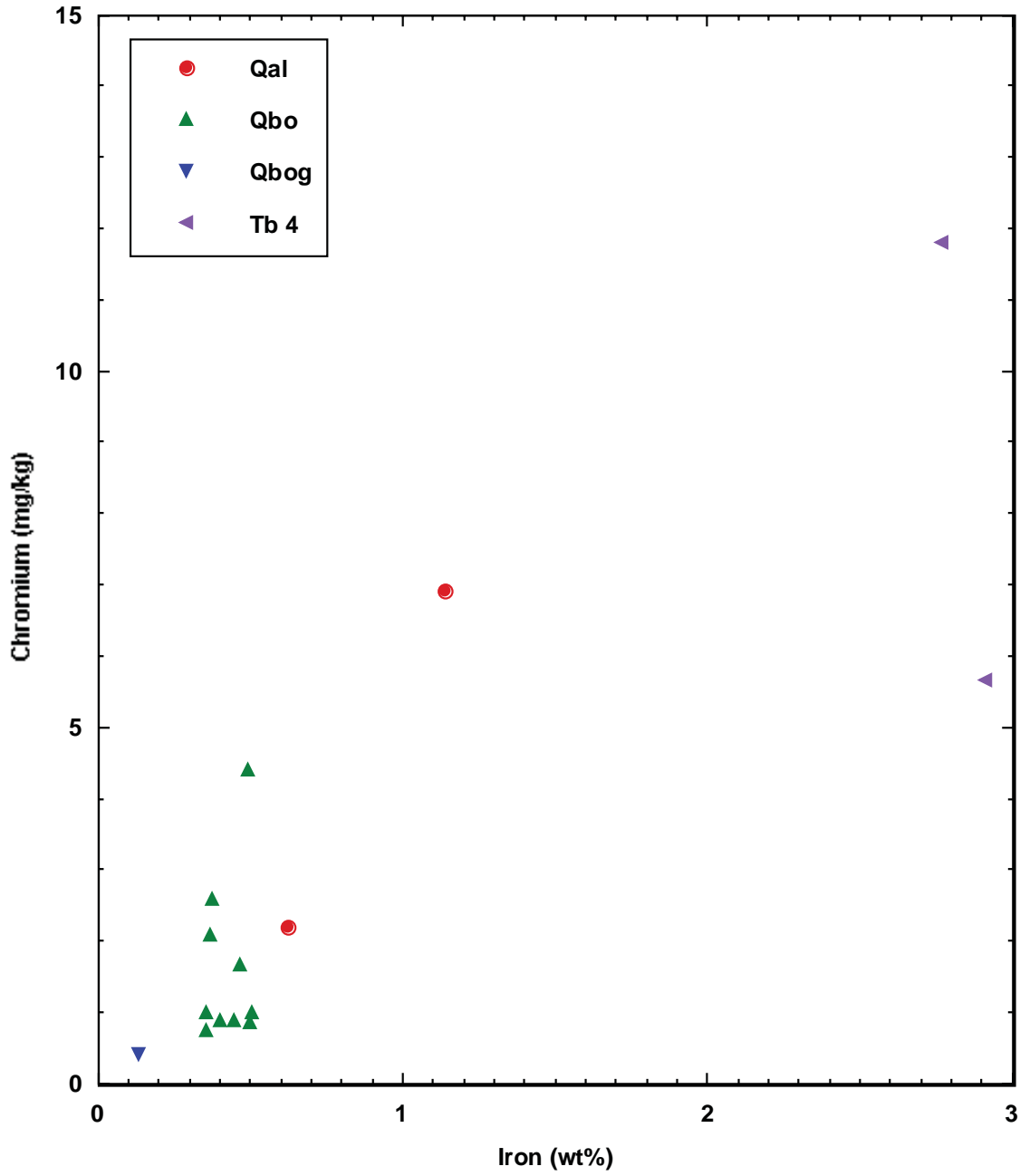


Figure B-1.7-11. Acid-soluble iron (wt%) versus acid-soluble chromium (mg/kg) at core hole SCC-5, Sandia Canyon, New Mexico.

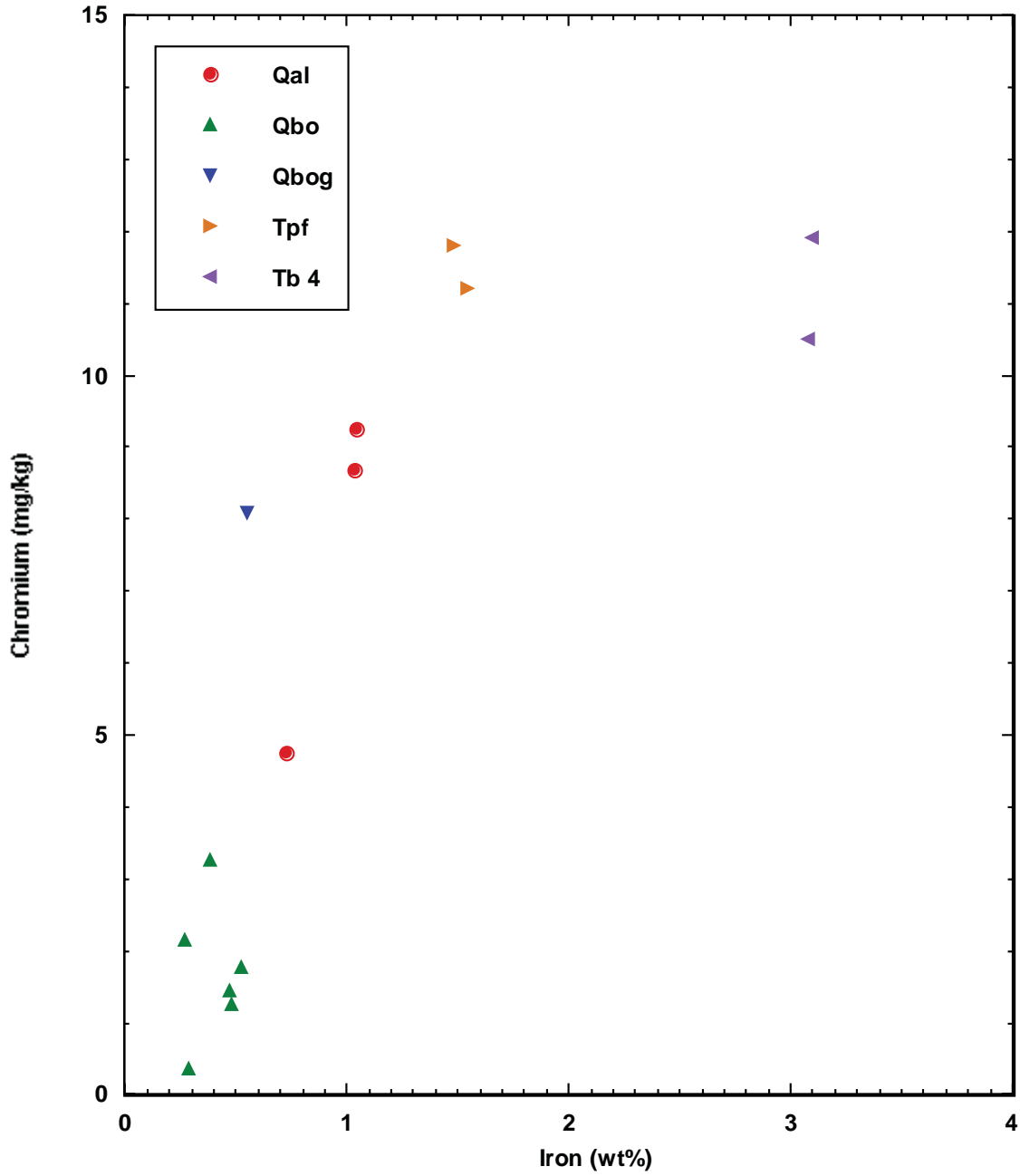


Figure B-1.7-12. Acid-soluble iron (wt%) versus acid-soluble chromium (mg/kg) at core hole SCC-6, Sandia Canyon, New Mexico.

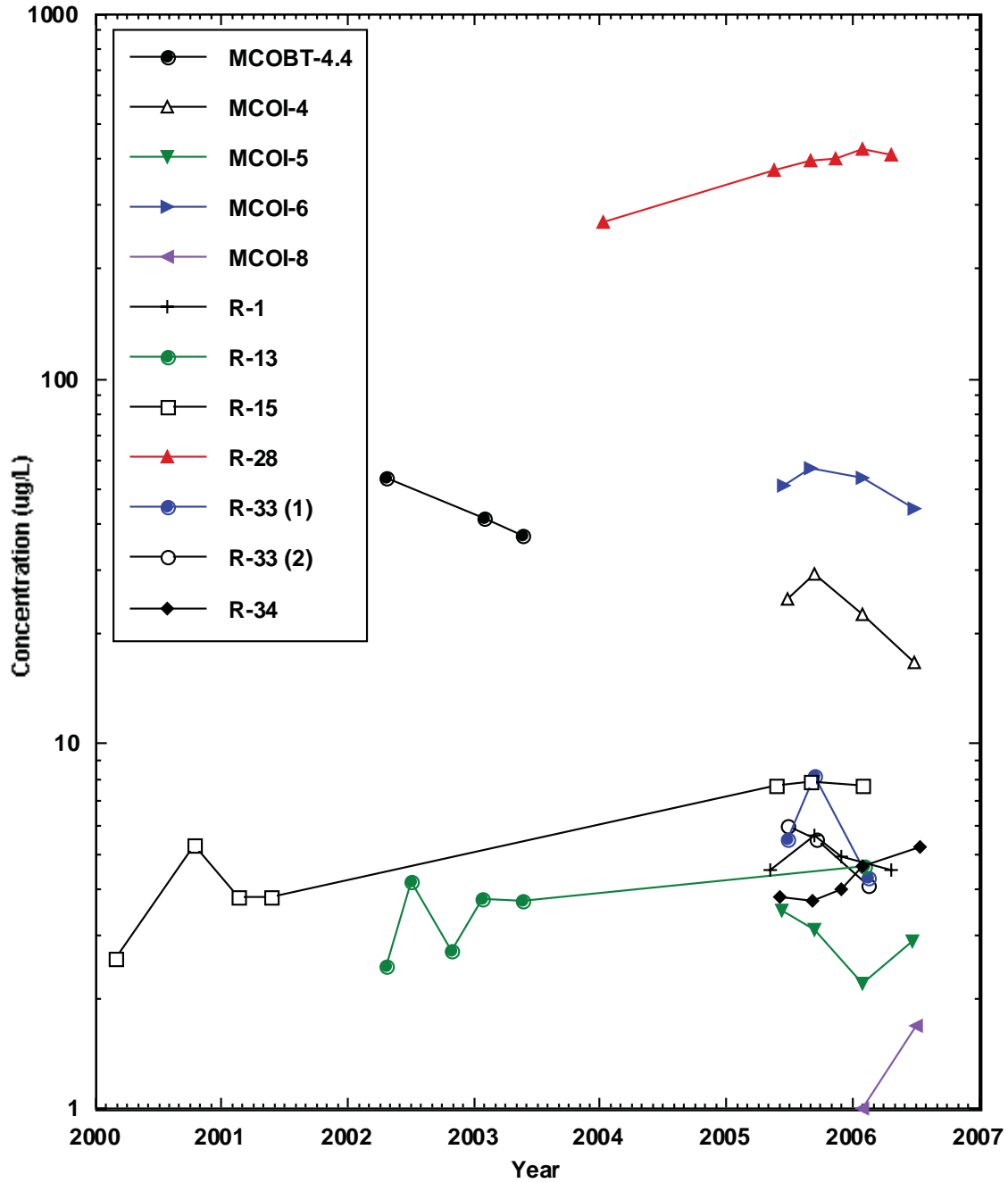


Figure B-1.7-13. Concentration of total dissolved chromium at MCOBT-4.4, MCOI-4, MCOI-5, MCOI-6, MCOI-8, R-1, R-13, R-15, R-28, R-33, and R-34, Mortandad Canyon, New Mexico.

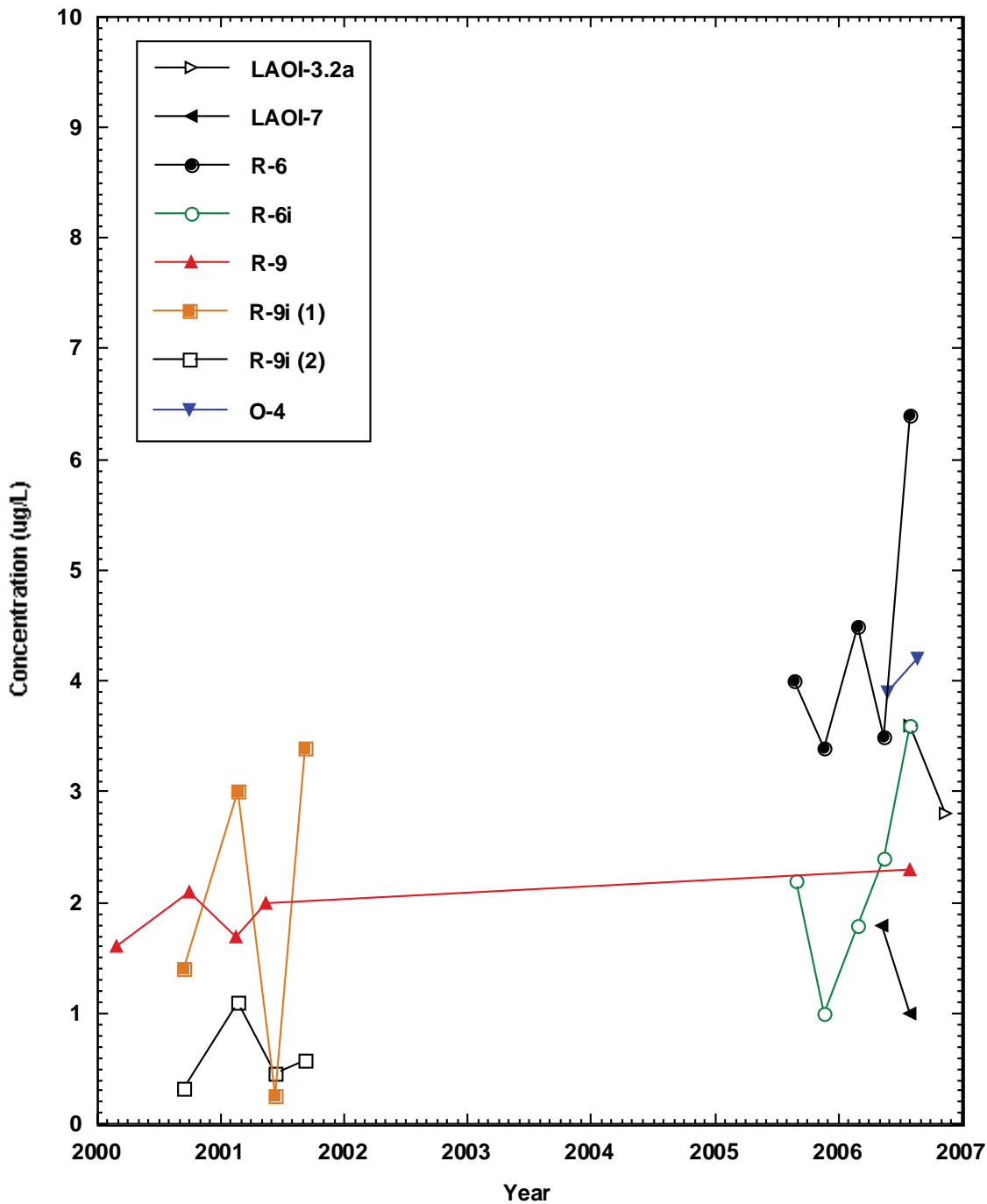


Figure B-1.7-14. Concentration of total dissolved chromium at LAOI-3.2a, LAOI-7, R-6, R-6i, R-9, R-9i (screens 1 and 2), and O-4, Los Alamos Canyon, New Mexico.

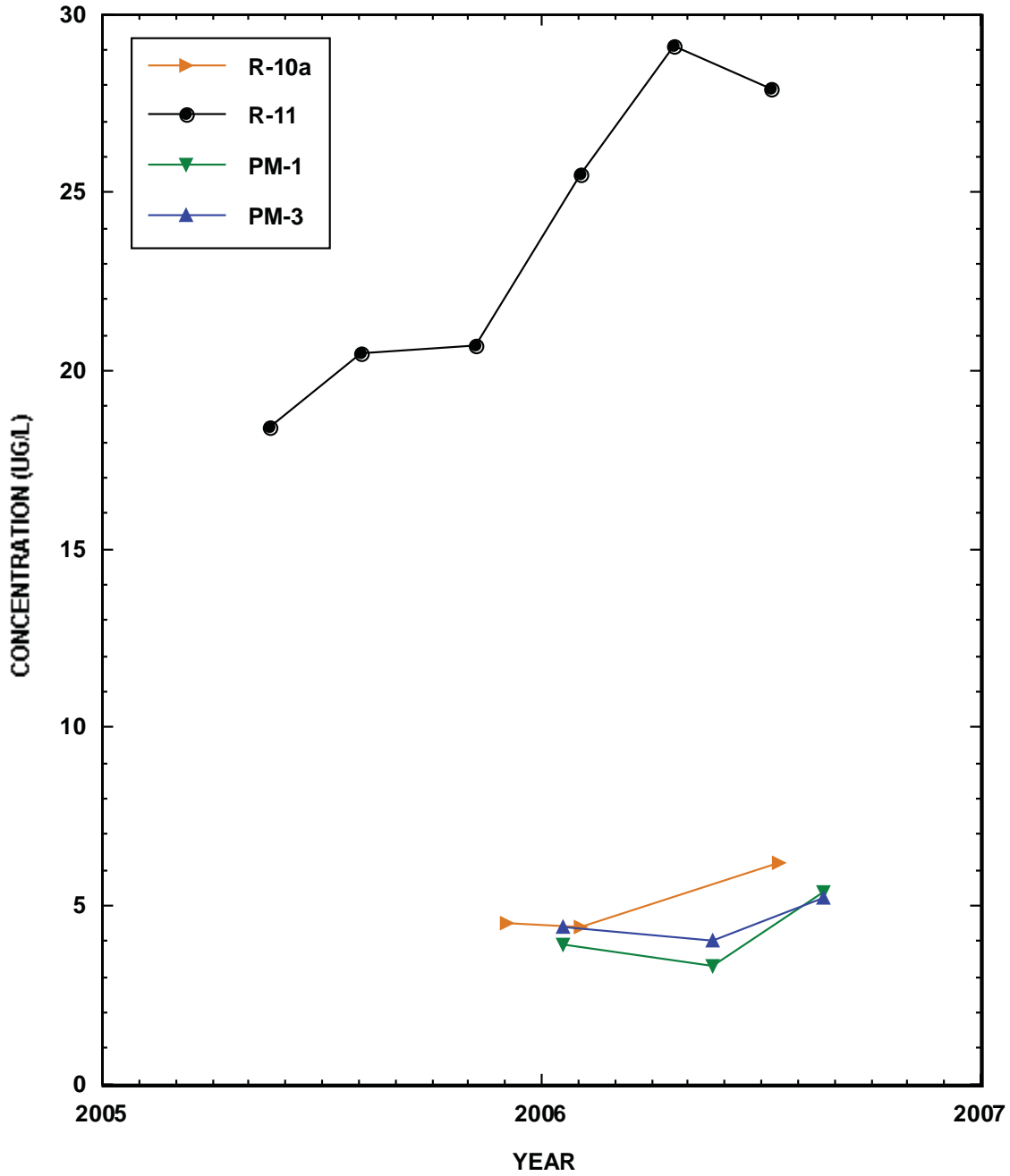


Figure B-1.7-15. Concentration of total dissolved chromium at R-10a, R-11, PM-1, and PM-3, Sandia Canyon, New Mexico.

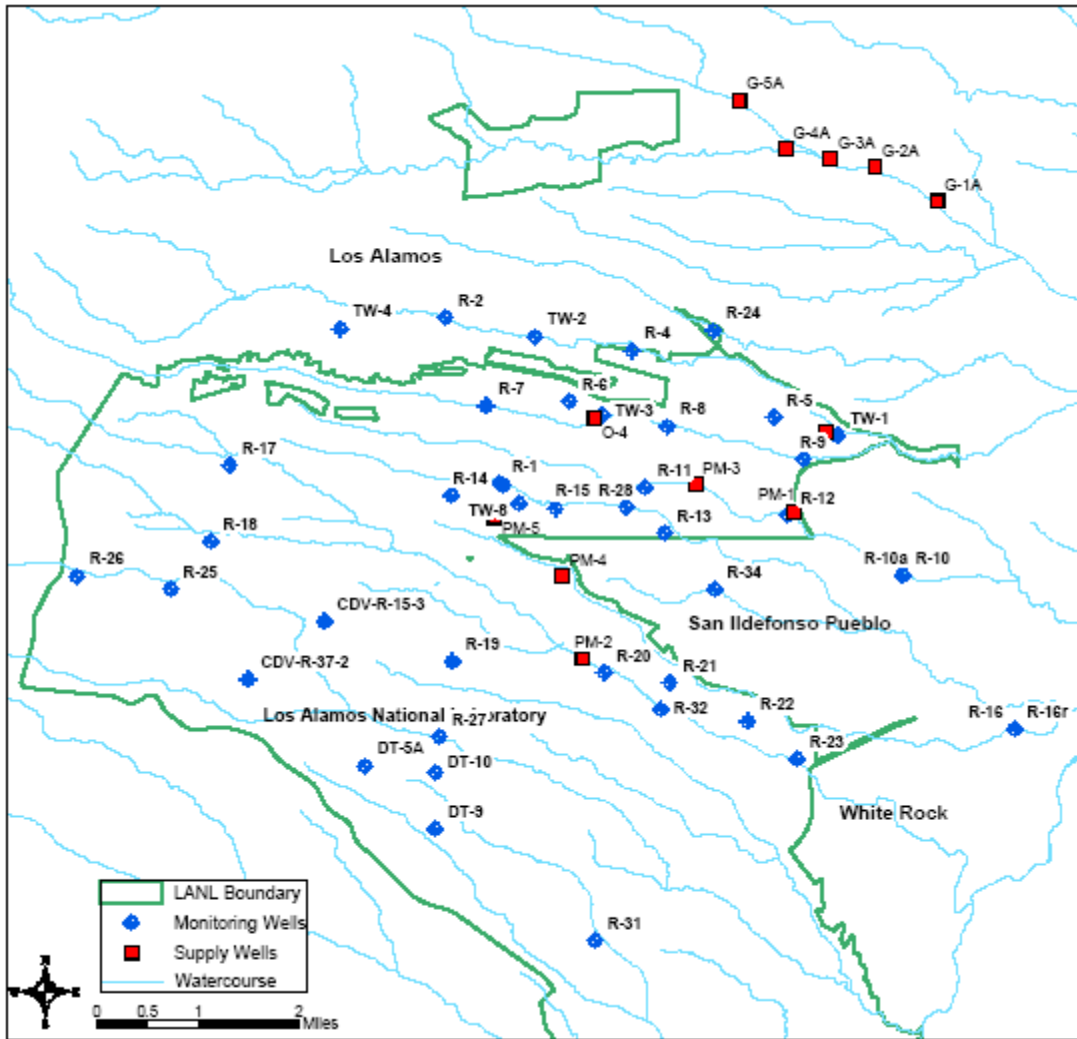
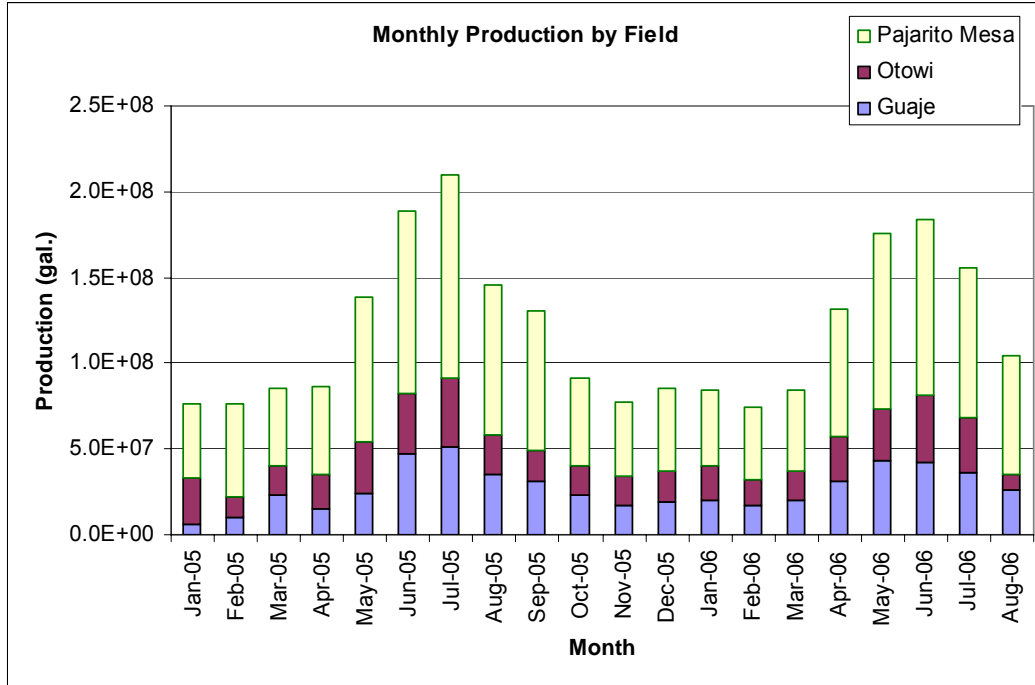


Figure B-2.0-1. Los Alamos County water supply wells, regional aquifer monitoring wells, and springs discharging regional aquifer at the Laboratory.

a.



b.

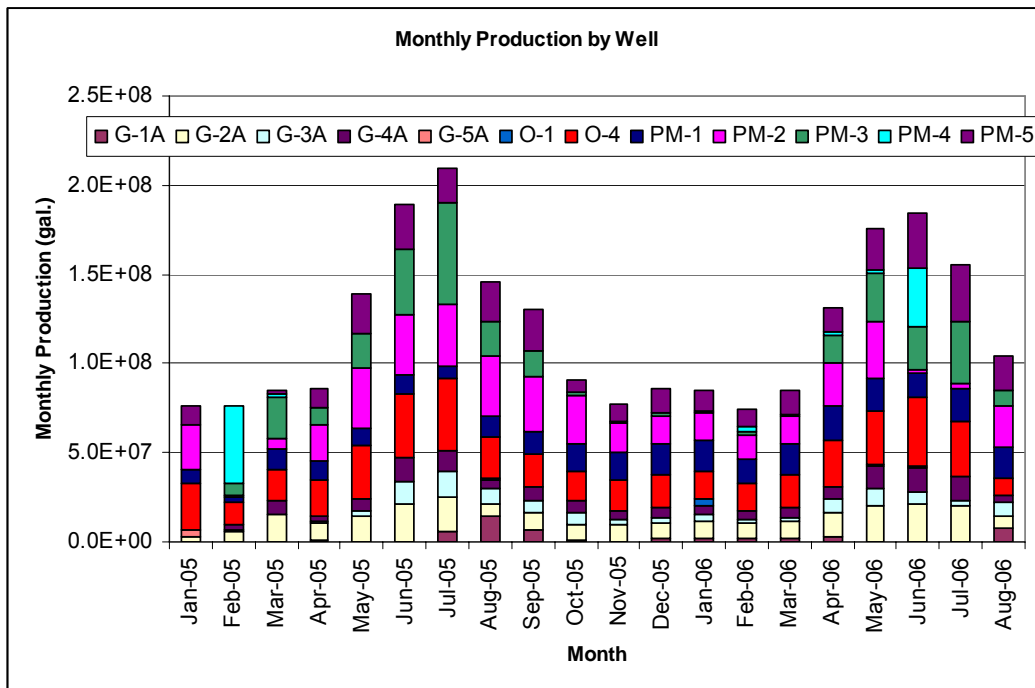


Figure B-2.0-2. Monthly water-supply production from (a) Los Alamos County well fields and (b) individual wells for 2005 and 2006.

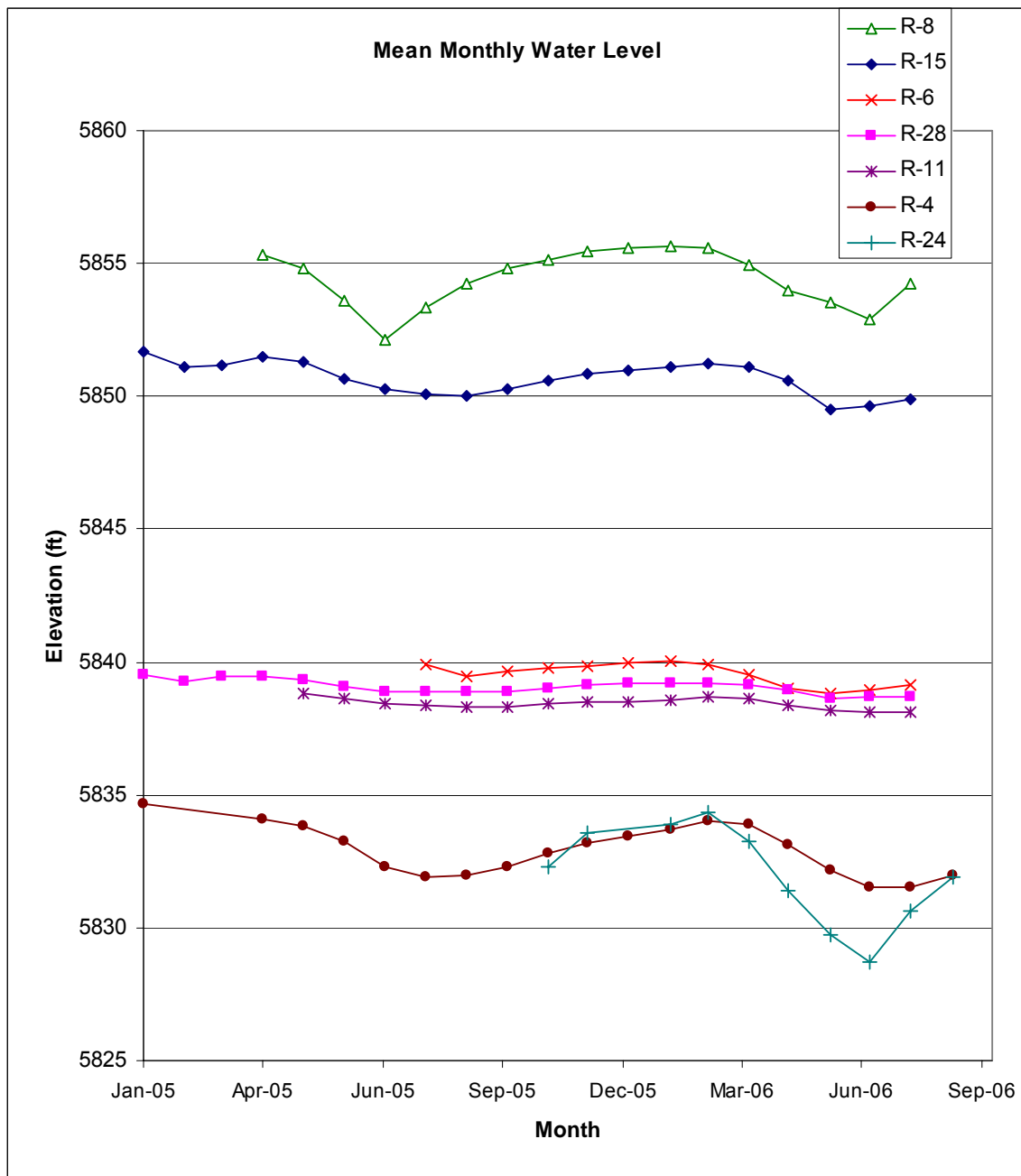


Figure B-2.0-3. Time series of mean monthly water levels in selected monitoring wells for 2005 and 2006.

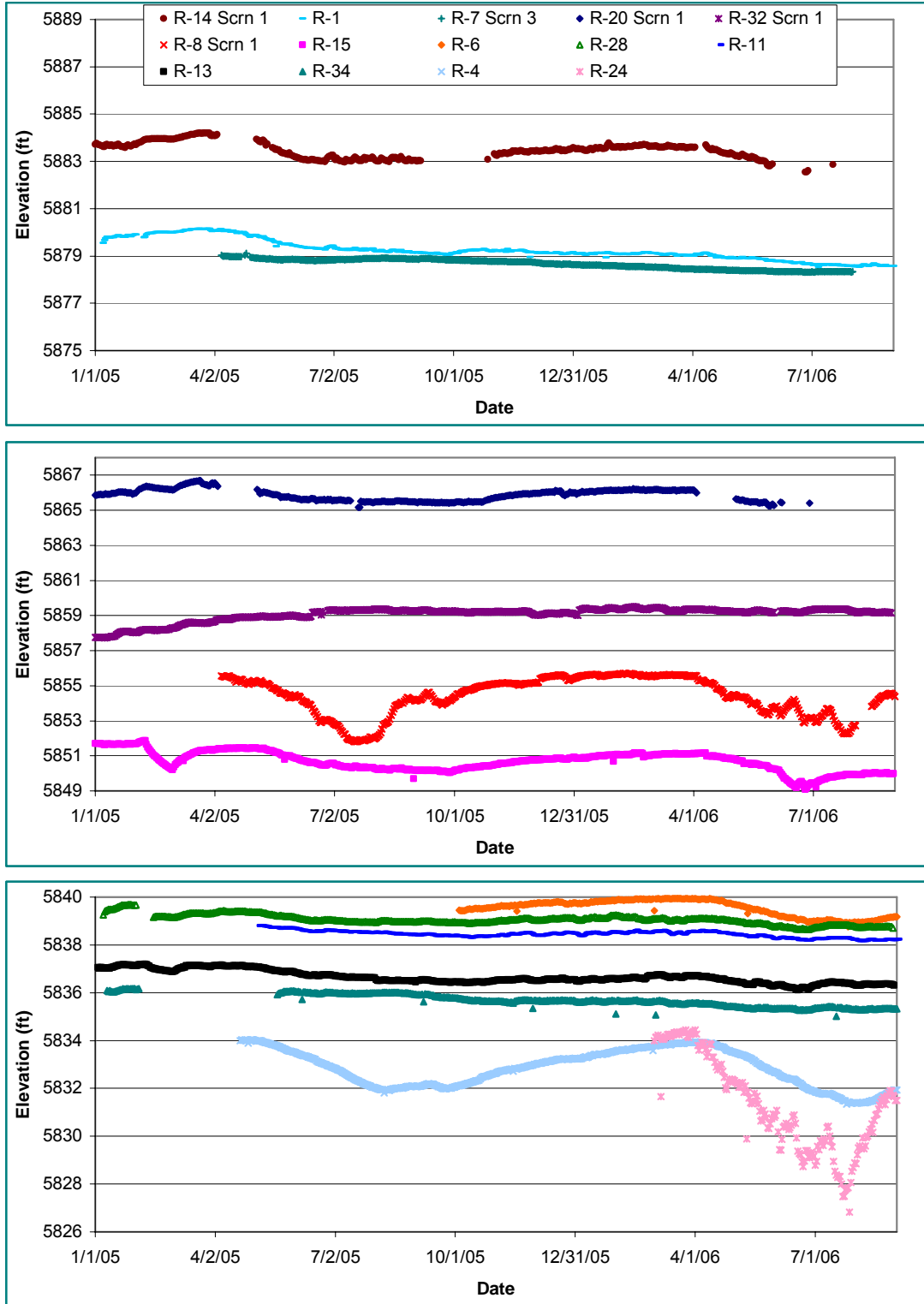


Figure B-2.0-4. Time series of mean daily water levels (corrected for atmospheric pressure) in selected wells for 2005 and 2006, showing relative seasonal transient response to water-supply pumping.

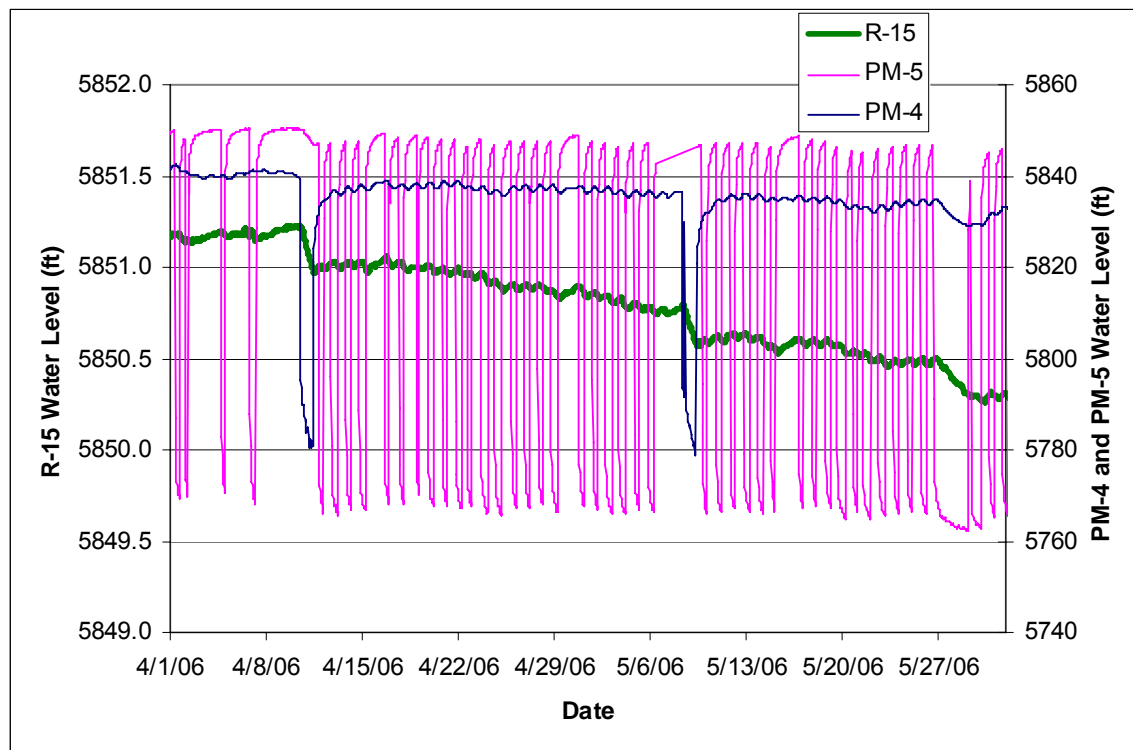


Figure B-2.0-5. R-15 water level corrected for atmospheric pressure showing response to pumping supply well PM-5 (note the differences in the axis scales for monitoring and pumping water-levels).

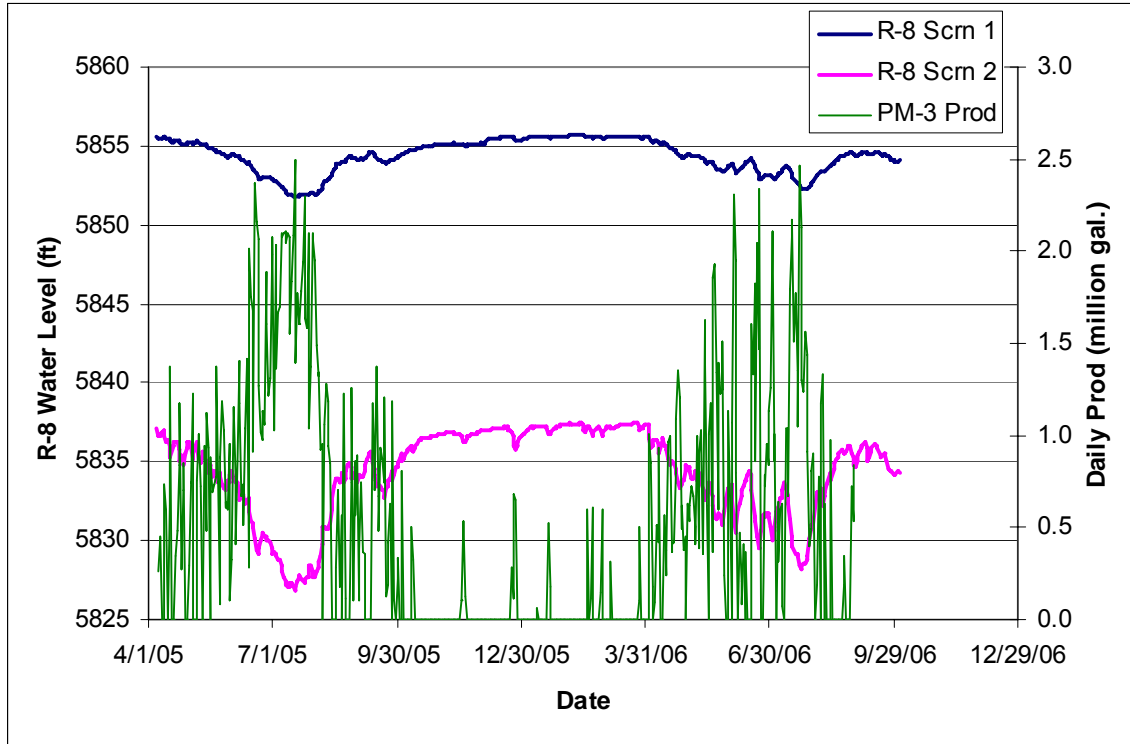
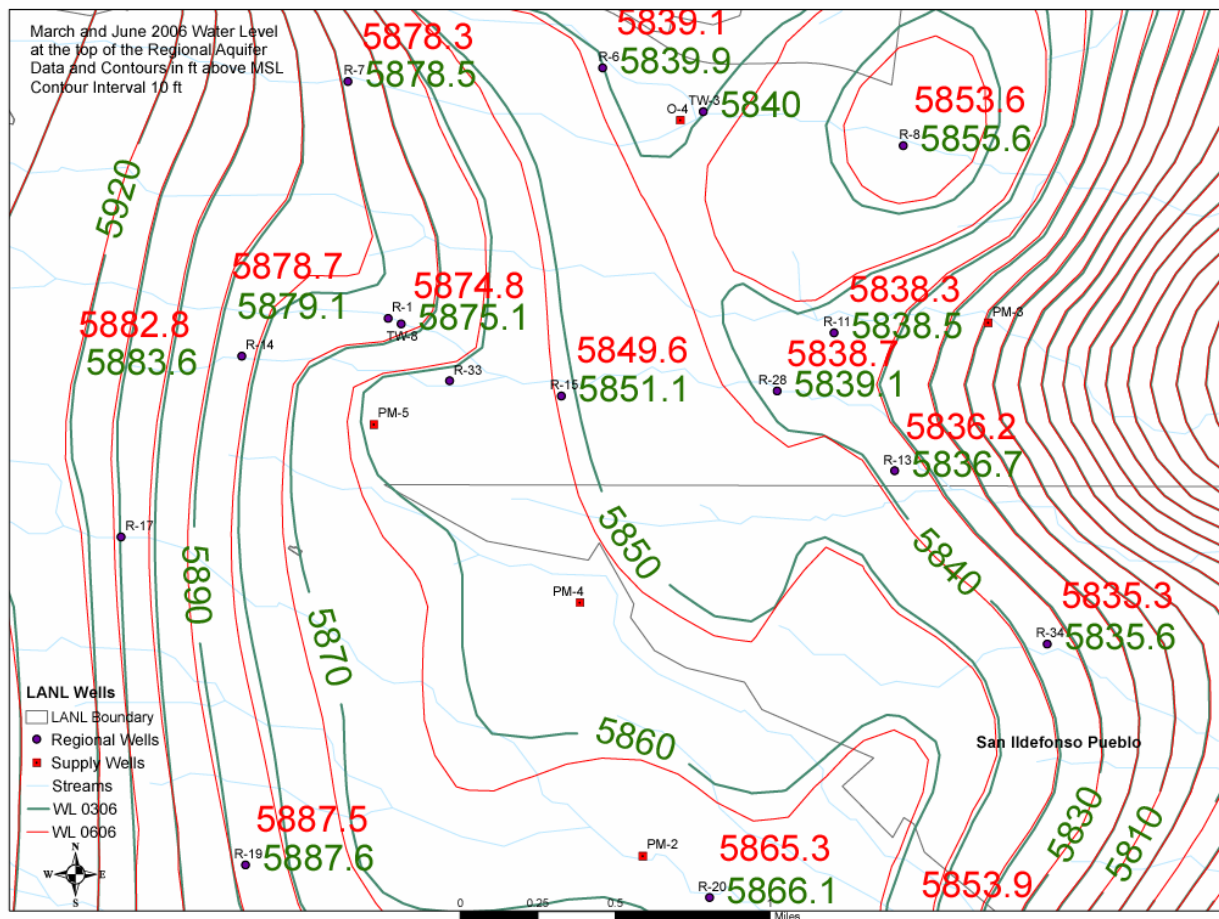


Figure B-2.0-6. R-8 water level showing response to pumping supply well PM-3.



**Figure B-2.0-7. Water table contour map for March and June 2006 using the water-level data measured at the screen closest to the top of the regional aquifer from all the monitoring wells. However, a substantial portion of these water-level measurements might not be representative of the water-table elevation. For more details, see text and Table B-2.0-2.**

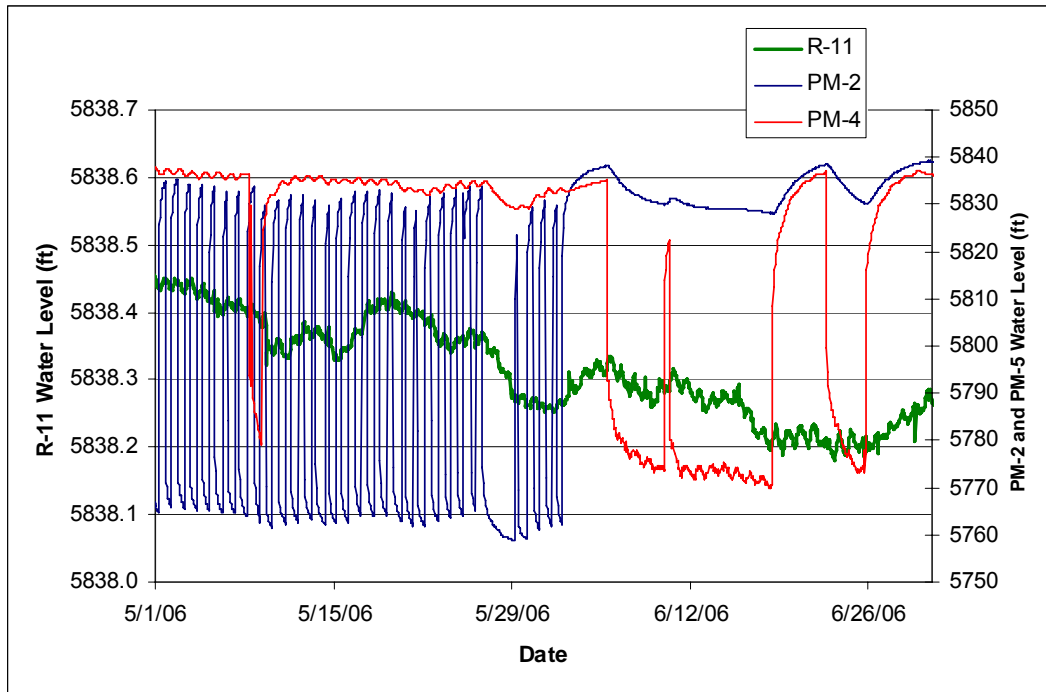


Figure B-2.0-8. R-11 water level corrected for atmospheric pressure showing response to pumping of supply wells PM-2 and PM-4 (note the differences in the axis scales for monitoring and pumping water levels).

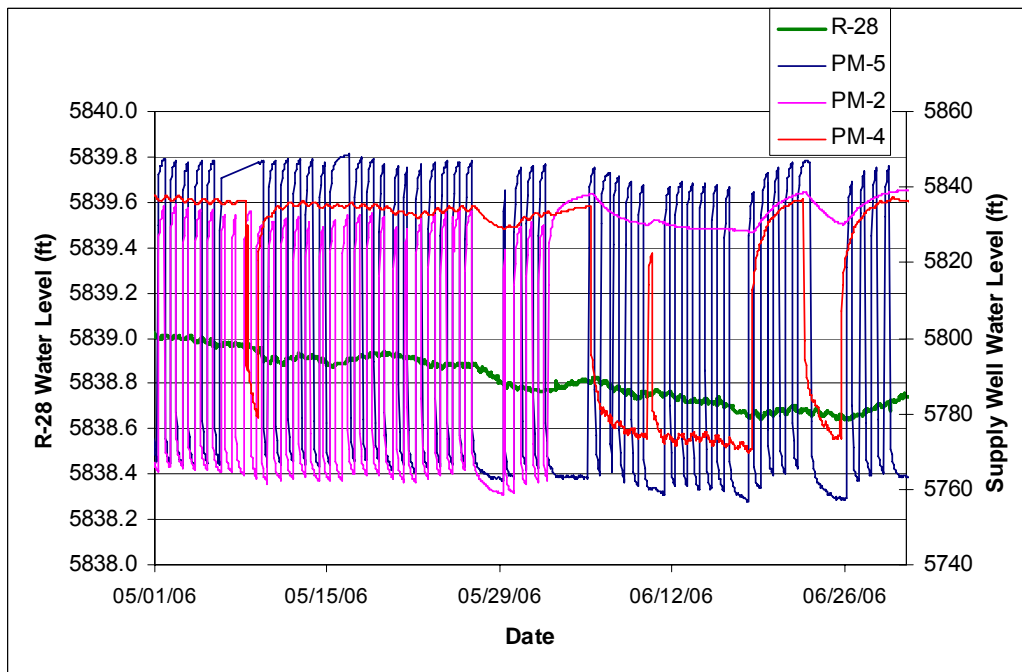


Figure B-2.0-9. R-28 water level corrected for atmospheric pressure showing response to pumping of supply wells PM-2, PM-4, and PM-5 (note the differences in the axis scales for monitoring and pumping water levels).

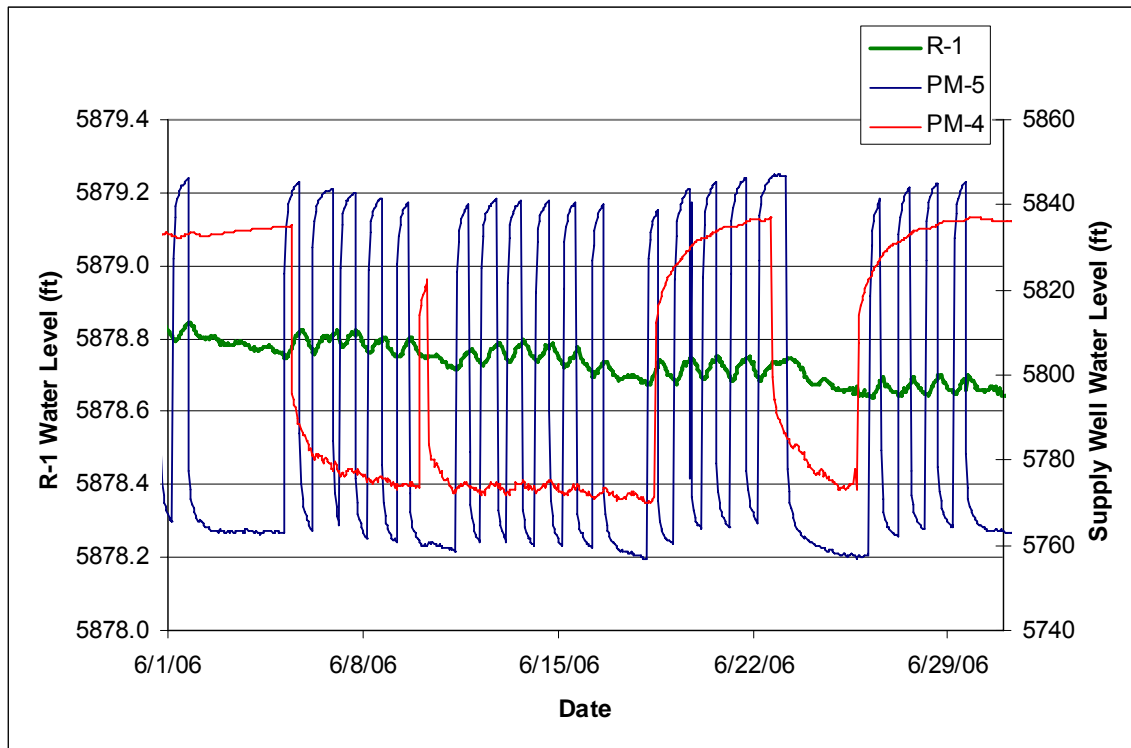


Figure B-2.0-10. R-1 water level corrected for atmospheric pressure showing response to pumping of supply well PM-5 (note the differences in the axis scales for monitoring and pumping water levels).

**Table B-1.0-1**  
**Summary Information for Alluvial and Intermediate Drill Holes**

Hole	Depth	Goal	Well Screen	Core Samples	Water Samples
SCA-1	2.2 ft	install alluvial well	1.3–1.9 ft	n/a <sup>a</sup>	n/a
SCA-2	19 ft	install alluvial well	10.1–14.8 ft	n/a	n/a
SCA-3	58.5 ft	install alluvial well	27.6–32.0 ft	n/a	n/a
SCA-4	43.8 ft	install alluvial well	37.0–41.5 ft	n/a	n/a
SCA-5	78.5 ft	install alluvial well	55.0–64.4 ft	n/a	n/a
SCC-1	400 ft	collect core and water	358.4–377.9 ft	21	1
SCC-2	388.6 ft	collect core and water	P&A <sup>b</sup>	20	4
SCC-3	344 ft	collect core and water	P&A	17	2
SCC-4	323 ft	collect core and water	P&A	16	1
SCC-5	287.5 ft	collect core and water	P&A	16	0
SCC-6	259.5 ft	collect core and water	P&A	14	0

<sup>a</sup> n/a = Not applicable. (Note: Core samples were collected for alluvial wells SCA-3, -4, and -5 but were used only for geologic logging; no cores from the SCA series wells were analyzed for contaminants.)

<sup>b</sup> P&A = Plugged and abandoned; no well installed.

**Table B-1.0-2**  
**Summary Information for Piezometers**

Piezometer Hole	Screen 1	Screen 2	Screen 3	Companion Alluvial well
SCP-1a,b,c	a = 37.8–38.3 ft	b = 39.4–39.9 ft	c = 41.2–41.7 ft	SCA-4
SCP-2a	a = 44.5–45.0 ft	n/a*	n/a	SCA-3
SCP-2b	b = 49.5–50.0 ft	n/a	n/a	SCA-3

\* n/a = Not applicable where piezometers were not nested in a single hole.

**Table B-1.1-1**  
**Summary of and Modifications to SC-Hole Stratigraphies**  
**Core Hole SC-1**

Depth (ft)	(b) Bag or (L) Lexan Sample	Observations
5	b	loose silt; Qbt 1v clasts up to 2 cm
10	b	crystal-rich sand
<b>Qal/Qbt 1g at 10-14.5 (~12) ft (new pick) [Kleinfelder 2002 places Qal/Qbo at 23 ft]</b>		
14.5	b	pink vitric ash flow, nonwelded, some intact core pieces
24	b	pink vitric ash flow, nonwelded, some intact core pieces
29	b	pink vitric ash flow, nonwelded, some intact core pieces
44	b	transition to buff-colored vitric ash flow, nonwelded, some intact core pieces
46.5–49	L	buff-colored vitric ash flow, nonwelded, intact core
54	b	buff-colored vitric ash flow, nonwelded, some intact core pieces

**Table B-1.1-1 (continued)**

Depth (ft)	(b) Bag or (L) Lexan Sample	Observations
59	b	buff-colored vitric ash flow, nonwelded, some intact core pieces
69	b	buff-colored vitric ash flow, nonwelded, some intact core pieces
<b>Qbt1g/Qbo at 69-76 (~73) ft (new pick) (This pick assumes that pink horizon beginning below marks top of Qbo, with little or no Qct between Qbt 1g and Qbo.)</b>		
76-77	b	pink vitric ash flow, nonwelded, intact core
79-81.5	L	pink vitric ash flow, nonwelded, intact core
86-86.5	b	pink vitric ash flow, nonwelded, some intact core pieces
96-97	b	buff-colored vitric ash flow, nonwelded, some intact core pieces
101.5-104	L	buff-colored vitric ash flow, nonwelded, intact core
105-106	b	buff-colored vitric ash flow, nonwelded, some intact core pieces

**Table B-1.1-1 (continued)  
Core Hole SC-2**

Depth (ft)	(b) Bag or (L) Lexan Sample	Observations
5	b	silty; moderate induration
10	b	silty, slight induration, lesser amounts of xl-rich sand
20	b	clasts of Qbt 1v to >2.5 cm (cut by 1 in core); some silty sand
<b>Qal/Qbt1g at 25 ft</b>		
26.5-29	b	intact core of Qbt 1g
31-32	b	some intact core pieces of Qbt 1g
41-42	b	friable Qbt 1g
46-47	b	friable Qbt 1g
<b>Qbt1g/Qct at 54 ft</b>		
56-57	b	very moist; small white vitric aphyric pumice in silt/clay matrix
59.3-60	b	moderately moist; small white vitric aphyric pumice in silt/clay matrix; trace obsidian (Kleinfelder 2002, 091687 noted perched saturation at 59.3 ft.)
71-72	b	silty, trace obsidian; clasts of sub-cm white vitric aphyric pumice and cm-size orange Qbo pumice
74-75.5	L	fine silt in upper section, to ~74.6 ft; pumice fall in lower half, vitric white aphyric pumice to 0.5 cm
81-82	b	cm-scale Qbo pumice, orange, plus sub-cm white aphyric pumice and trace obsidian
<b>Qct/Qbo at 82-92 (~87) ft (new pick) [Kleinfelder pick was at 67 ft]</b>		
92-93	b	fragments of orange Qbo; abundant angular lithics to 2 cm
101-102	b	buff-colored vitric ash flow, nonwelded, some intact core pieces
104-106.5	L	buff-colored vitric ash flow, nonwelded, intact core
116-117	b	buff-colored vitric ash flow, nonwelded, some intact core pieces
126.5-129	L	buff-colored vitric ash flow, nonwelded, intact core
144-146.5	L	buff-colored vitric ash flow, nonwelded, intact core

**Table B-1.1-1 (continued)**  
**Core Hole SC-3**

Depth (ft)	(b) Bag or (L) Lexan Sample	Observations
5	b	crystal-rich sand
10	b	crystal-rich sand
20	b	crystal-rich sand with moderate clay cementation
<b>Qal/Qct at 20-30 (~25) ft (new pick) (Kleinfelder 2002, 091687 included Qbt1g from 51.5–63ft; Qct from 63–96 ft.)</b>		
30	b	clay zone with sparse Qbt xls plus trace obsidian
<b>(Kleinfelder 2002, 091687 noted perched saturation at 35 ft during drilling.)</b>		
40	b	clay zone with common Qbt crystals, traces of obsidian
56.2-57.3	L	some very crystal-rich sands; core was wet (based on vesicular desiccation features)
56.3-56.5	b	fine- to medium-size aphyric pumice
65-65.5	b	pumice fall (note: one side of bag labeled "68-65.5")
67.5-68	b	crystal-rich sand
68-68.5	b	no sample (or mislabeled bag: see "65-65.5" above)
81-81.5	b	small aphyric pumice in clay cement; traces of vesicular obsidian glass
91-92	b	some Qbt crystals; traces of obsidian remain
<b>Qct/Qbo at 92-99.5 ft (97 ft Kleinfelder depth)</b>		
98.7-101.2	L	buff-colored vitric ash flow, nonwelded, intact core
118.7-121.2	L	buff-colored vitric ash flow, nonwelded, intact core

**Table B-1.1-1 (continued)**  
**Core Hole SC-4**

Depth (ft)	(b) Bag or (L) Lexan Sample	Observations
5	b	loamy sand with both rounded and angular gravel to 2 cm
10	b	crystal-rich sand with roots and twigs
20	b	indurated silt with ~10% Qbt crystals; clay matrix fine and dispersed
35	b	crystal-rich sand, ~90% Qbt crystals
44	b	very clay-rich, coarse and waxy clay aggregates; clasts of Qbt 1v to 3 cm
45.5-48	L	shallow end of core has clay-cemented colluvium of altered Qbt 1v; deeper end grades to dark-brown clay cementing crystal-rich sand
<b>Qal/Qbo at 50 ft</b>		
61-62	b	buff-colored vitric ash flow, nonwelded, some intact core pieces
79-80	L	buff-colored vitric ash flow, nonwelded, intact core
96.5-99	L	buff-colored vitric ash flow, nonwelded, intact core

Kleinfelder 2002, 091687

**Table B-1.1-1 (continued)**  
**Core Hole SC-5**

Depth (ft)	(b) Bag or (L) Lexan Sample	Observations
5	b	crystal-rich sand plus weakly clay-cemented silt
10	b	weakly cemented silt plus ~20% Qbt crystals
20	b	weakly cemented silt plus ~40% Qbt crystals
38	b	large (4-cm) fragment of Qbo or Qbt 1g; silt with glass shards
45-46	b	very loosely indurated silt; glass shards
<b>Qal/Qbo at 49.3 ft</b>		
49-51.5	L	clay-cemented crystal-rich sand; Qbt 1v clasts to 3 cm in upper part of core; sharp contact at 49.3 ft with intact core of buff-colored Qbo ash flow
54-56.5	L	buff-colored vitric ash flow, nonwelded, intact core
71.5-74	L	buff-colored vitric ash flow, nonwelded, intact core
82.5-84	L	buff-colored vitric ash flow, nonwelded, intact core

**Table B-1.2-1**  
**Core Sample Summaries: Stratigraphic Units Sampled and Core Collection Method**

Unit <sup>a</sup>	SCC-1	SCC-2	SCC-3	SCC-4	SCC-5	SCC-6
alluvium	2 (cs <sup>b</sup> )		2 (1 cs, 1 t <sup>c</sup> )	2 (cs)	2 (t)	3 (1cs, 2 t)
Qbt 1g		2 (cs)	1 (t)	1 (t)		
Qct		3 (cs)	1 (t)	2 (t)		
Qbo	13 (t)	10 (2 cs, 8 t)	10 (t)	9 (t)	11 (t)	6 (t)
Qbog	1 (t)	1 (t)	1 (t)	1 (t)	1 (t)	1 (t)
Tpf	3 (t)	2 (t)	1 (t)	1 (t)		2 (t)
Tb 4	2 (core <sup>d</sup> )	2 (core)	1 (core)		2 (core)	2 (core)

<sup>a</sup> Stratigraphic unit symbols include the lower vitric nonwelded ash flows of the Tshirege Member of the Bandelier Tuff (Qbt 1g), the Cerro Toledo Interval (Qct), ash flows of the Otowi Member of the Bandelier Tuff (Qbo), the Guaje Pumice Bed (Qbog), the Puye Formation (Tpf), and Cerros del Rio basalts (Tb 4).

<sup>b</sup> cs = Continuous sampler.

<sup>c</sup> t = Shelby Tube.

<sup>d</sup> Core = Core barrel.

**Table B-1.3-1  
Summary Information for Groundwater Samples Collected during Drilling**

Unit*	SCC-1	SCC-2	SCC-3	SCC-4
Qbt 1g/Qct		2 (Qbt 1g/Qct contact, TD in Qct)		
Qbo				1 (upper Qbo, TD in Qbo – likely drilling fluid, not native water)
Tpf	1 (silty Puye, TD in basalt)	1 (silty Puye, TD in Puye) 1 (silty Puye, TD in basalt)	1 (silty Puye, TD in Puye) 1 (silty Puye, TD in basalt)	

\* Stratigraphic unit symbols include the lower vitric nonwelded ash flows of the Tshirege Member of the Bandelier Tuff (Qbt 1g), the Cerro Toledo Interval (Qct), ash flows of the Otowi Member of the Bandelier Tuff (Qbo), and the Puye Formation (Tpf).

**Table B-1.4-1  
Borehole Geophysical Logs and Borehole Videos  
(All Depths in Feet)**

**Drill Hole SCC-1**

Date	Cased Footage (ft bgs)	Open-Hole Interval (ft bgs)	Tool (depth of use in ft bgs)
October 5, 2006	0-337.5	337.5-400	video (0-377.7)
October 5, 2006	0-337.5	337.5-400	natural gamma (0-393)
October 5, 2006	0-337.5	337.5-400	induction (340-392)

**Table B-1.4-1 (continued)  
Drill Hole SCC-2**

Date	Cased Footage (ft bgs)	Open-Hole Interval (ft bgs)	Tool (depth of use in ft bgs)
September 1, 2006	0-316.75	316.75-388.6	natural gamma (0-388)
September 5, 2006	0-316.75	316.75-388.6	video (315.3-367.3)
September 5, 2006	0-316.75	316.75-388.6	induction (317-380)

**Table B-1.4-1 (continued)  
Drill Hole SCC-3**

Date	Cased Footage (ft bgs)	Open-Hole Interval (ft bgs)	Tool (depth of use in ft bgs)
September 13, 2006	0-257.8	257.8-344	video (0-324)
September 13, 2006	0-327.5	327.5-344	natural gamma (0-340)
September 13, 2006	0-257.8	257.8-344	induction (259-339)

**Table B-1.4-1 (continued)**  
**Drill Hole SCC-4**

Date	Cased Footage (ft bgs)	Open-Hole Interval (ft bgs)	Tool (depth of use in ft bgs)
September 21, 2006	0–257.1	257.1–323	video (0–321)
September 21, 2006	0–257.1	257.1–323	natural gamma (0–322)
September 21, 2006	0–257.1	257.1–323	induction (256–316)

**Table B-1.4-1 (continued)**  
**Drill Hole SCC-5**

Date	Cased Footage (ft bgs)	Open-Hole Interval (ft bgs)	Tool (depth of use in ft bgs)
September 27, 2006	0–217.5	217.5–290	video (0–280)
September 27, 2006	0–217.5	217.5–290	natural gamma (0–287)
September 27, 2006	0–217.5	217.5–290	induction (228–289)

**Table B-1.4-1 (continued)**  
**Drill Hole SCC-6**

Date	Cased Footage (ft bgs)	Open-Hole Interval (ft bgs)	Tool (depth of use in ft bgs)
October 11, 2006	0–216	216–259.5	video (0–249.1)
October 11, 2006	0–216	216–259.5	natural gamma (0–257)
October 11, 2006	0–216	216–259.5	induction (216–256)

**Table B-2.0-1**  
**Summary of Water-I Level Changes at the Monitoring**  
**Boreholes between March and June 2006**

Well	Screen	Mar-06			Jun-06			Water level Change (ft)	Comment
		No. Data Points	Avg Water Level (ft)	Std Dev (ft)	No. Data Points	Avg Water Level (ft)	Std Dev (ft)		
CDV-R-15-3	4	652	6019.80	0.02	720	6019.79	0.01	-0.01	Response may not correlate to pumping
CDV-R-37-2	2	677	6137.31	0.03	720	6137.29	0.02	-0.02	Response may not correlate to pumping
G-3	Single	744	5760.98	2.49	720	5724.70	<b>4.74</b>	-36.28	Non pumping data shown for Guaje well field
R-1	Single	744	5879.06	0.19	720	5878.73	0.13	-0.33	
R-2	Single	744	5871.88	0.22	720	5871.72	0.13	-0.16	
R-4	Single	744	5833.86	0.21	720	5832.28	<b>0.30</b>	-1.58	Confined portion of aquifer, not phreatic water
R-5	3	744	5768.05	0.02	719	5767.81	0.02	-0.23	Deeper screen shows more response
R-6	Single	744	5839.91	0.38	720	5839.10	0.17	-0.81	
R-7	3	744	5878.49	0.03	720	5878.33	0.01	-0.16	
R-8	1	741	5855.59	0.03	720	5853.55	<b>0.38</b>	-2.03	No filter pack at screen, data questionable
R-9	Single	744	5691.97	0.21	720	5692.03	0.12	0.06	Probably not representative of water table
R-10a	Single	1	5741.26		720	5741.29	0.08	0.03	March data from April measurement
R-11	Single	744	5838.53	0.21	720	5838.25	0.13	-0.28	
R-12	3	744	5695.18	0.07	720	5695.21	0.04	0.03	Probably not representative of water table
R-13	Single	744	5836.68	0.19	720	5836.23	0.13	-0.45	
R-14	1	744	5883.61	0.04	13	5882.81	0.14	-0.80	Equipment problems limit number of data
R-15	Single	744	5851.02	0.21	720	5849.60	<b>0.38</b>	-1.42	Screen taps deeper zones of aquifer
R-16r	Single	744	5693.12	0.35	720	5693.35	0.10	0.23	Response does not correlate to pumping
R-18	Single	744	6117.40	0.31	720	6117.31	0.11	-0.09	Response may not correlate to pumping
R-19	3	744	5887.61	0.01	720	5887.48	0.01	-0.13	Deeper screens show more response
R-20	1	744	5866.15	0.06	12	5865.32	0.07	-0.83	June data incomplete, response may be greater
R-21	Single	744	5854.59	0.20	720	5853.90	0.13	-0.69	
R-22	1	744	5762.38	0.16	720	5762.43	0.08	0.04	
R-23	Single	744	5697.77	0.21	720	5697.82	0.12	0.05	
R-24	Single	735	5834.16	1.35	720	5829.84	<b>0.75</b>	-4.32	Confined portion of aquifer, not phreatic water
R-25	4	744	6347.29	0.16	720	6346.34	0.10	-0.95	Response does not correlate with pumping
R-25	5	744	6235.40	0.06	720	6235.37	0.05	-0.03	Response does not correlate with pumping
R-26	2	743	6539.10	0.18	713	6538.16	0.18	-0.93	Response does not correlate to pumping
R-28	Single	744	5839.07	0.21	720	5838.72	0.14	-0.35	
R-31	2	744	5827.89	0.14	567	5827.94	0.09	0.06	Response does not correlate to pumping
R-32	1	744	5859.34	0.07	604	5859.23	0.05	-0.11	Deeper screens show more response
R-34	Single	744	5835.57	0.31	720	5835.32	0.12	-0.25	
TW-1	Single	1	5855.35			No Data			March data from February measurement
TW-3	Single	1	5839.95			No Data			March data from February measurement
TW-4	Single	1	6071.45			6071.45		0.00	March data from February measurement
TW-8	Single	744	5875.05	0.19	720	5874.78	0.17	-0.27	
DT-5A	Single	744	5958.66	0.20		No Data			Long term data show steady decline
DT-9	Single	138	5915.55	0.08		No Data			Long term data show steady decline
DT-10	Single	744	5919.34	0.12	109	5919.47	0.05	0.13	Long term data show steady decline

**Table B-2.0-2**  
**Data for Monitoring Well Screens Located at the**  
**Top of the Regional Aquifer**

Well	Screen	Avg March 2006 Water Level (ft)	Screen Top (ft bgs)	Screen Bottom (ft bgs)	Screen Length (ft)	Geologic Unit	Screen Top Elev (ft)	Top of Screen from Water Table (ft)	Comment
CDV-R-15-3	4	6019.8	1235.1	1278.9	43.8	Tp	6023.8	4.0	Screen straddles water table
CDV-R-37-2	2	6137.3	1188.7	1213.8	25.1	Tt	6141.9	4.6	Screen straddles water table
G-3	Single	5761.0	560.0	1100.0	540.0	Tsf	5579.0	-182.0	Former supply well converted to monitoring
R-1	Single	5879.1	1031.1	1057.4	26.3	Tp	5850.1	-29.0	Compare with nearby TW-8
R-2	Single	5871.9	906.5	929.6	23.1	Tpf	5863.9	-7.9	
R-4	Single	5833.9	792.9	816.0	23.1	Tp	5784.6	-49.3	Screen monitors potential confined zone
R-5	3	5768.0	676.9	720.3	43.4	Tsf/Tsfb	5795.7	27.7	Long screen at top of regional aquifer
R-6	Single	5839.9	1205.0	1228.0	23.0	Tf	5790.8	-49.1	Screen significantly below water table
R-7	3	5878.5	895.5	937.4	41.9	Tp	5883.7	5.2	Screen straddles water table
R-8	1	5855.6	705.3	755.7	50.4	Tp	5839.4	-16.2	Screen below water table, no filter pack
R-9	Single	5692.0	683.0	748.5	65.5	Tsfb	5699.8	7.8	Screen straddles "deep" water table
R-10a	Single	5741.3	690.0	700.0	10.0	Tsf	5673.7	-67.5	Screen significantly below water table
R-11	Single	5838.5	855.0	877.9	22.9	Tp	5818.7	-19.8	Screen below water table
R-12	3	5695.2	801.0	839.0	38.0	Tsfb	5698.6	3.4	Screen straddles "deep" water table
R-13	Single	5836.7	958.3	1018.7	60.4	Tp	5714.7	-122.0	Screen significantly below water table
R-14	1	5883.6	1200.6	1233.2	32.6	Tp	5861.5	-22.1	Screen below water table
R-15	Single	5851.0	958.6	1020.3	61.7	Tp	5861.4	10.4	Screen straddles water table
R-16r	Single	5693.1	600.0	617.6	17.6	Tpt	5657.0	-36.1	Screen significantly below water table
R-18	Single	6117.4	1358.0	1381.0	23.0	Tpf	6046.8	-70.6	Screen significantly below water table
R-19	3	5887.6	1171.4	1215.4	44.0	Tpf	5894.9	7.3	Screen straddles water table
R-20	1	5866.1	904.6	912.2	7.6	Tb4	5789.8	-76.4	Screen significantly below water table
R-21	Single	5854.6	888.8	906.8	18.0	Tp	5767.4	-87.2	Screen significantly below water table
R-22	1	5762.4	872.3	914.2	41.9	Tb4	5778.2	15.8	Screen straddles water table
R-23	Single	5697.8	816.0	873.2	57.2	Tsf	5711.8	14.0	Screen straddles water table
R-24	Single	5834.2	825.0	848.0	23.0	Tsf	5722.4	-111.8	Screen monitors confined zone
R-25	4	6347.3	1184.6	1194.6	10.0	Tpf	6331.5	-15.8	Probable intermediate zone
R-25	5	6235.4	1294.7	1304.7	10.0	Tpf	6221.4	-14.0	Screen below water table
R-26	2	6539.1	1422.0	1445.0	23.0	Tp	6219.7	-319.4	Screen significantly below water table
R-28	Single	5839.1	934.3	958.1	23.8	Tpf	5794.3	-44.8	Screen significantly below water table
R-31	2	5827.9	515.0	545.7	30.7	Tb4	5847.5	19.6	Screen straddles water table
R-32	1	5859.3	867.5	875.2	7.7	Tb4	5770.1	-89.2	Screen significantly below water table
R-33	1	5860.0	995.5	1018.5	23.0	Tpp	5857.8	-2.2	Water level estimated, screen at water table
R-34	Single	5835.6	883.7	906.6	22.9	Tpp	5746.3	-89.3	Screen significantly below water table
TW-1	Single	5855.4	632.0	642.0	10.0	Tp	5737.2	-118.2	Water level erratic
TW-3	Single	5840.0	805.0	815.0	10.0	Tp	5821.9	-18.1	Screen below water table
TW-4	Single	6071.5	1195.0	1205.0	10.0	Tt	6049.6	-21.9	Screen below water table
TW-8	Single	5875.1	953.0	1065.0	112.0	Tp	5920.5	45.4	Screen straddles water table
DT-5A	Single	5958.7	1171.5	1788.5	617.0	Tp	5972.4	13.7	Screen straddles water table
DT-9	Single	5915.6	819.0	1500.0	681.0	Tp	6116.0	200.4	Screen straddles water table
DT-10	Single	5919.3	1078.4	1408.0	329.6	Tp	5941.5	22.2	Screen straddles water table

Note: Green highlighted cells indicate screens located appropriately to represent the water table; yellow cells indicate screens that are located to potentially represent the water table; orange cells indicate screens that potentially do not represent the regional phreatic water table; blue cells indicate screens that are located in Miocene basalt zones that do not appear to be representative of the phreatic water table.

## **Appendix C**

---

*Analytical Data Tables and Water-Level Data  
(on DVDs)*

